BioMed Research International

Angiogenesis and Vasculogenesis in Health and Disease

Guest Editors: Alessio D'Alessio, Francesco Moccia, Jie-Hui Li, Alessandra Micera, and Themis R. Kyriakides

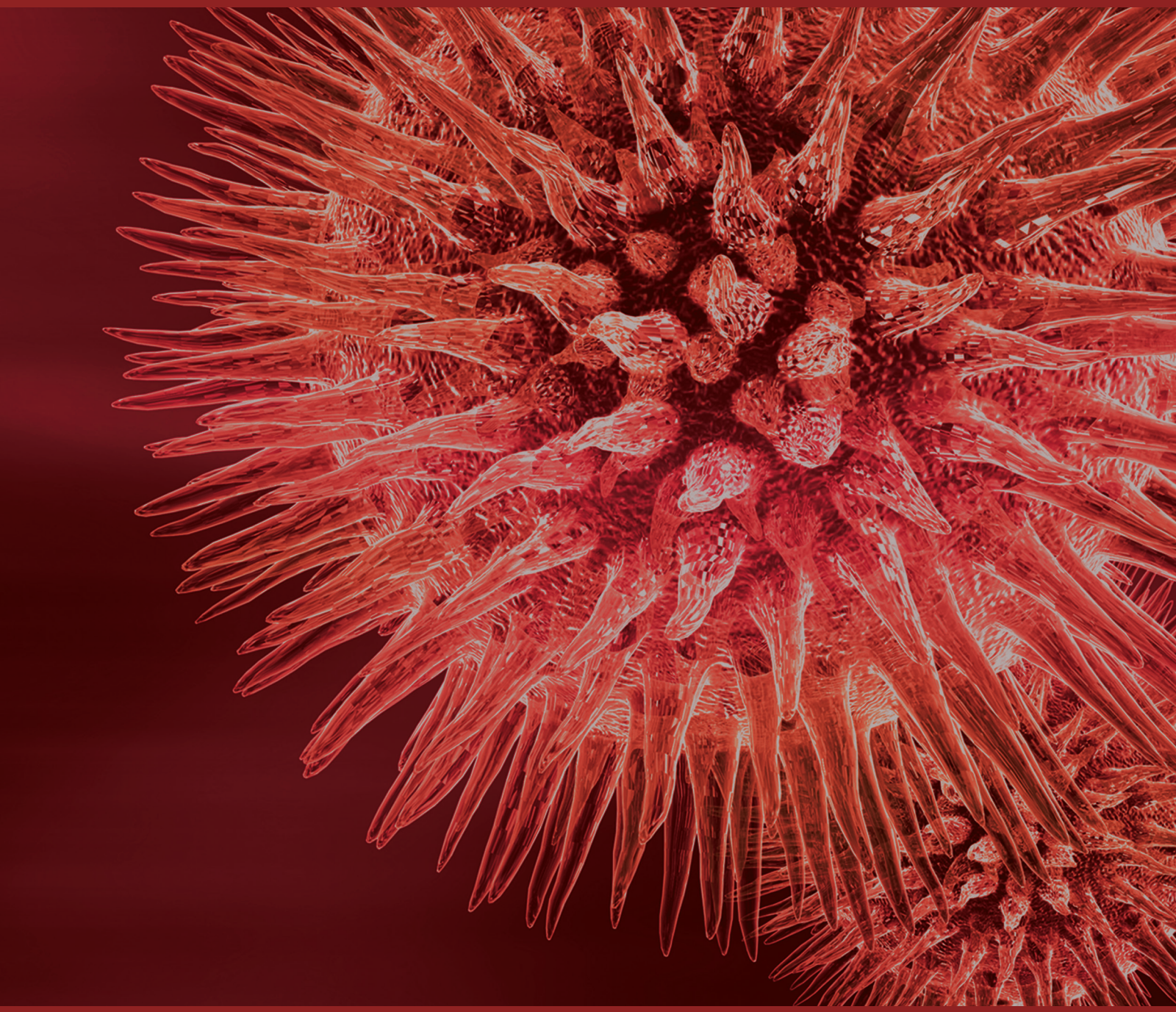

Angiogenesis and Vasculogenesis in Health and Disease

BioMed Research International

Angiogenesis and Vasculogenesis in Health and Disease

Guest Editors: Alessio DAlessio, Francesco Moccia, Jie-Hui Li, Alessandra Micera, and Themis R. Kyriakides

Contents

Hindawi Publishing Corporation
BioMed Research International
Volume 2015, Article ID 126582, 2 pages
http://dx.doi.org/10.1155/2015/126582

Editorial

Angiogenesis and Vasculogenesis in Health and Disease

Alessio D'Alessio,[1] Francesco Moccia,[2] Jie-Hui Li,[3] Alessandra Micera,[4] and Themis R. Kyriakides[5]

[1]*Institute of Histology and Embryology, School of Medicine, Catholic University of the Sacred Heart, 00168 Rome, Italy*
[2]*Department of Biology and Biotechnology "Lazzaro Spallanzani", University of Pavia, 27100 Pavia, Italy*
[3]*Department of Molecular and Cell Biology, Boston University Henry M. Goldman School of Dental Medicine, 650 Albany Street, Boston, MA 02118, USA*
[4]*IRCCS-G. B. Bietti Foundation, 00198 Rome, Italy*
[5]*Department of Pathology, Yale University School of Medicine, New Haven, CT 06510, USA*

Correspondence should be addressed to Alessio D'Alessio; alessio.dalessio@rm.unicatt.it

Received 5 May 2015; Accepted 5 May 2015

Angiogenesis is an important process that takes place during new blood vessel formation from preexisting ones. The first sign of vasculature occurs in the early phases of embryonic development when mesoderm-derived endothelial progenitor cells (EPCs) proliferate and form a primitive network of vessels during vasculogenesis. Vascular Endothelial Growth Factor (VEGF) is the most crucial factor in this process since it induces cell proliferation and migration. This primitive vascular structure, also known as the primary capillary plexus, is progressively remodeled in order to establish a mature circulatory network. Although vasculogenesis was thought to be restricted to embryonic development, recent studies support the existence of bone marrow-derived EPCs in adulthood that can contribute to neovascularization. In the adult, angiogenesis is mostly restricted to the ovarian cycle, injured tissues, and organ growth. Therefore, endothelial cells are considered stable and almost quiescent showing limited turnover in the adult vasculature. The lack of balance of pro- and antiangiogenic cues is considered one of the most crucial features that distinguish physiological from pathological angiogenesis. It is not surprising that we have witnessed an increase in interest in the field of angiogenesis research during the last decades with the main focus on trying to understand how to modulate blood vessel growth in order to develop new clinical approaches for a broad range of angiogenesis-related diseases. The main focus of this special issue is to highlight the complicated mechanism of angiogenesis in many different fields of cell biology. The special issue, which compiles a series of seven original research papers and two review articles, covers relevant aspects of vascular biology that are deeply discussed by experts in the field.

N. Irrera et al. investigated the effect of EPO-α and EPO-Z, two biosimilar recombinant human erythropoietins, on angiogenesis and cell proliferation in an experimental model of burn injury. Their study shows that although EPO-α and EPO-Z were both able to accelerate wound repair and angiogenesis, EPO-α was more effective in achieving complete skin regeneration. Authors hypothesize that the higher efficacy of EPO-α might be ascribed to an advantageous conformational structure, which renders this molecule more efficient in inducing cell proliferation and skin remodeling.

The interesting research article by I. Pafumi et al. describes a novel calcium-dependent machinery activated through the angiopoietin-1/2-tie receptor system. They employed the widely used human umbilical vein endothelial cells (HUVECs). The research team that has long-standing experience in the study of the intracellular calcium machinery in different experimental models suggests a novel Ca^{2+}-dependent mechanism activated by angiopoietins that controls important angiogenic processes, including cell migration and the formation of capillary-like structures *in vitro*.

W. D. Ito and collaborators generated a specific monoclonal antibody, namely, CTA 157-2, against membrane preparations of growing collateral vessels. They show that CTA 157-2 specifically binds to the cell surface and activates the proteasome on vascular resident EPCs. In particular, they propose a functional role of the 20S proteasome activity on EPCs function and vascular growth by reducing the extent of collateral proliferation *in vivo*.

The article by L. Gackowska et al. is an interesting study that evaluates the different expression patterns of adiponectin receptors 1 and 2 (AdipoR1, AdipoR2) in children with primary hypertension versus healthy patients. The authors employed different experimental approaches, including flow cytometry, PCR, and ELISA, to show that neutrophil AdipoRs upregulation is associated with early stages of vascular injury, hypertension severity, and low serum levels of adiponectin. These findings suggest the involvement of the innate immune system in the development and maintenance of primary hypertension in children.

The research article by J. L. de Carvalho and coauthors proposes an innovative approach in order to generate functional endothelial cells, derived from Human Adipose-Derived Stromal Cells (hASCs), which can be employed for vascular grafts. By using an experimental model consisting of decellularized rat aorta with preserved basal membrane, they employed hASC derived ECs to promote reendothelialization of the aorta.

B. Lorusso et al. focus on lymphatic endothelial cells. Indeed, similar to the blood vascular system, the lymphatic system plays an important role in a variety of physiological and pathological conditions including inflammation, wound healing, and the formation of tumor metastasis. Their study proposes an innovative approach to obtain purified and functional human lymphatic endothelial cells isolated from human lung (HL-LECs) of healthy patients. Authors underline the potential application of HL-LECs for understanding the mechanisms regulating the biology of the lymphatic system.

X. Zhang et al. investigate the potential therapeutic contribution of Oncostatin M (OSM) to angiogenesis after myocardial infarction in a knock-out animal model deficient in the OSM-specific receptor β subunit. Their results indicate that OSM treatment preserved cardiac function, prevented cardiac hypertrophy, and stimulated angiogenesis via upregulation of VEGF and bFGF in infarct border zone of ischemic myocardium.

Two interesting review articles are also reported in this special issue. In their review article, A. Zimna and M. Kurpisz first review some general concepts of angiogenesis, hypoxia, and the importance of O_2 homeostasis in the vascular network followed by a revision of recent studies concerning the contribution of the Hypoxia-Inducible Factor-1 (HIF-1) pathway and hypoxia in both physiological and pathological angiogenesis. Another review article by D. A. de Souza Junior and colleagues covers the current knowledge of how mast cell proteases, in particular chymases and tryptases, are implicated in tumor angiogenesis.

Acknowledgment

We want to express our sincerest gratitude to external reviewers who willingly shared their expertise on specific topics.

Alessio D'Alessio
Francesco Moccia
Jie-Hui Li
Alessandra Micera
Themis R. Kyriakides

Hindawi Publishing Corporation
BioMed Research International
Volume 2015, Article ID 747864, 12 pages
http://dx.doi.org/10.1155/2015/747864

Research Article

Isolation and Characterization of Human Lung Lymphatic Endothelial Cells

Bruno Lorusso,[1] Angela Falco,[1] Denise Madeddu,[1] Caterina Frati,[1] Stefano Cavalli,[1] Gallia Graiani,[1] Andrea Gervasi,[1] Laura Rinaldi,[1] Costanza Lagrasta,[2] Davide Maselli,[1] Letizia Gnetti,[2] Enrico M. Silini,[2] Eugenio Quaini,[3] Luca Ampollini,[4] Paolo Carbognani,[4] and Federico Quaini[1]

[1]*Department of Clinical and Experimental Medicine, University Hospital of Parma, 43126 Parma, Italy*
[2]*Department of Biomedical, Biotechnological, and Translational Sciences (S.Bi.Bi.T.), University Hospital of Parma, 43126 Parma, Italy*
[3]*Cardiovascular Department, Humanitas Clinical and Research Centre, 20089 Milan, Italy*
[4]*Department of Surgical Sciences, University Hospital of Parma, 43126 Parma, Italy*

Correspondence should be addressed to Federico Quaini; federico.quaini@unipr.it

Received 23 October 2014; Revised 24 December 2014; Accepted 12 January 2015

Academic Editor: Themis R. Kyriakides

Characterization of lymphatic endothelial cells from the respiratory system may be crucial to investigate the role of the lymphatic system in the normal and diseased lung. We describe a simple and inexpensive method to harvest, isolate, and expand lymphatic endothelial cells from the human lung (HL-LECs). Fifty-five samples of healthy lung selected from patients undergoing lobectomy were studied. A two-step purification tool, based on paramagnetic sorting with monoclonal antibodies to CD31 and Podoplanin, was employed to select a pure population of HL-LECs. The purity of HL-LECs was assessed by morphologic criteria, immunocytochemistry, flow cytometry, and functional assays. Interestingly, these cells retain *in vitro* several receptor tyrosine kinases (RTKs) implicated in cell survival and proliferation. HL-LECs represent a clinically relevant cellular substrate to study lymphatic biology, lymphoangiogenesis, interaction with microbial agents, wound healing, and anticancer therapy.

1. Introduction

The lymphatic system consists of a vascular network of blind-end, thin-walled capillaries and larger vessels that drain lymph, from the extracellular spaces of most organs, to the venous circulation through the thoracic duct. The lymphatic capillary wall is composed of a continuous single-cell layer of overlapped endothelial cells. Due to the discontinuous basement membrane, these vessels are highly permeable. The lymphatic system also includes lymphoid organs such as lymph nodes, tonsils, Payer's patches, spleen, and thymus. Lymphatic vessels are usually absent in avascular structures and in some vascularized organs such as brain, retina, and bone marrow. By regulating tissue fluid homeostasis, immune cell trafficking, and dietary fats absorption the lymphatic system plays a pivotal role in inflammation, wound healing, and tumour metastasis [1–4]. Recently, a murine model has been proposed in which pulmonary lymphatic function is required in late fetal life to prevent tissue edema and ensuring lung compliance at birth [5].

In the last fifteen years, an important aid in some aspects of *in vitro* and *in vivo* vascular biology has been prompted by the identification of lymphatic markers that can accurately discriminate lymphatic vessels from blood vessels. Thus, hyaluronan receptor Lyve-1 [6], the prospero-related homeobox gene transcription factor Prox1 [7], the membrane glycoprotein podoplanin (Pdn)/D2-40 [8], vascular endothelial growth factor receptor- (VEGFR-) 3 tyrosine kinase

[9], and its ligands VEGF-C and VEGF-D [10] have been documented in the specification and lineage commitment of the lymphatic system.

Evidence has also been provided that specific congenital or acquired disorders of the lymphatic system may lead to pathologic conditions such as lymphangitis, lymphoedema, lymphangioma, and lymphangiosarcoma [11].

Although lymphatics in the lung have been described over centuries ago [12] detailed reports on the precise identification of human lung lymphatics are at best sporadic.

Histologic characterization of pulmonary structures showed that lymphatic vessels are located in close proximity of the airways and major blood vessels, a phenomenon likely related to their role in alveolar clearance necessary to obtain an efficient respiration. Although not shared by experts in the field, according to several investigators, this specific function sees the lymphatic contribution of greater importance than that of blood vasculature [13–16]. In this regard, the low numerical incidence and flattening of lymphatics make it difficult to assess their morphometric evaluation in interalveolar septa of the normal human lung and therefore possible functional correlations [13, 15]. However, by immunohistochemistry [13] or cast scanning electron microscopy [15], measurable quantity of lymphatics mainly located in the interlobular and bronchovascular interstitium seems to be less than half of that of blood vessels [13]. Interestingly, an increased density and surface area of lymphatics was observed in the peribronchiolar space as compared to perivascular location [13].

Although lymphatics and lymphangiogenesis have been implicated in the pathogenesis of lung diseases, the assessment of their biologic and functional involvement is missing. Human studies have shown *de novo* lymphangiogenesis or lack of lymphatics, respectively, in patients affected by diffuse alveolar damage or severe asthma [17–19]. In idiopathic pulmonary fibrosis a severe injury of subpleural and interlobular lymphatics suggested alveolar clearance as a new putative pathogenetic mechanism of the disease [20, 21]. Structural and functional changes in the lymphatic vascular system have also been implicated in the setting of lung transplantation and allograft rejection [11].

It is clear that a better understanding of organ specific lymphatics may lead to identify cellular and molecular targets, whose modulation may interfere with several pathologic processes including neo-lymphangiogenesis induced by tumours and their metastatic diffusion.

Cell culture models may be crucial to elucidate the pathobiology of lung microvascular endothelium. However, most of our current knowledge is derived from experiments on cultured human umbilical cord vein endothelial cells (HUVECs).

Methods to obtain lymphatic endothelial cells from several tissues [22–25] have been reported and different isolation procedures have been proposed to isolate a relative pure population of pulmonary microvascular endothelial cells from humans and murine tissues [26–30]. Yet, a detailed description of protocols to harvest, culturing and propagate lymphatic endothelial cells (LECs) from the human lung has not been published.

Here, we describe a simple and inexpensive method, requiring minimum equipment and accessories, to obtain lymphatic (HL-LECs) and blood (HL-BECs) endothelial cells from healthy human lung using a two-step purification tool based on sequential sorting with monoclonal antibodies to CD31- and Pdn-coated paramagnetic beads.

HL-LECs were extensively characterized by morphology, including transmission electron microscopy (TEM), immunocytochemistry, and flow cytometry, and their ability to form tube-like structures on Matrigel was assessed.

2. Materials and Methods

2.1. Tissue Sampling. The study was performed on 55 patients affected by lung cancer and undergoing lobectomy or pneumonectomy at the Department of Surgical Sciences, University-Hospital of Parma. Patients were enrolled after informed consent to the employment of biologic samples for research purpose. The procedure was approved by the institutional review board for human studies (Ethical Committee) of the University-Hospital of Parma and in accord with principles listed in the Helsinki declaration.

Lung tissue was collected and transferred under sterile condition to the Laboratory of Pathology (S.Bi.Bi.T. Dept). Samples were processed by the medical staff ensuring the priority of their use for diagnostic purposes within 1 hour from resection. Fragments of 0.5–1 g were obtained at safety distance of minimum 7 cm from the tumour. The correct sampling procedure to exclude pathologic findings was carried out by subsequent histologic analysis.

Fresh, healthy lung tissues were shortly immersed in sterile PBS to perform cell isolation or fixed in 10% neutral buffered formalin and embedded in paraffin for histologic and immunohistochemical analysis.

2.2. Immunohistochemistry. To ensure that harvested pulmonary tissues did not contain tumour lesion or other pathologic conditions, fixed samples were stained with hematoxylin and eosin (H&E). Immunohistochemical detection of lymphatic vessels was performed on paraffin-embedded sections cut at 5 μm thickness. After deparaffinization, heat-induced antigen retrieval was carried out in 10 mM sodium citrate buffer (pH 6) for 15 minutes by microwave oven. Sections were cooled down to room temperature (RT), washed in distilled water, rinsed in PBS and incubated with 20% goat serum (Sigma Aldrich, St. Louis, MO, USA) for 30 minutes at RT to block unspecific binding.

Sections were incubated with primary antibodies: mouse anti-human CD31 (ready to use; overnight (o/n) 4°C; DAKO, Copenhagen, Denmark) and rabbit anti-human Pdn (1 : 100; o/n 4°C; ReliaTECH, Braunschweig, Germany). TRITC- and FITC-conjugated anti-mouse and anti-rabbit antibodies (Sigma Aldrich), respectively, were used to detect simultaneously the two epitopes. Nuclei were counterstained with 0.5 mg/mL 4′,6-Diamidino-2-phenylindole (DAPI; 18 minutes RT; Sigma Aldrich). Slides were mounted by Vectashield (Vector Laboratories, Burlingame, CA, USA) and analyzed using a fluorescence Microscope (Leica DMI6000B,

Heidelberg, Germany). Fluorescent images were digitally captured with "LAS Advanced Fluorescence" software (Leica) connected to the microscope provided by a digital camera (Leica DFC350FX).

2.3. Processing of Fresh Lung Tissue. Fragments of healthy lung specimens were washed several times with phosphate buffer solution (PBS) and finely minced with scissors and subjected to enzymatic digestion for 75 minutes at 37°C with 1 mg/mL collagenase/dispase solution (Roche, Basel, Switzerland). The resulting digestion product was squeezed over a 100 μm nylon mesh (BD Biosciences, San Josè, CA, USA) to remove aggregates. The harvested cells were washed, seeded on collagen coated wells of a 6-well plate (BD Biosciences) and cultured in complete growth medium consisting of endothelial growth medium-MV (EGM-MV; Lonza, Walkersville, MD, USA) plus 5% fetal bovine serum (FBS; Lonza) and 2 ng/mL recombinant human vascular endothelial growth factor-C (VEGF-C; ReliaTECH).

Twenty-four hours later, nonadherent cells and debris were removed, whereas the adherent cell population was washed with PBS and cultured in complete medium until 70–80% confluence (usually reached in 5–7 days).

2.4. LEC Isolation and Culture. Primary cultures were harvested by trypsin/EDTA (Sigma Aldrich), incubated with 20 μL FcR reagent and 20 μL anti-human CD31 immunolabeled magnetic microbeads, according to manufacturer's recommendations (CD31 Microbeads Kit; Miltenyi Biotec, Bergisch Gladbach, Germany).

In brief, after 15 minutes at 4°C, cells were loaded onto a MS Column (Miltenyi Biotec) and placed in the magnetic field of an OctoMACS Separator (Miltenyi Biotec). All recovered ECs, positively selected for CD31 by the magnetic particle concentrator, were cultured on collagen-coated T25 flasks (BD Biosciences) in complete medium.

When reached 80–90% of confluence, CD31 selected cells were detached by trypsinization, washed, resuspended in 100 μL PBS, and incubated, for 20 minutes at 4°C, with 1 μg mouse anti-human Pdn (ReliaTECH). After incubation, cells were washed, centrifuged, resuspended in 30 μL PBS 0.5% FBS, and incubated with 15 μL goat anti-mouse antibodies-coated magnetic microbeads (MiltenyiBiotec) for 15 minutes at 4°C. Cells were reloaded onto a MS Column placed in the magnetic field of an OctoMACS Separator and eluted with 2 mL PBS added with 0.5% FBS. The unsorted population, being the $CD31^{pos}/Pdn^{neg}$ cell fraction and magnetically labelled Pdn^{pos} ECs retained on the column were separately processed. After removal of column from the magnetic field, the magnetically retained Pdn sorted cells were eluted with 2 mL PBS containing 0.5% FBS and represented Lymphatic Endothelial Cells (LECs). LECs were seeded, cultured, and propagated with EGM-MV plus 5% FBS and 2 ng/mL VEGF-C. Pdn unsorted cells representing Blood Endothelial Cells (BECs) were seeded, cultured, and propagated with EGM-MV plus 5% FBS.

Human lung lymphatic endothelial cells (HL-LECs) and human lung blood endothelial cells (HL-BECs), routinely examined by inverted light microscopy (Olympus CK40, Tokyo, Japan), were serially sub-cultured at a split ratio of 1 : 5 onto biocoat T25 flask (1×10^4 cells/cm^2). HL-LEC could be easily expanded from passage 2 (P2) to 8 (P8) without changes in their morphology or evidence of cellular senescence. Several cryogenic vials (VWR International PBI, Radnor, PA, USA) containing 5×10^5 endothelial cells from each recovered cell lines were frozen in cryopreservation solution containing 90% (v/v) FBS (Sigma Aldrich) and 10% (v/v) dimethyl sulfoxide (Sigma Aldrich) for storage in liquid nitrogen and to create a master cell bank. The vials were placed overnight in a cryo 1°C freezing container (VWR International PBI) at −80°C and transferred after 24–48 hours in liquid nitrogen. All the experiments described here were performed on HL-LECs from P2 to P8.

2.5. TEM Analysis. HL-LECs were analyzed by transmission electron microscopy (TEM) to detect the typical subcellular features associated with the lymphatic endothelium.

HL-LECs were expanded and after trypsinization centrifuged to obtain a visible pellet. The pellet was fixed in Karnovsky solution (4% formaldehyde, 5% glutaraldehyde) for 90 minutes at RT After washing with phosphate buffer, pH 7.2, the pellet was embedded in agar to maintain cohesiveness for subsequent processing.

Sample were post-fixed in 1% osmium tetroxide (OsO_4) for 90 minutes at RT and dehydrated by increasing concentration of alcohol. Following this procedure, samples were washed with propylene oxide and embedded in epoxy resin (Durcupan ACM, Sigma Aldrich). After resin polymerization, samples were trimmed on sections of 0.5 μm thickness and subsequently stained with methylene blue and safranin to select morphologically the field of interest. Ultrathin sections were collected on a 300-mesh copper grid and, after staining with uranyl acetate and lead citrate, were qualitatively examined under a transmission electron microscope (Philips EM 208S).

2.6. Flow Cytometric Analysis. HL-LEC confluent monolayers at P3 and P8 were dissociated with trypsin/EDTA, the cell pellet resuspended in PBS with 1% FBS and aliquot at 1×10^5 cell/tube for antibody labeling. One hundred microlitres of the cell suspension were incubated for 30 minutes at 4°C with 1 μg mouse anti-human Pdn (ReliaTECH). Primary antibody binding was detected by goat anti-mouse IgG FITC. Negative controls were represented by omission of the primary antibody from the reaction. Live cells were gated using forward (FSC) versus side scatter (SSC) dot plot.

Cells were analyzed by a FACS-Diva software (FACScanto II, BD Biosciences) acquiring at least 50,000 events.

2.7. Immunocytochemistry. Immunocytochemistry was performed on HL-LEC cultured on chamber slides (BD Biosciences) pretreated with collagen solution type 1 (Sigma Aldrich). When 80% confluence was reached, cells were fixed in cold 4% paraformaldehyde in PBS, pH = 7.4 for 30 minutes at RT. After washing with PBS, HL-LECs were exposed to 20%

goat serum (Sigma Aldrich) for 30 minutes at RT to block unspecific binding.

Cells were then incubated with the following primary unconjugated antibodies: mouse anti-human CD31 (ready to use; o/n 4°C; DAKO), rabbit anti-human von Willebrand Factor (vWF) (1 : 200; o/n 4°C; DAKO), rabbit anti-human Prox-1 (1 : 20; 75 minutes 37°C; Acris, Herford, Germany) after light permeabilization with 0.1% Triton X100, mouse anti-human alpha-smooth muscle actin (α-SMA) (1 : 200; o/n 4°C; DAKO), mouse anti-human vascular endothelial growth factor receptor-2 (VEGFR-2/KDR) (1 : 100; o/n 4°C; ReliaT-ECH), rabbit anti-human VEGFR-3 (1 : 25; o/n 4°C; Abcam). Fluorochrome-conjugated secondary antibodies (1 : 70; 60 minutes 37°C; Sigma Aldrich) were employed to detect different epitopes by fluorescence microscopy. Nuclei were recognized by counterstaining with DAPI for 15 minutes at RT and cover slips mounted with Vectashield.

Samples were analyzed using a fluorescence microscope (DMI6000B Leica). Fluorescent images were digitally captured with "LAS Advanced Fluorescence" software (Leica) connected to a microscope provided by a digital camera (Leica DFC350FX).

D2-40, LYVE-1, Fibroblast Growth Factor Receptor (FGFR)-1, Epidermal Growth Factor Receptor (EGFR), hepatocyte growth factor receptor c-MET, type 1 Insulin-like Growth Factor Receptor (IGF-1R), Platelet-Derived Growth Factor Receptor (PDGFR)-beta, Tropomyosin-related kinases A (TrkA), and neurotrophin p75 receptor ($p75^{NTR}$) were investigated by immunoperoxidase. Briefly, after fixation, chamber slides of HL-LECs were immersed in 3% hydrogen peroxide solution for 10 minutes and then incubated with mouse anti-human D2-40 (1 : 50; o/n 4°C; Biocare Medical, Concord, CA, USA), rabbit anti-human LYVE-1 (1 : 50; o/n 4°C; Abcam, Cambridge, UK), rabbit anti-human FGFR-1 (1 : 40; o/n 4°C; Cell Signaling, Beverly, MA, USA), mouse anti-human EGFR (1 : 40; o/n 4°C; Zymed-Invitrogen, Grand Island, NY, USA), rabbit anti-human c-MET (according to manufacturer's recommendations; Ventana-Roche), rabbit anti-human IGF-1R (1 : 30; o/n 4°C; Cell Signaling), rabbit anti-human PDGFR-beta (1 : 25; o/n 4°C; Abcam), rabbit anti-human TrkA (1 : 40; o/n 4°C; Santa Cruz Biotechnology, Heidelberg, Germany), and rabbit anti-human $p75^{NTR}$ (1 : 70; o/n 4°C; Millipore, Darmstadt, Germany), respectively. The immunoreaction was revealed by anti-mouse and anti-rabbit secondary antibodies polymerized with horseradish peroxidase in Tris-HCl buffer following the instruction of the advance/HRP kit (DAKO). Cytologic preparations were then counterstained with hematoxylin and analysed by an optical microscope (Olympus BX60) connected to QICAM camera (QImaging, Surrey, BC, Canada).

For each epitope tested by either immunoperoxidase or immunofluorescence, negative controls were represented by samples incubated with secondary antibodies and omitting the primary antibodies from the reaction. The specificity of the immune reaction was documented by exposing our endothelial cell preparations to antibodies to CD45 used as an unrelated antigen (see Figure S4 in Supplementary Material available online at http://dx.doi.org/10.1155/2015/747864). Moreover, human dermal fibroblasts were employed as negative controls for the immunocytochemical detection of endothelial markers.

2.8. In Vitro Angiogenesis Assay. The tube formation assay was performed according to manufacturer's recommendations and previously reported methods with some modifications [31]. Briefly, 80 μL of Matrigel (BD Biosciences) were loaded at the bottom of well of the 96 well plates (BD Biosciences). After 30 minutes at 37°C, cells (2×10^4 cells/100 μL in each well) suspended in complete growth medium were gently layered on the top of Matrigel. After 24 hours, to assess tube-forming ability, images were captured using an inverted microscope (Olympus CK40) connected to a digital camera (Olympus DP21).

3. Results

3.1. Immunohistochemical Detection of Human Lung Lymphatics. A fragment of lung samples utilized for cell isolation was subjected to microscopic examination. Sections stained with H&E were analysed to exclude pathologic findings and to identify areas of preserved alveolar parenchyma (supplemental data, figure S1A). To detect lymphatic vessels, double immunolabelling with CD31 and the lymphatic marker Pdn was performed.

In agreement with previous studies [13–16], lymphatic vessels in healthy lung tissues were documented by the presence of $CD31^{pos}/Pdn^{pos}$ vascular profiles (supplemental data, figure S1B). Blood endothelial cells were labeled by CD31 only (supplemental data, figure S1B).

3.2. Isolation and Culture of HL-LEC and HL-BEC. After tissue digestion, primary cultures of a heterogeneous adherent cell population were obtained, mainly consisting of stromal cells, fibroblasts, macrophages and endothelial cell clusters at time displaying characteristic "cobblestone-like" morphology (Figures 1(a) and 1(b)). Sub-confluent cell monolayers were recovered with trypsin/EDTA and sorted with microbeads coated with anti-CD31 antibodies to remove contaminating cells (Figure 1(d)).

CD31 sorted ECs were cultured until confluence recovered with trypsin/EDTA and additionally sorted with anti-Pdn immunolabelled microbeads. By this approach, highly purified LECs from human lung tissue (HL-LEC) were successfully harvested (Figure 1(c)) and further expanded for their characterization (see below).

The negative selection from Pdn sorting was recovered and represented blood endothelial cells (BECs). Although also BECs were seeded, cultured, and propagated onto biocoat flask with EGM-MV plus 5% FBS, this cell population will not be detailed in our report.

This approach allowed us to isolate endothelial cells from 51 of the 55 processed human lung samples with a yield of 92%.

3.3. HL-LECs Propagation and Cryopreservation. HL-LECs were seeded, cultured and propagated (ratio 1 : 5) onto biocoat

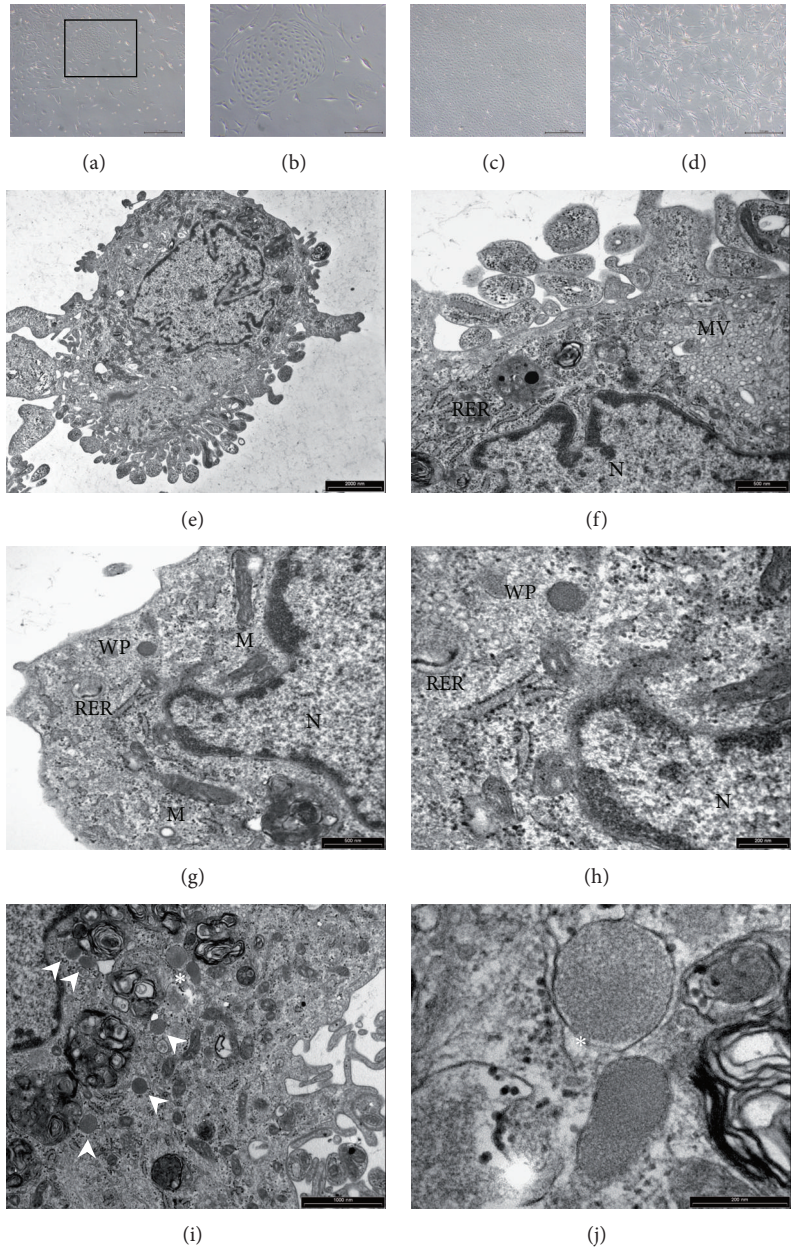

Figure 1: Morphology of human lung lymphatic endothelial cells (HL-LEC). (a)–(d): phase contrast microscopy. (a): an example of a mixed cell population obtained after enzymatic digestion of lung fragments. The black rectangle includes an area shown at higher magnification in (b) to illustrate a cluster of cells with cobblestone-like morphology, suggestive of an endothelial phenotype. (c): confluent monolayer of lymphatic endothelial cells selected by double immunomagnetic sorting with CD31 and Pdn antibodies. (d): fibroblastoid morphology of the CD31 negative cell population eluted after immunomagnetic sorting. (e)–(j): Transmission Electron Microscopy (TEM). (e): microphotograph of a single HL-LEC showing numerous surface microvilli. (f)–(h): ultrastructural characteristics of the lymphatic endothelium are documented by the presence of prominent micropinocytotic vesicles (MV), a well-developed rough endoplasmic reticulum (RER) and Weibel-Palade bodies (WP). (i)-(j): ultrastuctural image of a HL-LEC showing multiple Weibel-Palade bodies (white arrowheads) Two adjacent WPBs (asterisk), one transversally and one obliquely oriented, are shown at higher magnification in (j) to appreciate microtubular-like structures. M: mitochondria. N: nucleus. Scale bars: (a), (c), and (d) = 500 μm; (b) = 200 μm; (e) = 2 μm; (f) and (g) = 0.5 μm; (h) and (j) = 0.2 μm; (i) = 1 μm.

T25 flask (1×10^4 cells/cm^2) with EGM-MV plus 5% FBS and 2 ng/mL VEGF-C for at least 8 passages without significant changes in morphology, growth properties and evidence of cellular senescence (data not shown). A uniform monolayer was initially identified as endothelial cells according to morphologic criteria. In typical cultures, from P2 to P8, the doubling time of HL-LEC was 32.3 ± 2.5 hours.

At several passages, cells were aliquoted and cryopreserved. Subsequently, random cryogenic vials were thawed with a good recovery (data not shown).

3.4. TEM Analysis. The typical ultrastructural features of the lymphatic endothelium were documented by TEM. Lung derived cultured endothelial cells showed prominent microvilli on the cell surface (Figure 1(e)). In addition to the presence of abundant cytoplasmic microvescicles and a well-developed rough endoplasmic reticulum (Figure 1(f)), electron-dense rod-shaped microtubulated bodies, originally described by Weibel and Palade [32], were detected in cultured HL-LECs (Figures 1(g)–1(j)). Moreover, as previously reported [33], numerous autophagic vacuoles and parallel aggregates of intermediate filaments were frequently observed in expanded endothelial cells (data not shown).

3.5. Immunophenotypic Characterization of HL-LECs

3.5.1. Flow Cytometric Analysis. To ascertain the efficiency in cell separation and the lymphatic nature of HL-LECs, FACS analysis of the expression of Pdn was performed. As shown in Figures 2(b) and 2(c), 100% of isolated and cultured lymphatic endothelial cell lines from human lung tissues were positive for the lymphatic specific marker at P3 and this property was preserved until P8. Cells eluted from Pdn immunomagnetic sorting representing HL-BECs did not express the lymphatic associated antigen at FACS analysis (Figure 2(d)).

3.5.2. Immunocytochemical Analysis. To ensure the purity of cells recovered by double immunomagnetic sorting, immunocytochemistry was performed on LECs cultured on chamber slides.

The pan-endothelial marker CD31 is an integral membrane glycoprotein, also known as Platelet Endothelial Adhesion Molecule-1 (PECAM-1), which is constitutively expressed on the surface of mature endothelial cells. CD31 is highly enriched at junctions between adjacent endothelial cells, both *in vitro* and *in vivo* [34, 35]. Accordingly, virtually all our cultured LECs were positive for CD31 with abundant membrane expression (Figure 3(a)). Similarly, von Willebrand factor (vWF) glycoprotein, exhibited as strong granular cytoplasmic expression (Figure 3(b)). Interestingly, vWF is stored in endothelial cell in Weibel-Palade bodies [32] further strengthening their detection by TEM. In contrast, the expression of α-SMA was constantly absent in our preparation of HL-LEC (data not shown).

To define the lymphatic phenotype, three specific cell markers D2-40, LYVE-1 and Prox-1 were examined.

D2-40/podoplanin is a mucin-type transmembrane glycoprotein and unlike CD31, which recognizes both blood and lymphatic endothelial epitopes, its immunoreactivity is restricted and selectively expressed in LEC. Results of our investigation documented that all LECs lines obtained from the human lung expressed Pdn at a rate of 100% (Figure 3(c)).

LYVE-1, the lymphatic receptor for the extracellular matrix mucopolysaccharide hyaluronan, was widely expressed in our preparations of LECs showing a characteristic pattern on cell membrane surface (Figure 3(d)).

Prox-1, a key control gene in the program that specifies lymphatic endothelial cell fate, was consistently expressed by lymphatic endothelial cells isolated from healthy human lung tissue (Figures 3(e), 3(f), and 3(g)).

Importantly, the expression of these markers was preserved in cells expanded at least for 8 passages.

Thus, by immunocytochemistry, our population of HL-LEC possesses the distinct phenotypic characteristics of the lymphatic endothelium.

3.6. HL-LECs Express Multiple Tyrosine-Kinase Receptors. Receptor tyrosine kinases (RTKs) are transmembrane receptors that phosphorylate tyrosine residues with specificity in various protein substrates. RTKs play an important role in cell signaling and are involved in a variety of processes. In particular, in lymphatic endothelial cells RTKs are highly relevant due to their essential role in cell survival, proliferation, migration, and lymph-angiogenesis [36].

Thus, the presence of TK receptors in our primary cultures of human HL-LECs was investigated.

VEGFR-2 is thought to be the principal mediator of angiogenesis, although is also expressed at low levels in LECs. VEGFR-3 is a crucial receptor for the growth of lymphatic vessels during development and in adult life. Ligand binding promotes receptor dimerization, which may occur between two VEGFR-3 molecules (homodimerization) or between a VEGFR-3 and a VEGFR-2 molecule (heterodimerization). These biochemical events play a fundamental role in lymph-angiogenesis [36, 37]. As shown in Figures 4(a) and 4(b), both VEGFR-2 and VEGFR-3 were unambiguously expressed by human HL-LECs *in vitro*. Immunofluorescence signals of these epitopes were not detected in negative control cell lines (supplemental figure S3).

EGFR, also known as ErbB1 and HER-1, the first type I receptor tyrosine kinase identified, is a member of the ErbB, or HER, family of receptors (EGFR, HER-2, HER-3, HER-4). EGFR is a transmembrane protein with an internal tyrosine kinase domain. Activation by one of its many ligands leads to dimerization of EGFR, either with another EGFR (homodimerization) or one of the other receptors from the HER family (heterodimerization), which activates the catalytic system of the tyrosine kinase [36, 38]. This results in the activation of multiple pathways that promote survival, proliferation, and angiogenesis. These activities are mediated primarily through the mitogen-activated protein kinase (MAPK) and phosphatidylinositol 3-kinase (PI3K)-Akt pathways [38]. The typical expression of EGFR protein in primary cultures of HL-LEC is shown in Figure 4(e).

Similarly, FGFR-1 belongs to a highly conserved receptor tyrosine kinases family: FGFR1–4. This receptor activates an array of downstream signaling pathways, such as MAPK and PI3K/Akt pathways. Both these pathways regulate key cell behaviors such as survival, proliferation, differentiation, and lymphangiogenic effects in target cells [39]. As shown in Figure 4(f), virtually all HL-LECs *in vitro* express FGFR-1.

The type 1 Insulin-like Growth Factor Receptor (IGF-1R) belongs to the RTK superfamily and mediates crucial signaling pathways implicated in growth, proliferation, differentiation and apoptosis. Upon ligand binding at the plasma

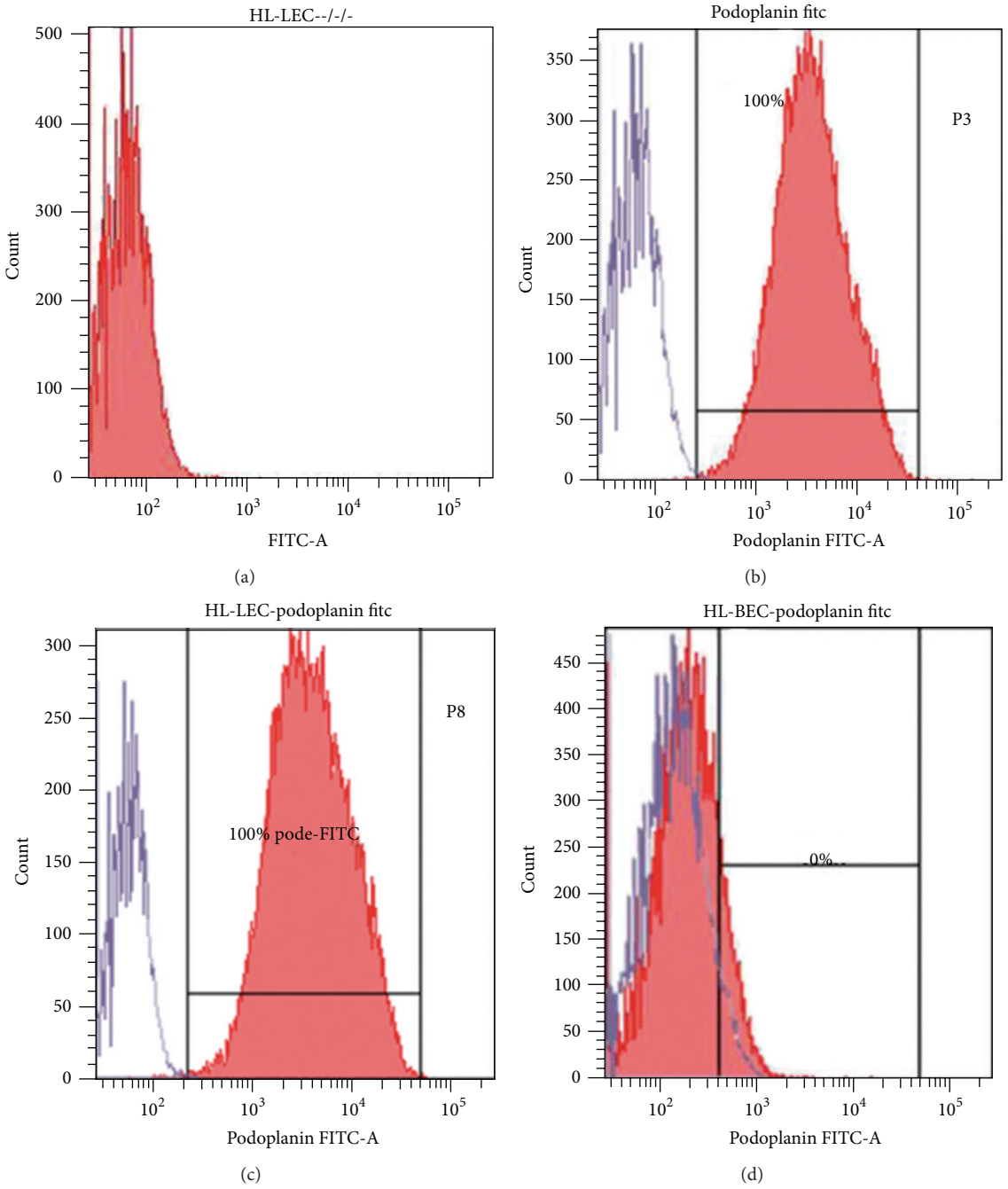

Figure 2: Fluorescence activated cell sorting. (a)–(c): Representative flow cytometric assay of lymphatic endothelial cells from the human lung (HL-LEC) expanded after double immunomagnetic sorting. (a): negative control represented by the omission of primary antibodies. (b) and (c): virtually 100% of HL-LECs show strong specific positivity for antibodies against Pdn both at passage 3 (P3, (b)) and 8 (P8, (c)). (d): FACS plot of HL-BECs eluted from Pdn immunomagnetic sorting (P4).

membrane, signaling events mediated by the IGF-1R occurs primarily through activation of PI3K-Akt and MAPK pathways [40]. HL-LECs cultured *in vitro* express IGF-1R, as shown in Figure 4(g).

The c-MET receptor tyrosine kinase, along with its ligand Hepatocyte Growth Factor (HGF), plays an important role in the regulation and control of tissue homeostasis under normal physiological conditions. However, HGF/c-MET axis has also been implicated in the regulation of cancer cell growth, angiogenesis, invasion, and metastasis. In addition to the interaction with other angiogenic signals, c-MET appears to act as an independent angiogenic factor [41, 42]. HL-LECs express c-MET receptor with its characteristic pattern (Figure 4(h)).

PDGFR-beta is a master regulator of lymphangiogenesis possessing diverse range of biologic activities, including

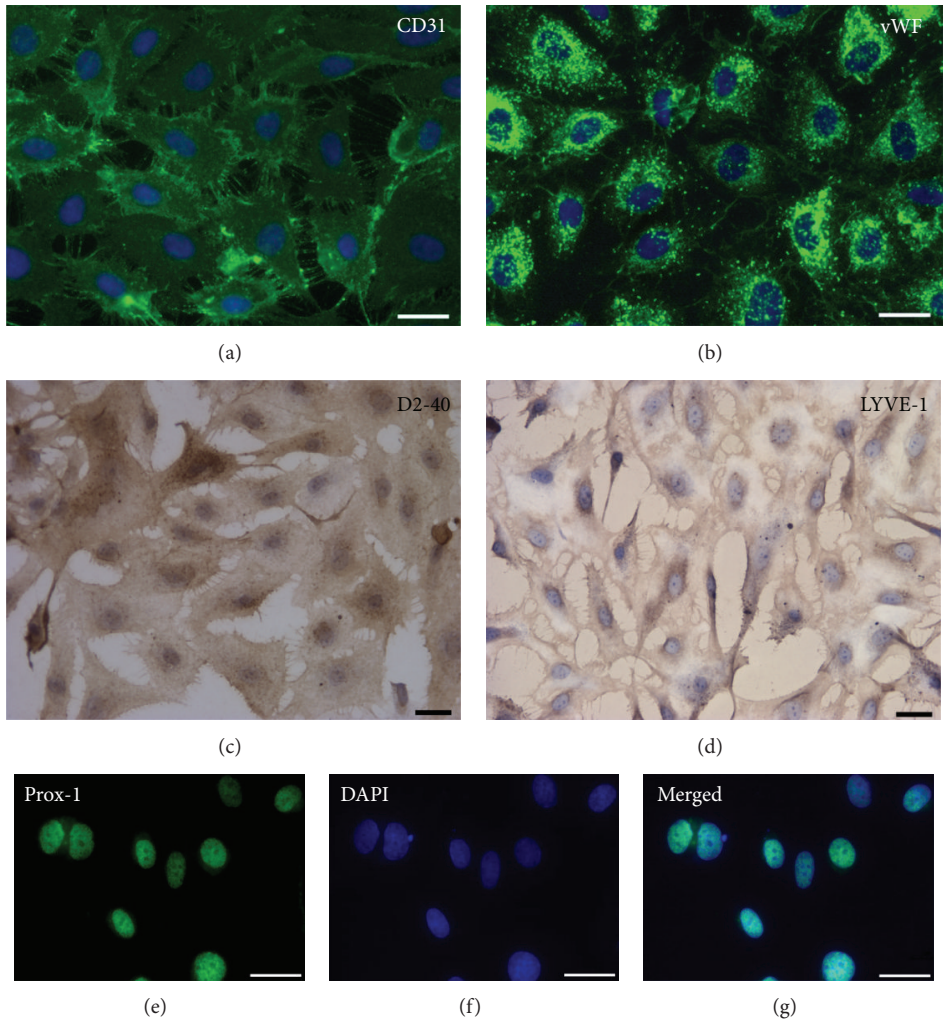

Figure 3: Immunocytochemical characterization of cultured human lung endothelial cells (HL-LECs). (a) and (b): the surface expression of the pan-endothelial marker CD31 and the dot-like cytoplasmic abundance of von Willebrand Factor (vWF) are shown in green by immunofluorescence. (c) and (d): immunoperoxidase detection of lymphatic associated antigens D2-40 and LYVE-1 (brownish) in HL-LEC. (e)–(g): the specific lymphatic lineage commitment of HL-LECs is documented by the nuclear expression of Prox-1 transcription factor (green). Nuclei are counterstained by DAPI in (a), (b), (f) and (g) and by Haematoxylin in (c) and (d). The immunocytochemical analysis was conducted on HL-LECs at passage 4 (P4). Scale bars: (a)–(g) = 25 μm.

cell survival, proliferation and chemotaxis [43]. Accordingly, we could observe that our preparations of HL-LEC widely expressed *in vitro* PDGFR-beta (Figure 4(d)).

Finally, the expression of neurotrophin receptors TrkA and $p75^{NTR}$ were evaluated, because recent studies have shown that both receptors are involved in vascular biology. The high-affinity TrkA receptor serves as a receptor for certain neurotrophic factors, including nerve growth factor (NGF), brain-derived neurotrophic factor (BDNF), and neurotrophin 3 (NT3), and plays a critical role in the development and maintenance of the central and peripheral nervous systems. The low-affinity $p75^{NTR}$, expressed in Schwann cells and neurons and belonging to the tumor necrosis factor family, contributes to a plethora of signaling complexes associates with several co-receptors, including the TrkA [44–47]. As shown in Figures 4(i) and 4(j), HL-LEC identified by our laboratory express TrkA and $p75^{NTR}$.

3.7. In Vitro Angiogenesis Assay. The formation of capillary-like tubes is a rather specific functional characteristic of endothelial cells [31, 48]. To determine whether our cell population had angiogenic property at least *in vitro*, we investigated the capacity of HL-LEC to organize into tubule-like networks on Matrigel. $CD31^{pos}/Pdn^{pos}$ LECs were able to form tube-like structures in response to a matrix, which mimics the physical and functional properties of basement membrane (Supplemental data, figure S5).

4. Discussion

The blood vascular system has been intensively studied since its discovery, however, only in recent years, the lymphatic system has emerged as a crucial player in physiologic processes and in a variety of diverse pathologic conditions such as inflammation, wound healing, and tumour metastasis.

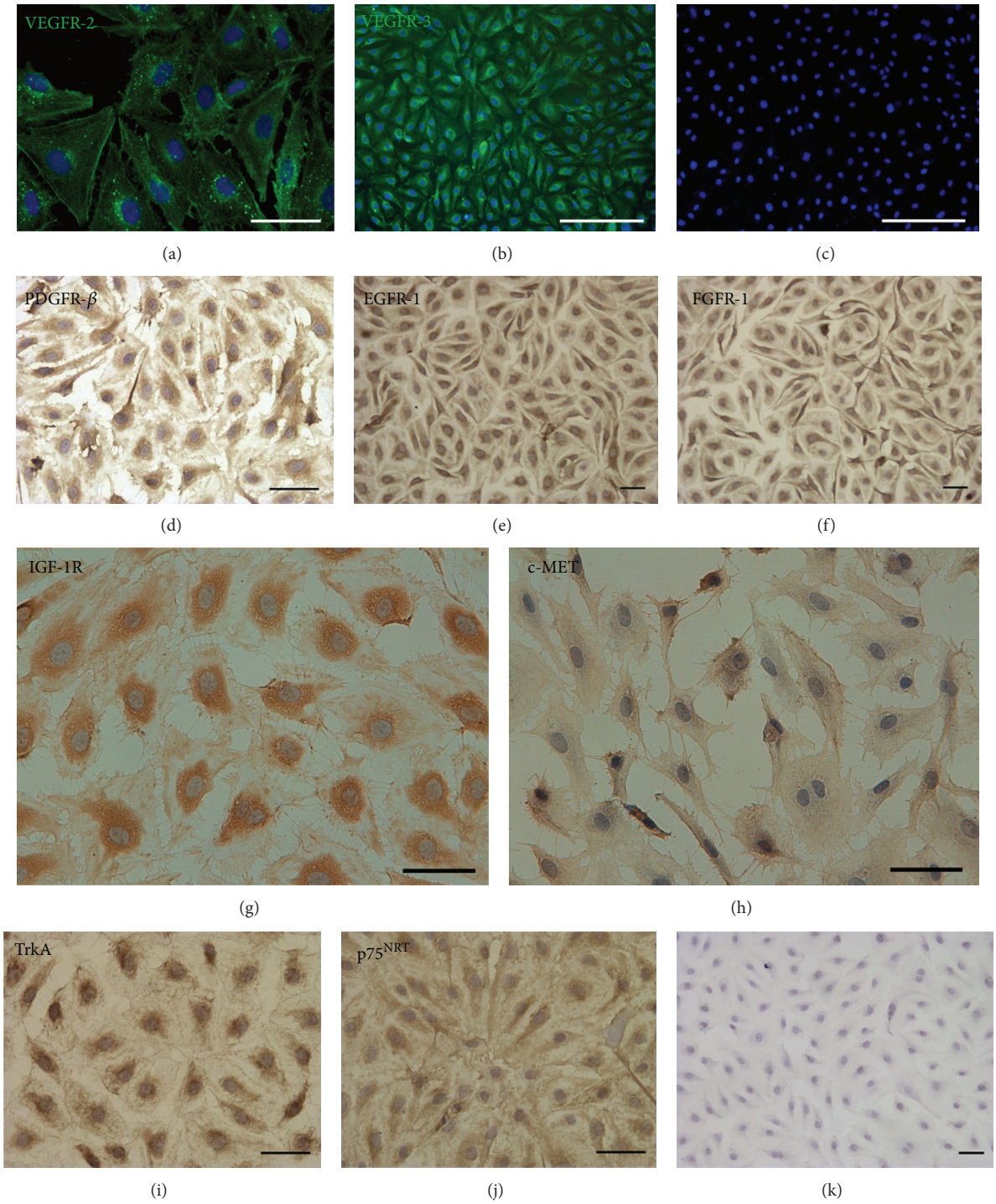

Figure 4: Detection of Receptor Tyrosine Kinases on HL-LECs (P4). (a) and (b) (immunofluorescence): green fluorescence corresponds to the surface expression of vascular endothelial growth factor receptor- (VEGFR-) 2 and VEGFR-3, respectively, in cultured HL-LECs. (c): representative image of a negative control in which the primary antibody was omitted from the reaction. Nuclei are shown by the blue fluorescence of DAPI. (d)–(j) (immunoperoxidase): the brownish precipitate on the surface of HL-LECs on each panel corresponds respectively to the expression of Platelet-Derived Growth Factor Receptor- (PDGFR-) beta, Epidermal Growth Factor Receptor- (EGFR-) 1, Fibroblast Growth Factor Receptor- (FGFR-) 1, type 1 Insulin-like Growth Factor Receptor (IGF-1R), the Hepatocyte Growth Factor receptor c-MET, Tropomyosin-related kinases A (TrkA), and neurotrophin p75 receptor ($p75^{NTR}$). (k): representative image of a negative control in which the primary antibody was omitted from the reaction. Nuclei are counterstained with Haematoxylin. Scale bars: (a), (d), (e), (f), (g), (h), (i), (j), and (k) = 50 μm; (b) and (c) = 250 μm.

Specifically, pulmonary lymphatic vessels are required for efficient respiration, mainly attributable to alveolar clearance in which their essential contribution has been established. Lymphatics have been also implicated in the pathogenesis of idiopathic pulmonary fibrosis, lymphangioleiomyomatosis and metastatic cancer, representing a potential novel approach to develop effective target therapies of severe lung diseases [1, 13, 17, 20].

The endothelium forms the inner cellular lining of blood and lymphatic vessels. Endothelial cell phenotypes are differentially regulated in space and time, giving rise to the phenomenon of "EC heterogeneity" implying that each vascular bed has unique structural and functional properties [49].

Cell culture models may be crucial to study the pathophysiologic role of the lung microvascular endothelium. Most of our knowledge is derived from studies on cultured human umbilical cord vein endothelial cells (HUVECs) due to their accessibility and reproducible isolation, but do not represent a model of the adult human microcirculation. Most studies have been successful in the identification and purification of blood endothelial cells from lung microcirculation. In addition, methodologies as automated cell sorting are costly, time consuming and not easily accessible to every laboratory. Moreover, only recently, lymphatic endothelial cell lines have been produced and although expensive are commercially available.

Therefore, our laboratory developed a protocol, for the routine and large scale in-house use, to harvest, isolate and expand human lung lymphatic endothelial cells.

We believe that several steps were critical to the success and effectiveness of our procedure to obtain a pure population of lymphatic endothelial cells from human lung microcirculation.

First, the fast (within one hour) processing of biological material immediately after resection ensured the preservation of cell viability and biological properties. Furthermore, daily observation of endothelial cell morphology and growth was crucial to determine the optimal time for bead separation and to avoid overgrowth of unwanted cells. Finally, cell sorting using markers such as CD31 and Pdn that are undoubtedly, abundantly, and specifically expressed by lymphatic endothelial cells both *in vivo* and *in vitro* allowed reproducible and efficient results in the isolation of HL-LEC. The immunocytochemical detection of cell surface markers confirmed that isolated cells were of lymphatic origin. These phenotypic characteristics were confirmed by flow cytometry.

The absence of α-smooth muscle actin was important to rule out contaminating cells in cultures immediately after the double selection for CD31 and Pdn. These data were further strengthened by the presence of lymphatic endothelium-specific markers such as Lyve-1 and Prox-1.

We also documented that our harvested and expanded HL-LEC are functionally competent. Indeed, when plated on a reconstituted basement membrane matrix, HL-LEC rapidly attached, aligned, and formed capillary-like tubules, mimicking lymphangiogenesis. Lymphangiogenesis is the formation of new lymphatic vessels from preexisting ones, an important biological process associated with diverse pathologic states. This assay is easy and cost-effective, and implies that HL-LECs are able to activate signaling pathways involved in cell adhesion, migration and protease activity ultimately leading to tubule-like microvessel formation.

To obtain insights on lymphatic endothelial cell biology, we determined whether our preparations of HL-LEC express relevant receptor tyrosine kinases (RTKs).

RTKs are central players in signal transduction networks and ligand binding activates the intrinsic protein tyrosine kinase domain triggering the intracellular signaling cascade.

We documented that virtually all HL-LECs, *in vitro*, retain the expression of VEGFR-2, VEGFR-3, EGFR-1, FGFR-1, c-Met, IGF-R1, PDGFR-beta, TrkA, and $p75^{NRT}$. In addition to their implication in cell survival, proliferation, migration, and lympho-angiogenesis, RTKs have become the most studied class of drug target by the pharmaceutical industry.

5. Conclusion

We have been able to reproducibly isolate human lung lymphatic endothelial cells from healthy pulmonary tissue by double magnetic cell sorting using a combination of commercially available antibodies. The few unsuccessful attempts occurred during the initial application of our procedures and were mainly attributable to setting the time of tissue digestion and microbial contamination. Full characterization of HL-LECs confirmed the high levels of purity and successful cultures yield large number of cells that could be expanded for several passages and cryopreserved being viable for further studies.

HL-LEC may represent an important tool for *in vitro* studies on lymphatic biology, lympho-angiogenesis, wound healing, inflammation, anti-cancer therapy, and interaction with microbial agents. Our report suggests a purification strategy to isolate BECs and LECs that can be applied to other human tissues. We believe that organ- and patient-specific endothelial cells are essential to elucidate signalling pathways involved in the pathogenetic mechanisms of lung diseases and to provide novel approaches to reach the goal of a true personalized therapy.

Conflict of Interests

The authors declare that there is no conflict of interests regarding the publication of this paper.

Authors' Contribution

Bruno Lorusso and Federico Quaini designed the study and wrote the paper. Angela Falco, Denise Madeddu, Caterina Frati, Gallia Graiani, Andrea Gervasi, Laura Rinaldi, and Davide Maselli acquired and analyzed the data. Letizia Gnetti and Enrico M. Silini are responsible for morphologic and histopathologic analysis. Eugenio Quaini, Luca Ampollini, and Paolo Carbognani are responsible for selection and

enrollment of patients and surgical procedures. Stefano Cavalli and Costanza Lagrasta critically revised the paper prior to submission.

Acknowledgments

The authors wish to thank Gabriella Becchi (Department of Biomedical, Biotechnological and Translational Sciences, University-Hospital of Parma, Italy), Emilia Corradini (Department of Biomedical, Biotechnological and Translational Sciences-University-Hospital of Parma, Italy), and Sabrina Bonomini (Department of Clinical and Experimental Medicine, University-Hospital of Parma, Italy) for technical assistance. This work was supported in part by a local grant to FQ from funding of the University of Parma.

References

[1] G. Oliver and M. Detmar, "The rediscovery of the lymphatic system: old and new insights into the development and biological function of the lymphatic vasculature," *Genes & Development*, vol. 16, no. 7, pp. 773–783, 2002.

[2] G. Oliver, "Lymphatic vasculature development," *Nature Reviews Immunology*, vol. 4, no. 1, pp. 35–45, 2004.

[3] G. Oliver and K. Alitalo, "The lymphatic vasculature: recent progress and paradigms," *Annual Review of Cell and Developmental Biology*, vol. 21, pp. 457–483, 2005.

[4] T. Tammela and K. Alitalo, "Lymphangiogenesis: molecular mechanisms and future promise," *Cell*, vol. 140, no. 4, pp. 460–476, 2010.

[5] Z. Jakus, J. P. Gleghorn, D. R. Enis et al., "Lymphatic function is required prenatally for lung inflation at birth," *Journal of Experimental Medicine*, vol. 211, no. 5, pp. 815–826, 2014.

[6] S. Banerji, J. Ni, S.-X. Wang et al., "LYVE-1, a new homologue of the CD44 glycoprotein, is a lymph-specific receptor for hyaluronan," *Journal of Cell Biology*, vol. 144, no. 4, pp. 789–801, 1999.

[7] J. T. Wigle, N. Harvey, M. Detmar et al., "An essential role for *Prox1* in the induction of the lymphatic endothelial cell phenotype," *The EMBO Journal*, vol. 21, no. 7, pp. 1505–1513, 2002.

[8] S. Breiteneder-Geleff, A. Soleiman, H. Kowalski et al., "Angiosarcomas express mixed endothelial phenotypes of blood and lymphatic capillaries: podoplanin as a specific marker for lymphatic endothelium," *The American Journal of Pathology*, vol. 154, no. 2, pp. 385–394, 1999.

[9] A. Kaipainen, J. Korhonen, T. Mustonen et al., "Expression of the fms-like tyrosine kinase 4 gene becomes restricted to lymphatic endothelium during development," *Proceedings of the National Academy of Sciences of the United States of America*, vol. 92, no. 8, pp. 3566–3570, 1995.

[10] N. Ferrara, H.-P. Gerber, and J. LeCouter, "The biology of VEGF and its receptors," *Nature Medicine*, vol. 9, no. 6, pp. 669–676, 2003.

[11] M. H. Witte, M. J. Bernas, C. P. Martin, and C. L. Witte, "Lymphangiogenesis and lymphangiodysplasia: from molecular to clinical lymphology," *Microscopy Research and Technique*, vol. 55, no. 2, pp. 122–145, 2001.

[12] T. Bartholin, *Vasa Lymphatica in Homine Nuper Inventa*, Hafniae Paulli, Copenhagen, Denmark, 1654.

[13] F. Sozio, A. Rossi, E. Weber et al., "Morphometric analysis of intralobular, interlobular and pleural lymphatics in normal human lung," *Journal of Anatomy*, vol. 220, no. 4, pp. 396–404, 2012.

[14] M. Kambouchner and J.-F. Bernaudin, "Intralobular pulmonary lymphatic distribution in normal human lung using D2-40 antipodoplanin immunostaining," *Journal of Histochemistry and Cytochemistry*, vol. 57, no. 7, pp. 643–648, 2009.

[15] D. E. Schraufnagel, "Lung lymphatic anatomy and correlates," *Pathophysiology*, vol. 17, no. 4, pp. 337–343, 2010.

[16] M. P. Pusztaszeri, W. Seelentag, and F. T. Bosman, "Immunohistochemical expression of endothelial markers CD31, CD34, von Willebrand factor, and Fli-1 in normal human tissues," *Journal of Histochemistry and Cytochemistry*, vol. 54, no. 4, pp. 385–395, 2006.

[17] S. El-Chemaly, S. J. Levine, and J. Moss, "Lymphatics in lung disease," *Annals of the New York Academy of Sciences*, vol. 1131, pp. 195–202, 2008.

[18] M. Yamashita, N. Iwama, F. Date et al., "Characterization of lymphangiogenesis in various stages of idiopathic diffuse alveolar damage," *Human Pathology*, vol. 40, no. 4, pp. 542–551, 2009.

[19] R. V. Mandal, E. J. Mark, and R. L. Kradin, "Organizing pneumonia and pulmonary lymphatic architecture in diffuse alveolar damage," *Human Pathology*, vol. 39, no. 8, pp. 1234–1238, 2008.

[20] C. G. Glasgow, S. El-Chemaly, and J. Moss, "Lymphatics in lymphangioleiomyomatosis and idiopathic pulmonary fibrosis," *European Respiratory Review*, vol. 21, no. 125, pp. 196–206, 2012.

[21] S. El-Chemaly, D. Malide, E. Zudaire et al., "Abnormal lymphangiogenesis in idiopathic pulmonary fibrosis with insights into cellular and molecular mechanisms," *Proceedings of the National Academy of Sciences of the United States of America*, vol. 106, no. 10, pp. 3958–3963, 2009.

[22] Y. Zeng, K. Opeskin, J. Goad, and E. D. Williams, "Tumor-induced activation of lymphatic endothelial cells via vascular endothelial growth factor receptor-2 is critical for prostate cancer lymphatic metastasis," *Cancer Research*, vol. 66, no. 19, pp. 9566–9575, 2006.

[23] S. Norgall, M. Papoutsi, J. Rössler, L. Schweigerer, J. Wilting, and H. A. Weich, "Elevated expression of VEGFR-3 in lymphatic endothelial cells from lymphangiomas," *BMC Cancer*, vol. 7, article 105, 2007.

[24] E. Garrafa, L. Trainini, A. Benetti et al., "Isolation, purification, and heterogeneity of human lymphatic endothelial cells from different tissues," *Lymphology*, vol. 38, no. 4, pp. 159–166, 2005.

[25] S. Fiorentini, A. Luganini, V. Dell'Oste et al., "Human cytomegalovirus productively infects lymphatic endothelial cells and induces a secretome that promotes angiogenesis and lymphangiogenesis through interleukin-6 and granulocyte-macrophage colony-stimulating factor," *Journal of General Virology*, vol. 92, no. 3, pp. 650–660, 2011.

[26] J. D. Catravas, C. Snead, C. Dimitropoulou et al., "Harvesting, identification and barrier function of human lung microvascular endothelial cells," *Vascular Pharmacology*, vol. 52, no. 5-6, pp. 175–181, 2010.

[27] S. A. A. Comhair, W. Xu, L. Mavrakis, M. A. Aldred, K. Asosingh, and S. C. Erzurum, "Human primary lung endothelial cells in culture," *American Journal of Respiratory Cell and Molecular Biology*, vol. 46, no. 6, pp. 723–730, 2012.

[28] N. Fujino, H. Kubo, C. Ota et al., "A novel method for isolating individual cellular components from the adult human distal

lung," *The American Journal of Respiratory Cell and Molecular Biology*, vol. 46, no. 4, pp. 422–430, 2012.

[29] M. L. Fehrenbach, G. Cao, J. T. Williams, J. M. Finklestein, and H. M. DeLisser, "Isolation of murine lung endothelial cells," *The American Journal of Physiology—Lung Cellular and Molecular Physiology*, vol. 296, no. 6, pp. L1096–L1103, 2009.

[30] L. S. Mackay, S. Dodd, I. G. Dougall et al., "Isolation and characterisation of human pulmonary microvascular endothelial cells from patients with severe emphysema," *Respiratory Research*, vol. 14, article 23, 2013.

[31] I. Arnaoutova, J. George, H. K. Kleinman, and G. Benton, "The endothelial cell tube formation assay on basement membrane turns 20: state of the science and the art," *Angiogenesis*, vol. 12, no. 3, pp. 267–274, 2009.

[32] E. R. Weibel and G. E. Palade, "New cytoplasmic components in arterial endothelia," *The Journal of Cell Biology*, vol. 23, pp. 101–112, 1964.

[33] E. Sölder, B. C. Böckle, V. A. Nguyen et al., "Isolation and characterization of CD133+ CD34+ VEGFR-2+ CD45− fetal endothelial cells from human term placenta," *Microvascular Research*, vol. 84, no. 1, pp. 65–73, 2012.

[34] A. Woodfin, M.-B. Voisin, and S. Nourshargh, "PECAM-1: a multi-functional molecule in inflammation and vascular biology," *Arteriosclerosis, Thrombosis, and Vascular Biology*, vol. 27, no. 12, pp. 2514–2523, 2007.

[35] P. Baluk, J. Fuxe, H. Hashizume et al., "Functionally specialized junctions between endothelial cells of lymphatic vessels," *Journal of Experimental Medicine*, vol. 204, no. 10, pp. 2349–2362, 2007.

[36] M. A. Lemmon and J. Schlessinger, "Cell signaling by receptor tyrosine kinases," *Cell*, vol. 141, no. 7, pp. 1117–1134, 2010.

[37] K. Alitalo, T. Tammela, and T. V. Petrova, "Lymphangiogenesis in development and human disease," *Nature*, vol. 438, no. 7070, pp. 946–953, 2005.

[38] R. S. Herbst, J. V. Heymach, and S. M. Lippman, "Molecular origins of cancer: lung cancer," *New England Journal of Medicine*, vol. 359, no. 13, pp. 1367–1380, 2008.

[39] G. Liang, Z. Liu, J. Wu, Y. Cai, and X. Li, "Anticancer molecules targeting fibroblast growth factor receptors," *Trends in Pharmacological Sciences*, vol. 33, no. 10, pp. 531–541, 2012.

[40] M. M. Chitnis, J. S. P. Yuen, A. S. Protheroe, M. Pollak, and V. M. Macaulay, "The type 1 insulin-like growth factor receptor pathway," *Clinical Cancer Research*, vol. 14, no. 20, pp. 6364–6370, 2008.

[41] J. S. de Bono and T. A. Yap, "c-MET: an exciting new target for anticancer therapy," *Therapeutic Advances in Medical Oncology*, vol. 3, no. 1, supplement, pp. S3–S5, 2011.

[42] Y. Feng, P. S. Thiagarajan, and P. C. Ma, "MET signaling: novel targeted inhibition and its clinical development in lung cancer," *Journal of Thoracic Oncology*, vol. 7, no. 2, pp. 459–467, 2012.

[43] R. Cao, M. A. Björndahl, P. Religa et al., "PDGF-BB induces intratumoral lymphangiogenesis and promotes lymphatic metastasis," *Cancer Cell*, vol. 6, no. 4, pp. 333–345, 2004.

[44] R. Romon, E. Adriaenssens, C. Lagadec, E. Germain, H. Hondermarck, and X. Le Bourhis, "Nerve growth factor promotes breast cancer angiogenesis by activating multiple pathways," *Molecular Cancer*, vol. 9, article 157, 2010.

[45] K. Nakamura, F. Tan, Z. Li, and C. J. Thiele, "NGF activation of TrkA induces vascular endothelial growth factor expression via induction of hypoxia-inducible factor-1α," *Molecular and Cellular Neuroscience*, vol. 46, no. 2, pp. 498–506, 2011.

[46] G. Graiani, C. Emanueli, E. Desortes et al., "Nerve growth factor promotes reparative angiogenesis and inhibits endothelial apoptosis in cutaneous wounds of type 1 diabetic mice," *Diabetologia*, vol. 47, no. 6, pp. 1047–1054, 2004.

[47] A. Caporali, E. Pani, A. J. G. Horrevoets et al., "Neurotrophin p75 receptor ($p75^{NTR}$) promotes endothelial cell apoptosis and inhibits angiogenesis: implications for diabetes-induced impaired neovascularization in ischemic limb muscles," *Circulation Research*, vol. 103, no. 2, pp. e15–e26, 2008.

[48] H. K. Kleinman and G. R. Martin, "Matrigel: basement membrane matrix with biological activity," *Seminars in Cancer Biology*, vol. 15, no. 5, pp. 378–386, 2005.

[49] W. C. Aird, "Endothelial cell heterogeneity," *Cold Spring Harbor Perspectives in Medicine*, vol. 2, no. 1, Article ID a006429, 2012.

Hindawi Publishing Corporation
BioMed Research International
Volume 2015, Article ID 968927, 9 pages
http://dx.doi.org/10.1155/2015/968927

Research Article

Epoetin Alpha and Epoetin Zeta: A Comparative Study on Stimulation of Angiogenesis and Wound Repair in an Experimental Model of Burn Injury

Natasha Irrera,[1] Alessandra Bitto,[1] Gabriele Pizzino,[1] Mario Vaccaro,[1] Francesco Squadrito,[1] Mariarosaria Galeano,[2] Francesco Stagno d'Alcontres,[2] Ferdinando Stagno d'Alcontres,[2] Michele Buemi,[1] Letteria Minutoli,[1] Michele Rosario Colonna,[2] and Domenica Altavilla[3]

[1]*Department of Clinical and Experimental Medicine, University of Messina, 98125 Messina, Italy*
[2]*Department of Dentistry and Medical and Surgical Experimental Sciences, University of Messina, 98125 Messina, Italy*
[3]*Department of Paediatric, Gynaecological, Microbiological and Biomedical Sciences, University of Messina, 98125 Messina, Italy*

Correspondence should be addressed to Francesco Squadrito; fsquadrito@unime.it

Received 19 December 2014; Revised 2 April 2015; Accepted 15 April 2015

Academic Editor: Themis R. Kyriakides

Deep second-degree burns are characterized by delayed formation of granulation tissue and impaired angiogenesis. Erythropoietin (EPO) is able to stimulate angiogenesis and mitosis, activating vascularization and cell cycle. The aim of our study was to investigate whether two biosimilar recombinant human erythropoietins, EPO-α and EPO-Z, may promote these processes in an experimental model of burn injury. A total of 84 mice were used and a scald burn was produced on the back after shaving, in 80°C water for 10 seconds. Mice were then randomized to receive EPO-α (400 units/kg/day/sc) or EPO-Z (400 units/kg/day/sc) or their vehicle (100 μL/day/sc 0.9% NaCl solution). After 12 days, both EPO-α and EPO-Z increased VEGF protein expression. EPO-α caused an increased cyclin D1/CDK6 and cyclin E/CDK2 expression compared with vehicle and EPO-Z ($p < 0.001$). Our study showed that EPO-α and EPO-Z accelerated wound closure and angiogenesis; however EPO-α resulted more effectively in achieving complete skin regeneration. Our data suggest that EPO-α and EPO-Z are not biosimilars for the wound healing effects. The higher efficacy of EPO-α might be likely due to its different conformational structure leading to a more efficient cell proliferation and skin remodelling.

1. Introduction

Erythropoietin (EPO) is a renal glycoprotein hormone that regulates red blood cell production by inhibiting apoptosis of erythroid precursor cells, but it is also involved in the mechanisms of proliferation and differentiation in hematopoietic tissues [1, 2]. EPO acts through its specific cytokine receptor, the erythropoietin receptor (EPOR), allocated on cell surface [3, 4] of many different haematopoietic and nonhaematopoietic tissues and cells [5]. EPOR has been identified on neurons, astrocytes, microglia, endothelial cells, macrophages, fibroblasts, keratinocytes, mast cells, melanocytes, liver, and uterus. When activated, the receptor promotes the Janus Kinase (JAK)/Signal Transducer and Activator of Transcription (STAT) pathway, stimulating mitosis and differentiation in all these cell lines [6, 7].

Several studies have suggested that EPO may be involved in the regulation of physiological wound healing process. It has been demonstrated that locally erythropoietin administration into subcutaneous fibrin chambers was able to promote the formation of wound granulation tissue in a rat model of wound healing [8]. This effect was ascribed to the stimulation of physiological angiogenesis and upregulation of iNOS expression in skin.

Furthermore, additional studies have shown that EPO may interact with vascular endothelial cells and vascular

endothelial growth factor (VEGF), involved in the angiogenic process, thus stimulating cellular motility and mitosis in endothelium and leading to the formation of new capillaries [9, 10]. These experimental evidences prompted the use of EPO in improving impaired wound healing; as a matter of fact our group already demonstrated the efficacy of recombinant EPO in ameliorating skin repair during diabetes and burn injury [11, 12].

Recombinant human erythropoietin (rHuEPO) has been largely used in the clinical setting and new formulations have been synthesized, such as Epoetin alpha (EPO-α) and Epoetin Z (EPO-Z) [13–15]. EPO-α was the first generation recombinant erythropoietin with the same amino acid sequence as human erythropoietin and it exerts the maximum therapeutic effect when administered subcutaneously [16]. EPO-Z is a new generation biosimilar with the same amino acid sequence of EPO-α and overlapping carbohydrate composition; it may be used as an alternative choice for the treatment of patients with end-stage renal diseases and anemia. EPO-Z was developed and registered in agreement with the European Medicines Agency (EMEA) guidelines. The regulatory approval of EPO-Z is based both on extensive physicochemical/molecular, preclinical, and clinical characterization studies and on a comprehensive postmarketing surveillance program, as required for all European "biosimilars."

However, biosimilars may have some differences in the materials used for their preparation and may show variability in manufacturing processes, and, in addition, the active form may differ with regard to the size and the complexity of the structure [17]. The biotechnological techniques used for the preparation of the compounds make the molecules more heterogeneous, and this is the result of changes in structure such as glycosylation and/or alterations in amino acid sequence. These variations are often responsible for immune effects [18–20].

Since the new EPO-Z has never been tested for its skin repair effects, the purpose of our study was to investigate whether EPO-α and EPO-Z may display overlapping specific action in an experimental model of burn injury.

2. Materials and Methods

2.1. Animals and Experimental Burn Model. The protocol was evaluated and accepted by the Ethics Committee of the University of Messina and all animal procedures were carried out according to Guide for the Care and Use of Laboratory Animals. A total of 84 male C57BL/6 mice weighing 20–22 g were used in this study and were purchased by Charles River Italy (Calco, Italy). Animals were housed and maintained under controlled environmental conditions (12 h light/dark cycle, temperature approximately 23°C) and provided with standard laboratory food and water *ad libitum*. Skin injury was performed on the shaved back of mice: after general anaesthesia with sodium pentobarbital (80 mg/kg/i.p.), hair on the back was shaved using a depilatory cream to reduce any possible injury due to hair removal. Burn injury was produced with 80°C water, and mice were immersed for 10 seconds with a burn template so that the dorsum was exposed to hot water through a 2 × 3 cm window. In this way, we produced a deep-dermal second-degree burn; post-burn sedation and analgesia were provided with diazepam (50 mg/L added to drinking water) for 7 days to alleviate pain. Following thermal injury, animals were divided into 3 groups and randomized to receive EPO-α (400 I.U./kg/day in 100 μL 0.9% NaCl subcutaneously), EPO-Z (400 I.U./kg/day in 100 μL 0.9% NaCl subcutaneously), or vehicle (100 μL/day 0.9% NaCl subcutaneously). The dose chosen in this study has been previously shown effective for EPO-α in previous studies for the treatment of wound healing [11, 12]. Neither lower dose regimens nor different schedule treatments showed beneficial effects in preliminary experiments (results not shown). At 3, 6, and 12 days 7 animals per group were sacrificed and the remaining 7 animals from each group were observed and treated to assess the time to final wound closure. At the time of sacrifice blood was collected by cardiac puncture, and burn areas were excised and used for histological and molecular analysis.

2.2. Erythrocyte Count and Haemoglobin Level. Number of erythrocytes and haemoglobin (Hb) level were evaluated from blood samples at 12 days after burn injury. Red blood cell count was carried out on stained smears according to the standard morphologic criteria for mouse [11, 12].

2.3. Western Blot Determination of VEGF, Cyclin D1, CDK6, Cyclin E, CDK2, p15, and p27. Skin samples were homogenized in lysis buffer (1% Triton X100, 20 mM Tris/HCl, pH 8.0, 137 mM NaCl, 10% glycerol, 5 mM EDTA, 1 mM phenylmethylsulfonyl fluoride, 1% aprotinin, and 15 μg/mL leupeptin). Protein samples (30 μg) were denatured in a reducing buffer (62 mmol/L Tris pH 6.8, 10% glycerol, 2% SDS, 5% β-mercaptoethanol, and 0.003% bromophenol blue) and separated by electrophoresis on a sodium dodecyl sulphate (SDS) polyacrylamide gel (10% or 12%). The separated proteins were transferred onto a PVDF membrane using a transfer buffer (39 mmol/L glycine, 48 mmol/L Tris, and pH 8.3, 20% methanol) at 100 V for 1 hour. The membranes were stained with Ponceau S (0.005% in 1% acetic acid) to confirm blotting, blocked with 5% nonfat dry milk in TBS-0.1% Tween for 1 hour at room temperature, washed 3 times for 10 minutes each in TBS-0.1% Tween, and then incubated with a primary antibody for cyclin D1, CDK6, cyclin E, CDK2, p15, or p27 (Cell Signaling, Beverly, MA) and VEGF (Abcam, Cambridge, UK) in TBS-0.1% Tween overnight at 4°C. The day after, antibody was removed by washing the membranes 3 times for 10 minutes each in TBS-0.1% Tween. Membranes were incubated with a secondary antibody peroxidase-conjugated (Pierce, Rockford, IL) for 1 hour at room temperature. After washing, the membranes were analyzed by the enhanced chemiluminescence system according to the manufacturer's protocol (Amersham, Little Chalfont, UK). The VEGF, cyclin D1, CDK6, cyclin E, CDK2, p15, and p27 protein signals were quantified by scanning densitometry using a bioimage analysis system (Bio-Profil Celbio, Milan, Italy). Equal loading of protein was assessed on stripped blots by β-actin staining with a rabbit monoclonal antibody (Cell Signaling, Beverly, MA).

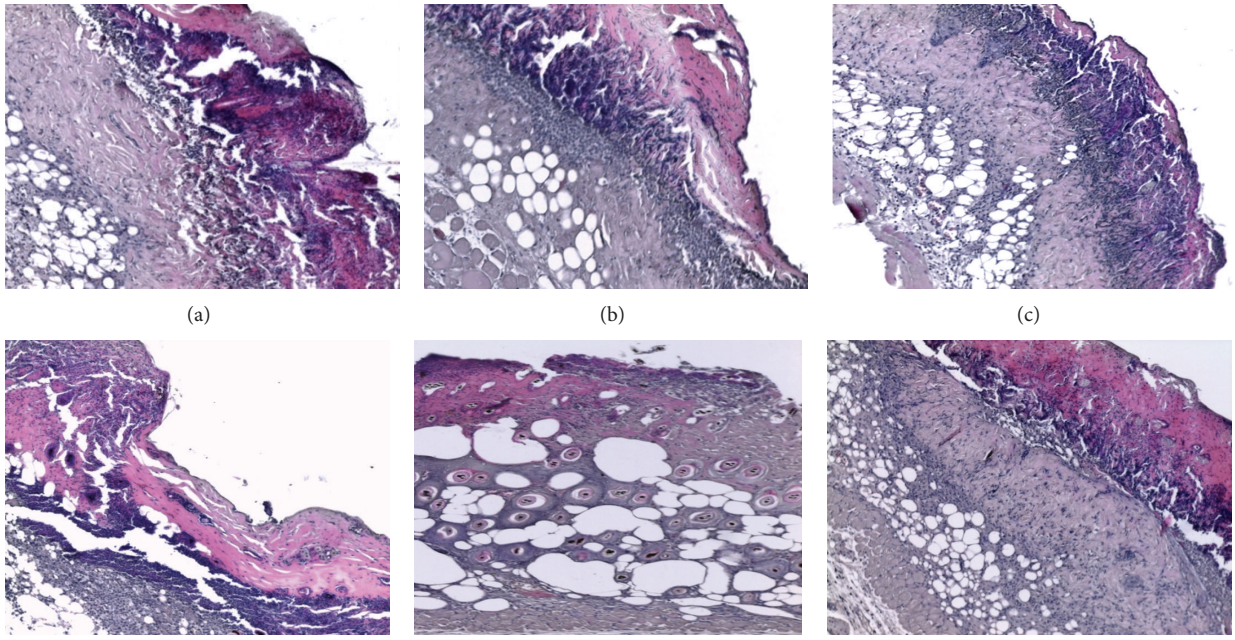

Figure 1: H&E stained sections of burned skin at days 3 and 6 examined under light microscopy. The untreated group (a) as well as groups treated with EPO-α (b) and EPO-Z (c) show extensive skin defects, necrosis and inflammatory cells in the subcutaneous layer, and absence of hair follicles and skin glands. At day 6 the untreated group (d) shows the persistence of the crust and of necrotic and inflammatory areas; EPO-α treatment (e) promotes the reduction of the inflammatory infiltrate, partial restoration of the dermal structure with the presence of hair follicles and sweat glands; EPO-Z treated skin (f) shows the presence of a partial regeneration behind the crust, with some areas of necrosis and inflammatory cells infiltration.

2.4. Histologic Evaluation. Skin samples were removed from the animals of each experimental group and fixed in 10% buffered formalin at room temperature for at least 24 hours. Perpendicular sections to the anterior-posterior axis of the burn area were dehydrated in graded ethanol, cleared in xylene, and embedded in paraffin according to routine procedures. Five-micrometer-thick sections of paraffin-embedded tissues were mounted on glass slides, hydrated to distilled water, and then stained with hematoxylin and eosin. In particular, histological slides were examined at ×10 to ×20 magnification to observe morphologic alterations or improvements (i.e., presence or absence of reepithelialization, crusting, blistering, granulation tissue and collagen matrix organization, inflammation, congestion, and edema), as previously reported [11, 12]. Evaluations were obtained from a pathologist without knowledge of the treatments.

2.5. Immunohistochemistry for CD31. Paraffin-embedded tissues were sectioned (5 μm) and rehydrated, and antigen unmasking was performed by using 0.05 M sodium citrate buffer (pH 6.0). Specimens were treated with 3% hydrogen peroxide to block endogenous peroxides and with horse normal serum (Vector Laboratories, Burlingame, CA, USA) to avoid nonspecific staining. Slides were then incubated overnight at 4°C in a humid box with primary antibody to detect CD31 (Abcam, Cambridge, UK). The day after, sections were washed with PBS, a secondary antibody was used (Vector Laboratories), and the reaction was revealed adding a DAB solution (diaminobenzidine tetrahydrochloride, Sigma, Milan, Italy) for 1–3 minutes. Slides were counterstained with haematoxylin, dehydrated, mounted, and examined by a pathologist without knowledge of the treatments, by using masked slides from ×10 to ×40 magnification with a Leica (Leica Microsystems, Milan, Italy) microscope.

2.6. Statistical Analysis. All data are expressed as means ± S.D. Comparisons between different treatments were analysed by one-way ANOVA followed by Bonferroni's multiple-comparison test. The histological score analysis was carried out by two-way ANOVA followed by Bonferroni's multiple-comparison test. The possibility of error was set at $p < 0.05$ and it was considered statistically significant. Graphs were drawn using GraphPad Prism (version 5.0 for Windows).

3. Results and Discussion

3.1. Erythrocyte Count and Blood Hb. Since EPO is effective in stimulating the erythroid lineage, we evaluated the number of red cells and Hb in our experimental groups, to confirm that EPO-α and EPO-Z may promote the production of erythrocytes and haemoglobin. We have already observed in our previous studies that rHuEPO stimulates erythroid lineage [11, 12]. As expected, the administration of EPO-α and EPO-Z increased both the number of circulating erythrocytes

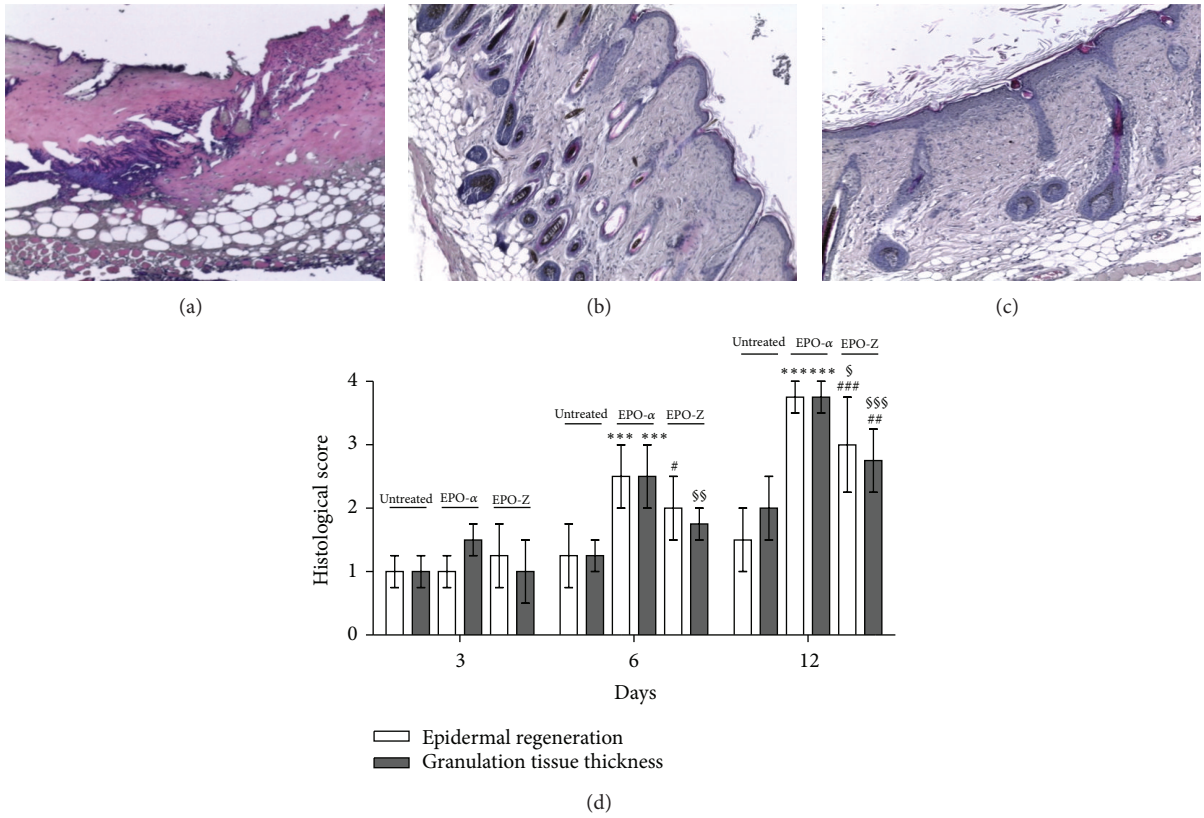

Figure 2: H&E stained sections of burned skin at day 12 observed under light microscopy. Skin of untreated animals (a) shows necrosis surrounded by a contraction of the *panniculus carnosus* as well as disorganized dermal-epidermal layers. Animals treated with EPO-α (b) demonstrate a well regenerated tissue with a keratin layer and reorganized subdermal structures. Animals treated with EPO-Z (c) show a still incomplete healing process characterized by a linear external layer with a low staining of hair keratin compared with the EPO-α treated group. The graph (d) represents the mean of epidermal regeneration and granulation tissue thickness at several time points in the studied animals. $^{***}p < 0.001$ versus untreated; $^{\#}p < 0.05$ versus untreated; $^{\#}p < 0.05$ versus untreated; $^{\#\#\#}p < 0.001$ versus untreated; $^{\S}p < 0.05$ versus EPO-Z; $^{\S\S}p < 0.01$ versus EPO-Z; $^{\S\S\S}p < 0.001$ versus EPO-Z. Significance between treatments is considered within the same day of observation.

and Hb at day 12 (data not shown). No difference was observed between the two compounds. Our results confirm that these two molecules equally stimulate erythroid lineage, as reported in clinical studies, and act as biosimilars [15].

3.2. Skin Repair. Wound healing is characterized not only by the stimulation of angiogenesis, but also by the formation and remodelling of matrix components and, in this setting, macrophages are responsible for the production of growth factors. Since EPOR is located on the surface of these cells, EPO may stimulate macrophages, and this mechanism of action explains the role of erythropoietin in the skin repair process [21].

Additionally, an in vitro study, evaluating the effects of EPO and EPO receptors in human hair follicles (HFs) [22], showed that also hair follicle cells synthesize EPO protein in situ and express EPO receptor. These structures are well-known not only for producing hair but also for their important contribution to tissue repair through reepithelialization, and both investigators and clinicians have noted for years that hair-bearing areas tend to heal more quickly than areas lacking follicles [23, 24]. Langton et al. [25] demonstrated that acute wound healing is delayed in absence of HFs. HFs-derived keratinocytes are responsible for reepithelization during wound healing [26], while HF dermal sheath cells are a key source of fibroblasts in response to wounding and have a role in replacing skin dermis [27].

In our study, at day 3, control group as well as groups treated with EPO-α and EPO-Z showed extensive skin defects, necrosis and inflammatory cells in the subcutaneous layer, and absence of hair follicles and skin glands. At day 6, the control group showed the persistence of the crust and of necrotic and inflammatory areas. The treatment with EPO-α promoted the reduction of the inflammatory infiltrate and determined partial restoration of the dermal structure with the presence of hair follicles and sweat glands; instead EPO-Z treated skin showed only the presence of a partial regeneration behind the crust, with some areas of necrosis and inflammatory cells infiltration (Figure 1).

At the end of experimental period (day 12), skin of control animals showed necrosis surrounded by a contraction of the *panniculus carnosus* as well as disorganized dermal-epidermal layers. We observed that animals treated with EPO-α demonstrated a well regenerated tissue with

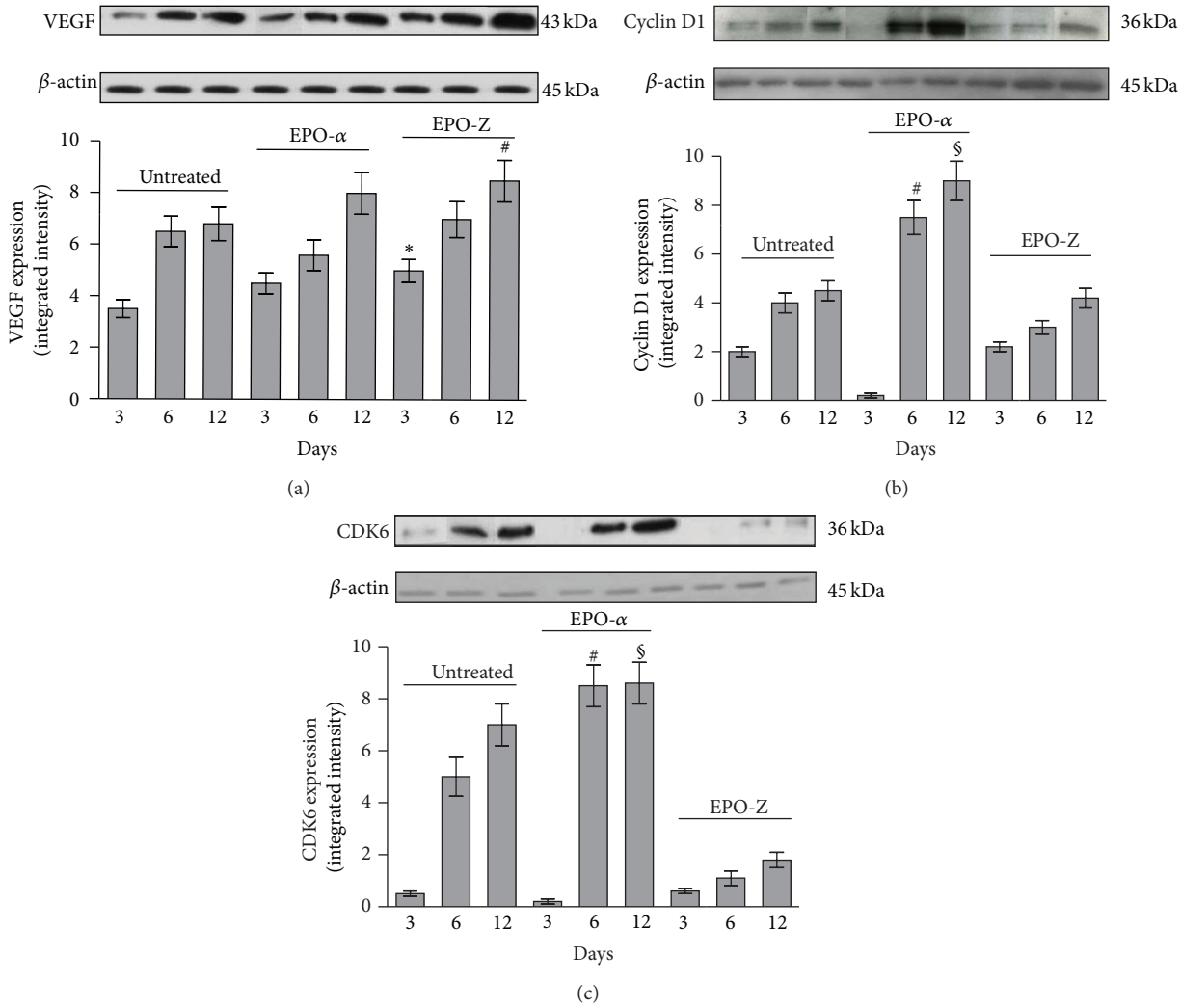

Figure 3: Effects of EPO-α and EPO-Z on VEGF (a) protein expression in skin tissue samples. EPO-α increases the expression of VEGF at all time points even if not significantly. The administration of EPO-Z significantly increases the expression of VEGF at both 3 and 12 days. $^{*}p < 0.01$ versus untreated; $^{\#}p < 0.01$ versus untreated. Effects of EPO-α and EPO-Z treatment on cyclin D1 (b) and CDK6 (c) proteins expression in skin tissue samples. $^{\#}p < 0.001$ versus untreated and EPO-Z, $^{\S}p < 0.001$ versus untreated and EPO-Z. Values are expressed as mean and SD for each group. Significance between treatments is considered within the same day of observation.

a keratin layer and reorganized subdermal structures. Animals treated with EPO-Z showed a still incomplete healing process compared with the EPO-α treated group (Figure 2).

Therefore, the use of EPO-α caused reduced inflammation, restored dermal layers, and accelerated complete healing with a "*restitutio ad integrum*" of skin structures, such as hair follicles. By contrast, EPO-Z did not determine a complete healing compared with EPO-α: tissue structures were organized, inflammation was reduced, and matrix components were visible but incompletely formed.

3.3. Angiogenesis: Expression of VEGF. A deep second-degree burn is characterized by the disruption and alteration of the whole epidermis; furthermore, the burned area shows a non-regenerating, mesenchyma-mediated wound healing, with delayed formation of granulation tissue, decreased deposition of collagen, and impaired angiogenesis. EPO can protect epidermis, dermis, and its vital structures, in particular capillaries and blood vessels, from further damage following burn injury [28]. In fact, it has been demonstrated that erythropoietin may also act on nonhaematopoietic tissues via the EPOR, stimulating tissue healing, particularly following injury [29, 30].

The angiogenic process is the result of the interaction of several factors and VEGF has a pivotal role in orchestrating wound healing, promoting endothelial cell proliferation from the very first moments. In a previous study we demonstrated that the synergism between VEGF and EPO promotes the angiogenic process, confirming the role of rHuEPO as a growth factor in an experimental model of wound healing [11].

In the present experiment we compared EPO-α and EPO-Z in the stimulation of angiogenesis. Physiologically, the healing of burn wounds causes an increase in VEGF

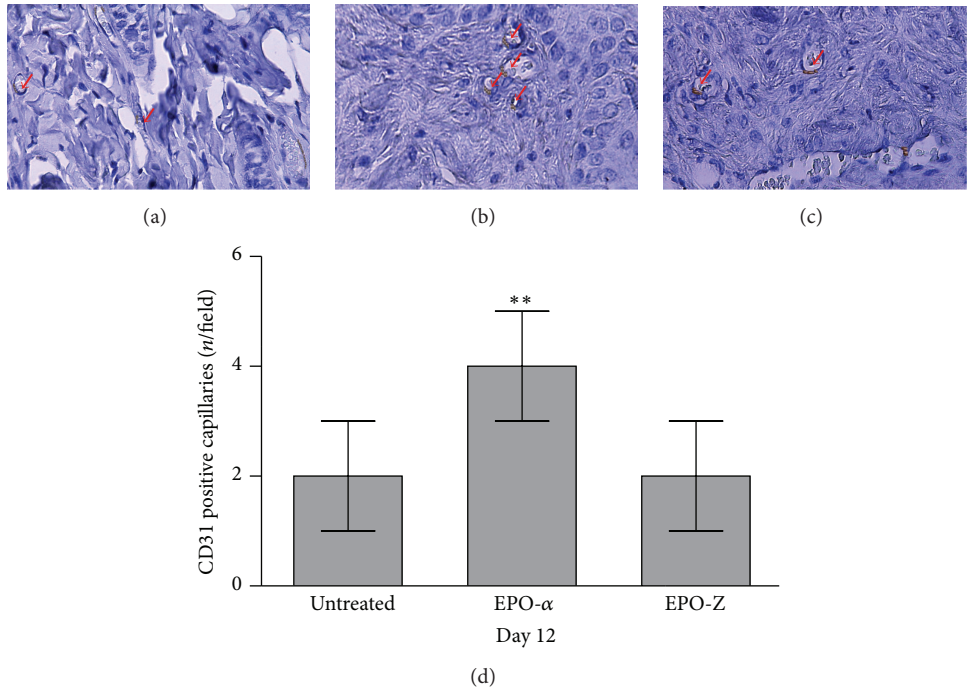

Figure 4: CD31 immunostaining of burned skin from mice untreated (a) or treated with EPO-α (b) or EPO-Z (c) at day 12. Arrows indicate staining positivity in small capillaries; administration of EPO-α stimulates neovessel formation, as shown in the graph, (d) more than EPO-Z ($^{**}p = 0.0017$ versus untreated and EPO-Z).

compared to normal conditions. For this reason, we studied VEGF expression in wounds at days 3, 6, and 12 after treatment. As shown in Figure 3, EPO-α and of EPO-Z stimulated VEGF expression at all time points, and EPO-Z stimulation was significant at days 3 and 12. The reason for this apparent discrepancy could be due to the fact that VEGF is not the only and one factor involved in new vessel formation, and indeed during impaired wound healing conditions the receptor of VEGF (VEGF-R2) and other growth mediators are downregulated. As a matter of fact, despite a lower increase in VEGF (as compared to EPO-Z), EPO-α caused a faster and more organized skin healing underlying that VEGF increase alone is not sufficient. To prove the efficacy of angiogenesis stimulation, besides VEGF synthesis, we investigated the newly formed capillaries through CD31 immunostaining which was investigated in skin samples at days 6 and 12. At day 6 no CD31 staining was observed in skin tissue (data not shown). As demonstrated in Figure 4, at day 12 untreated animals presented a positive staining (Figure 4(a)) and the administration of EPO-α further increased the staining in small capillaries, indicating a sustained angiogenesis (Figure 4(b)). EPO-Z did not improve neovascularisation at day 12, confirming the delayed healing observed with H&E staining (Figure 4(c)).

3.4. Regulation of Cell Cycle Machinery. The processes of (i) angiogenesis, (ii) matrix remodelling, and (iii) wound healing are promoted by activation of cell cycle and cell proliferation executed in a timely and orderly manner. The phases of cell cycle in mammalian cells are controlled by different types of cyclins. Cyclins, cyclins-dependent kinases (CDKs), and negative regulators, such as cyclin-dependent kinase inhibitors belonging to the p16 and p21 family, work together to regulate cell cycle progression. Cyclin D1 and cyclin E are fundamental in the activation of the G1 phase. Cyclin D1 and cyclin E increase is followed by a concomitant upregulation of CDK6 and CDK2 activity. Both complexes trigger progression of the G1 phase and entry into the S phase. Cell cycle negative regulators are divided into 2 families, the p21 family (p21, p27, and p57) and the p16 family (p15, p16, p18, and p19). Any alteration in the complex equilibrium between cyclin/CDK complexes and their negative regulators could be responsible for an impaired cell growth and, in turn, for a delayed tissue repair [31, 32].

It has been demonstrated that EPO gene expression is related to the upregulation of cyclins/CDK and the administration of EPO may promote DNA synthesis, as well as cell proliferation, and upregulates the expression of cyclins [33]. In agreement with this finding, it has also been shown that improvement of neovascularisation induced by EPO may be attributed to a direct effect mediated not only by VEGF, but also by endothelial cell proliferation [34].

In our experiment we tested not only EPO-α and EPO-Z for the same efficacy in promoting wound healing in experimental burn wounds but also whether these effects were dependent upon the activation of cyclins and cyclin-dependent kinases (CDKs). The cell cycle positive regulators were evaluated at days 3, 6, and 12 following burn injury. The burn wounds of mice treated with vehicle showed a moderate expression of cyclin D1 and CDK6 at days 3, 6, and 12

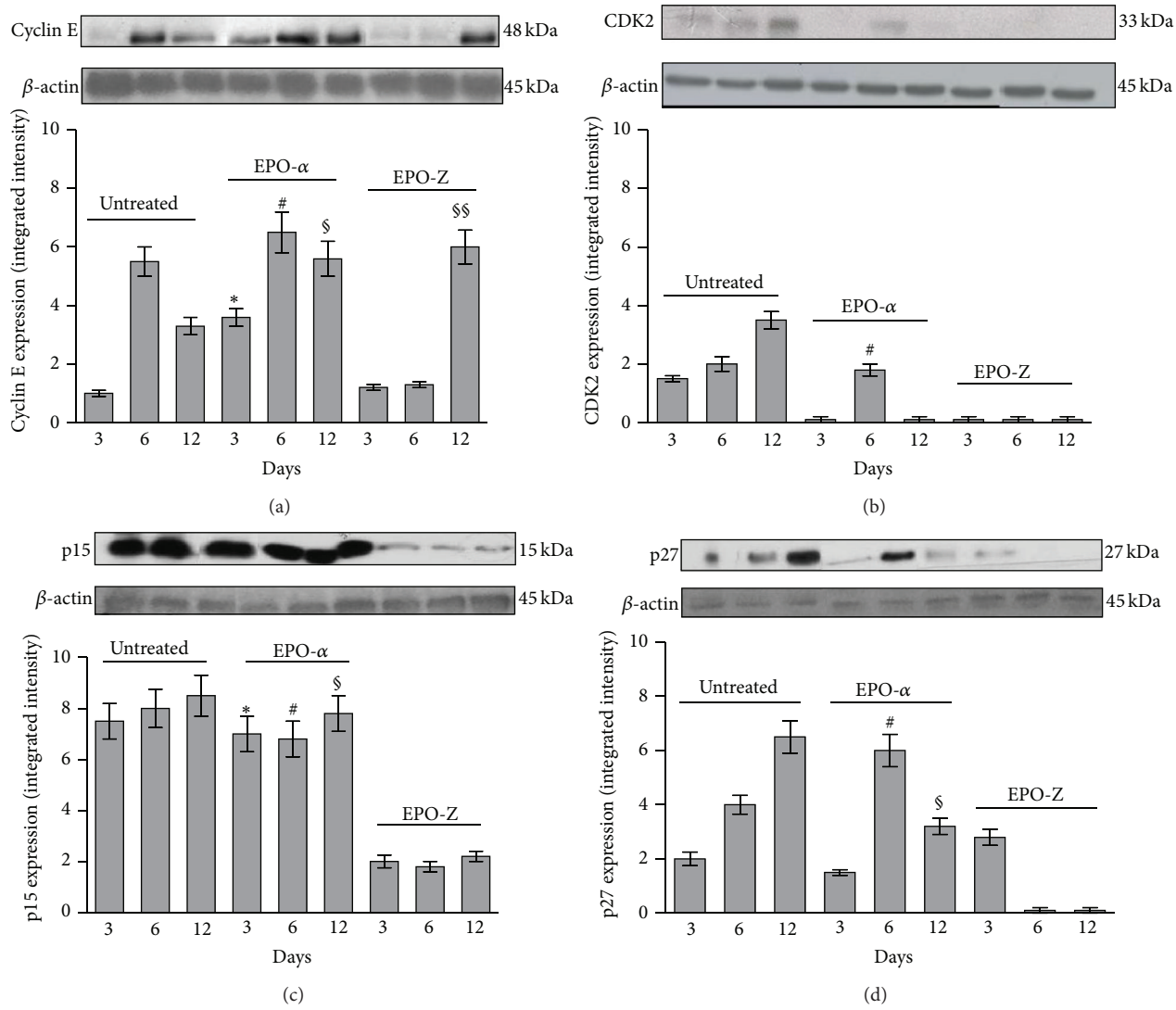

FIGURE 5: Effects of EPO-α and EPO-Z treatment on cyclin E (a) and CDK2 (b) protein expression in skin tissue samples. $^{*}p < 0.001$ versus untreated; $^{\#}p < 0.001$ versus EPO-Z; $^{\S}p < 0.001$ versus untreated and EPO-Z. Effects of EPO-α and EPO-Z treatment on p15 (c) and p27 (d) protein expression in skin tissue samples. $^{*}p < 0.001$ versus EPO-Z; $^{\#}p < 0.001$ versus EPO-Z; $^{\S}p < 0.001$ versus EPO-Z. Values are expressed as mean and SD for each group. Significance between treatments is considered within the same day of observation.

(Figures 3(b) and 3(c)). The administration of EPO-α significantly upregulated the expression of cyclin D1 at days 6 and 12 ($p < 0.001$) compared to the treatment with vehicle and EPO-Z (Figure 3; $p < 0.001$).

CDK6, the kinase responsible for the activation of cyclin D, showed a trend similar to its cyclin in wounds treated with vehicle (Figures 3(b) and 3(c)). The administration of EPO-α determined a significant increase in the expression of CDK6 at days 6 and 12 ($p < 0.001$). EPO-Z did not cause significant differences in the expression of CDK6.

The expression of cyclin E in skin of mice treated with vehicle increased only at day 6. The treatment with EPO-α significantly enhanced the expression of cyclin E at all time points; the administration of EPO-Z increased cyclin E expression only at day 12 (Figure 5(a)). CDK2 expression did not show any significant upregulation following the treatment with both EPO-α and EPO-Z compared to the animals treated only with vehicle (Figure 5(b)).

Interestingly, we observed an opposite situation for the expression of p15 protein: in fact, in this case, the treatment with EPO-Z reduced only the expression of the inhibitor p15 in a significant manner and at all time points, while EPO-Z did not modify the expression of the cyclins (Figure 5(c)). However, the only reduction in the expression of the inhibitor p15 is not sufficient to activate the cell cycle and accelerate the wound healing process following burn injury.

On the other hand, the treatment with EPO-α did not modify the expression of this inhibitor in a significant way.

The expression of p27 was increased at days 6 and 12 in burn mice treated with vehicle and EPO-α and only at day 3 in mice treated with EPO-Z (Figure 5(d)).

Under normal conditions, the progression of granulation tissue and cell proliferation are controlled by cyclin D_1/CDK6 and cyclin E/CDK2 complexes. Our data demonstrate that EPO-α increased more efficiently the expression of cyclins. In this way, cell cycle is certainly promoted and this event contributes to the regeneration of the burned tissue and its damaged structures. Therefore it is tempting to speculate that the better wound healing effect of EPO-α is due to a greater ability to prime the cell cycle machinery.

4. Conclusions

It has been demonstrated that EPO represents particularly promising approach for the treatment of burn wounds [35–37]. EPO-α and EPO-Z are biosimilars, and they should have overlapping therapeutic efficacy. In fact both compounds did not show significant differences in Hb levels, in erythrocytes number, and in expression of VEGF. EPO-α and EPO-Z also accelerate wound closure and angiogenesis, but EPO-α resulted more effectively in achieving complete skin regeneration. We hypothesize that the superiority in this specific therapeutic effect of EPO-α with respect to EPO-Z might be related to a more robust activation of the cell cycle machinery. At this moment, we do not have a clear-cut explanation for this "dissimilarity." It could be hypothesized that molecular differences in manufacturing processes used for the preparation of these two formulations or changes in structure, for example, in glycosylation of some residues, may lead to a different activation of cell cycle and may account for the different wound healing effect. In addition, these possible conformational changes might be responsible for a lower receptor affinity that determines an alteration of receptor bond and therefore of the correlated signalling of response.

However further experiments are needed to fully elucidate the molecular mechanisms underlying this difference between the two biosimilars.

All these data propose that the abnormalities of wound healing in burn injury might be a result of significant alterations in the cell cycle machinery of the repair tissue, and the administration of EPO might be suggested as a potential strategy to restore the impaired wound healing, stimulating both angiogenesis and cell cycle of the damaged burned tissue.

Conflict of Interests

The authors declare that there is no conflict of interests regarding the publication of this paper.

Authors' Contribution

Natasha Irrera and Alessandra Bitto equally contributed to this work.

References

[1] W. Jelkmann, "Biology of erythropoietin," *Clinical Investigator*, vol. 72, no. 6, pp. S3–S10, 1994.

[2] M. Piagnerelli and J.-L. Vincent, "The use of erythropoiesis-stimulating agents in the intensive care unit," *Critical Care Clinics*, vol. 28, no. 3, pp. 345–362, 2012.

[3] H. Youssoufian, G. Longmore, D. Neumann, A. Yoshimura, and H. F. Lodish, "Structure, function, and activation of the erythropoietin receptor," *Blood*, vol. 81, no. 9, pp. 2223–2236, 1993.

[4] J. Rossert and K.-U. Eckardt, "Erythropoietin receptors: their role beyond erythropoiesis," *Nephrology Dialysis Transplantation*, vol. 20, pp. 1025–1028, 2005.

[5] M. Brines and A. Cerami, "Discovering erythropoietin's extra-hematopoietic functions: biology and clinical promise," *Kidney International*, vol. 70, no. 2, pp. 246–250, 2006.

[6] F. P. Barbone, D. L. Johnson, F. X. Farrell et al., "New epoetin molecules and novel therapeutic approaches," *Nephrology Dialysis Transplantation*, vol. 14, no. 2, pp. 80–84, 1999.

[7] P. J. Connolly, S. K. Wetter, W. V. Murray et al., "Synthesis and erythropoietin receptor binding affinities of N, N-disubstituted amino acids," *Bioorganic and Medicinal Chemistry Letters*, vol. 10, no. 17, pp. 1995–1999, 2000.

[8] Z. A. Haroon, K. Amin, X. Jiang, and M. O. Arcasoy, "A novel role for erythropoietin during fibrin-induced wound-healing response," *American Journal of Pathology*, vol. 163, no. 3, pp. 993–1000, 2003.

[9] D. Ribatti, M. Presta, A. Vacca et al., "Human erythropoietin induces a pro-angiogenic phenotype in cultured endothelial cells and stimulates neovascularization in vivo," *Blood*, vol. 93, no. 8, pp. 2627–2636, 1999.

[10] M. Buemi, A. Lacquaniti, D. Bolignano et al., "The erythropoietin and regenerative medicine: a lesson from fish," *European Journal of Clinical Investigation*, vol. 39, no. 11, pp. 993–999, 2009.

[11] M. Galeano, D. Altavilla, D. Cucinotta et al., "Recombinant human erythropoietin stimulates angiogenesis and wound healing in the genetically diabetic mouse," *Diabetes*, vol. 53, no. 9, pp. 2509–2517, 2004.

[12] M. Galeano, D. Altavilla, A. Bitto et al., "Recombinant human erythropoietin improves angiogenesis and wound healing in experimental burn wounds," *Critical Care Medicine*, vol. 34, no. 4, pp. 1139–1146, 2006.

[13] C. Baldamus, S. Krivoshiev, M. Wolf-Pflugmann, M. Siebert-Weigel, R. Koytchev, and A. Bronn, "Long-term safety and tolerability of epoetin zeta, administered intravenously, for maintenance treatment of renal anemia," *Advances in Therapy*, vol. 25, no. 11, pp. 1215–1228, 2008.

[14] V. Wizemann, B. Rutkowski, C. Baldamus, P. Scigalla, and R. Koytchev, "Comparison of the therapeutic effects of epoetin zeta to epoetin alfa in the maintenance phase of renal anemia treatment," *Current Medical Research & Opinion*, vol. 24, no. 3, pp. 625–637, 2008.

[15] S. Krivoshiev, V. V. Todorov, J. Manitius, S. Czekalski, P. Scigalla, and R. Koytchev, "Comparison of the therapeutic effects of epoetin zeta and epoetin alfa in the correction of renal anaemia," *Current Medical Research and Opinion*, vol. 24, no. 5, pp. 1407–1415, 2008.

[16] T. McGowan, N. M. Vaccaro, J. S. Beaver, J. Massarella, and M. Wolfson, "Pharmacokinetic and pharmacodynamic profiles of

extended dosing of epoetin alfa in anemic patients who have chronic kidney disease and are not on dialysis," *Clinical Journal of the American Society of Nephrology*, vol. 3, no. 4, pp. 1006–1014, 2008.

[17] S. D. Roger, "Biosimilars: how similar or dissimilar are they?" *Nephrology*, vol. 11, no. 4, pp. 341–346, 2006.

[18] G. Barosi, A. Bosi, M. P. Abbracchio et al., "Key concepts and critical issues on epoetin and filgrastim biosimilars: a position paper from the Italian Society of Hematology, Italian Society of Experimental Hematology, and Italian Group for Bone Marrow Transplantation," *Haematologica*, vol. 96, no. 7, pp. 937–942, 2011.

[19] A. S. Tsiftsoglou, S. Ruiz, and C. K. Schneider, "Development and regulation of biosimilars: current status and future challenges," *BioDrugs*, vol. 27, no. 3, pp. 203–211, 2013.

[20] S. Tamilvanan, N. L. Raja, B. Sa, and S. K. Basu, "Clinical concerns of immunogenicity produced at cellular levels by biopharmaceuticals following their parenteral administration into human body," *Journal of Drug Targeting*, vol. 18, no. 7, pp. 489–498, 2010.

[21] Z. A. Haroon, K. Amin, X. Jiang, and M. O. Arcasoy, "A novel role for erythropoietin during fibrin-induced wound-healing response," *American Journal of Pathology*, vol. 163, no. 3, pp. 993–1000, 2003.

[22] B. M. Kang, S. H. Shin, M. H. Kwack et al., "Erythropoietin promotes hair shaft growth in cultured human hair follicles and modulates hair growth in mice," *Journal of Dermatological Science*, vol. 59, no. 2, pp. 86–90, 2010.

[23] G. H. Bishop, "Regeneration after experimental removal of skin in man," *American Journal of Anatomy*, vol. 76, no. 2, pp. 153–181, 1945.

[24] V. Martinot, V. Mitchell, P. Fevrier, A. Duhamel, and P. Pellerin, "Comparative study of split thickness skin grafts taken from the scalp and thigh in children," *Burns*, vol. 20, no. 2, pp. 146–150, 1994.

[25] A. K. Langton, S. E. Herrick, and D. J. Headon, "An extended epidermal response heals cutaneous wounds in the absence of a hair follicle stem cell contribution," *Journal of Investigative Dermatology*, vol. 128, no. 5, pp. 1311–1318, 2008.

[26] M. Ito, Y. Liu, Z. Yang et al., "Stem cells in the hair follicle bulge contribute to wound repair but not to homeostasis of the epidermis," *Nature Medicine*, vol. 11, no. 12, pp. 1351–1354, 2005.

[27] C. A. B. Jahoda and A. J. Reynolds, "Hair follicle dermal sheath cells: unsung participants in wound healing," *The Lancet*, vol. 358, no. 9291, pp. 1445–1448, 2001.

[28] C. I. Günter, A. Bader, U. Dornseifer et al., "A multi-center study on the regenerative effects of erythropoietin in burn and scalding injuries: study protocol for a randomized controlled trial," *Trials*, vol. 14, no. 1, article 124, 2013.

[29] E. Bodó, A. Kromminga, W. Funk et al., "Human hair follicles are an extrarenal source and a nonhematopoietic target of erythropoietin," *The FASEB Journal*, vol. 21, no. 12, pp. 3346–3354, 2007.

[30] M. V. A. Arroyo, M. A. Castilla, F. R. G. Pacheco et al., "Role of vascular endothelial growth factor on erythropoietin-related endothelial cell proliferation," *Journal of the American Society of Nephrology*, vol. 9, no. 11, pp. 1998–2004, 1998.

[31] P. Nurse, "A long twentieth century of the cell cycle and beyond," *Cell*, vol. 100, no. 1, pp. 71–78, 2000.

[32] J. Bartkova, B. Grøn, E. Dabelsteen, and J. Bartek, "Cell-cycle regulatory proteins in human wound healing," *Archives of Oral Biology*, vol. 48, no. 2, pp. 125–132, 2003.

[33] H.-S. Peng, X.-H. Xu, R. Zhang et al., "Multiple low doses of erythropoietin delay the proliferation of hepatocytes but promote liver function in a rat model of subtotal hepatectomy," *Surgery Today*, vol. 44, no. 6, pp. 1109–1115, 2014.

[34] H. Sorg, C. Krueger, T. Schulz, M. D. Menger, F. Schmitz, and B. Vollmar, "Effects of erythropoietin in skin wound healing are dose related," *The FASEB Journal*, vol. 23, no. 9, pp. 3049–3058, 2009.

[35] D. Schmauss, F. Rezaeian, T. Finck, H. G. Machens, R. Wettstein, and Y. Harder, "Treatment of secondary burn wound progression in contact burns—a systematic review of experimental approaches," *Journal of Burn Care & Research*, 2015.

[36] M. Tobalem, Y. Harder, F. Rezaeian, and R. Wettstein, "Secondary burn progression decreased by erythropoietin," *Critical Care Medicine*, vol. 41, no. 4, pp. 963–971, 2013.

[37] A. Bader, S. Ebert, S. Giri et al., "Skin regeneration with conical and hair follicle structure of deep second-degree scalding injuries via combined expression of the EPO receptor and beta common receptor by local subcutaneous injection of nanosized rhEPO," *International Journal of Nanomedicine*, vol. 7, pp. 1227–1237, 2012.

Hindawi Publishing Corporation
BioMed Research International
Volume 2015, Article ID 549412, 13 pages
http://dx.doi.org/10.1155/2015/549412

Review Article

Hypoxia-Inducible Factor-1 in Physiological and Pathophysiological Angiogenesis: Applications and Therapies

Agnieszka Zimna and Maciej Kurpisz

Institute of Human Genetics, Polish Academy of Sciences, Strzeszynska 32, 60-479 Poznań, Poland

Correspondence should be addressed to Maciej Kurpisz; kurpimac@man.poznan.pl

Received 19 December 2014; Revised 10 April 2015; Accepted 17 April 2015

Academic Editor: Alessio D'Alessio

The cardiovascular system ensures the delivery of oxygen and nutrients to all cells, tissues, and organs. Under extended exposure to reduced oxygen levels, cells are able to survive through the transcriptional activation of a series of genes that participate in angiogenesis, glucose metabolism, and cell proliferation. The oxygen-sensitive transcriptional activator HIF-1 (hypoxia-inducible factor-1) is a key transcriptional mediator of the response to hypoxic conditions. The HIF-1 pathway was found to be a master regulator of angiogenesis. Whether the process is physiological or pathological, HIF-1 seems to participate in vasculature formation by synergistic correlations with other proangiogenic factors such as VEGF (vascular endothelial growth factor), PlGF (placental growth factor), or angiopoietins. Considering the important contributions of HIF-1 in angiogenesis and vasculogenesis, it should be considered a promising target for treating ischaemic diseases or cancer. In this review, we discuss the roles of HIF-1 in both physiological/pathophysiological angiogenesis and potential strategies for clinical therapy.

1. Angiogenesis

The circulatory system is the first biological system that is established during mammalian development [1]. Vessel formation occurs via only two basic mechanisms: vasculogenesis and angiogenesis [2]. During embryonic development, the primary vascular plexus is formed by vasculogenesis. This phenomenon involves *de novo* blood vessel formation from precursor cells called angioblasts (precursors of endothelial cells), whereas angiogenesis is the process by which blood vessels are formed from preexisting vessels. This process involves the remodelling of blood vessels into the large and small vessels that are typical for networks containing arteries, capillaries, and veins [3, 4]. Angiogenesis occurs in adult organisms and in embryos during development [3].

Angiogenesis consists of several basic steps. Briefly, biological signals such as hypoxia, ischaemia, and/or blood vessel damage upregulate the expression of proangiogenic growth factors that activate their receptors [5, 6]. Vascular permeability increases in response to VEGF, thereby allowing the extravasation of plasma proteins that form a primitive scaffold for migrating endothelial cells [7]. Angiopoietin-1 and angiopoietin-2 (Ang-1 and Ang-2) exert antagonistic functions during vessel development. Ang-1, which is a known natural inhibitor of vascular permeability, protects against plasma leakage, whereas Ang-2 is involved in vessel destabilisation via the detachment of smooth muscle cells and the promotion of permeabilisation [8, 9]. Subsequently, matrix metalloproteinases (MMPs) enhance angiogenesis through the degradation of matrix components [10]. Proliferating endothelial cells migrate to distant sites and then assemble as a solid cord that subsequently forms a lumen [11]. Integrins $\alpha\beta$ promote endothelial cell adhesion and migration, whereas VE-cadherin increases cell survival and promotes endothelial cell adhesion [12–14]. Once the vessels are formed, pericytes and smooth muscle cells surround the newly created capillaries to stabilise the walls and to prevent leakage. Other factors such as Ang-1, PDGF-BB (platelet-derived growth factor BB), and PDGFR (platelet-derived growth factor receptor) participate in the maturation of blood vessels [8, 15]. Further expansion of the lumen diameter is called arteriogenesis [11].

Angiogenesis occurs in physiological states such as embryonic development, wound healing, or vessel penetration into avascular regions and in pathological states such as solid tumours formation, eye diseases, or chronic inflammatory disorders such as rheumatoid arthritis, psoriasis, and periodontitis [16, 17]. Pathophysiological angiogenesis exhibits differences in molecular pathways in comparison to physiological angiogenesis. Mutations in oncogenes and tumour suppressor genes and disruptions in growth factor activity play crucial roles during tumour angiogenesis [17]. The activation of the most prominent proangiogenic factor VEGF might be due to physiological stimuli such as hypoxia or inflammation or due to oncogene activation and tumour suppression function loss [18, 19]. Additionally, physiological angiogenesis such as that which occurs during embryonic development or wound healing seems to be dependent on VEGF signalling, whereas tumour angiogenesis adopts the ability to shift its dependence from VEGF to other proangiogenic pathways, for example, through the recruitment of myeloid cells and the upregulation of alternative vascular growth factors (PlGF and FGF, fibroblast growth factor) [17]. Moreover, tumour vessels are distinct from normal vasculature because they are disorganised and tortuous. Many morphological and functional differences exist between normal and tumour vasculature. For instance, tumour vessels are leakier than normal vessels, and endothelial cells growing within tumours carry genetic abnormalities [20, 21]. Elucidating the molecular mechanism of pathological angiogenesis might lead to the identification of potential therapeutic targets.

Angiogenesis is a multistep process that requires the involvement of many biological signals and stimuli regardless of whether it is a physiological or pathological action. Proangiogenic factors are activated in response to some physical signals. Blood vessel damage, infarction, and blood flow reduction lead to decreases in O_2 supply [11]. This state is called hypoxia, which is a potent angiogenic trigger that stimulates proangiogenic factor activity.

2. Hypoxia

2.1. O_2 Homeostasis. Constant oxygen supply is essential for proper tissue function, development, and homeostasis. Thus, the vasculature network plays a crucial role in delivering oxygen particles (O_2), nutrients, and other molecules within the entire human body [22]. Significantly, the first physiological system that becomes functional during mammalian embryonic development is the circulatory system. Governing O_2 homeostasis in tissues by supplying an oxygen concentration adequate for the demand generated by the metabolic outputs of the tissue is essential. Oxygenic balance can be upset by rapid cellular division during embryonic development, by tumour growth, or by vasculature dysfunction due to vessel occlusion or rupture [23]. Notably, normal physiological O_2 concentrations vary greatly from normal oxygen tension in the air depending on the type of tissue. For instance, arterial blood has a normal pO_2 of 14%; myocardium, 10%; and skeletal muscle, 5%. In contrast, the natural pO_2 levels of bone marrow, thymus, and cartilage are at or below 1% [24, 25]. The state when the O_2 level decreases relative to physiological levels (characteristic for particular tissues) is called hypoxia [1].

2.2. Hypoxia-Inducible Factor-1. Adaptation to low oxygen tension (hypoxia) in cells and tissues requires the activation of several genes that participate in angiogenesis, cell proliferation/survival, glucose and iron metabolism. In eukaryotic cells, hypoxia-inducible factor-1 (HIF-1) is a primary transcriptional mediator of the hypoxic response and master regulator of O_2 homeostasis [26]. Hypoxia-inducible factor-1 was first discovered as a transcription factor that regulates erythropoietin (EPO) expression in response to low oxygen levels in the blood [27, 28]. HIF-1 consists of two different subunits, α and β (also known as aryl hydrocarbon nuclear receptor translocator (ARNT)); both subunits are members of the basic helix-loop-helix Per-Arnt-Sim (bHLH-PAS) transcription factor family [29, 30]. PAS and bHLH motifs are required for heterodimerisation between the HIF-1α and HIF-1β subunits [31]. Additionally, the bHLH domain of the HIF-1α/ARNT dimer is essential for DNA binding on hypoxia response elements (HREs) with the consensus sequence (G/ACGTG) in the promoters or enhancers of target genes [32]. Transcriptional activation and interactions with coactivators (such as CBP/p300) of HIF-1α are mediated by two domains, that is, C-TAD and N-TAD, which are on the C-terminus of the protein [33–35]. HIF-1β is a constitutively expressed subunit, whereas HIF-1α is translated continuously and degraded subsequently through ubiquitination under normoxic conditions [36, 37]. Thus far, three isoforms of HIF-α have been discovered (Figure 1(a)), that is, the previously discussed subunit HIF-1α and two other subunits, HIF-2α (also called endothelial PAS protein (EPAS)) and HIF-3α (IPAS). The second isoform is expressed constitutively in the endothelium, lung, and cartilage and shares 48% amino acid sequence identity with HIF-1α. The third protein, HIF-3α, also called inhibitory PAS (IPAS), is a negative regulator of HIF-1 that dimerises with the HIF-1α subunit and prevents its DNA-binding activity. The entire set of HIF-α subunits dimerises with ARNT and binds to HREs [38–40].

Under extended exposure to hypoxic conditions, HIF-1α is expressed as long as a balance between O_2 supply and usage in tissues cannot be reached [36, 37]. When oxygen tension is sufficient, *de novo* synthesised cytoplasmic HIF-1α is hydroxylated by a family of prolyl hydroxylase enzymes (PHDs) on proline 402 and 564 residues located within ODDD (O_2-dependent degradation domain) [41, 42]. The hydroxylation of the abovementioned prolines is the key mechanism of negative regulation of HIF-1α activity and results in the binding of the von Hippel-Lindau (VHL) E3 ligase complex, which ubiquitinates HIF-1α, targeting it to proteasomal degradation [43–45]. The second major mechanism that modulates HIF-1α activity is the hydroxylation of asparagine residue 803 (Asn803) in the C-TAD domain. In this case, asparagine is hydroxylated under normoxic conditions by factor inhibiting HIF-1 (FIH-1), which prevents the interaction of HIF-1α within CBP/p300 (CREB-binding protein/E1A binding protein p300) [46–49]. Hydroxylases (PHDs and FIH-1) are strictly Fe(II)- and 2-oxoglutarate-dependent dioxygenases that are activated

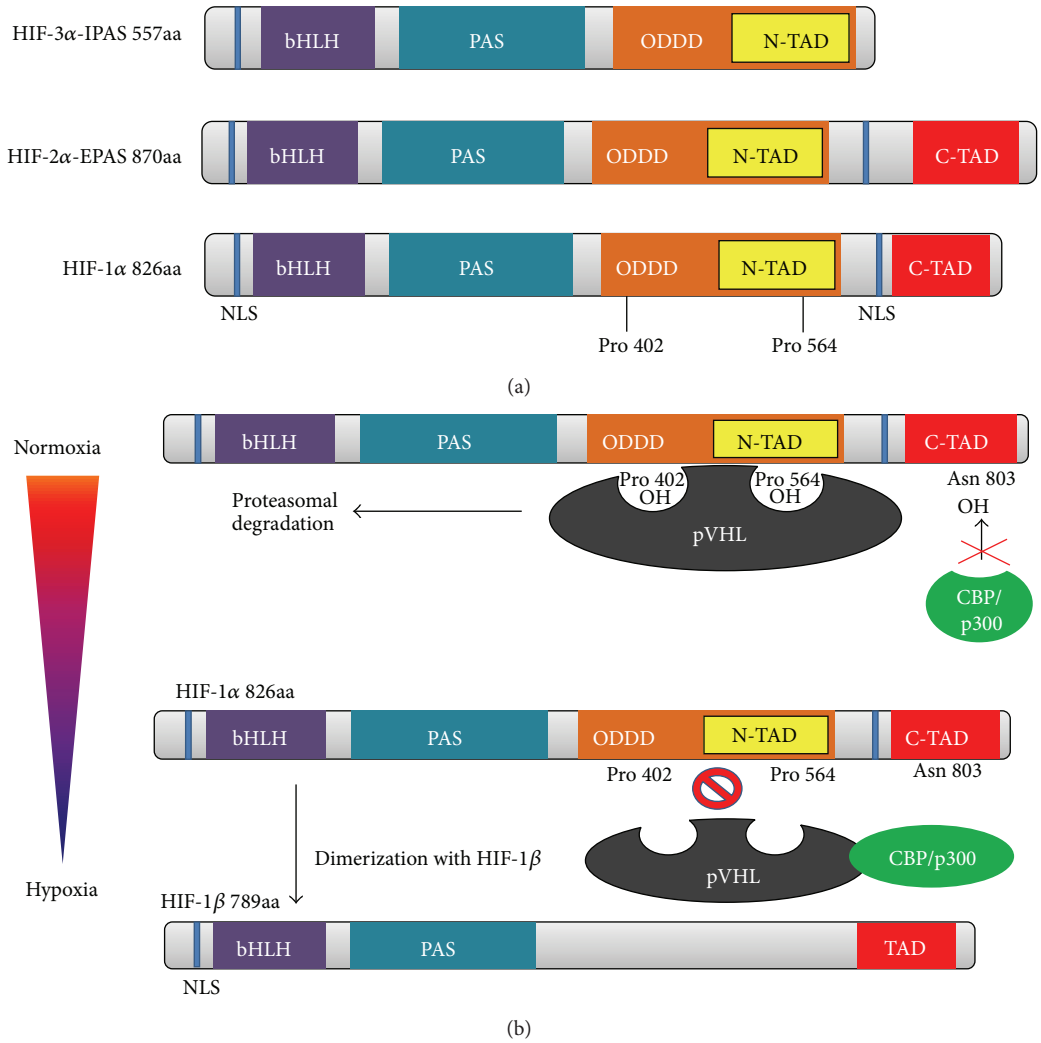

FIGURE 1: *Schematic representation of HIF-α gene structures and DNA binding.* (a) HIF-1α and HIF-2α contain the following domains: a nuclear localisation domain (NLS), DNA binding and dimerisation domains (bHLH/PAS), oxygen-dependent degradation domain (ODDD), and cofactor interaction and transcriptional activity domains (N-TAD/C-TAD). HIF-3α lacks a C-TAD domain. NLS: nuclear localisation signal; bHLH: basic helix-loop-helix domain; PAS: Per-ARNT-Sim motif; ODDD: oxygen-dependent degradation domain; N-TAD: N-terminal transactivation domain; C-TAD: C-terminal transactivation domain. (b) Dimerisation of HIF-1α with HIF-1β under hypoxic conditions results in the formation of the HIF-1 transcription factor, which binds to hypoxia response elements (HREs) and activates the transcription of O_2-dependent genes (according to [134]).

only in the presence of molecular oxygen. Under hypoxic conditions, substrates and coactivators of hydroxylation such as O_2, Fe(II), and 2-oxoglutarate become limited, which leads to the attenuation of HIF-1α hydroxylation [50, 51]. HIF-1α accumulates in the cytosol and is subsequently translocated into the nucleus where it dimerises with the HIF-1β subunit. The HIF-1α/β dimer binds to HREs that are located within O_2-regulated genes (Figure 2) [34, 35]. HIF-1 target gene members include a stress response gene family that mediates the adaptation of cells/tissues to chronic or acute hypoxia; this family includes glucose transporters, glycolytic enzymes, and angiogenic and haematopoietic growth factors [52].

2.3. HIF-1 Activity and Target Genes. Recently, HIF-1 has been shown to regulate more than 2% of genes in vascular endothelial cells either directly or indirectly [53]. The modulation of cell responses is followed by the transcriptional activation of target genes by the HIF-1α/β dimer (Figure 1(b)) [54, 55]. For example, hypoxia upregulates the expression of erythropoietin (EPO), which is required for red blood cell production. The generation of new erythrocytes increases the delivery of oxygen to tissues to reach O_2 homeostasis [56]. Additionally, low oxygen levels influence glucose metabolism in cells. Under hypoxic conditions, cells generate only 2 ATP molecules by oxygen-independent glycolysis instead of 38 ATP molecules by the oxygen-dependent tricarboxylic acid cycle (TCA) under normoxic conditions [57, 58]. To maintain the energetic balance under hypoxic conditions, cells increase their ability to produce ATP by increasing glucose uptake via the enhancement of glycolytic enzyme and

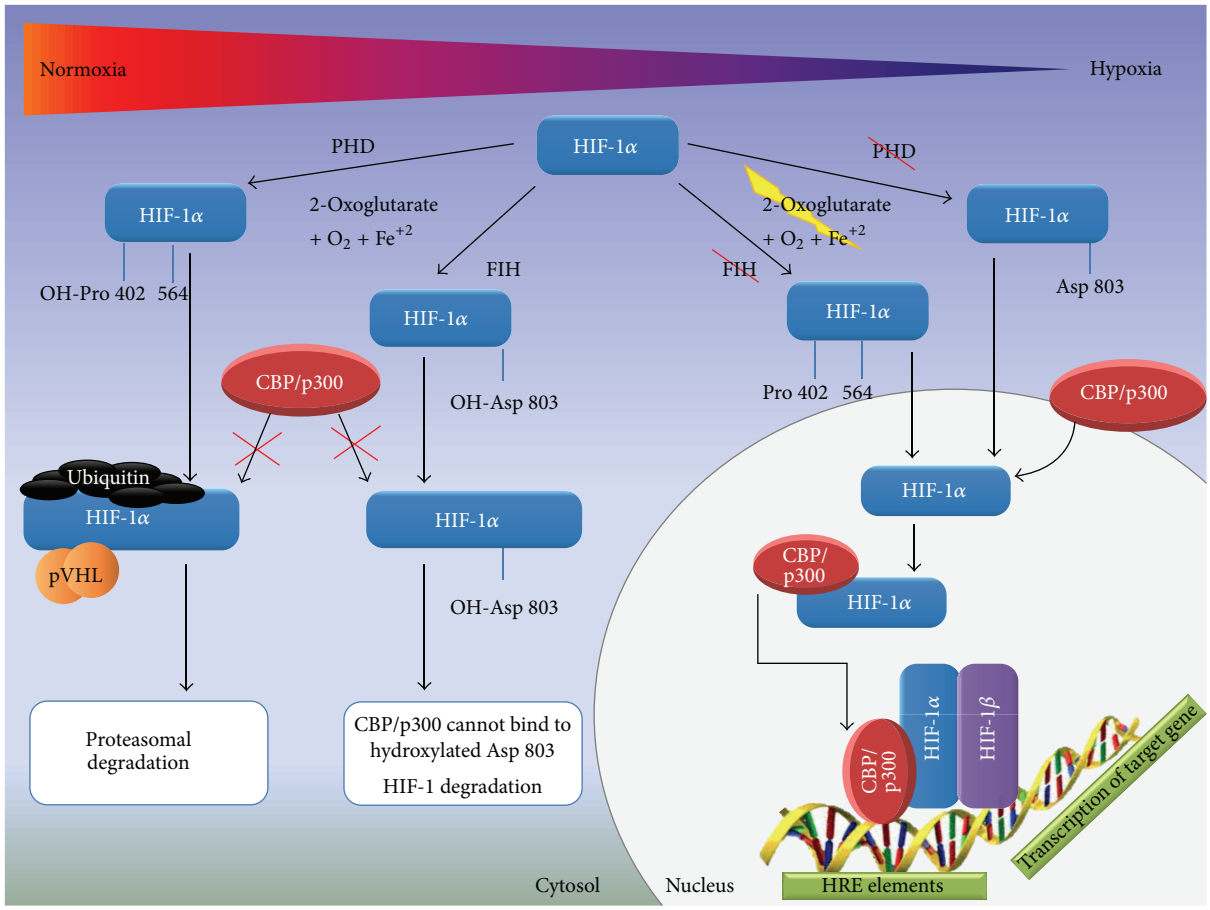

FIGURE 2: *HIF-1α under normoxic and hypoxic conditions.* In the presence of molecular oxygen, 2-oxoglutarate, and Fe^{2+}, HIF-1α is hydroxylated on proline 402 and 564 residues located within ODDD (O_2-dependent degradation domain) by prolyl hydroxylase enzymes (PHDs). Hydroxylation results in the binding of the von Hippel-Lindau (VHL) E3 ligase complex, which ubiquitinates HIF-1α, targeting it to proteasomal degradation. The hydroxylation of the asparagine residue prevents CBP/p300 binding to HIF-1α. Under hypoxic conditions, substrates and coactivators of hydroxylation such as O_2, Fe(II), and 2-oxoglutarate become limited, which leads to the attenuation of HIF-1α hydroxylation. HIF-1α accumulates in the cytosol and is subsequently translocated into the nucleus where it dimerises with the HIF-1β subunit. The HIF-1α/β dimer binds to HREs and regulates target gene expression.

transporter expression [59–61]. Furthermore, cell proliferation and survival may be enhanced under hypoxic conditions. Factors such as IGF-2 (insulin growth factor-2) and TGFα (transforming growth factor) are upregulated through HIF-1 activity [62, 63]. Additionally, myoblasts cultured under hypoxic conditions show increased proliferation compared to cells maintained under normoxic conditions. Myogenic gene expression analysis revealed that the genes *MyoD* and *Myf5* (both involved in myogenic cell proliferation and differentiation) were upregulated in hypoxic cells, whereas no significant influence of myogenic gene expression was observed in normoxic cells [64].

3. Hypoxia-Induced Angiogenesis

3.1. Physiological Vasculogenesis and Angiogenesis under Hypoxic Conditions. Vasculogenesis is a characteristic embryonic process that involves *de novo* blood vessel formation and that leads to establishing a primary vascular plexus. O_2 tension plays a crucial role in organogenesis and vasculogenesis during embryonic development [1]. During the first stage of embryogenesis, before the circulatory system develops, the oxygen tension is relatively low and does not exceed 3% [65, 66]. The developing embryo requires an increase in the oxygen level, which leads to the formation of primary vessels from angioblasts. Because the uterine environment is hypoxic it is thereby obvious that hypoxia may be the primary stimulus of vessel formation [3, 4]. Hypoxia also stimulates EC (endothelial cell) behaviour. Under *in vitro* conditions, HIF-1α promotes the arterial differentiation of endothelial progenitor cells (EPCs) over venous differentiation by regulating the expression of genes that inhibit the venous specification factor Coup-TFII (Hey2 and delta-like ligand 4 (Dll4)) [67]. In contrast, HIF-1β enhances the differentiation of hemangioblasts from mesodermal progenitors [68]. Mouse model studies have demonstrated the participation of both HIF-1 dimer subunits in vasculogenesis [69, 70]. For instance, HIF-1α- or HIF-1β (ARNT) deficient mouse embryos showed

aberrant placental architecture with fewer foetal blood vessels [71–73]. Additionally, a lack of the HIF-1β gene results in defective vascular development in the yolk sac, branchial arches, cranium, and somites [74, 75]. These defects are lethal for embryos at day 10.5. HIF-1 subunit deficiencies markedly decrease VEGF mRNA and protein expression, leading to defects in blood vessel formation and neural fold termination [70, 74, 75].

Current studies have indicated that hypoxia and HIF-1 expression in adult organisms may contribute to angiogenesis in the following ways: by transcriptionally activating several angiogenic genes and their receptors (*VEGF*, *PlGF*, *PDGFB*, *ANGPT1*, and *ANGPT2*) [76, 77]; by regulating proangiogenic chemokines and receptors (*SDF-1α*, stromal cell derived factor 1α, and *S1P*, sphingosine-1-phosphate, and receptors *CXCR4*, C-X-C chemokine receptor type 4, and *S1PRs*, sphingosine-1-phosphate receptors), thus facilitating the recruitment of endothelial progenitor cells to the site of hypoxia [78]; and by enhancing EC proliferation and division (regulating genes involved in the cell cycle and DNA replication) [53]. Summarising these findings, we conclude that HIF-1 can orchestrate the process of angiogenesis.

HIF-1 participates in every step of angiogenesis. Cross activity between HIF-1 and proangiogenic factors is a basic relationship during capillary formation under hypoxia. Every step of the vessel formation cascade is supported by HIF-1. Notably, vascular endothelial growth factor isoforms (VEGF-A, VEGF-B, VEGF-C, and VEGF-D) are the primary factors that participate in angiogenesis [79], and angiogenesis initiated by hypoxia and by HIF-1 is often VEGF-dependent primarily because HIF-1 is a master stimulator of vascular endothelial growth factor. The sprouting of new vessels is a complex process that involves a wide range of proangiogenic factors and their receptors. Under hypoxic conditions, HIF-1 accumulation upregulates the principal proangiogenic factor VEGF directly [80, 81]. VEGF activity induces the expression of Flt-1 (fms-related tyrosine kinase) and KDR (kinase insert domain receptor) receptors [82, 83]. As long as the oxygen balance is disrupted, VEGF will bind its receptors and stimulate capillary outgrowth. Additionally, VEGF is known as a factor that enhances the expression of other proangiogenic factors such as PlGF and FGF. We can assume that when the blood flow is sufficient to supply oxygen to cells and tissues, HIF-1α will be degraded, thereby inhibiting *VEGF* gene and protein expression and stopping the entire cascade of proangiogenic factors. In conclusion, HIF-1 may regulate the expression of proangiogenic factors either directly (by binding to HREs) or indirectly (cascade effect) [84]. Aside from VEGFs, other factors participate in angiogenesis, including placental growth factor (PlGF), platelet-derived growth factor (PDGF), angiopoietins 1 and 2 (ANGPT1 and ANGPT2), and metalloproteinases (MMPs). Receptors such as Flt-1, KDR, Tie 1, and Tie 2 that transduce these signals and thereby maintain the cascade of new vessel formation are also important. Analyses of proangiogenic genes revealed the presence of HREs within the promoters of some genes [85, 86].

As was mentioned above, angiogenesis is a multistep process [87]. During the first step, hypoxia and HIF-1 stimulate VEGF and their receptors directly, and the cascade of new vessel creation begins. Second, the extracellular matrix must be degraded by metalloproteinases to allow the migrating endothelial cells to form tubes. Metalloproteinase 2 (MMP-2) expression has been shown to be enhanced by HIF-1α [88]. Next, integrins $\alpha\beta$ (induced by HIF) [89] stimulate endothelial cell proliferation and adhesion, and HIF-1 controls EC behaviour. The Manalo group examined the influence of hypoxia and HIF-1 on the endothelial cell transcriptome. Microarray analysis demonstrated the upregulation of several genes that are responsible for the cell cycle and DNA replication. Additionally, it was proven that ECs cultured under low density and hypoxic conditions exhibit increased proliferation. In conclusion, HIF-1 can stimulate cell proliferation and division under hypoxia-induced angiogenesis by transcriptionally regulating the genes involved in the basic biological functions of cells [53]. Finally, the last step of angiogenesis is vessel maturation, which involves the recruitment of vascular supporting cells (pericytes and smooth muscle cells) and the formation of the basement membrane. In this case, HIF-2α is a primary enhancer of genes that determine blood vessel stabilisation. For example, fibronectin is a component of the basement membrane, and HIF-2α is involved in the upregulation of this gene [90]. Considering these findings, we can assume that HIF-1 regulates almost every step of capillary formation.

Increasing knowledge regarding the influence of HIF-1 on angiogenesis has been applied to *in vitro* studies that attempt to develop treatments for ischaemic diseases. For example, the adenoviral transfer of HIF-1α and HIF-2α into rabbit ischaemic limbs resulted in an increase in blood flow followed by induction of vessel sprouting. Additionally, these capillaries were highly enlarged compared to those of rabbits transduced with *VEGF-A*. As another consequence of *VEGF* gene transfer, the newly formed vessels were leaky, and the area of transfer was surrounded by oedema compared to animals treated with AdHIF-1α and AdHIF-2α [91]. In turn, *in vivo* studies demonstrated that the deletion of HIF-2α in murine ECs caused VEGF-induced acute vessel permeability. Furthermore, immortalised HIF-2α-deficient ECs exhibited decreased adhesion to extracellular matrix proteins and diminished expression of fibronectin, integrins, endothelin B receptor, angiopoietin-2, and delta-like ligand 4 (Dll4) [90]. Artificial hypoxia induced by $CoCl_2$ (0.5 mM) stimulates angiogenic responses in SCAPs (stem cells from apical papilla) cocultured with HUVECs (human umbilical vein endothelial cells). Hypoxic conditions induced upregulated HIF-1α and VEGF expression in HUVECs, whereas *ephrin-B2* gene was enhanced in SCAPs. Notably, this gene plays a central role in heart morphogenesis and angiogenesis by regulating cell adhesion and cell migration. Additionally, synergistic effects between HIF-1, VEGF, and ephrin-B2 led to an increase in the endothelial tubule number, vessel length, and branching points [92].

In conclusion, hypoxia-induced angiogenesis is a complex process that has been tested in both *in vitro* and *in vivo* studies. Moreover, the application of HIF-1 therapy in phase I clinical studies of critical limb ischaemia resulted in complete recovery of the ischaemic region [93]. Increased knowledge

of the role of HIF-1 in angiogenesis may provide promising treatment methods for ischaemic diseases as partly described in Section 4.1 of this paper.

3.2. The Effect of Hypoxia on Pathophysiological Angiogenesis and the Role of HIF-1 in Tumour Angiogenesis. Low oxygen tension has been linked with many pathophysiological disorders and human diseases. Hypoxia is a component of tumour development and metastasis, while angiogenesis is principal for tumour growth and progression [94, 95]. Current studies have suggested that in terms of malignant transformation the activation of HIF-dependent angiogenesis in cancer occurs in two basic ways: by hypoxic conditions prevailing in the tumour cell mass or by genetic alterations caused by tumour transformation, genetic disorders, or molecular interactions that stimulate HIF activity, irrespective of oxygen tension. Undeniably, HIF plays a critical role in stimulating angiogenesis. However, notably, proangiogenic activity is directly linked with HIF-dependent VEGF activation, which results in an "angiogenic switch" in growing tumour masses [96].

Hypoxia is best characterised as an HIF activator. When intensively proliferating cells form a solid tumour, the balance between oxygen supply and demand is impaired; therefore, hypoxic environments (intratumoural hypoxia) prevail in growing cell masses. This prevalence is the reason why newly activated HIF-1α is not ubiquitinated and targeted to proteasomal degradation. Accumulating HIF-1 upregulates the expression of a number of proangiogenic genes including *VEGF* and their receptors *Flt-1*, *Flk-1*, *Ang-1*, *Ang-2*, and *Tie-2* receptor, and all of these genes are essential for sprouting new vessels. Among these factors, VEGF is considered a primary effector of tumour angiogenesis. Moreover, the expression of VEGF can enhance the expression of other proangiogenic factors and their receptors; thus, vessel outgrowth is stimulated by multiple factors [95, 97]. This phenomenon, which is called "angiogenic switching," allows tumour cells to induce angiogenesis, thereby stimulating tumour progression by supplying oxygen and nutrients through the newly created capillaries [96].

The above-presented data suggest that hypoxia directly enhances angiogenesis by promoting VEGF expression. In contrast, HIF-1-dependent angiogenesis can be activated by factors other than hypoxia. HIF-1α accumulation does not always occur under low O_2 tension. Thus, HIF-1 can also be regulated by oxygen-independent mechanisms. The malignant transformation of cells may cause a whole range of genetic alterations that block the ubiquitination and proteasomal degradation of HIF-1α [84, 98]. Carcinogenesis is linked with aberrations in tumour suppressor genes also known as antioncogene genes. The protein products of these genes may control cell division, the cell cycle, or apoptosis. When cells exhibit DNA damage, these proteins are responsible for repressing the cell cycle or cell division or for promoting apoptosis. The most important tumour suppressors are pRb, p53, p21, and PTEN. Some evidence has indicated that altered antioncogenes can enhance angiogenesis via HIF-dependent VEGF stimulation. For instance, deleting the p53 tumour suppressor gene in a human cancer cell line promotes the neovascularisation and growth of tumours in mice. This vascularisation was followed by increased HIF-1α levels and augmented HIF-1-dependent transcriptional activation of vascular endothelial growth factor (VEGF) [99]. Additionally, mutation in the tumour suppressor gene PTEN led to hypoxia-independent HIF-1α accumulation and to activated HIF-1-mediated proangiogenic gene expression [100]. In breast cancer, HER2 (receptor tyrosine kinase) signalling induces HIF-1α protein synthesis rather than inhibiting its degradation, thus manifesting a novel mechanism of HIF-1-dependent VEGF expression regulation [101]. These findings suggest that not only the hypoxic environment can lead to angiogenesis in the case of malignant transformation. Additionally, the genetic alteration of single gene may be a cause of hypoxia-independent stimulation of HIF. Some evidence has indicated that genetic diseases are involved in the activation of HIF and thereby the stimulation of angiogenesis. von Hippel-Lindau is a genetic disease that predisposes individuals to benign and malignant tumours [102]. This condition is defined by a mutation in the *VHL* gene; thus, pVHL is not translated. This protein is a ligase that ubiquitinates HIF-1α and causes its degradation by proteasomes; thus, maintaining the balance of HIF-1 under normoxia is crucial. A loss of pVHL allows HIF-1α to dimerise with HIF-1β and to activate the transcription of a number of proangiogenic genes, including *VEGF*. Patients suffering from this disease have frequent malignancies in the central nervous system and/or retinal hemangioblastomas or clear cell renal carcinomas [103–106]. However despite homology between HIF-1α and HIF-2α there are evidences that in VHL-defective renal cell carcinoma HIF isoforms exhibit different or opposite effect on gene expression and proliferation of tumour cells [107]. Genetic predisposition is not the only factor that can stimulate oxygen-independent HIF angiogenesis involving *VEGF* gene activation. Cases where some other molecules can stimulate HIF-dependent angiogenesis have been demonstrated. As an example, we can recall a phenomenon based on the feedback loop of HIF-1 and a product of the anaerobic metabolic pathway. The abovementioned mechanism that activates HIF-1-dependent angiogenesis in cancer cells is the phenomenon called the Warburg effect. Because anaerobic conditions prevail in tumour cell masses, cancer cells produce energy primarily by glycolysis. As a side effect, cells also produce high levels of lactates and pyruvates. These molecules have been reported to increase HIF-1α accumulation and to regulate hypoxia-inducible gene expression, thus promoting *VEGF* transcription and translation and resulting in tumour angiogenesis [108].

Strong interactions between HIF-1α and VEGF lead to the rapid activation of the vessel formation cascade; however, these vessels exhibit several dysfunctions. The process of intratumoural vessel formation is a consequence of imbalanced activity of angiogenic activators and inhibitors. These vessels are not fully functional and exhibit structural abnormalities. A loss of stabilisation with pericytes and smooth muscle cells and a lack of an arterial and venous phenotype lead to leakage, poor blood flow, and perfusion [109, 110]. However, these vessels are able to deliver nutrients and oxygen to growing tumour cell masses. Thus, we can also

conclude that tumours with vasculature are more sensitive to various therapies. Due to vascularisation, chemotherapeutics and inhibitors may be better distributed across tumour cells, thus leading to the inhibition of malignant cell growth.

4. Hypoxia as a Potential Therapeutic Tool

Hypoxia-inducible factor-1 has been considered a potential therapeutic target in many diseases. Predominantly, HIF-1 therapies focus on diseases common to developing countries such as ischaemic disorders (including cardiovascular disease and limb ischaemia) and cancer. Nonetheless, HIF-1 is also a potential therapeutic agent for treating endometriosis and blindness. Depending on the type of disease and the expected therapeutic effect, HIF-1 therapies have different approaches. The function of HIF-1 in therapies can be classified into two different strategies: HIF-1 upregulation (ischaemia) and HIF-1 inhibition (cancer and endometriosis) (Figure 3).

4.1. Activation of HIF-1-Dependent Angiogenesis in Ischaemic Diseases. The neovascularisation of ischaemic regions is a fundamental assumption of therapeutic angiogenesis. The induction of capillary outgrowth for therapeutic purposes is stimulated by the administration of angiogenic growth factors or sequences that encode these proteins. Thus far, multiple angiogenic factors such as VEGF, PlGF, FGF, and PDGF have been applied in *in vitro* studies and in preclinical and clinical trials [111–114]. However, therapies using only one proangiogenic agent to initiate angiogenesis were shown to be insufficient; thus, these therapies may require supplementation with other factors that can stabilise new capillaries. Therefore, hypoxia-induced angiogenesis may be a successful strategy [115]. HIF-1 regulates cell-type specific proangiogenic factors and cytokines either directly or indirectly. Promoting HIF-1 activity is essential in ischaemic diseases. Thus far, HIF-1 therapies have been based on two approaches: the administration of HIF-1α/2α or the induction of HIF-1 expression by the modification/administration/inhibition of molecules associated with HIF activity.

Basic strategies of therapeutic angiogenesis involve the administration of proangiogenic factors using vectors, combined therapies with stem cells or fusion/recombinant proteins. Hypoxia-inducible gene transfer led to the enhancement of angiogenesis in both myocardium and ischaemic skeletal muscles. Additionally, AdHIF-1α and AdHIF-2α injection did not induce tissue oedema in contrast to regions treated with AdVEGF. In conclusion, HIF application in this case resulted in the formation of stable and mature vessels compared to VEGF treatment, where the newly formed vessels were leaky [91]. To prevent oxygen-dependent degradation of HIF-1α, attempts to modify this subunit were made. An alternative approach of applying AdCA5 adenovirus encoding a constitutively active form of the HIF-1α subunit due to a deletion and a point mutation in the region responsible for O_2-dependent degradation was proposed. In a model of endovascular limb ischaemia, intramuscular injection of AdCA5 improved the recovery of blood flow by stimulating both angiogenesis and arteriogenesis [116]. Furthermore, therapy with AdCA5 induced the upregulation of several proangiogenic genes/proteins that are targets for therapeutic angiogenesis in hindlimb and cardiac ischaemia models, including FGF-2, hepatocyte growth factor, MCP-1, PDGF-B, PlGF, SDF-1, and VEGF. Moreover, AdCA5 injection into mouse eyes enhanced neovascularisation in multiple capillary beds, including those not responsive to VEGF alone. Due to the upregulation of *PlGF* and *VEGF* expression after AdCA5 treatment, both genes acted synergistically, which led to neovascularisation of the retina [117]. Combined therapy using AdCA5 gene therapy and prolyl-4-hydroxylase inhibitor dimethyloxalylglycine- (DMOG-) treated BMDACs (bone marrow-derived angiogenic cells) acted synergistically to increase the recovery of blood flow after femoral artery ligation, thereby preventing tissue necrosis. This synergistic effect is due to AdCA5 enhancement of BMDAC homing, whereas DMOG treatment increases the retention of grafted cells in the ischaemic tissues. Another combined therapy with modified stem cells was applied in cerebral ischaemia. Rat bone marrow-derived mesenchymal stem cells (BMSCs) were infected with adenoviral particles containing constitutively expressed HIF-1α due to mutations in proline 564 and asparagine 803 sites. Genetically modified cells were transplanted in a rat middle cerebral artery occlusion model (MCAO). At 7 days after intervention, improved motor function, reduced cerebral infarction, and increased VEGF protein expression that led to revascularisation were observed [118]. The stabilisation and administration of HIF-1α may be achieved by the construction of a fusion protein. For instance, DNA-binding and dimerisation domains of HIF-1α were fused with the transactivation domain of herpes simplex virus (VP16). A plasmid vector encoding this structure was used in a rabbit hindlimb ischaemia model. The administration of HIF-1α/VP16 resulted in the improvement of blood flow in the ischaemic region as determined by an increase in the number of blood vessels [119]. Additionally, using promoters specific for particular cells or tissues, angiogenesis could have occurred in the designated site. The construction of a vector encoding O_2-independent HIF-1α under the keratin 14 promoter (K14-HIF-1ΔODD) resulted in the upregulation of HIF-1α in a skin. The activation of HIF-1α increased skin capillary density. Moreover, the new vessels were not leaky, and enhanced skin vascularity was not associated with oedema compared to the capillaries that formed after K14-VEGF therapy [120].

Another approach leading to HIF-1-dependent angiogenesis is associated with the modification/administration of molecules that regulate HIF-1α activity. The stabilisation of HIF-1α under normoxic conditions is focused on the inhibition of prolyl hydroxylase activity. As mentioned above, PHDs require O_2, Fe(II), and 2-oxoglutarate (2-OG) for their enzymatic activity [50, 51]. The delivery of small molecules such as an iron chelator (DFO) or 2-OG analogue (N-oxalylglycine) may inhibit the enzyme activity [121, 122]. For instance, HIF-1 can be enhanced by the suppression of prolyl hydroxylase activity using dimethyloxalylglycine (DMOG). The systemic administration of DMOG in a mouse model of hindlimb ischaemia results in the elevation of HIF-1α protein expression, which leads to neovascularisation in

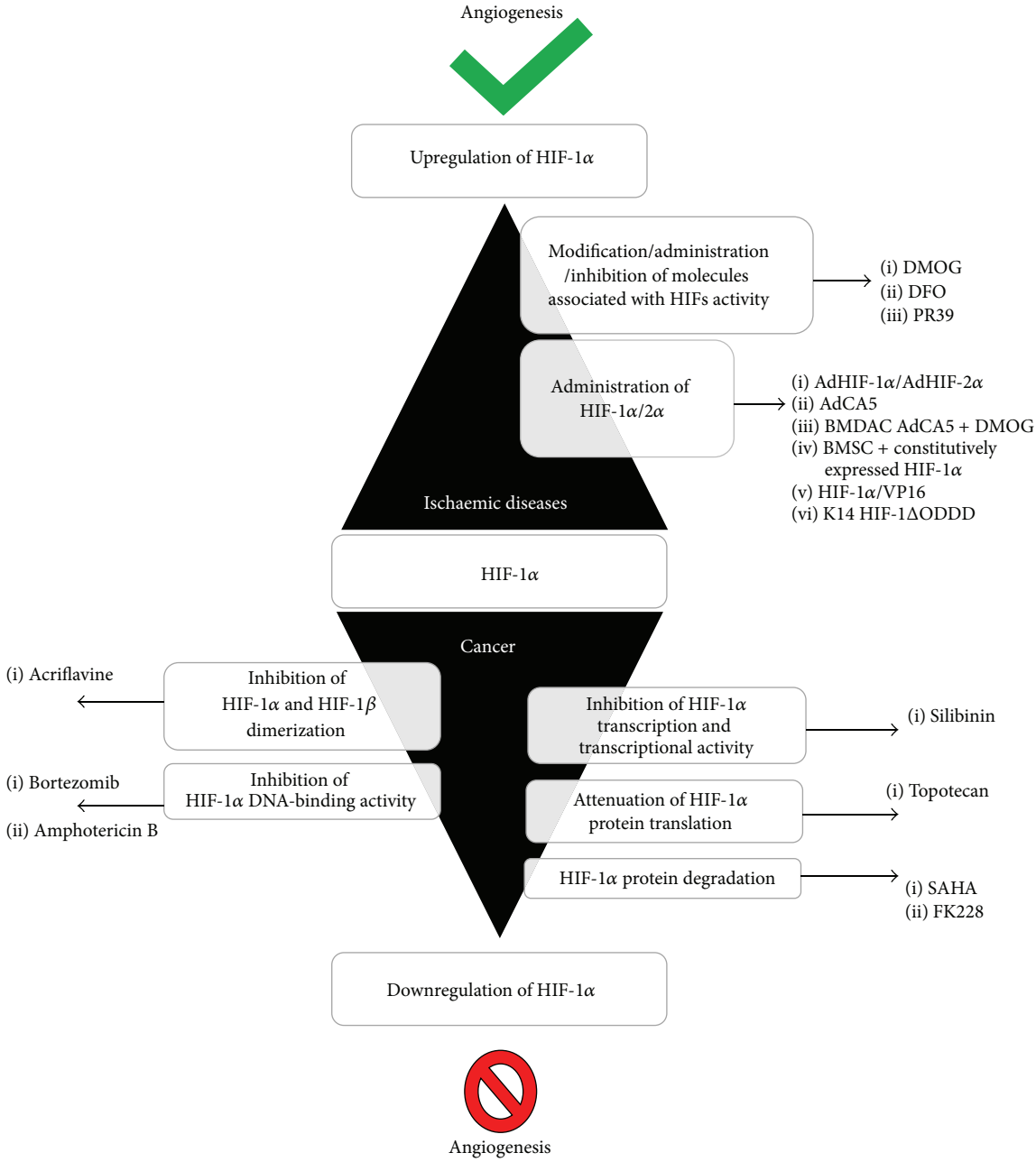

Figure 3: *Different strategies in HIF-1α therapies*. Depending on the type of disease and the expected therapeutic effect, different approaches are used in HIF-1 therapies: HIF-1 upregulation (ischaemia) to induce angiogenesis or HIF-1 inhibition to attenuate angiogenesis (cancer). DMOG: dimethyloxalylglycine; DFO: 2-OG analogue (N-oxalylglycine); PR39: macrophage-derived peptide; AdHIF-1α and AdHIF-2α: adenoviral vector; AdCA5: adenovirus encoding a constitutively active form of the HIF-1α; BMDAC: bone marrow-derived angiogenic cells; HIF-1α/VP16: DNA-binding and dimerisation domains of HIF-1α fused with the transactivation domain of herpes simplex virus; K14-HIF-1ΔODD: vector encoding O_2-independent HIF-1α under the keratin 14 promoter. Silibinin: nontoxic flavonoid; topotecan: chemotherapeutic agent that is a topoisomerase inhibitor; SAHA and FK228: histone deacetylase inhibitors; acriflavine, bortezomib; amphotericin B: anti-HIF drugs.

the infarcted region [121]. Then, capillary growth is followed by HIF-induced VEGF and Flk-1 upregulation. A novel strategy involves the preconditioning of rat bone marrow-derived mesenchymal stem cells (BMSCs) using DMOG to enhance their survival and therapeutic efficacy after transplantation into infarcted rat hearts. After DMOG treatment, these cells exhibited enhanced expression of survival and proangiogenic factors such as HIF-1α, vascular endothelial growth factor, and glucose transporter 1. Thus, the transplantation of DMOG-treated BMSCs reduced heart infarction size and promoted angiogenesis in the ischaemic region [123]. An alternative to the use of PHD inhibitor molecules is

the administration of a molecule that stabilises HIF-1α under normoxic conditions. PR39, which is a macrophage-derived peptide, achieved this effect by inhibiting HIF-1α degradation through the ubiquitin-proteasome system. The introduction of the PR39 peptide resulted in a significant increase in HIF-1α protein levels irrespective of ischaemia or hypoxia. Therefore, angiogenesis can be induced in the postinfarcted myocardium of transgenic mice [124].

4.2. Inhibition of HIF-1-Dependent Angiogenesis in Cancer Therapies. Cancer therapies are based on the targeted inhibition of proangiogenic factors. Current treatments are focused on the inhibition of VEGF activity. Because of studies regarding VEGF antiangiogenic therapy, patients were treated with bevacizumab (VEGF inhibitor) or sunitinib (VEGFR2 inhibitor) [125]. Since the discovery that the HIF-1 pathway regulates the activation of many proangiogenic factors in tumours and may promote metastasis, the HIF-1α subunit has been considered an attractive target for new cancer therapeutics. The inhibition of HIF-1-dependent angiogenesis involves the regulation of HIF-1α activity by molecules that modulate HIF-1α transcription and transcriptional activity, HIF-1α and HIF-1β dimerisation, HIF-1α protein translation, HIF-1α DNA binding, and HIF-1α protein degradation [24, 126].

Thus far, the Food and Drug Administration has approved several anti-HIF drugs. For instance, bortezomib and amphotericin B functionally inhibit HIF-1α, thereby preventing p300 recruitment by enhancing the interaction between FIH-1 and the HIF-1α C-terminal transactivation domain (C-TAD) [127, 128]. In contrast, silibinin is a nontoxic flavonoid that is able to inhibit hypoxia-dependent HIF-1α accumulation and to inhibit HIF-1 transcriptional activity in HeLa and hepatoma cells [129]. Silibinin is also a potent inhibitor of cell proliferation. Two other drugs, SAHA and FK228, are histone deacetylase inhibitors that were found to promote HIF-1α degradation by upregulating p53 and VHL. These drugs have been successfully used in the United States. HIF-1 activity might also be attenuated by previously used chemotherapeutics such as anthracycline and doxorubicin, which act by inhibiting HIF-1α DNA-binding activity, and acriflavine, which prevents HIF subunit dimerisation [130, 131].

Clinical trials are presently focused on other drugs that may attenuate HIF-1-dependent angiogenesis. Currently, flavopiridol (Alvocidib) is in phase III clinical trials. This synthetic flavonoid, which is derived from an alkaloid Indian plant, was found to be a potent inhibitor of the transcription of HIF-1α and of many other genes involved in cell cycle arrest [132, 133]. Other clinical studies (phases I and II) are being conducted with many other drugs that involve HIF-1 degradation, downregulation, or inactivation.

Conflict of Interests

The authors declare that no conflict of interests exists regarding the publication of this paper.

Acknowledgments

This study was supported by the National Science Centre Grants nos. 2012/07/N/NZ3/01687 and 2014/13/B/NZ3/04646 and by the National Centre for Research and Development Grant no. STRATEGMED1/233624/5/NCBR/2014.

References

[1] G. L. Semenza, "Hypoxia-inducible factor 1 and cardiovascular disease," *Annual Review of Physiology*, vol. 76, pp. 39–56, 2014.

[2] P. Carmeliet, "Mechanisms of angiogenesis and arteriogenesis," *Nature Medicine*, vol. 6, no. 4, pp. 389–395, 2000.

[3] W. Risau, "Mechanisms of angiogenesis," *Nature*, vol. 386, no. 6626, pp. 671–674, 1997.

[4] W. Risau and I. Flamme, "Vasculogenesis," *Annual Review of Cell and Developmental Biology*, vol. 11, pp. 73–91, 1995.

[5] P. Carmeliet, "Angiogenesis in health and disease," *Nature Medicine*, vol. 9, no. 6, pp. 653–660, 2003.

[6] G. D. Yancopoulos, S. Davis, N. W. Gale, J. S. Rudge, S. J. Wiegand, and J. Holash, "Vascular-specific growth factors and blood vessel formation," *Nature*, vol. 407, no. 6801, pp. 242–248, 2000.

[7] B. P. Eliceiri, R. Paul, P. L. Schwartzberg, J. D. Hood, J. Leng, and D. A. Cheresh, "Selective requirement for Src kinases during VEGF-induced angiogenesis and vascular permeability," *Molecular Cell*, vol. 4, no. 6, pp. 915–924, 1999.

[8] G. Thurston, J. S. Rudge, E. Ioffe et al., "Angiopoietin-1 protects the adult vasculature against plasma leakage," *Nature Medicine*, vol. 6, no. 4, pp. 460–463, 2000.

[9] P. C. Maisonpierre, C. Suri, P. F. Jones et al., "Angiopoietin-2, a natural antagonist for Tie2 that disrupts in vivo angiogenesis," *Science*, vol. 277, no. 5322, pp. 55–60, 1997.

[10] A. R. Nelson, B. Fingleton, M. L. Rothenberg, and L. M. Matrisian, "Matrix metalloproteinases: biologic activity and clinical implications," *Journal of Clinical Oncology*, vol. 18, no. 5, pp. 1135–1149, 2000.

[11] E. M. Conway, D. Collen, and P. Carmeliet, "Molecular mechanisms of blood vessel growth," *Cardiovascular Research*, vol. 49, no. 3, pp. 507–521, 2001.

[12] B. P. Eliceiri and D. A. Cheresh, "The role of αv integrins during angiogenesis: insights into potential mechanisms of action and clinical development," *Journal of Clinical Investigation*, vol. 103, no. 9, pp. 1227–1230, 1999.

[13] M. Corada, M. Mariotti, G. Thurston et al., "Vascular endothelial-cadherin is an important determinant of microvascular integrity in vivo," *Proceedings of the National Academy of Sciences of the United States of America*, vol. 96, no. 17, pp. 9815–9820, 1999.

[14] K. A. Knudsen, C. Frankowski, K. R. Johnson, and M. J. Wheelock, "A role for cadherins in cellular signaling and differentiation," *Journal of Cellular Biochemistry*, vol. 30-31, pp. 168–176, 1998.

[15] P. Lindahl, M. Hellström, M. Kalén, and C. Betsholtz, "Endothelial-perivascular cell signaling in vascular development: lessons from knockout mice," *Current Opinion in Lipidology*, vol. 9, no. 5, pp. 407–411, 1998.

[16] P. J. Polverini, "The pathophysiology of angiogenesis," *Critical Reviews in Oral Biology and Medicine*, vol. 6, no. 3, pp. 230–247, 1995.

[17] A. S. Chung, J. Lee, and N. Ferrara, "Targeting the tumour vasculature: insights from physiological angiogenesis," *Nature Reviews Cancer*, vol. 10, no. 7, pp. 505–514, 2010.

[18] R. S. Kerbel, "Tumor angiogenesis," *The New England Journal of Medicine*, vol. 358, no. 19, pp. 2039–2049, 2008.

[19] N. Ferrara and R. S. Kerbel, "Angiogenesis as a therapeutic target," *Nature*, vol. 438, no. 7070, pp. 967–974, 2005.

[20] R. K. Jain, "Molecular regulation of vessel maturation," *Nature Medicine*, vol. 9, no. 6, pp. 685–693, 2003.

[21] J. A. Nagy, S.-H. Chang, A. M. Dvorak, and H. F. Dvorak, "Why are tumour blood vessels abnormal and why is it important to know?" *British Journal of Cancer*, vol. 100, no. 6, pp. 865–869, 2009.

[22] G. L. Semenza, "Life with oxygen," *Science*, vol. 318, no. 5847, pp. 62–64, 2007.

[23] J. A. Bertout, S. A. Patel, and M. C. Simon, "The impact of O_2 availability on human cancer," *Nature Reviews Cancer*, vol. 8, no. 12, pp. 967–975, 2008.

[24] B. L. Krock, N. Skuli, and M. C. Simon, "Hypoxia-induced angiogenesis: good and evil," *Genes and Cancer*, vol. 2, no. 12, pp. 1117–1133, 2011.

[25] Z. Yun, Q. Lin, and A. J. Giaccia, "Adaptive myogenesis under hypoxia," *Molecular and Cellular Biology*, vol. 25, no. 8, pp. 3040–3055, 2005.

[26] J. I. Bárdos and M. Ashcroft, "Negative and positive regulation of HIF-1: a complex network," *Biochimica et Biophysica Acta—Reviews on Cancer*, vol. 1755, no. 2, pp. 107–120, 2005.

[27] G. L. Semenza and G. L. Wang, "A nuclear factor induced by hypoxia via de novo protein synthesis binds to the human erythropoietin gene enhancer at a site required for transcriptional activation," *Molecular and Cellular Biology*, vol. 12, no. 12, pp. 5447–5454, 1992.

[28] G. L. Wang and G. L. Semenza, "Characterization of hypoxia-inducible factor 1 and regulation of DNA binding activity by hypoxia," *The Journal of Biological Chemistry*, vol. 268, no. 29, pp. 21513–21518, 1993.

[29] R. J. Kewley, M. L. Whitelaw, and A. Chapman-Smith, "The mammalian basic helix-loop-helix/PAS family of transcriptional regulators," *International Journal of Biochemistry and Cell Biology*, vol. 36, no. 2, pp. 189–204, 2004.

[30] G. L. Wang, B.-H. Jiang, E. A. Rue, and G. L. Semenza, "Hypoxia-inducible factor 1 is a basic-helix-loop-helix-PAS heterodimer regulated by cellular O_2 tension," *Proceedings of the National Academy of Sciences of the United States of America*, vol. 92, no. 12, pp. 5510–5514, 1995.

[31] S. T. Crews, "Control of cell lineage-specific development and transcription by bHLH-PAS proteins," *Genes and Development*, vol. 12, no. 5, pp. 607–620, 1998.

[32] R. H. Wenger, D. P. Stiehl, and G. Camenisch, "Integration of oxygen signaling at the consensus HRE," *Science's STKE*, vol. 2005, no. 306, article re12, 2005.

[33] J. L. Ruas, L. Poellinger, and T. Pereira, "Functional analysis of hypoxia-inducible factor-1 alpha mediated transactivation. Identification of amino acid residues critical for transcriptional activation and/or interaction with CREB-binding protein," *The Journal of Biological Chemistry*, vol. 277, no. 41, pp. 38723–38730, 2002.

[34] B.-H. Jiang, J. Z. Zheng, S. W. Leung, R. Roe, and G. L. Semenza, "Transactivation and inhibitory domains of hypoxia-inducible factor 1α: modulation of transcriptional activity by oxygen tension," *The Journal of Biological Chemistry*, vol. 272, no. 31, pp. 19253–19260, 1997.

[35] C. W. Pugh, J. F. O'Rourke, M. Nagao, J. M. Gleadle, and P. J. Ratcliffe, "Activation of hypoxia-inducible factor-1: definition of regulatory domains within the α subunit," *The Journal of Biological Chemistry*, vol. 272, no. 17, pp. 11205–11214, 1997.

[36] B.-H. Jiang, G. L. Semenza, C. Bauer, and H. H. Marti, "Hypoxia-inducible factor 1 levels vary exponentially over a physiologically relevant range of O_2 tension," *The American Journal of Physiology—Cell Physiology*, vol. 271, no. 4, pp. C1172–C1180, 1996.

[37] S. Salceda and J. Caro, "Hypoxia-inducible factor 1α (HIF-1α) protein is rapidly degraded by the ubiquitin-proteasome system under normoxic conditions. Its stabilization by hypoxia depends on redox-induced changes," *Journal of Biological Chemistry*, vol. 272, no. 36, pp. 22642–22647, 1997.

[38] M. Ema, S. Taya, N. Yokotani, K. Sogawa, Y. Matsuda, and Y. Fujii-Kuriyama, "A novel bHLH-PAS factor with close sequence similarity to hypoxia-inducible factor 1α regulates the *VEGF* expression and is potentially involved in lung and vascular development," *Proceedings of the National Academy of Sciences of the United States of America*, vol. 94, no. 9, pp. 4273–4278, 1997.

[39] Y.-Z. Gu, S. M. Moran, J. B. Hogenesch, L. Wartman, and C. A. Bradfield, "Molecular characterization and chromosomal localization of a third α-class hypoxia inducible factor subunit, HIF3α," *Gene Expression*, vol. 7, no. 3, pp. 205–213, 1998.

[40] Y. Makino, R. Cao, K. Svensson et al., "Inhibitory PAS domain protein is a negative regulator of hypoxia-inducible gene expression," *Nature*, vol. 414, no. 6863, pp. 550–554, 2001.

[41] W. G. Kaelin Jr., "Proline hydroxylation and gene expression," *Annual Review of Biochemistry*, vol. 74, pp. 115–128, 2005.

[42] V. Srinivas, L.-P. Zhang, X.-H. Zhu, and J. Caro, "Characterization of an oxygen/redox-dependent degradation domain of hypoxia-inducible factor α (HIF-α) proteins," *Biochemical and Biophysical Research Communications*, vol. 260, no. 2, pp. 557–561, 1999.

[43] N. Masson and P. J. Ratcliffe, "HIF prolyl and asparaginyl hydroxylases in the biological response to intracellular O_2 levels," *Journal of Cell Science*, vol. 116, no. 15, pp. 3041–3049, 2003.

[44] N. Masson, C. Willam, P. H. Maxwell, C. W. Pugh, and P. J. Ratcliffe, "Independent function of two destruction domains in hypoxia-inducible factor-α chains activated by prolyl hydroxylation," *EMBO Journal*, vol. 20, no. 18, pp. 5197–5206, 2001.

[45] L. A. McNeill, K. S. Hewitson, J. M. Gleadle et al., "The use of dioxygen by HIF prolyl hydroxylase (PHD1)," *Bioorganic & Medicinal Chemistry Letters*, vol. 12, no. 12, pp. 1547–1550, 2002.

[46] K. S. Hewitson, L. A. McNeill, M. V. Riordan et al., "Hypoxia-inducible factor (HIF) asparagine hydroxylase is identical to factor inhibiting HIF (FIH) and is related to the cupin structural family," *The Journal of Biological Chemistry*, vol. 277, no. 29, pp. 26351–26355, 2002.

[47] D. Lando, D. J. Peet, D. A. Whelan, J. J. Gorman, and M. L. Whitelaw, "Asparagine hydroxylation of the HIF transactivation domain: a hypoxic switch," *Science*, vol. 295, no. 5556, pp. 858–861, 2002.

[48] D. Lando, D. J. Peet, J. J. Gorman, D. A. Whelan, M. L. Whitelaw, and R. K. Bruick, "FIH-1 is an asparaginyl hydroxylase enzyme that regulates the transcriptional activity of hypoxia-inducible factor," *Genes and Development*, vol. 16, no. 12, pp. 1466–1471, 2002.

[49] P. C. Mahon, K. Hirota, and G. L. Semenza, "FIH-1: a novel protein that interacts with HIF-1α and VHL to mediate repression

of HIF-1 transcriptional activity," *Genes and Development*, vol. 15, no. 20, pp. 2675–2686, 2001.

[50] W. G. Kaelin Jr. and P. J. Ratcliffe, "Oxygen sensing by metazoans: the central role of the HIF hydroxylase pathway," *Molecular Cell*, vol. 30, no. 4, pp. 393–402, 2008.

[51] C. J. Schofield and Z. Zhang, "Structural and mechanistic studies on 2-oxoglutarate-dependent oxygenases and related enzymes," *Current Opinion in Structural Biology*, vol. 9, no. 6, pp. 722–731, 1999.

[52] Q. Ke and M. Costa, "Hypoxia-inducible factor-1 (HIF-1)," *Molecular Pharmacology*, vol. 70, no. 5, pp. 1469–1480, 2006.

[53] D. J. Manalo, A. Rowan, T. Lavoie et al., "Transcriptional regulation of vascular endothelial cell responses to hypoxia by HIF-1," *Blood*, vol. 105, no. 2, pp. 659–669, 2005.

[54] P. J. Kallio, I. Pongratz, K. Gradin, J. McGuire, and L. Poellinger, "Activation of hypoxia-inducible factor 1α: posttranscriptional regulation and conformational change by recruitment of the Arnt transcription factor," *Proceedings of the National Academy of Sciences of the United States of America*, vol. 94, no. 11, pp. 5667–5672, 1997.

[55] P. J. Kallio, K. Okamoto, S. O'Brien et al., "Signal transduction in hypoxic cells: inducible nuclear translocation and recruitment of the CBP/p300 coactivator by the hypoxia-inducible factor-1α," *The EMBO Journal*, vol. 17, no. 22, pp. 6573–6586, 1998.

[56] G. L. Semenza, M. K. Nejfelt, S. M. Chi, and S. E. Antonarakis, "Hypoxia-inducible nuclear factors bind to an enhancer element located 3′ to the human erythropoietin gene," *Proceedings of the National Academy of Sciences of the United States of America*, vol. 88, no. 13, pp. 5680–5684, 1991.

[57] T. N. Seagroves, H. E. Ryan, H. Lu et al., "Transcription factor HIF-1 is a necessary mediator of the pasteur effect in mammalian cells," *Molecular and Cellular Biology*, vol. 21, no. 10, pp. 3436–3444, 2001.

[58] C. V. Dang and G. L. Semenza, "Oncogenic alterations of metabolism," *Trends in Biochemical Sciences*, vol. 24, no. 2, pp. 68–72, 1999.

[59] G. L. Semenza, P. H. Roth, H.-M. Fang, and G. L. Wang, "Transcriptional regulation of genes encoding glycolytic enzymes by hypoxia-inducible factor 1," *The Journal of Biological Chemistry*, vol. 269, no. 38, pp. 23757–23763, 1994.

[60] R. H. Wenger, "Cellular adaptation to hypoxia: O_2-sensing protein hydroxylases, hypoxia-inducible transcription factors, and O_2-regulated gene expression," *The FASEB Journal*, vol. 16, no. 10, pp. 1151–1162, 2002.

[61] G. L. Semenza, "Regulation of metabolism by hypoxia-inducible factor 1," *Cold Spring Harbor Symposia on Quantitative Biology*, vol. 76, pp. 347–353, 2011.

[62] D. Feldser, F. Agani, N. V. Iyer, B. Pak, G. Ferreira, and G. L. Semenza, "Reciprocal positive regulation of hypoxia-inducible factor 1alpha and insulin-like growth factor 2," *Cancer Research*, vol. 59, no. 16, pp. 3915–3918, 1999.

[63] B. Krishnamachary, S. Berg-Dixon, B. Kelly et al., "Regulation of colon carcinoma cell invasion by hypoxia-inducible factor 1," *Cancer Research*, vol. 63, no. 5, pp. 1138–1143, 2003.

[64] M. Koning, P. M. N. Werker, M. J. A. van Luyn, and M. C. Harmsen, "Hypoxia promotes proliferation of human myogenic satellite cells: a potential benefactor in tissue engineering of skeletal muscle," *Tissue Engineering A*, vol. 17, no. 13-14, pp. 1747–1758, 2011.

[65] J. A. Mitchell and J. M. Yochim, "Intrauterine oxygen tension during the estrous cycle in the rat: its relation to uterine respiration and vascular activity," *Endocrinology*, vol. 83, no. 4, pp. 701–705, 1968.

[66] F. Rodesch, P. Simon, C. Donner, and E. Jauniaux, "Oxygen measurements in endometrial and trophoblastic tissues during early pregnancy," *Obstetrics and Gynecology*, vol. 80, no. 2, pp. 283–285, 1992.

[67] H. Diez, A. Fischer, A. Winkler et al., "Hypoxia-mediated activation of Dll4-Notch-Hey2 signaling in endothelial progenitor cells and adoption of arterial cell fate," *Experimental Cell Research*, vol. 313, no. 1, pp. 1–9, 2007.

[68] D. M. Adelman, E. Maltepe, and M. C. Simon, "Multilineage embryonic hematopoiesis requires hypoxic ARNT activity," *Genes and Development*, vol. 13, no. 19, pp. 2478–2483, 1999.

[69] N. V. Iyer, L. E. Kotch, F. Agani et al., "Cellular and developmental control of O_2 homeostasis by hypoxia-inducible factor 1α," *Genes & Development*, vol. 12, no. 2, pp. 149–162, 1998.

[70] K. R. Kozak, B. Abbott, and O. Hankinson, "ARNT-deficient mice and placental differentiation," *Developmental Biology*, vol. 191, no. 2, pp. 297–305, 1997.

[71] D. M. Adelman, M. Gertsenstein, A. Nagy, M. C. Simon, and E. Maltepe, "Placental cell fates are regulated in vivo by HIF-mediated hypoxia responses," *Genes and Development*, vol. 14, no. 24, pp. 3191–3203, 2000.

[72] K. D. Cowden Dahl, B. H. Fryer, F. A. Mack et al., "Hypoxia-inducible factors 1α and 2α regulate trophoblast differentiation," *Molecular and Cellular Biology*, vol. 25, no. 23, pp. 10479–10491, 2005.

[73] K. Takeda, V. C. Ho, H. Takeda, L. J. Duan, A. Nagy, and G.-H. Fong, "Placental but not heart defects are associated with elevated hypoxia-inducible factor α levels in mice lacking prolyl hydroxylase domain protein 2," *Molecular and Cellular Biology*, vol. 26, no. 22, pp. 8336–8346, 2006.

[74] E. Maltepe, J. V. Schmidt, D. Baunoch, C. A. Bradfield, and M. C. Simon, "Abnormal angiogenesis and responses to glucose and oxygen deprivation in mice lacking the protein ARNT," *Nature*, vol. 386, no. 6623, pp. 403–407, 1997.

[75] D. L. Ramírez-Bergeron, A. Runge, D. M. Adelman, M. Gohil, and M. C. Simon, "HIF-dependent hematopoietic factors regulate the development of the embryonic vasculature," *Developmental Cell*, vol. 11, no. 1, pp. 81–92, 2006.

[76] A. E. Greijer, P. van der Groep, D. Kemming et al., "Upregualtion of gene expression by hypoxia is mediated predominantly by hypoxia-inducible factor I (HIF-I)," *Journal of Pathology*, vol. 206, no. 3, pp. 291–304, 2005.

[77] G. L. Semenza, "Angiogenesis in ischemic and neoplastic disorders," *Annual Review of Medicine*, vol. 54, pp. 17–28, 2003.

[78] D. J. Ceradini, A. R. Kulkarni, M. J. Callaghan et al., "Progenitor cell trafficking is regulated by hypoxic gradients through HIF-1 induction of SDF-1," *Nature Medicine*, vol. 10, no. 8, pp. 858–864, 2004.

[79] J. E. Park, G.-A. Keller, and N. Ferrara, "The vascular endothelial growth factor (VEGF) isoforms: differential deposition into the subepithelial extracellular matrix and bioactivity of extracellular matrix-bound VEGF," *Molecular Biology of the Cell*, vol. 4, no. 12, pp. 1317–1326, 1993.

[80] Y. Liu, S. R. Cox, T. Morita, and S. Kourembanas, "Hypoxia regulates vascular endothelial growth factor gene expression in endothelial cells: Identification of a 5′ enhancer," *Circulation Research*, vol. 77, no. 3, pp. 638–643, 1995.

[81] J. A. Forsythe, B.-H. Jiang, N. V. Iyer et al., "Activation of vascular endothelial growth factor gene transcription by hypoxia-inducible factor 1," *Molecular and Cellular Biology*, vol. 16, no. 9, pp. 4604–4613, 1996.

[82] H.-P. Gerber, F. Condorelli, J. Park, and N. Ferrara, "Differential transcriptional regulation of the two vascular endothelial growth factor receptor genes. Flt-1, but not Flk-1/KDR, is up-regulated by hypoxia," *The Journal of Biological Chemistry*, vol. 272, no. 38, pp. 23659–23667, 1997.

[83] J. Waltenberger, U. Mayr, S. Pentz, and V. Hombach, "Functional upregulation of the vascular endothelial growth factor receptor KDR by hypoxia," *Circulation*, vol. 94, no. 7, pp. 1647–1654, 1996.

[84] C. W. Pugh and P. J. Ratcliffe, "Regulation of angiogenesis by hypoxia: role of the HIF system," *Nature Medicine*, vol. 9, no. 6, pp. 677–684, 2003.

[85] D. R. Mole, C. Blancher, R. R. Copley et al., "Genome-wide association of hypoxia-inducible factor (HIF)-1α and HIF-2α DNA binding with expression profiling of hypoxia-inducible transcripts," *The Journal of Biological Chemistry*, vol. 284, no. 25, pp. 16767–16775, 2009.

[86] J. Schödel, S. Oikonomopoulos, J. Ragoussis, C. W. Pugh, P. J. Ratcliffe, and D. R. Mole, "High-resolution genome-wide mapping of HIF-binding sites by ChIP-seq," *Blood*, vol. 117, no. 23, pp. e207–e217, 2011.

[87] P. Carmeliet and R. K. Jain, "Molecular mechanisms and clinical applications of angiogenesis," *Nature*, vol. 473, no. 7347, pp. 298–307, 2011.

[88] Y. Ben-Yosef, A. Miller, S. Shapiro, and N. Lahat, "Hypoxia of endothelial cells leads to MMP-2-dependent survival and death," *The American Journal of Physiology—Cell Physiology*, vol. 289, no. 5, pp. C1321–C1331, 2005.

[89] S. Keely, L. E. Glover, C. F. MacManus et al., "Selective induction of integrin β1 by hypoxia-inducible factor: implications for wound healing," *The FASEB Journal*, vol. 23, no. 5, pp. 1338–1346, 2009.

[90] N. Skuli, L. Liu, A. Runge et al., "Endothelial deletion of hypoxia-inducible factor-2α (HIF-2α) alters vascular function and tumor angiogenesis," *Blood*, vol. 114, no. 2, pp. 469–477, 2009.

[91] H. Niemi, K. Honkonen, P. Korpisalo et al., "HIF-1α and HIF-2α induce angiogenesis and improve muscle energy recovery," *European Journal of Clinical Investigation*, vol. 44, no. 10, pp. 989–999, 2014.

[92] C. Yuan, P. Wang, L. Zhu et al., "Coculture of stem cells from apical papilla and human umbilical vein endothelial cell under hypoxia increases the formation of three-dimensional vessel-like structures *in vitro*," *Tissue Engineering Part A*, vol. 21, no. 5-6, 2015.

[93] S. Rajagopalan, J. Olin, S. Deitcher et al., "Use of a constitutively active hypoxia-inducible factor-1α transgene as a therapeutic strategy in no-option critical limb ischemia patients: phase I dose-escalation experience," *Circulation*, vol. 115, no. 10, pp. 1234–1243, 2007.

[94] L. Holmgren, M. S. O'Reilly, and J. Folkman, "Dormancy of micrometastases: balanced proliferation and apoptosis in the presence of angiogenesis suppression," *Nature Medicine*, vol. 1, no. 2, pp. 149–153, 1995.

[95] J. Folkman, "Tumour angiogenesis," in *Cancer Medicine*, J. F. Holland, R. C. Bast Jr., D. L. Morton, E. Frei III, D. W. Kufe, and R. R. Weichselbaum, Eds., pp. 181–204, Williams & Wilkins, Baltimore, Md, USA, 1997.

[96] E. B. Rankin and A. J. Giaccia, "The role of hypoxia-inducible factors in tumorigenesis," *Cell Death and Differentiation*, vol. 15, no. 4, pp. 678–685, 2008.

[97] J. M. Brown and A. J. Giaccia, "The unique physiology of solid tumours: opportunities (and problems) for cancer therapy," *Cancer Research*, vol. 58, no. 7, pp. 1408–1416, 1998.

[98] G. L. Semenza, "Hypoxia, clonal selection, and the role of HIF-1 in tumor progression," *Critical Reviews in Biochemistry and Molecular Biology*, vol. 35, no. 2, pp. 71–103, 2000.

[99] R. Ravi, B. Mookerjee, Z. M. Bhujwalla et al., "Regulation of tumor angiogenesis by p53-induced degradation of hypoxia-inducible factor 1α," *Genes and Development*, vol. 14, no. 1, pp. 34–44, 2000.

[100] W. Zundel, C. Schindler, D. Haas-Kogan et al., "Loss of PTEN facilitates HIF-1-mediated gene expression," *Genes and Development*, vol. 14, no. 4, pp. 391–396, 2000.

[101] E. Laughner, P. Taghavi, K. Chiles, P. C. Mahon, and G. L. Semenza, "HER2 (neu) signaling increases the rate of hypoxia-inducible factor 1α (HIF-1α) synthesis: novel mechanism for HIF-1-mediated vascular endothelial growth factor expression," *Molecular and Cellular Biology*, vol. 21, no. 12, pp. 3995–4004, 2001.

[102] W. G. Kaelin Jr., "Molecular basis of the VHL hereditary cancer syndrome," *Nature Reviews Cancer*, vol. 2, no. 9, pp. 673–682, 2002.

[103] P. H. Maxwell, M. S. Wlesener, G. W. Chang et al., "The tumour suppressor protein VHL targets hypoxia-inducible factors for oxygen-dependent proteolysis," *Nature*, vol. 399, no. 6733, pp. 271–275, 1999.

[104] O. Iliopoulos, A. Kibel, S. Gray, and W. G. Kaelin Jr., "Tumour suppression by the human von Hippel-Lindau gene product," *Nature Medicine*, vol. 1, no. 8, pp. 822–826, 1995.

[105] K. Kondo, J. Klco, E. Nakamura, M. Lechpammer, and W. G. Kaelin Jr., "Inhibition of HIF is necessary for tumor suppression by the von Hippel-Lindau protein," *Cancer Cell*, vol. 1, no. 3, pp. 237–246, 2002.

[106] J. K. Maranchie, J. R. Vasselli, J. Riss, J. S. Bonifacino, W. M. Linehan, and R. D. Klausner, "The contribution of VHL substrate binding and HIF1-α to the phenotype of VHL loss in renal cell carcinoma," *Cancer Cell*, vol. 1, no. 3, pp. 247–255, 2002.

[107] R. R. Raval, K. W. Lau, M. G. B. Tran et al., "Contrasting properties of hypoxia-inducible factor 1 (HIF-1) and HIF-2 in von Hippel-Lindau-associated renal cell carcinoma," *Molecular and Cellular Biology*, vol. 25, no. 13, pp. 5675–5686, 2005.

[108] H. Lu, R. A. Forbes, and A. Verma, "Hypoxia-inducible factor 1 activation by aerobic glycolysis implicates the Warburg effect in carcinogenesis," *The Journal of Biological Chemistry*, vol. 277, no. 26, pp. 23111–23115, 2002.

[109] Z. Wang, C. Dabrosin, X. Yin et al., "Broad targeting of angiogenesis for cancer prevention and therapy," *Seminars in Cancer Biology*, 2015.

[110] P. N. Span and J. Bussink, "Biology of hypoxia," *Seminars in Nuclear Medicine*, vol. 45, no. 2, pp. 101–109, 2015.

[111] A. Zimna, A. Janeczek, N. Rozwadowska et al., "Biological properties of human skeletal myoblasts genetically modified to simultaneously overexpress the pro-angiogenic factors vascular endothelial growth factor-A and fibroblast growth factor-4," *Journal of Physiology and Pharmacology*, vol. 65, no. 2, pp. 193–207, 2014.

[112] S. Kolakowski Jr., M. F. Berry, P. Atluri et al., "Placental growth factor provides a novel local angiogenic therapy for ischemic cardiomyopathy," *Journal of Cardiac Surgery*, vol. 21, no. 6, pp. 559–564, 2006.

[113] S. Rajagopalan, E. R. Mohler III, R. J. Lederman et al., "Regional angiogenesis with vascular endothelial growth factor in peripheral arterial disease: a phase II randomized, double-blind, controlled study of adenoviral delivery of vascular endothelial growth factor 121 in patients with disabling intermittent claudication," *Circulation*, vol. 108, no. 16, pp. 1933–1938, 2003.

[114] R. J. Lederman, F. O. Mendelsohn, R. D. Anderson et al., "TRAFFIC Investigators. Therapeutic angiogenesis with recombinant fibroblast growth factor-2 for intermittent claudication (the TRAFFIC study): a randomised trial," *The Lancet*, vol. 359, no. 9323, pp. 2953–2958, 2002.

[115] K. Hirota and G. L. Semenza, "Regulation of angiogenesis by hypoxia-inducible factor 1," *Critical Reviews in Oncology/Hematology*, vol. 59, no. 1, pp. 15–26, 2006.

[116] T. H. Patel, H. Kimura, C. R. Weiss, G. L. Semenza, and L. V. Hofmann, "Constitutively active HIF-1α improves perfusion and arterial remodeling in an endovascular model of limb ischemia," *Cardiovascular Research*, vol. 68, no. 1, pp. 144–154, 2005.

[117] B. D. Kelly, S. F. Hackett, K. Hirota et al., "Cell type-specific regulation of angiogenic growth factor gene expression and induction of angiogenesis in nonischemic tissue by a constitutively active form of hypoxia-inducible factor 1," *Circulation Research*, vol. 93, no. 11, pp. 1074–1081, 2003.

[118] C. Yang, H. Liu, and D. Liu, "Mutant hypoxia-inducible factor 1α modified bone marrow mesenchymal stem cells ameliorate cerebral ischemia," *International Journal of Molecular Medicine*, vol. 34, no. 6, pp. 1622–1628, 2014.

[119] K.-G. Shyu, M.-T. Wang, B.-W. Wang et al., "Intramyocardial injection of naked DNA encoding HIF-1α/VP16 hybrid to enhance angiogenesis in an acute myocardial infarction model in the rat," *Cardiovascular Research*, vol. 54, no. 3, pp. 576–583, 2002.

[120] D. A. Elson, G. Thurston, L. E. Huang et al., "Induction of hypervascularity without leakage or inflammation in transgenic mice overexpressing hypoxia-inducible factor-1α," *Genes and Development*, vol. 15, no. 19, pp. 2520–2532, 2001.

[121] M. Milkiewicz, C. W. Pugh, and S. Egginton, "Inhibition of endogenous HIF inactivation induces angiogenesis in ischaemic skeletal muscles of mice," *Journal of Physiology*, vol. 560, no. 1, pp. 21–26, 2004.

[122] G. L. Wang and G. L. Semenza, "Desferrioxamine induces erythropoietin gene expression and hypoxia-inducible factor 1 DNA-binding activity: Implications for models of hypoxia signal transduction," *Blood*, vol. 82, no. 12, pp. 3610–3615, 1993.

[123] X. Liu, J. Wang, X. Ji, S. Yu, and L. Wei, "Preconditioning of bone marrow mesenchymal stem cells by prolyl hydroxylase inhibition enhances cell survival and angiogenesis in vitro and after transplantation into the ischemic heart of rats," *Stem Cell Research & Therapy*, vol. 5, no. 5, p. 111, 2014.

[124] J. Li, M. Post, R. Volk et al., "PR39, a peptide regulator of angiogenesis," *Nature Medicine*, vol. 61, pp. 49–55, 2000.

[125] K. Mittal, H. Koon, P. Elson et al., "Dual VEGF/VEGFR inhibition in advanced solid malignancies," *Cancer Biology & Therapy*, vol. 15, no. 8, pp. 975–981, 2014.

[126] Y. Hu, J. Liu, and H. Huang, "Recent agents targeting HIF-1α for cancer therapy," *Journal of Cellular Biochemistry*, vol. 114, no. 3, pp. 498–509, 2013.

[127] D. H. Shin, Y.-S. Chun, D. S. Lee, L. E. Huang, and J.-W. Park, "Bortezomib inhibits tumor adaptation to hypoxia by stimulating the FIH-mediated repression of hypoxia-inducible factor-1," *Blood*, vol. 111, no. 6, pp. 3131–3136, 2008.

[128] E. J. Yeo, Y. S. Chun, Y. S. Cho et al., "YC-1: a potential anticancer drug targeting hypoxia-inducible factor 1," *Journal of the National Cancer Institute*, vol. 95, no. 7, pp. 516–525, 2003.

[129] P. García-Maceira and J. Mateo, "Silibinin inhibits hypoxia-inducible factor-1α and mTOR/p70S6K/4E-BP1 signalling pathway in human cervical and hepatoma cancer cells: implications for anticancer therapy," *Oncogene*, vol. 28, no. 3, pp. 313–324, 2009.

[130] Y. M. Lee, S.-H. Kim, H.-S. Kim et al., "Inhibition of hypoxia-induced angiogenesis by FK228, a specific histone deacetylase inhibitor, via suppression of HIF-1α activity," *Biochemical and Biophysical Research Communications*, vol. 300, no. 1, pp. 241–246, 2003.

[131] S. Shankar, R. Davis, K. P. Singh, R. Kurzrock, D. D. Ross, and R. K. Srivastava, "Suberoylanilide hydroxamic acid (Zolinza/vorinostat) sensitizes TRAIL-resistant breast cancer cells orthotopically implanted in BALB/c nude mice," *Molecular Cancer Therapeutics*, vol. 8, no. 6, pp. 1596–1605, 2009.

[132] E. W. Newcomb, M. A. Ali, T. Schnee et al., "Flavopiridol downregulates hypoxia-mediated hypoxia-inducible factor-1α expression in human glioma cells by a proteasome-independent pathway: implications for in vivo therapy," *Neuro-Oncology*, vol. 7, no. 3, pp. 225–235, 2005.

[133] M. V. Blagosklonny, "Flavopiridol, an inhibitor of transcription: implications, problems and solutions," *Cell Cycle*, vol. 3, no. 12, pp. 1537–1542, 2004.

[134] C. J. Yeom, L. Zeng, Y. Zhu, M. Hiraoka, and H. Harada, "Strategies to assess hypoxic/HIF-1-active cancer cells for the development of innovative radiation therapy," *Cancers*, vol. 3, no. 3, pp. 3610–3631, 2011.

Hindawi Publishing Corporation
BioMed Research International
Volume 2015, Article ID 317905, 10 pages
http://dx.doi.org/10.1155/2015/317905

Research Article

OSM Enhances Angiogenesis and Improves Cardiac Function after Myocardial Infarction

Xiaotian Zhang,[1] Di Zhu,[1] Liping Wei,[2] Zhijing Zhao,[1] Xin Qi,[2] Zongjin Li,[3] and Dongdong Sun[1]

[1]*Department of Cardiology, Xijing Hospital, Fourth Military Medical University, 127 West Changle Road, Xi'an, Shaanxi 710032, China*
[2]*Department of Cardiology, Tianjin Union Medicine Center, Tianjin 300121, China*
[3]*Department of Pathophysiology, Nankai University School of Medicine, 94 Weijin Road, Tianjin 300071, China*

Correspondence should be addressed to Zongjin Li; zongjinli@nankai.edu.cn and Dongdong Sun; wintersun3@gmail.com

Received 8 August 2014; Revised 12 November 2014; Accepted 15 November 2014

Academic Editor: Francesco Moccia

Oncostatin M (OSM) has been reported to stimulate angiogenesis by upregulating VEGF and bFGF, implying that it could be a therapeutic strategy in treating ischemic diseases. The present study was aimed at investigating whether OSM could improve cardiac function via prompting angiogenesis following myocardial infarction (MI). Wild type (WT) and Oβ knock-out (O$\beta^{-/-}$) mice were, respectively, randomized into sham group, MI + vehicle group, and MI + OSM group. WT mice displayed significantly impaired cardiac function after MI. OSM treatment attenuated cardiac dysfunction in WT MI mice, while Oβ deletion abrogated the protective effects. Besides, OSM attenuated heart hypertrophy and pulmonary congestion evidenced by decreased heart weight/body weight and lung weight/body weight ratio. Further, reduction of apoptosis and fibrosis in infarct border zone was observed in OSM treated WT MI mice compared with vehicle. Moreover, in WT mice subjected to MI, OSM treatment significantly increased capillary density along with upregulation of p-Akt and angiogenic factors VEGF and bFGF in comparison with vehicle, and this phenomenon was not found in O$\beta^{-/-}$ mice. In conclusion, OSM treatment preserved cardiac function, inhibited apoptosis and fibrosis, and stimulated angiogenesis via upregulating VEGF and bFGF in infarct border zone of ischemic myocardium, indicating that OSM could be a novel therapeutic target for MI.

1. Introduction

Myocardial infarction (MI) remains one of the major causes of mortality and disability worldwide [1, 2]. Loss of cardiomyocytes in the infarction area and remodeling of the spared myocardium result in cardiac dysfunction [3]. Although MI triggers a spontaneous angiogenic response which could reestablish myocardial blood flow, this protective response is usually insufficient to restore the physiological level of perfusion [4]. Hence, therapeutic induction of angiogenesis is recognized to be a valid approach to restore the supply of oxygen and nutrients to the ischemic regions and improve compromised cardiac function [5, 6].

Oncostatin M (OSM) is a member of the interleukin-6 (IL-6) cytokine family produced by inflammatory cells. Murine OSM binds to its receptor Oβ, which exists as a part of a heterodimer with the glycoprotein 130 (gp130) signal transducer, and exerts multiple physiological functions. Previous studies have reported that OSM is involved in regulating cell proliferation, differentiation, survival, regeneration, and remodeling of various tissues [7]. Gwechenberger et al. reported that OSM contributed to the process of cardiomyocytes repair after myocardial infarction [8] and Pöling et al. have confirmed that blocking OSM signaling attenuates inflammatory dilative cardiomyopathy [9]. Besides, OSM also has the ability to upregulate some potent angiogenic factors, such as vascular endothelial growth factor (VEGF) [10], basic fibroblast growth factor (bFGF) [11, 12], and angiopoietin2 (Ang2) [13]. Whether OSM could induce angiogenesis in the heart after myocardial infarction thus restoring myocardial perfusion remains largely unknown.

Therefore, the aim of the study was to establish the role of OSM in enhancing VEGF and bFGF production, reducing cardiomyocytes fibrosis and apoptosis, and improving cardiac function after myocardial infarction.

2. Methods

2.1. Experimental Animals. Animal experiments were performed following the guidelines in accordance with the National Institutes of Health Guidelines on the Use of Laboratory Animals and were approved by the Fourth Military Medical University Ethic Committee on Animal Care. 129-Osmrtm1.1Nat/J mice were purchased from Jackson Laboratory (Bar Harbor, Maine, USA) which possess loxP sites on both sides of the second exon (first coding exon) of the oncostatin M receptor (Oβ) gene. 129-Osmrtm1.1Nat/J mice were crossed with C-Tg (CMV-cre) 1 Cgn/J mice (Jackson Laboratory, USA) to knockout oncostatin M receptor Oβ. PCR analysis was used to screen O$\beta^{-/-}$ mice, and O$\beta^{+/+}$ mice (weight 23–25 g) were used as control. Mice were randomly allocated into six groups: (1) sham (WTS); (2) myocardial infarction (MI) + vehicle (WTMI); (3) WTMI + OSM; (4) O$\beta^{-/-}$ sham (O$\beta^{-/-}$S); (5) O$\beta^{-/-}$MI + vehicle (O$\beta^{-/-}$MI); (6) O$\beta^{-/-}$MI + OSM. MI was induced by permanent left anterior descending (LAD) coronary artery ligation. Sham groups underwent identical surgical procedure without coronary ligation.

2.2. Surgical Procedures. Mice were anesthetized with 3% isoflurane, then orally intubated with a 22G IV catheter, and ventilated with a rodent respirator (Harvard Apparatus, Hilliston, USA). MI was produced by temporarily exteriorizing the heart via a left thoracic incision and placing a 6-0 silk suture around the left anterior descending coronary artery. The lungs were inflated by positive end-expiratory pressure and the chest was closed with 6.0 nylon suture. After surgery, the animals were weaned from the respirator and then placed on a heating pad for recovery. Sham mice underwent the same surgical procedures except for the fact that the suture placed under the left coronary artery was not tied.

2.3. OSM Treatment Protocol. OSM-treated mice received OSM injection after operation. OSM (R&D Systems, Inc., Minneapolis, MN, USA) was dissolved in sterile PBS containing 0.1% bovine serum albumin and injected intraperitoneally twice a day with 60 ng per gram of body weight for 14 days. Vehicle group received the same volume of sterile PBS containing 0.1% bovine serum albumin as for 14 days.

2.4. Echocardiography for Determination of Cardiac Function. Echocardiography was conducted 4 weeks after MI. Mice were sedated using 3% isoflurane and transthoracic echocardiography was performed by Vevo 2100 ultrasound system (Visual-Sonics, Toronto, Canada) with a 30 MHz linear transducer. Left ventricular ejection fraction (EF), left ventricular fractional shortening (FS), diastolic left ventricular internal diameter (LVIDd), and systolic left ventricular internal diameter (LVIDs) were calculated by the use of computer algorithms. All measurements were calculated based on the statistics of 4 consecutive cardiac cycles and all of these measurements were performed in a blinded manner [14].

2.5. Determination of Apoptosis. Heart samples were fixed in 4% paraformaldehyde and then paraffin embedded at day 14 as previously described [15]. Then, the hearts were cut into 5 μm sections. Terminal deoxynucleotidyl transferase-mediated dUTP nick-end labeling (TUNEL) staining was carried out using a commercially available kit according to the manufacturer's instructions (Promega, Madison, WI, USA). Nuclei were stained by DAPI (Roche). Ten fields in the infarct border zone were randomly selected from each section for the calculation of the percentage of apoptotic nuclei (apoptotic nuclei/total nuclei) and the obtained ratios were averaged for statistical analysis.

2.6. Determination of Cardiac Fibrosis. To determine cardiac fibrosis of the heart, paraffin embedded sections (4 μm) of the heart were stained by Masson's trichrome staining. In brief, the sections were deparaffinized in histo-clear and rehydrated using sequential passage through 100 to 70% ethanol for 6 min each followed by washing in distilled water three times. The slides were then stained with Weigert's iron hematoxylin for 10 min and washed under tap water for 10 min. The sections were washed again in distilled water and then stained with Biebrich scarlet-acid fuchsin solution for 15 min, in phosphomolybdic-phosphotungstic acid solution for 15 min and aniline blue solution, and stained for 10 min. The sections were rinsed briefly in distilled water and were treated with 1% acetic acid solution for 5 min. After a final wash in distilled water, the sections were dehydrated through sequential gradient of 70–100% alcohol followed by histo-clear wash and then mounted using Permount. The heart tissue sections were digitally imaged in high pixel resolution on an Epson Scanner.

2.7. Quantitative Real-Time PCR. RNA was isolated by using a NucleoSpin RNA II kit (Macherey-Nagel GmbH) and cDNA prepared with a Reverse Transcription System kit (Promega Corp). Quantitative real-time polymerase chain reaction was performed using predesigned Taqman Gene Expression Assays and AmpliTaq Gold DNA polymerase following the manufacturer's instructions (Applied Biosystems Inc.). The ratio of the mRNA levels for each sample was calculated by normalizing the comparative quantitation values to those of GAPDH mRNA. PCR was performed in a GeneAmp PCR system 2400 Thermal Cycler (Perkin-Elmer, Norwalk, CT, USA). Primers used were as follows: GAPDH, 5′-ACG GCA AAT TCA ACG GCA CAG TCA-3′ (forward) and 5′-TGG GGG CAT CGG CAG AAG G-3′ (reverse); Collagen I, 5′-TGC CGT GAC CTC AAG ATG TG-3′ (forward) and 5′-CAC AAG CGT GCT GTA GGT GA-3′ (reverse); Collagen III, 5′-AGA TCA TGT CTT CAC TCA AGT C-3′ (forward) and 5′-TTT ACA TTG CCA TTG GCC TAG-3′ (reverse).

2.8. Determination of Capillary Density. Capillary density was performed 14 days after the surgical procedure by

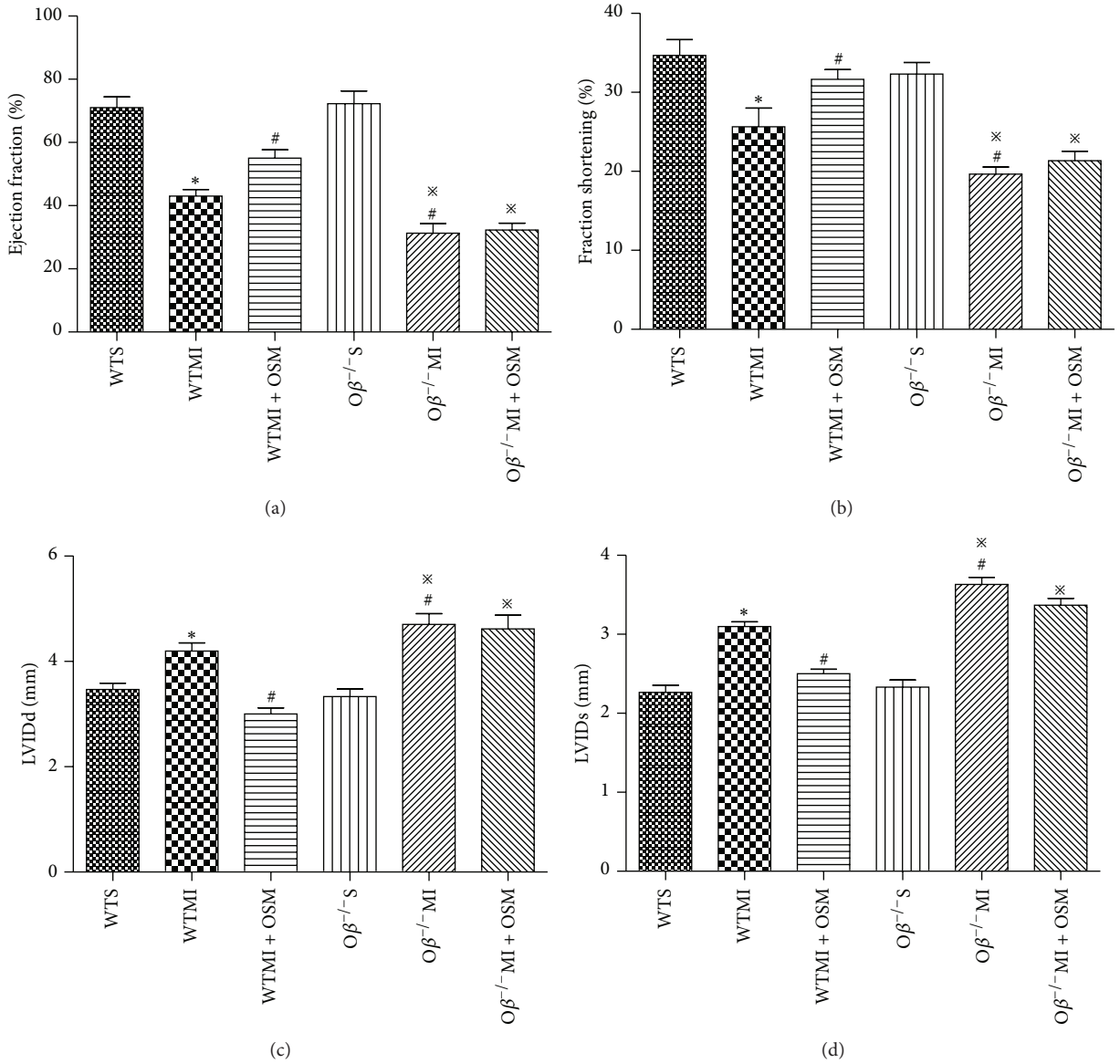

Figure 1: OSM treatment improved cardiac function after MI. Echocardiographic analysis of cardiac (a) ejection fraction, (b) fraction shortening, (c) left ventricular internal diastolic diameter (LVIDd), and (d) left ventricular internal systolic diameter (LVIDs) in the six groups of mice 28 days after operation. The values are means ± SD. $^{*}P < 0.05$ versus WT group, $^{\#}P < 0.05$ versus WT + MI group, and $^{※}P < 0.05$ versus O$\beta^{-/-}$S group. $N = 18$ in each group.

immunohistochemistry. Mice were sacrificed, hearts were removed, and paraffin-embedded sections were prepared. Endothelial cells were labeled using goat polyclonal anti-CD31 (Santa Cruz Biotechnology, Santa Cruz, CA) followed by a biotinylated horse anti-goat secondary antibody (Vector Laboratories). The reaction product (brown) was visualized with 3,3′-diaminobenzidine substrate using the Vector ABC Vectastain Elite Kit (Vector Laboratories, Burlingame, CA). Images were captured and stored in digital Tiff file format for later image analysis. Counts of capillary and arteriolar density per square millimeter were obtained after superimposing a calibrated morphometric grid on each digital image using Adobe Photoshop Software.

2.9. Western Blot Assay. Protein was isolated from homogenized heart tissue following standard protocols. Total proteins were loaded onto an SDS-PAGE gel and transferred electrophoretically to nitrocellulose membranes (Millipore, Billerica, MA). After blocking with 5% skim milk, the membranes were incubated with the appropriate primary antibody of the recommended dilution at 4°C overnight. The membranes were washed and further incubated with horseradish peroxidase—linked secondary antibody at 37°C for 60 min. The blots were developed with an enhanced chemiluminescence reagent kit (Millipore, Billerica, MA) and visualized with UVP Bioimaging Systems. Vision Works LS Acquisition and Analysis Software were used to analyze blot densities.

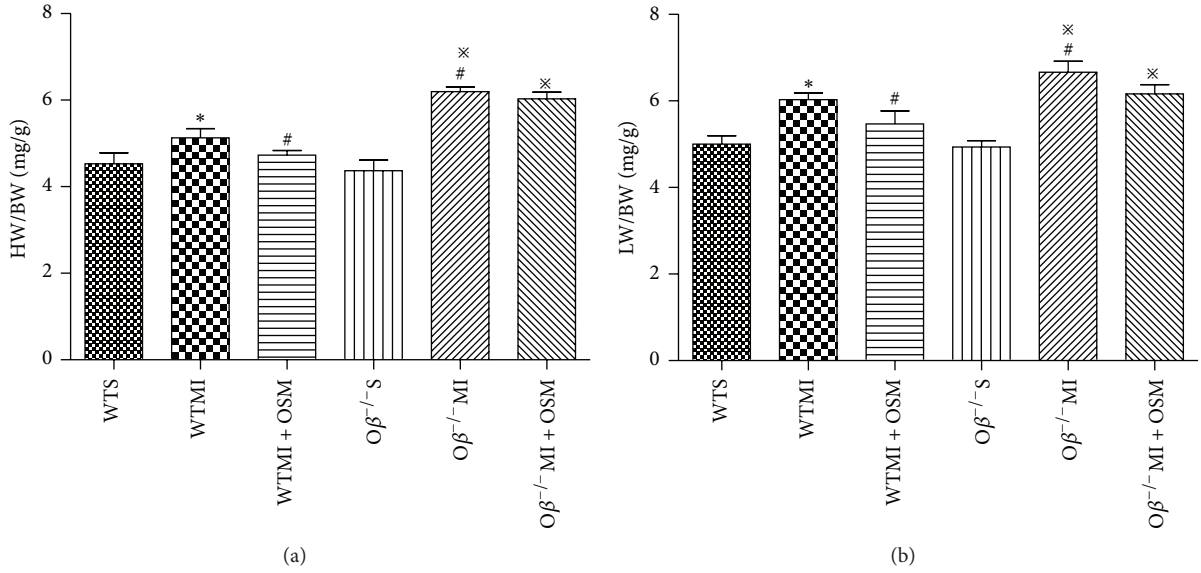

Figure 2: OSM prevented cardiac hypertrophy in response to MI. (a) HW/BW ratio in mice from all groups 14 days after MI. (b) LW/BW ratio in mice from all groups 14 days after MI. The values are means ± SD. $^{*}P < 0.05$ versus WT group, $^{\#}P < 0.05$ versus WT + MI group, and $^{※}P < 0.05$ versus O$\beta^{-/-}$S group. $N = 18$ in each group.

Primary antibodies used in this study were as follows: OSM (R&D systems, Minneapolis, MN), Oβ (R&D systems, Minneapolis, MN), cleaved caspase 3 (Cell Signaling, USA), caspase 3 (Cell Signaling, USA), β-actin (Cell Signaling, USA), p-Akt (Cell Signaling, USA), Akt (Cell Signaling, USA), VEGF (R&D systems, Minneapolis, MN), and bFGF (UBI, Lake Placid, NY). Secondary antibodies were horseradish peroxidase-conjugated goat anti-rabbit IgG (R&D systems, Minneapolis, MN) and rabbit anti-goat IgG (R&D systems, Minneapolis, MN).

2.10. Statistical Analysis. Continuous variables that approximated the normal distribution were expressed as means ± standard deviation (SD). Comparisons between groups were subjected to ANOVA followed by Bonferroni correction for post hoc t-test. Data expressed as proportions were assessed with a Chi-square test. Two sided tests have been used throughout, and $P < 0.05$ was considered statistically significant. SPSS software package version 14.0 (SPSS, Chicago, IL) was used for data analysis.

3. Results

3.1. OSM Treatment Improved Cardiac Function after MI. To determine whether OSM treatment could improve cardiac function in MI mice, echocardiographic investigations were carried out at day 28 after operation. In WT mice, MI induced significant cardiac function deterioration, evidenced by decreased EF value (WTMI versus WTS: 43.25 ± 2.12 versus 71.37 ± 3.49%, Figure 1(a)) and FS value (WTMI versus WTS: 25.37 ± 2.33 versus 34.67 ± 2.03%, Figure 1(b)) and increased LVIDd and LVIDs (Figures 1(c) and 1(d)). Deletion of Oβ, which abrogated OSM signaling, did not influence normal cardiac function before MI but resulted in a significant decline of left ventricular function after operation compared with WTMI mice (EF: O$\beta^{-/-}$MI versus WTMI: 31.24 ± 3.12 versus 43.25 ± 2.12%; FS: O$\beta^{-/-}$MI versus WTMI: 19.67 ± 0.88 versus 25.37 ± 2.33%, Figures 1(a) and 1(b)). Furthermore, a major improvement of cardiac function was observed when WTMI mice were treated with OSM (EF: WTMI + OSM versus WTMI: 55.38 ± 2.68 versus 43.59 ± 2.12%; FS: WTMI + OSM versus WTMI: 31.67 ± 1.20 versus 25.93 ± 2.33%, Figures 1(a) and 1(b)). However, the protective effect of OSM on cardiac function after MI was inhibited in Oβ knockout mice, indicating that OSM exerted cardiac protection in MI through Oβ receptor.

3.2. OSM Prevented Cardiac Hypertrophy in Response to MI. In order to investigate cardiac hypertrophy and pulmonary congestion, heart weight/body weight (HW/BW) ratio and lung wet weight/body weight (LW/BW) ratio were calculated 14 days after MI surgery. HW/BW ratio in WTMI mice was significantly increased compared with WT mice (WTMI versus WTS: 5.13 ± 0.12 versus 4.53 ± 0.15 mg/g, Figure 2(a)), and the change was reversed by OSM treatment (WTMI + OSM versus WTMI: 4.73 ± 0.06 versus 5.13 ± 0.12 mg/g, Figure 2(a)). However, Oβ deletion abrogated the beneficial effect of OSM (Figure 2(a)). Likewise, the increased LW/BW ratio in WTMI mice was reversed by OSM treatment (WTMI versus WTS: 6.03 ± 0.09 versus 5.00 ± 0.12 mg/g; WTMI + OSM versus WTMI: 5.47 ± 0.18 versus 6.03 ± 0.09 mg/g, Figure 2(b)), and the effect of OSM was inhibited in O$\beta^{-/-}$ mice (Figure 2(b)).

3.3. OSM Treatment Attenuated Cardiomyocyte Apoptosis after MI. The effect of OSM on the survival of myocardium

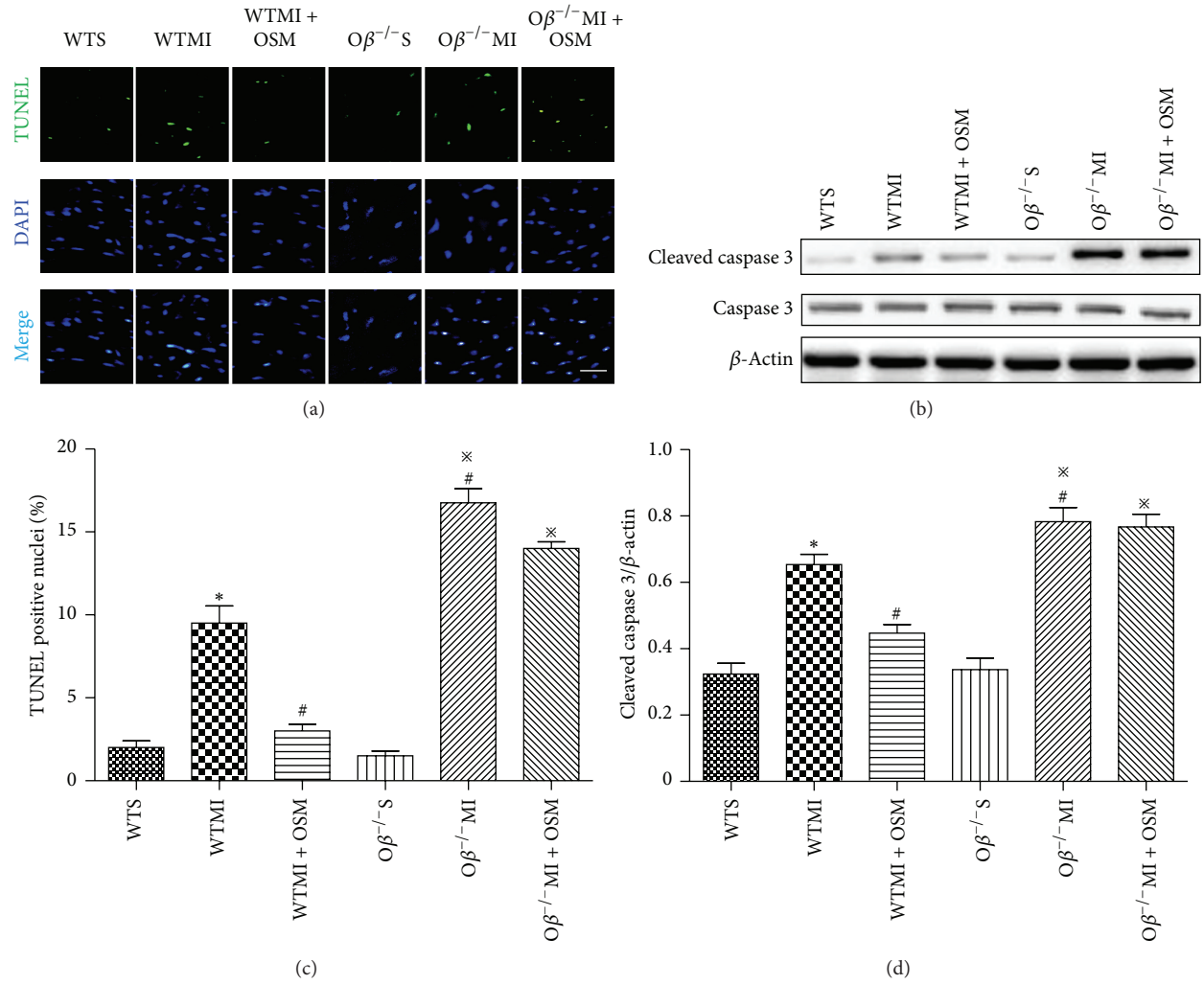

Figure 3: OSM treatment attenuated cardiomyocyte apoptosis after MI. (a) Representative digital micrographs showing cardiomyocyte apoptosis in the border zone of all groups of mice. Bar: 25 μm. (b) Western blot assay of cleaved caspase 3 and caspase 3 in the border zone of the six groups of mice. (c) Quantitative analysis of cardiomyocyte apoptosis after MI in counts/high-power field (HPF). (d) Quantitative data of the expression of cleaved caspase 3 in the six groups of mice. The values are means ± SD. $^{*}P < 0.05$ versus WT group, $^{\#}P < 0.05$ versus WT + MI group, and $^{※}P < 0.05$ versus O$\beta^{-/-}$S group. $N = 6$ in each group.

in response to ischemia was evaluated at postoperative day 14 using TUNEL staining method. The ratio of apoptotic cardiomyocytes was significantly increased in WTMI mice compared with WT group, and this change was attenuated by OSM treatment (WTMI versus WTS: 9.52 ± 1.04 versus 2.00 ± 0.41%; WTMI + OSM versus WTMI: 3.27 ± 0.41 versus 9.52 ± 1.04%, Figures 3(a) and 3(c)). Oβ knockout MI mice demonstrated more severe cardiomyocyte apoptosis than WTMI mice (O$\beta^{-/-}$MI versus WTMI: 16.75 ± 0.85 versus 9.52 ± 1.04%), and OSM treatment no longer exerted the function of decreasing cardiomyocytes' susceptibility to ischemia damage (O$\beta^{-/-}$MI + OSM versus O$\beta^{-/-}$MI: 15.29 ± 1.08 versus 16.75 ± 0.85%, Figures 3(a) and 3(c)). Western blot analysis showed that the expression of cleaved caspase 3 was consistent with the extent of apoptosis as determined by the TUNEL staining (Figures 3(b) and 3(d)).

3.4. Postischemic Myocardial Interstitial Fibrosis Was Prevented by OSM Administration. 14 days after MI, myocardial interstitial fibrosis in the border zone was detected by Masson's trichrome staining and quantified with percentage of fibrosis area. WTMI mice induced an increase of fibrosis area in comparison with WT mice (WTMI versus WTS: 16.75 ± 0.85 versus 1.75 ± 0.48%, Figures 4(a) and 4(b)). Oβ knockout MI mice revealed even severe cardiomyocyte fibrosis compared with WTMI mice (O$\beta^{-/-}$MI versus WTMI: 23.50 ± 1.32 versus 16.75 ± 0.85%, Figures 4(a) and 4(b)). OSM treatment resulted in remarkable reduction of fibrosis area in WT mice subjected to MI (WTMI + OSM versus WTMI: 7.52 ± 0.65 versus 16.75 ± 0.85%, Figures 4(a) and 4(b)), while it did not decrease fibrosis area in Oβ deletion MI mice. mRNA expressions of Collagens I and III in the border zone were consistent with the extent of fibrosis area

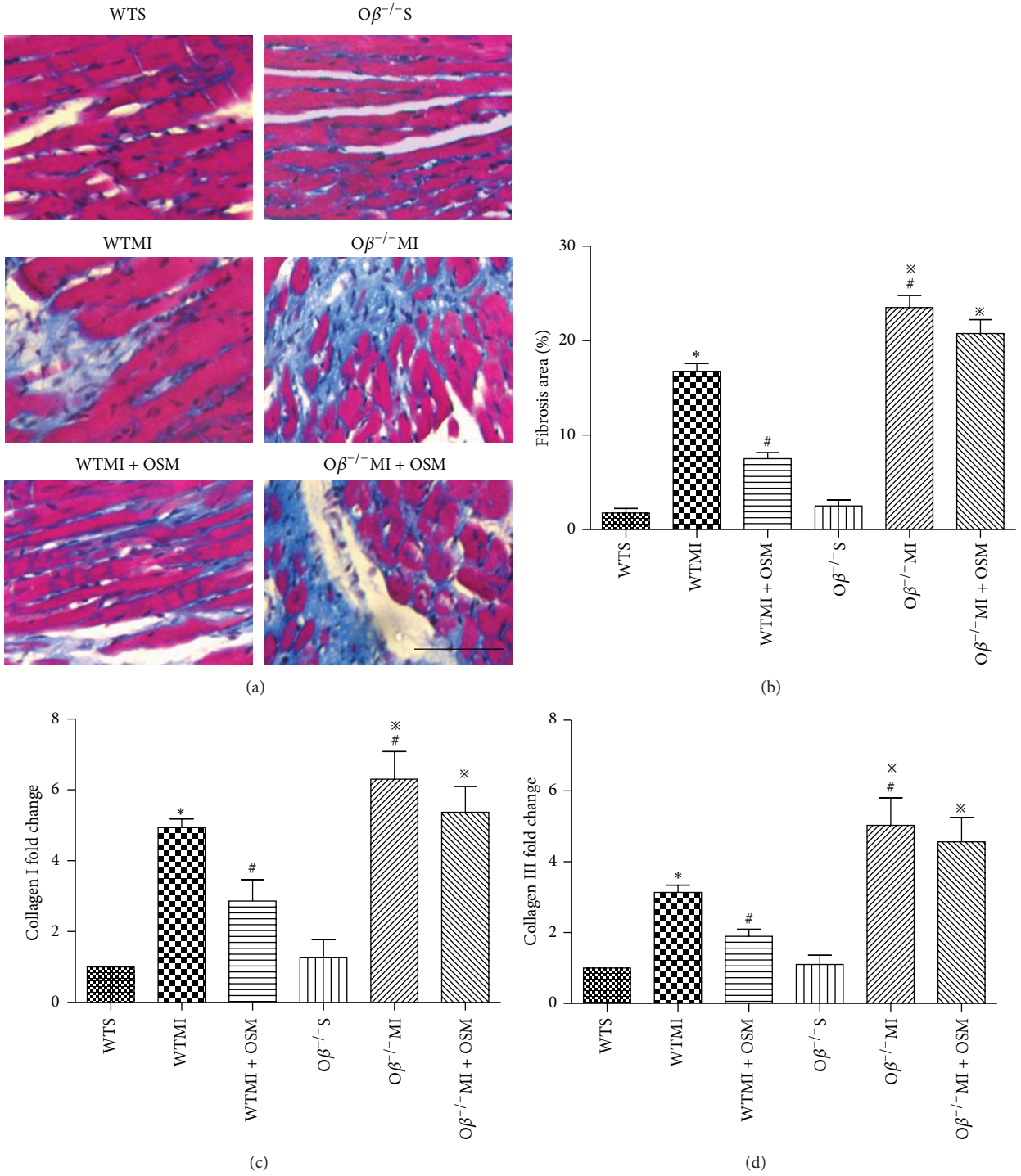

FIGURE 4: Postischemic myocardial interstitial fibrosis was prevented by OSM administration. (a) Representative images of Masson's trichrome-stained heart sections in all groups of mice 14 days after operation. Bar: 50 μm. (b) Quantitative analysis of myocardial interstitial fibrosis in all groups. (c) mRNA fold change of the expression of Collagen I. (d) mRNA fold change of the expression of Collagen III. The values are means ± SD. $^{*}P < 0.05$ versus WT group, $^{\#}P < 0.05$ versus WT + MI group, and $^{※}P < 0.05$ versus O$\beta^{-/-}$S group. $N = 6$ in each group.

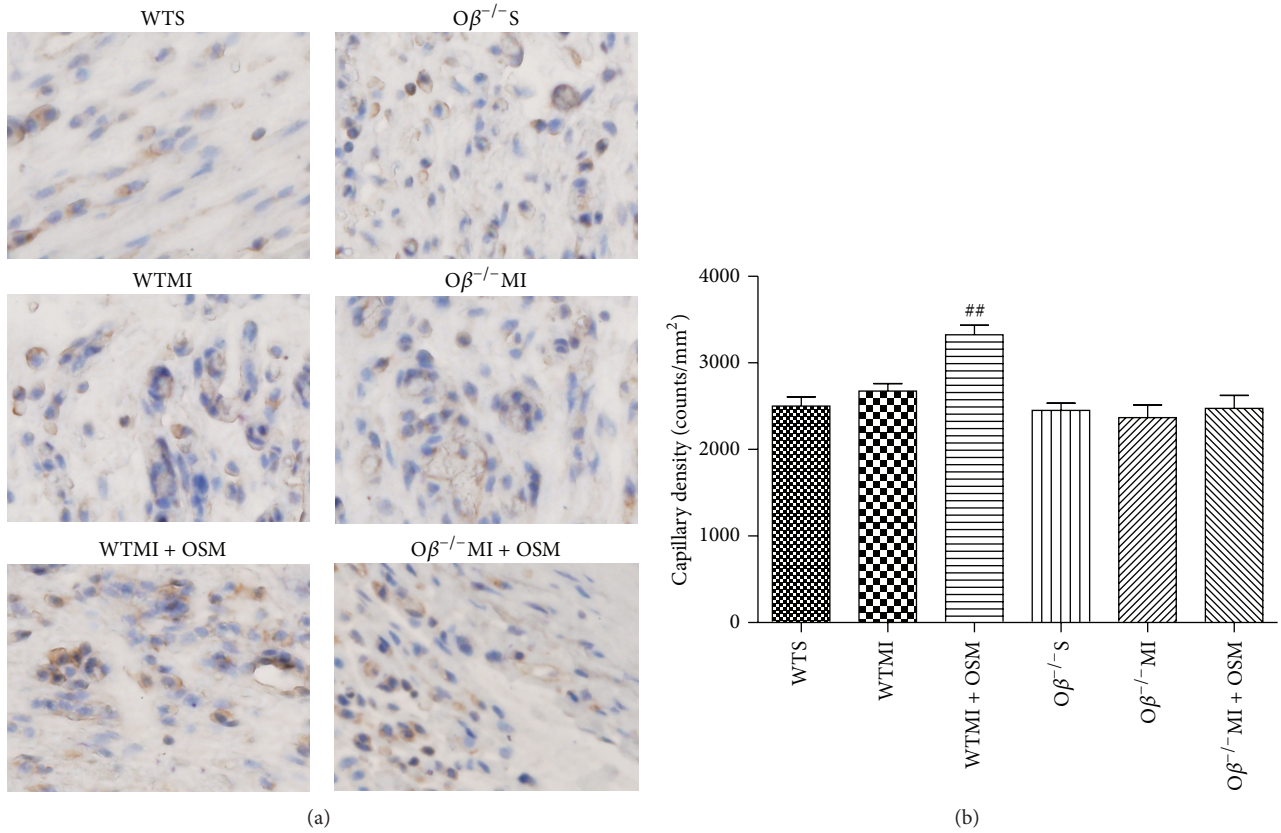

Figure 5: Treatment with OSM promoted angiogenesis by increasing capillary density after MI. (a) Representative digital micrographs showing capillary density/CD31 immunostaining 14 days after surgical intervention in different experimental groups. Magnification: 200x. (b) Quantitative analysis of capillary density in counts/mm^2. The values are means ± SD. $^{\#\#}P < 0.01$ versus WT + MI group. $N = 6$ in each group.

as determined by Masson's trichrome staining (Figures 4(c) and 4(d)).

3.5. Treatment with OSM Promoted Angiogenesis by Increasing Capillary Density after MI. The role of OSM treatment on the degree of angiogenesis following myocardial infarction was measured by capillary density through anti-CD31 immunohistochemistry staining 14 days after surgical intervention. WTMI mice revealed a minor increase of capillary density (WTMI versus WTS: 2675 ± 85 versus 2500 ± 108, $P = 0.25$), while OSM treatment significantly increased the capillary density (WTMI + OSM versus WTMI: 3325 ± 111 versus 2675 ± 85, Figures 5(a) and 5(b)). Conversely, no significant increase of capillary density was found in O$\beta^{-/-}$MI mice in comparison with the O$\beta^{-/-}$S mice and OSM treatment could no longer enhance angiogenesis as those detected in WT mice (O$\beta^{-/-}$MI versus O$\beta^{-/-}$S: 2370 ± 146 versus 2450 ± 84; O$\beta^{-/-}$MI + OSM versus O$\beta^{-/-}$MI: 2475 ± 149 versus 2370 ± 146, Figures 5(a) and 5(b)).

3.6. OSM Upregulated p-Akt, VEGF, and bFGF in Ischemic Myocardium. Finally, we investigated the possible mechanisms responsible for the angiogenic effect of OSM during the process of myocardial infarction. 14 days after operation, MI group revealed increased OSM expressions in infarct border zone, which were even higher in OSM-treated groups (Figure 6(a)). WTMI mice revealed decreased levels of both p-Akt and VEGF compared with WT mice, and the changes were reversed by OSM treatment (Figures 6(b) and 6(c)). Decreased p-Akt and VEGF levels were observed in O$\beta^{-/-}$MI mice compared with O$\beta^{-/-}$S mice, while OSM treatment could not reverse the alteration as those detected in WT mice (Figures 6(b) and 6(c)). Another well-known angiogenic factor bFGF was investigated 14 days after operation. Similarly, expression of bFGF was decreased in WT mice after the MI surgery, and OSM treatment could reverse the change in WT mice, while nonattenuation was found in Oβ KO mice (Figure 6(d)). Taken together, Akt/VEGF and bFGF were both involved in the angiogenic effect of OSM during myocardial infarction.

4. Discussion

Our present study revealed that (1) OSM treatment preserved cardiac function and attenuated myocardial apoptosis and fibrosis in a mouse MI model; (2) OSM promoted angiogenesis in the infarct border zone after MI probably via upregulating angiogenic factors VEGF and bFGF;

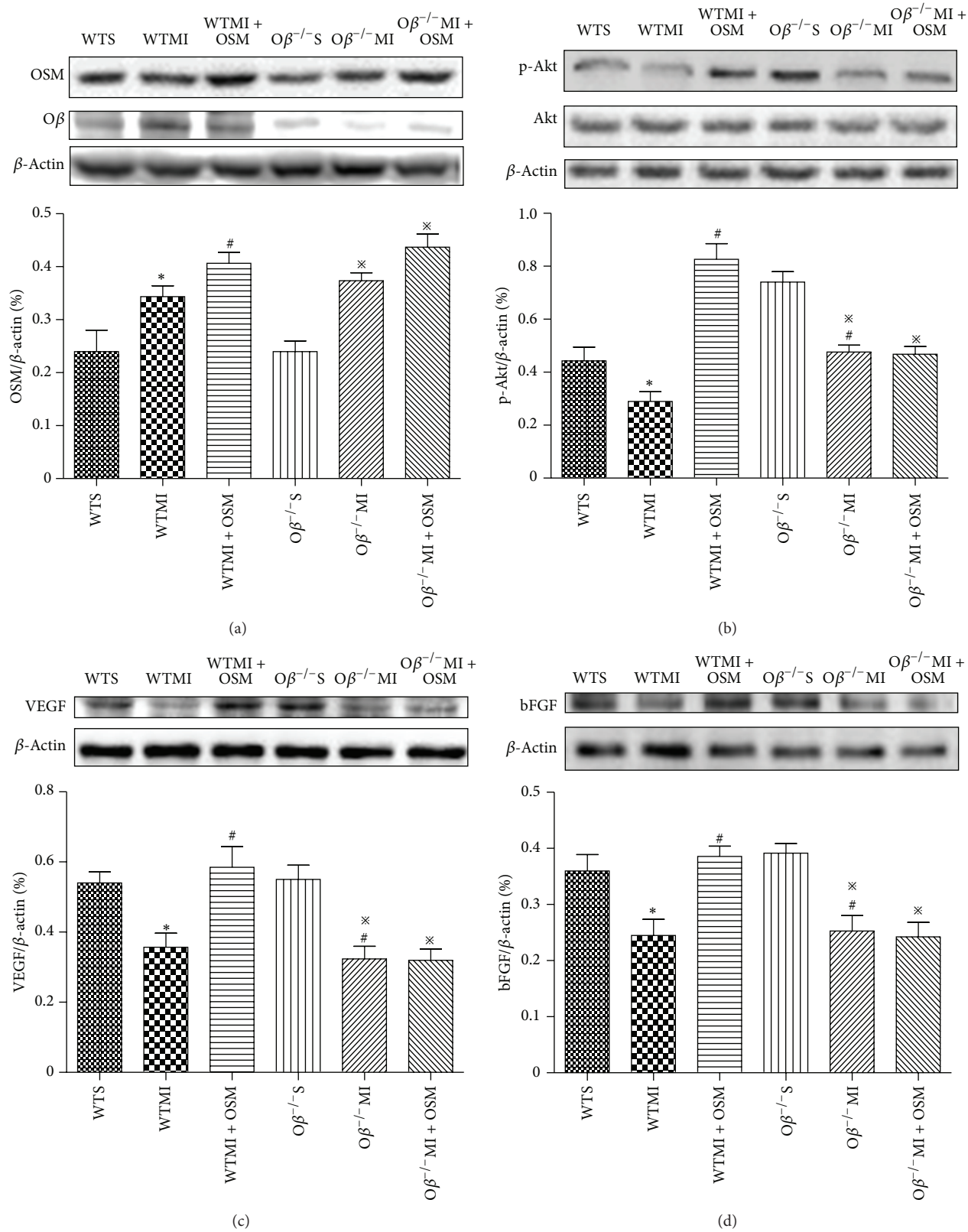

FIGURE 6: OSM increased levels of p-Akt, VEGF, and bFGF in ischemic myocardium. (a) Western blot analysis of the expressions of OSM in different groups of mice. (b) Western blot analysis of the levels of p-Akt and Akt in six groups. (c) Western blot analysis of the expression of VEGF in different groups of mice. (d) Western blot analysis of the expression of bFGF in the six groups of mice. The values are means ± SD. $^{*}P < 0.05$ versus WT group, $^{\#}P < 0.05$ versus WT + MI group, and $^{※}P < 0.05$ versus Oβ$^{-/-}$S group. $N = 6$ in each group.

(3) the beneficial effect of OSM in MI mice was abrogated when OSM receptor Oβ was knocked out.

After LAD ligation, myocardial apoptosis is increased as a result of ischemia, and the lost myocardial mass is replaced by fibrosis due to the fact that myocardium has limited regenerative abilities. Thereafter, therapies which can increase angiogenesis and the blood supply to tissue are highly desirable [5, 14, 16]. Despite some progress that has been made in the past two decades, these proangiogenic treatments have, until today, not resulted in routine clinical applications [17]. VEGF is one of the most widely used angiogenic factors in previous studies [18]. Numerous experimental reports demonstrated the proangiogenic activity and the associated benefit on cardiac function of VEGF administration in porcine or rodent models of MI [13, 19]. Nevertheless, VEGF alone stimulates the formation of immature, leaky, and disorganized blood vessel, and this phenomenon emphasizes the need of timely regulated angiogenic signal for the formation of a stable and functional microvascular network capable of restoring blood flow to ischemic tissues [20]. bFGF is another potent angiogenic factor which has been reported to induce angiogenesis in the ischemic heart and promoted cardiac repair after MI [17]. Interestingly, Cao et al. reported that bFGF-induced angiogenesis leads to the formation of stable and mature blood vessels in the mouse cornea [21], contrary to VEGF-stimulated angiogenesis. The knowledge brought the idea that a combination of VEGF and bFGF might be a better therapy to induce angiogenesis following MI.

The inflammatory cytokine OSM has been reported to increase VEGF expression in various tissue types and upregulate endothelial bFGF expression *in vitro*, so we hypothesized that it might induce mature vessels after MI. In the present study, we demonstrated for the first time that OSM induced angiogenesis by upregulating expressions of both VEGF and bFGF in a MI mouse model, thus restoring blood flow of ischemic heart and reducing apoptosis and fibrosis due to less damage of cardiomyocytes. VEGF is an endogenous proangiogenic factor that can be induced immediately after MI due to a spontaneous angiogenic response of the heart, but the protein at the border zone is only increased during day 1 after MI. At day 14, VEGF level is lower than that before MI [22]. We observed in this study that supplement of OSM stimulated VEGF expression till 14 days after operation, indicating that OSM treatment might support the insufficient spontaneous angiogenic process induced by MI. The beneficial effect of OSM treatment was confirmed by improvement of cardiac function 28 days after operation, which was consistent with previous studies reported by Kubin et al. [23].

There are two types of OSM receptors, namely, type I receptor consisting of LIFR (leukemia inhibitory factor receptor-) gp130 and type II receptor formed by a complex of OSM receptor Oβ and gp130 [24]. Murine OSM binds exclusively to type II receptor while human OSM has the exceptional capability to recruit both receptors. In the mouse MI model exploited in the present study, Oβ knockout completely abrogated protective effects of OSM following operation, which further confirmed that OSM exerted its angiogenic function in MI mice through and merely through type II receptor.

5. Conclusions

The present study provided direct evidence that OSM increased cardiac function and inhibited apoptosis and fibrosis through inducing angiogenesis via upregulating VEGF and bFGF in a mouse MI model. These findings suggested that OSM might be a promising therapeutic tool in treating MI.

Conflict of Interests

The authors declare that there is no conflict of interests regarding the publication of this paper.

Authors' Contribution

Xiaotian Zhang, Di Zhu, and Liping Wei contributed equally to this work.

Acknowledgments

This work was supported by the National Natural Science Foundation of China (nos. 81100579, 81270128, 81270263, 81200158, 81300149, and 81100234), by Xijing Hospital, boosting academic program (2012), and by Scientific and Technological Project in Shaanxi Province (2013K12-02-01).

References

[1] A. S. Go, D. Mozaffarian, V. L. Roger et al., "Heart Disease and Stroke Statistics—2014 update: a report from the American Heart Association," *Circulation*, vol. 129, no. 3, pp. e28–e292, 2014.

[2] A. S. Go, D. Mozaffarian, V. L. Roger et al., "Heart disease and stroke statistics—2013 update: a report from the American Heart Association," *Circulation*, vol. 127, pp. e6–e245, 2013.

[3] B. Messner, J. Kern, D. Wiedemann et al., "5-Methoxyleoligin, a lignan from Edelweiss, stimulates CYP26B1-dependent angiogenesis in vitro and induces arteriogenesis in infarcted rat hearts in vivo," *PLoS ONE*, vol. 8, no. 3, Article ID e58342, 2013.

[4] K. Albrecht-Schgoer, W. Schgoer, J. Holfeld et al., "The angiogenic factor secretoneurin induces coronary angiogenesis in a model of myocardial infarction by stimulation of vascular endothelial growth factor signaling in endothelial cells," *Circulation*, vol. 126, no. 21, pp. 2491–2501, 2012.

[5] M. Siragusa, R. Katare, M. Meloni et al., "Involvement of phosphoinositide 3-kinase γ in angiogenesis and healing of experimental myocardial infarction in mice," *Circulation Research*, vol. 106, no. 4, pp. 757–768, 2010.

[6] A. Bronckaers, P. Hilkens, W. Martens et al., "Mesenchymal stem/stromal cells as a pharmacological and therapeutic approach to accelerate angiogenesis," *Pharmacology and Therapeutics*, vol. 143, pp. 181–196, 2014.

[7] P. J. Hohensinner, C. Kaun, K. Rychli et al., "The inflammatory mediator oncostatin M induces stromal derived factor-1 in human adult cardiac cells," *The FASEB Journal*, vol. 23, no. 3, pp. 774–782, 2009.

[8] M. Gwechenberger, D. Moertl, R. Pacher, and M. Huelsmann, "Oncostatin-M in myocardial ischemia/reperfusion injury may

regulate tissue repair," *Croatian Medical Journal*, vol. 45, no. 2, pp. 149–157, 2004.

[9] J. Pöling, P. Gajawada, M. Richter et al., "Therapeutic targeting of the oncostatin M receptor-β prevents inflammatory heart failure," *Basic Research in Cardiology*, vol. 109, no. 1, article 396, 2014.

[10] S. L. Fossey, M. D. Bear, W. C. Kisseberth, M. Pennell, and C. A. London, "Oncostatin M promotes STAT3 activation, VEGF production, and invasion in osteosarcoma cell lines," *BMC Cancer*, vol. 11, article 125, 2011.

[11] E. S. Wijelath, B. Carlsen, T. Cole, J. Chen, S. Kothari, and W. P. Hammond, "Oncostatin M induces basic fibroblast growth factor expression in endothelial cells and promotes endothelial cell proliferation, migration and spindle morphology," *Journal of Cell Science*, vol. 110, part 7, pp. 871–879, 1997.

[12] M. Vasse, J. Pourtau, V. Trochon et al., "Oncostatin M induces angiogenesis in vitro and in vivo," *Arteriosclerosis, Thrombosis, and Vascular Biology*, vol. 19, no. 8, pp. 1835–1842, 1999.

[13] K. Rychli, C. Kaun, P. J. Hohensinner et al., "The inflammatory mediator oncostatin M induces angiopoietin 2 expression in endothelial cells in vitro and in vivo," *Journal of Thrombosis and Haemostasis*, vol. 8, no. 3, pp. 596–604, 2010.

[14] S. Araki, Y. Izumiya, S. Hanatani et al., "Akt1-mediated skeletal muscle growth attenuates cardiac dysfunction and remodeling after experimental myocardial infarction," *Circulation: Heart Failure*, vol. 5, no. 1, pp. 116–125, 2012.

[15] C.-N. Hao, J.-J. Huang, Y.-Q. Shi et al., "Pulsed electromagnetic field improves cardiac function in response to myocardial infarction," *The American Journal of Translational Research*, vol. 6, no. 3, pp. 281–290, 2014.

[16] R. S. Adluri, M. Thirunavukkarasu, L. Zhan et al., "Glutaredoxin-1 overexpression enhances neovascularization and diminishes ventricular remodeling in chronic myocardial infarction," *PLoS ONE*, vol. 7, no. 3, p. e34790, 2012.

[17] C. Cochain, K. M. Channon, and J.-S. Silvestre, "Angiogenesis in the infarcted myocardium," *Antioxidants & Redox Signaling*, vol. 18, no. 9, pp. 1100–1113, 2013.

[18] R. S. Adluri, M. Thirunavukkarasu, L. Zhan et al., "Thioredoxin 1 enhances neovascularization and reduces ventricular remodeling during chronic myocardial infarction: a study using thioredoxin 1 transgenic mice," *Journal of Molecular and Cellular Cardiology*, vol. 50, no. 1, pp. 239–247, 2011.

[19] D. Ribatti and E. Crivellato, "'Sprouting angiogenesis', a reappraisal," *Developmental Biology*, vol. 372, no. 2, pp. 157–165, 2012.

[20] M. Murakami, "Signaling required for blood vessel maintenance: molecular basis and pathological manifestations," *International Journal of Vascular Medicine*, vol. 2012, Article ID 293641, 15 pages, 2012.

[21] R. Cao, A. Eriksson, H. Kubo, K. Alitalo, Y. Cao, and J. Thyberg, "Comparative evaluation of FGF-2-, VEGF-A-, and VEGF-C-induced angiogenesis, lymphangiogenesis, vascular fenestrations, and permeability," *Circulation Research*, vol. 94, no. 5, pp. 664–670, 2004.

[22] T. Zhao, W. Zhao, Y. Chen, R. A. Ahokas, and Y. Sun, "Vascular endothelial growth factor (VEGF)-A: role on cardiac angiogenesis following myocardial infarction," *Microvascular Research*, vol. 80, no. 2, pp. 188–194, 2010.

[23] T. Kubin, J. Pöling, S. Kostin et al., "Oncostatin M is a major mediator of cardiomyocyte dedifferentiation and remodeling," *Cell Stem Cell*, vol. 9, no. 5, pp. 420–432, 2011.

[24] F. Beigel, M. Friedrich, C. Probst et al., "Oncostatin M mediates STAT3-dependent intestinal epithelial restitution via increased cell proliferation, decreased apoptosis and upregulation of SERPIN family members," *PLoS ONE*, vol. 9, no. 4, Article ID e93498, 2014.

Hindawi Publishing Corporation
BioMed Research International
Volume 2015, Article ID 719316, 11 pages
http://dx.doi.org/10.1155/2015/719316

Research Article

Activation of Cell Surface Bound 20S Proteasome Inhibits Vascular Cell Growth and Arteriogenesis

Wulf D. Ito,[1,2,3,4] Natalie Lund,[1,2] Ziyang Zhang,[1,5,6] Friedrich Buck,[7] Heinrich Lellek,[8] Andrea Horst,[9] Hans-Günther Machens,[6] Heribert Schunkert,[1,10] Wolfgang Schaper,[3] and Thomas Meinertz[2]

[1] *Medical Department II, Experimental Angiology, University Hospital Lübeck, Ratzeburger Allee 160, 23538 Lübeck, Germany*
[2] *Department of Cardiology, University Hospital Hamburg Eppendorf, Martinistraße 52, 20246 Hamburg, Germany*
[3] *Max-Planck Institute of Heart and Lung Research, Ludwigstraße 43, 61231 Bad Nauheim, Germany*
[4] *Cardiovascular Center Oberallgaeu-Kempten, Academic Teaching Hospital, University of Ulm, Im Stillen 2, 87509 Immenstadt, Germany*
[5] *Department of Orthopedics, Hand Surgery Division, Tongji Hospital, Tongji Medical College, Huazhong University of Science and Technology, Wuhan, Hubei, China*
[6] *Department of Plastic Surgery and Hand Surgery, Klinikum Rechts der Isar, Technical University of Munich, Ismaninger Straße 22, 81675 Munich, Germany*
[7] *Department of Clinical Chemistry, University Hospital Hamburg Eppendorf, Martinistraße 52, 20246 Hamburg, Germany*
[8] *Department of Medicine, University Hospital Hamburg Eppendorf, Martinistraße 52, 20246 Hamburg, Germany*
[9] *Institute of Experimental Immunology and Hepatology, University Medical Center Hamburg-Eppendorf, Martinistraße 52, 20246 Hamburg, Germany*
[10] *Department of Cardiology, German Heart Center Munich, Technical University of Munich, and Deutsches Zentrum für Herz-Kreislauf-Forschung (DZHK), Standard Munich Heart Alliance, Lazarettstraße 36, 80636 Munich, Germany*

Correspondence should be addressed to Wulf D. Ito; wulf.ito@kliniken-oa.de

Received 19 December 2014; Revised 17 February 2015; Accepted 21 February 2015

Academic Editor: Francesco Moccia

Arteriogenesis is an inflammatory process associated with rapid cellular changes involving vascular resident endothelial progenitor cells (VR-EPCs). Extracellular cell surface bound 20S proteasome has been implicated to play an important role in inflammatory processes. In our search for antigens initially regulated during collateral growth mAb CTA 157-2 was generated against membrane fractions of growing collateral vessels. CTA 157-2 stained endothelium of growing collateral vessels and the cell surface of VR-EPCs. CTA 157-2 bound a protein complex (760 kDa) that was identified as 26 kDa $\alpha 7$ and 21 kDa $\beta 3$ subunit of 20S proteasome in mass spectrometry. Furthermore we demonstrated specific staining of 20S proteasome after immunoprecipitation of VR-EPC membrane extract with CTA 157-2 sepharose beads. Functionally, CTA 157-2 enhanced concentration dependently AMC (7-amino-4-methylcoumarin) cleavage from LLVY (*N*-Succinyl-Leu-Leu-Val-Tyr) by recombinant 20S proteasome as well as proteasomal activity in VR-EPC extracts. Proliferation of VR-EPCs (BrdU incorporation) was reduced by CTA 157-2. Infusion of the antibody into the collateral circulation reduced number of collateral arteries, collateral proliferation, and collateral conductance *in vivo*. In conclusion our results indicate that extracellular cell surface bound 20S proteasome influences VR-EPC function *in vitro* and collateral growth *in vivo*.

1. Introduction

Vascular plasticity as seen during angiogenesis and arteriogenesis (the growth of collateral arteries from preexisting arteriolar anastomoses) requires rapid adaptation of endothelial and smooth muscle cells to environmental changes such as hypoxia and shear force [1–3]. Thus on-site protein turnover is of exquisite importance. The ubiquitin-proteasome pathway is involved in most regulatory mechanisms in which such a timely response is required, presumably because it

offers extremely high substrate specificity and the ability to alter quickly the rate of proteolysis [4]. One example is the regulation of hypoxia inducible transcription factor HIF 1 alpha that plays an important role during angiogenesis [5–7].

While oxygen tension plays a paramount role during angiogenesis the growth of preexisting arteriolar or arterial anastomoses into collateral arteries (arteriogenesis) is mainly driven by local changes of hemodynamical forces, which lead to rapid adaptations of arteriolar anastomoses via pronounced morphological changes [1, 2, 8]. Maximal proliferation is observed during the first three days after induction of a hemodynamically relevant stenosis and is associated with a pronounced accumulation of activated macrophages. The first cellular changes are visible within 24 hours after induction of a hemodynamically relevant stenosis, which indicates that the molecular response occurs very quickly [8–10].

Arteriogenesis (collateral growth) thus is an entity of its own that has to be clearly distinguished from angiogenesis, the sprouting of capillaries [8–11].

In addition to circulating cells recent studies suggest an important role of tissue resident vascular progenitor cells during postnatal neovascularization [10, 12–15]. $CD133^+$ pluripotent cells were found in liver, intestine, muscles, and exocrine glands [14]. In cardiac tissue, cardiovascular progenitor cells were found to be developed from a Flk-1 positive stem cell population [16]. We previously demonstrated that collateral growth was associated with proliferation and differentiation of resident perivascular cells suggesting that tissue resident cells play a dominant role during adult neovascularization [17].

In this study we embarked on a search for regulatory elements particularly of collateral growth on the cell membranous level that might explain the rapid adaptation of vascular cells during the initial phase of collateral growth. We utilized a model of arteriogenesis in the rat hindlimb that allowed us to identify and isolate a single collateral vessel early after induction of collateral growth [8]. This collateral artery was used for all biochemical and histological analyses except for those experiments where isolated vascular resident progenitor cells in culture were utilized as described in the Materials and Methods and Results sections. Based upon the generation of monoclonal antibodies against membrane preparations of this collateral vessel and immunohistochemical screening for collateral selectivity we generated a monoclonal antibody (CTA 157-2) that bound to the cell membrane of cells in the endothelial lining of growing collateral vessels as well as of isolated vascular resident endothelial progenitor cells (VR-EPCs) that were recently characterized by our group [18]. Interestingly CTA 157-2 was found to bind and activate extracellular proteasome. Furthermore the antibody reduced proliferation of VR-EPCs *in vitro* and collateral growth *in vivo* pointing towards an important functional role of cell surface bound proteasome during vascular resident endothelial progenitor cell proliferation and collateral growth.

2. Materials and Methods

All investigations conformed to the Guide for the Care and Use of Laboratory Animals published by the US National Institutes of Health (NIH Publication number 85-23, revised 1996) and Section 8 of the German Law for the Protection of Animals. Except for the immunization all *in vivo* experiments were performed on male Sprague Dawley rats (weight 200 g, Charles River Laboratories, Germany) under general anesthesia as previously described in detail [8].

2.1. Generation of Collateral Prone Antibody CTA 157-2. For collateral membrane proteins collection, 25 male SD rats were used. The right femoral artery of SD rats was ligated under general anesthesia as previously described [8]. Animals were killed twelve hours after femoral artery occlusion. Collateral arteries were identified using postmortem angiographies as previously described [8], excised, and shock frozen. Our previous experiments had shown that no degradation of mRNA or proteins occurred during this procedure. Collateral arteries were then homogenized in membrane braking buffer containing 50 mmol Tris HCl pH 7,5, 0,32 M Sucrose, 3 mM $MgCl_2$, 10 mM iodoacetamide, 0.02% Na Azide, 5 mmol EDTA, and proteinase inhibitors (all reagents: Sigma; St. Louis, USA). They were centrifuged twice at 1000 g and 4°C. Protein concentration of supernatant was determined and centrifuged at 100,000 g, 4°C for 1 h.

The antibody was generated according to standard protocols originally described by the Nobel laureates Kohler and Milstein [19]. Three C57/B16 (weight 20 g, Charles River Laboratories, Germany) mice were used for immunization. Anesthesia was induced by intraperitoneal injections of Ketamine (100 mg/kg body wt, Atarost) and 2% Xylazine (5 mg/kg body wt, Bayer). C57/B16 mice were immunized with membrane preparations of collateral arteries in TiterMax adjuvant (Sigma; St. Louis, USA) by 3 intraperitoneal injections at 2 weekly intervals. Two days after a fourth terminal boost, spleens were harvested and lymphocytes were fused with SP2/O mouse myeloma cells as previously described [20]. We screened and selected clones using cryosections of activated collateral arteries and control vessels.

For *in vitro* and *in vivo* investigations, the antibody was purified using Affinity Pak Immobilized Protein-L Columns (Pierce, Rockford, USA) according to manufacturer's instructions.

Immunohistochemistry staining of proliferating collaterals and control nonproliferating vessels was performed as described previously [8]. For double staining, CTA 157-2 was linked to NHS-Rhodamine (Pierce, Rockford, USA) using protocols provided by the manufacturers.

2.2. Isolation and Culture of Adult Vascular Resident Cells. Rat vascular resident cells were isolated as described before [18]. Briefly, rat hearts were perfused *ex vivo* with Krebs-Ringer buffer containing 0.06% collagenase. Cardiac microvasculature cells were then collected from the recirculation medium. Cells were grown under standard cell culture conditions using Dulbecco's Modified Eagle Medium (DMEM) supplemented with 10% Fetal Calf Serum (FCS), glutamine, and antibiotics. Confluent monolayers were split routinely 1 : 4 after washing with PBS and treatment with trypsin-EDTA. All reagents were purchased from Invitrogen (Karlsruhe, Germany).

2.3. Clonogenic Assay. After sorting, CTA 157-2 positive cells were cultured with DMEM + 10% FCS. When reaching 80% confluence, cells were detached and sorted by DAKO Cytomation MoFlo High Speed Cell Sorter (DAKO, Denmark) and single cells were placed in a 96-well plate. Cell growth was examined and counted every day by Nikon eclipse TS100 microscope (Nikon, Japan). After 7 days, wells with colony forming units were selected and subcultured for further studies.

2.4. Staining for Immunohistochemistry and FACS Analysis

2.4.1. Antibodies. Primary antibodies were anti-vimentin (V9) (Dianova, Hamburg, Germany); anti-PI3-kinase p85 (Upstate, New York, USA); anti-paxillin (C-18) polyclonal goat antibody (Santa Cruz; CA, USA); anti-plectin (C-20) polyclonal goat antibody (Santa Cruz; CA, USA); anti-vinculin polyclonal goat antibody (Santa Cruz; CA, USA); mouse monoclonal anti-p 27^{kip1} antibody (Abcam, Cambridge, UK); and polyclonal rabbit anti-bovine 20S proteasome antibody (Zymed, San Francisco, CA, USA).

Secondary staining was performed with FITC-coupled goat anti-mouse or donkey anti-goat antibody (Dianova, Hamburg, Germany). For light microscopic analysis secondary staining was performed with a peroxidase coupled goat anti-rabbit or goat anti-mouse antibody (Dianova, Hamburg, Germany). Revelation was performed using DAB (3,3′-diaminobenzidine). Counterstaining for light microscopic images was performed with hematoxylin.

2.4.2. Immunohistochemistry. Immunohistochemistry on tissue sections was performed as described previously [8]. For double labelling in immunohistochemistry and flow cytometric analysis CTA 157-2 was linked to NHS-Rhodamine (Pierce, Rockford, IL) or NHS-Dye 680 (MoBiTec), respectively, using protocols provided by the manufacturers. After fixing the cells either with ethanol 70% at pH 2 or with acetone : methanol 1 : 1 followed by blocking with 1% FCS in PBS they were treated with primary antibodies for 45 minutes at 37°C. Secondary antibodies were incubated for 45 minutes at 37°C. Nuclei were stained with 1 μg/mL Hoechst 33342 (Cambrex, Verviers, Belgium). Double staining was analyzed with a confocal laser scanning microscope (Zeiss, Oberkochen, Germany). Staining with labeled CTA 157-2 was performed either before or after permeabilization as indicated.

2.5. Chromatographic Purification of VR-EPCs Membrane Proteins. Membrane fractions were separated via ion-exchange chromatography on a Source 30 Q column (running buffer: 50 mmol Bis-Tris pH 6.5, 0.25% Triton; elution buffer: 50 mmol Bis-Tris pH 6.5, 0.25% Triton, 0.2, 0.3, 0.5, and 2 M NaCl; Pharmacia Biotech, Freiburg, Germany). Fractions were collected and tested for antibody binding in a nondenaturing slot-blot. Positive fractions were further separated via gel filtration using a Superdex Tricorn 200 HR 10/30 column (running buffer: 20 mmol Bis-Tris pH 6.5, 60 mmol NaCl; Amersham Biosciences, Uppsala, Sweden). Positive fractions were further separated via high liquid chromatography on a Mini Q Tricorn column (running buffer: 20 mmol Bis-Tris, pH 6.5 50 mmol NaCl; elution buffer 50 mmol Bis-Tris, pH 6.5, linear gradient of 2 M NaCl from 0 to 50%; Pharmacia Biotech, Freiburg, Germany). Positive fractions were run on 10% SDS page.

2.6. Mass Spectrometry (MS). Protein spots were cut out, the proteins were reduced with DTT, the cysteine residues were modified with iodoacetamide, and the protein in-gel was digested with trypsin (modified trypsin, Promega). After digestion the peptides were extracted from the gel, desalted on a C18mZipTip (Millipore), eluted with 1 μL 60% methanol/5% formic acid, and analyzed by nanoelectrospray mass spectrometry in a QTOF II instrument (Micromass, Manchester). The MS/MS spectra obtained by collision-induced fragmentation of the peptides were evaluated by the Mascot MS/MS ion search algorithm (Matrix Sciences, London).

2.7. Proteasome Activity Assay. 20S proteasome activity was measured using the 20S Proteasome Activity Assay Kit according to the protocol provided by the manufacturer (Chemicon International Inc., Temecula, CA). 10 μg of recombinant 20S proteasome was treated with different concentrations of CTA 157-2 and IgM control (0, 4, 8, 10, 15, and 20 mg/mL, resp.) as well as with lactacystin (0, 0.75, 1.5, 3, and 6 μg/mL, resp.) for 15 minutes at room temperature before adding the proteasome substrate (Suc-LLVY-AMC). Afterwards samples were incubated for 2 h at 60°C and the fluorescence was recorded using a 355/460 filter set in a fluorometer. Proteasome activity as total amount of proteasome substrate cleaved was calculated from a standard curve and related to the zero value for comparison between the experiments. A total of 8 independent experiments were performed.

2.8. Immunoprecipitation and Staining with a Second Polyclonal Rabbit Anti-Bovine 20S Proteasome Antibody. Purified CTA 157-2 (5–10 mg/mL) antibody was dissolved in 0.1 M $NaHCO_3$ buffer containing 0.5 M NaCl, pH 8.4 (binding buffer 1). Cyanogen-bromide activated resin (Sigma Chemicals, St. Louis, MO) was washed and swollen in cold 1 mM HCl for at least 30 minutes and washed in distilled water followed by washing with the coupling buffer and transferred to the solution with the antibody as described by the manufacturer. Antibody and gel were mixed at 4°C overnight. Unreacted antibody was washed away with binding buffer and unreacted groups were blocked with 0.2% glycine pH 0.8 for 2 hours at room temperature. The blocking solution was removed by washing with the binding buffer 1 and then with acetate buffer (0.1 M. pH 4, containing NaCl 0.5 M). The CTA 157-2 coupled sepharose beads were equilibrated with TNT buffer containing Tris 1 M pH 7.4, NaCl 5 M, Triton 10%, and proteinase inhibitors. CTA 157-2 positive cells were also dissolved in TNT buffer and preincubated with uncoupled cyanogen-bromide beads before incubation with the CTA 157-2 coupled sepharose beads at 4°C overnight. After incubation the beads were centrifuged and washed three times with TNT buffer before subjecting them to gel

electrophoreses and western blotting. After blocking, blots were incubated with a polyclonal rabbit anti-bovine 20S proteasome antibody (Zymed, San Francisco, CA, USA). Revelation with ECL was performed after incubation with a peroxidase coupled goat anti-rabbit antibody as described above. For control experiments a control IgM antibody was linked to the resin. All experiments were performed on cellular extracts of CTA 157-2 positive and CTA 157-2 negative cells.

2.9. Western Blots. VR-EPCs were homogenized in lysis buffer (Cell Signaling, Massachusetts, USA) containing a cocktail of protease inhibitors, and the protein concentration was determined by Lowry assay (BioRad, Germany). Samples were separated in 10% PAGE-SDS gels. After transfer to nitrocellulose membranes, samples were blocked in 5% albumin and incubated with primary antibodies for 2 hours at room temperature. After 4 washing steps with PBS, membranes were incubated with peroxidase-conjugated secondary antibodies (Dianova, Hamburg, Germany). Finally, detection was performed using a chemiluminescence system (GE Healthcare, Germany).

2.10. Flow Cytometric Analyses. For flow cytometric analysis of CTA 157-2 the antibody was linked to NHS-Dye 680 (MoBiTec, Göttingen, Germany) using protocols provided by the manufacturers. VR-EPCs were harvested, washed with PBS, and incubated for one hour with the antibody. Finally, cells were fixed and analyzed with a flow cytometer (FACSCalibur, Becton Dickinson, USA). For quantification we used DIVA software (Becton Dickinson, USA).

2.11. In Vitro and In Vivo Evaluation of VR-EPCs Functions Using CTA 157-2 Monoclonal Antibody. CTA 157-2 and control IgM antibody (both 10 μg/mL) were added into the culture medium of subconfluent VR-EPCs. After 2 days, assessment of *in vitro* proliferation was performed as described previously using the BrdU Flow Kit (PharMingen GmbH, Germany). After incubation with Bromodeoxyuridine (BrdU, 0.3 mg/mL) for 2 hours, the number of positive BrdU cells was counted by flow cytometry (FACSCalibur, Becton Dickinson, USA) as described previously [21]. A total of 5 independent experiments were performed. For *in vivo* assay, femoral artery occlusions were performed. CTA 157-2 (0.1 mg/mL at 10 μL/h) as well as the carrier alone was infused directly into the collateral circulation via osmotic minipump (ALZET, USA). After 7 days, proliferation of the collateral artery was detected by BrdU labeling and detection Kit 2 (Roche Diagnostics, Germany) as described previously [8], and the proliferation index was calculated as the number of BrdU-positive nuclei to the total number of nuclei inside the vessel wall ($n = 6$ per group). Postmortem angiographies ($n = 6$ per group) were obtained 7 days after femoral artery occlusion as described previously using postmortem perfusion of the distal hindlimb with a barium based contrast agent and exposition on single paper wrapped films (X-OMAT MA 13 × 18 cm, Kodak, France) in an X-ray chamber (Faxitron X-ray cooperation, Model 43855D, USA).

2.12. Collateral Proliferation. Collateral proliferation ($n = 6$ per group) was detected 7 days after cell administration as described previously with BrdU labeling and detection Kit 2 (Roche Diagnostics, Germany).

2.13. Determination of Collateral Dependent Conductance. Measurement of total collateral dependent conductance was performed one week after femoral artery occlusion in the anesthetized animal. In order to determine collateral conductance a method previously established and validated for the rabbit hindlimb was adapted to investigate the functionality of collateral vessels in the rat hindlimb at maximal vasodilatation [22]. We determined total collateral dependent conductance instead of pure collateral conductance because due to animal size placement of a pressure transducer distal to the collateral circulation distorts pressure and blood flow measurements in the rat hindlimb. Furthermore it has been shown that total collateral dependent conductance reflects collateral conductance within the first week after femoral artery occlusion [22, 23]. Systemic blood pressure, identical to blood pressure, was measured invasively via a catheter placed into the carotid artery and connected to a pressure transducer (FME TBD1220, Ser. number 2955; För Medical Instruments). Venous blood pressures were determined via a 1.4F Millar ultraminiature pressure only catheter (För Medical Instruments) that was inserted into the jugular vein and advanced to the vena cava superior. Collateral blood flow was determined via an ultrasonic flow probe (Transonic flow probe, V-Series; style: 0.7 mm, Probe: 0.5 PSB 263, Transonic Systems Inc., NY, USA) placed around the collateral stem region (common iliac artery) and connected to the respective flow meter (Transducer Ts 420, transit-time perivascular flowmeter Transonic Systems Inc., NY, USA). Measurements were performed under maximal vasodilatation using adenosine at increasing concentrations ranging from 15 to 300 μg/Kg per minute via a catheter inserted into the left carotid artery and advanced to the bifurcation as described previously. All measurements were recorded online on a computer using the MacLab interface (PowerLab; UmacLab). Total collateral dependent conductance was calculated as described previously dividing collateral blood flow by the arteriovenous pressure difference [22].

2.14. Statistical Analysis. All cell culture and biochemical analyses were repeated in at least 3 independent experiments. Data are shown as mean ± SEM. Statistical comparisons between 2 groups were performed with two-tailed Student's t-test. Multiple comparisons between groups were applied when necessary with ANOVA followed by post hoc analysis. Differences among means were considered significant when $P < 0.05$.

3. Results

3.1. Monoclonal Collateral Targeting IgM Antibody (CTA) 157-2 Stains Particularly the Endothelium of Proliferating Collateral Arteries. The immunohistochemical screening of monoclonal antibodies raised against membrane preparations of collateral arteries revealed that collateral targeting IgM

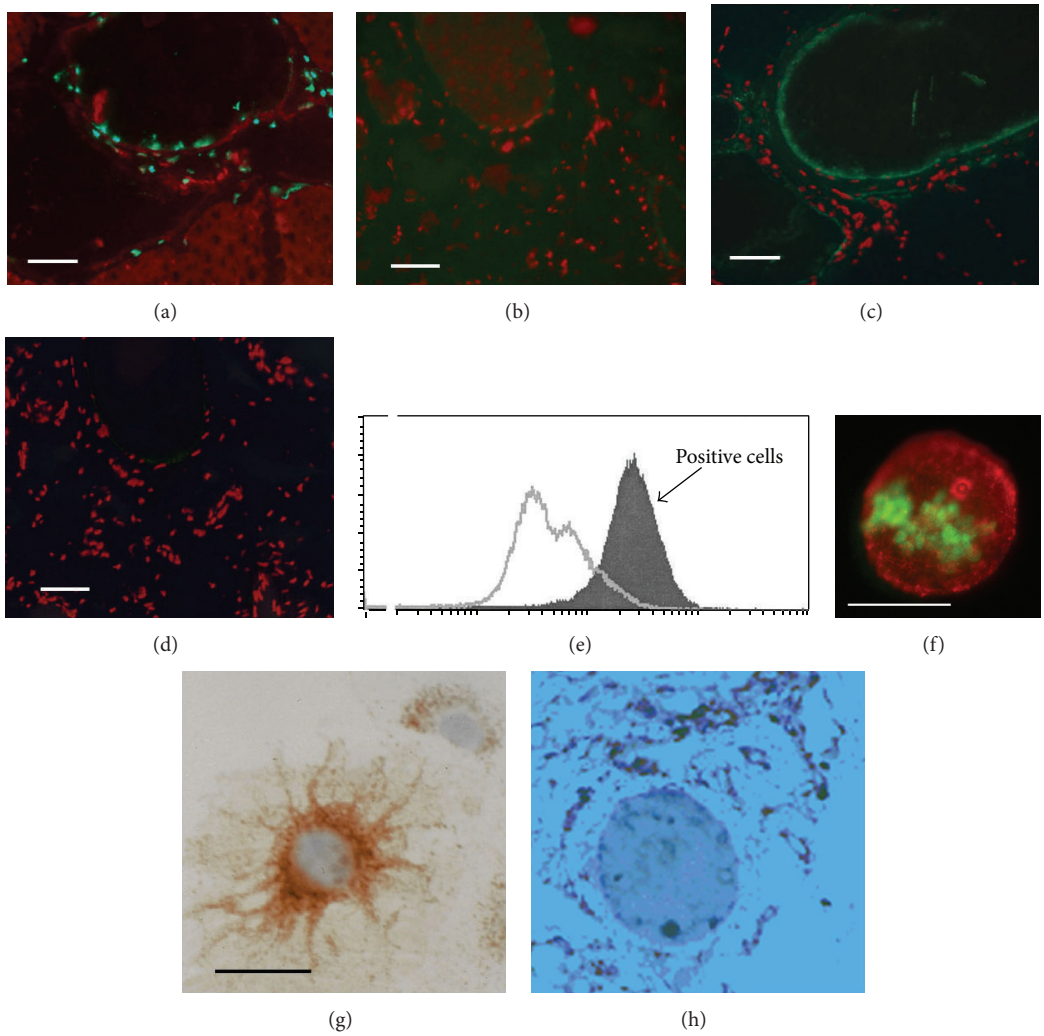

Figure 1: mAb CTA 157-2 staining of the endothelial lining of proliferating collateral vessels but not of control vessels ((a) and (c) parallel sections of proliferating collateral vessel; (a) BrdU staining (green fluorescence), (c) mAb CTA 157-2 staining (green fluorescence); (b) and (d) parallel sections of control vessel; (b) absence of BrdU staining (green fluorescence), (d) absence of mAb CTA 157-2 staining (green fluorescence); scale bar 40 μm). All slides were counterstained with propidium iodide as nuclear staining (red fluorescence). (e) Flow cytometric analysis of nonpermeabilized VR-EPCs after staining with mAb CTA 157-2 demonstrating specific extracellular staining of all cells (filled curve). Open curve shows staining with control antibody. (f) Fluorescence microscopy of BrdU treated cells stained with CTA 157-2 (red fluorescence) before permeabilization followed by permeabilization and staining of BrdU (green fluorescence) demonstrating focal distribution of the antigen on the cell membrane of proliferating VR-EPCs. (g) Light microscopic image of a vascular resident progenitor cell with immunohistochemical staining for total (intra- and extracellular) 20S proteasome (brown color; hematoxylin counterstain: blue): most 20S proteasome is found intracellularly, predominantly, and perinuclearly. (h) Light microscopic image of total 20S proteasome (brown color; hematoxylin counterstain: blue): most total (presumably intracellular) 20S proteasome is found in perinuclear cells.

antibody (CTA) 157-2 particularly stained the endothelial surfaces of proliferating collateral arteries (Figures 1(a)–1(d)). Other tissues like nerve tissue and other large vessels were stained as well albeit at a much lower level. The staining in these cases appeared to be restricted to the intracellular space. Thus this antibody appeared to be particularly suitable for the identification of novel players in collateral growth and was selected for further analysis.

3.2. Extracellular Staining of Vascular Resident Endothelial Progenitor Cell Membranes by CTA 157-2 as Demonstrated via Flow Cytometric Analysis. Using flow cytometric analysis we were able to demonstrate that CTA 157-2 stained an antigen present on the cell membrane of vascular resident endothelial progenitor cells (VR-EPCs), which were previously thoroughly characterized by our group [18] (Figure 1(e)). Fluorescence microscopy of these cells loaded with BrdU and stained with CTA 157-2 before permeabilization followed by permeabilization and staining of BrdU demonstrated a focal distribution of the antigen on proliferating cells (Figure 1(f)). This staining pattern contrasted with staining for total 20S proteasome that showed predominantly an intracellular perinuclear distribution as described previously [4] (Figure 1(g)). In histological section of collateral vessels this predominantly

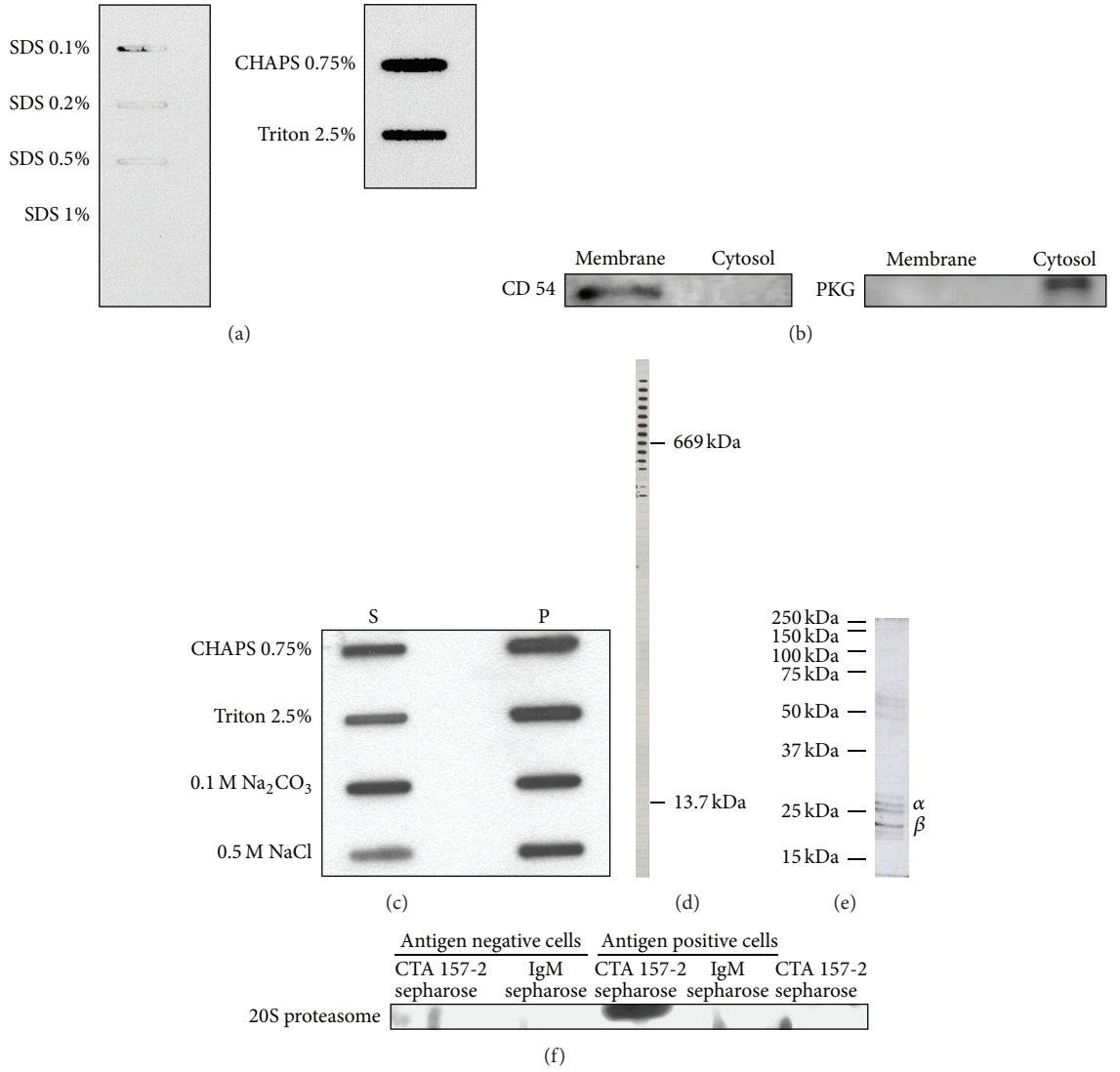

Figure 2: (a) Slot blot analysis of binding capacity of CTA 157-2 with different concentrations of SDS, CHAPS, and Triton. (b) Confirmation of purity of membrane fractions with anti-CD 54 antibody and cytosolic fractions with anti-PKG antibody. (c) Solubility of VR-EPC membrane fraction in different detergents (S: soluble phase; P: precipitate). (d) CTA 157-2 staining of different fractions collected after gel chromatography of cell membrane preparations along with stained marker proteins of defined sizes reveals that CTA 157-2 stains a protein complex of 700 kDa. (e) This complex separates on conventional SDS page into several subunits identified as 26 kD α7 and 21 kD β3 proteasome in mass spectrometry. (f) Specific staining of 20S proteasome after immunoprecipitation with CTA 157-2 of VR-EPC extracts (antigen positive cells). No staining after immunoprecipitation of antigen negative rat heart microvascular cells (antigen negative cells). No staining after immunoprecipitation with IgM control and of CTA 157-2 sepharose beads.

intracellular proteasome was mainly found in perivascular cells, presumably macrophages that are known to accumulate during collateral growth (Figure 1(h)).

3.3. CTA 157-2 Stains a 700 kDa Antigen Identified as Proteasome after Chromatographic Purification of Endothelial Membrane Fractions. In our attempt to identify the antigen stained by CTA 157-2 we had to learn that SDS even at lower concentration inhibited binding of CTA 157-2 to this antigen suggesting that this antibody detects a tertiary protein structure (Figure 2(a)). For this reason classical western blots could not be performed and classical methods of protein identification like screening of c-DNA expression libraries were deemed to fail. The purity of the membrane preparation was confirmed after staining with antibodies against CD 54, a membrane bound cell adhesion molecule, and soluble PKG a cytosolic protein on western blot. Only the membrane fractions expressed CD 54 whereas PKG was only found in the cytosolic fraction (Figure 2(b)). We tested the solubility of the complex in membrane fractions using different detergents and were able to demonstrate that part of the complex was solubilized already with NaCl. Only nonionic or zwitterionic

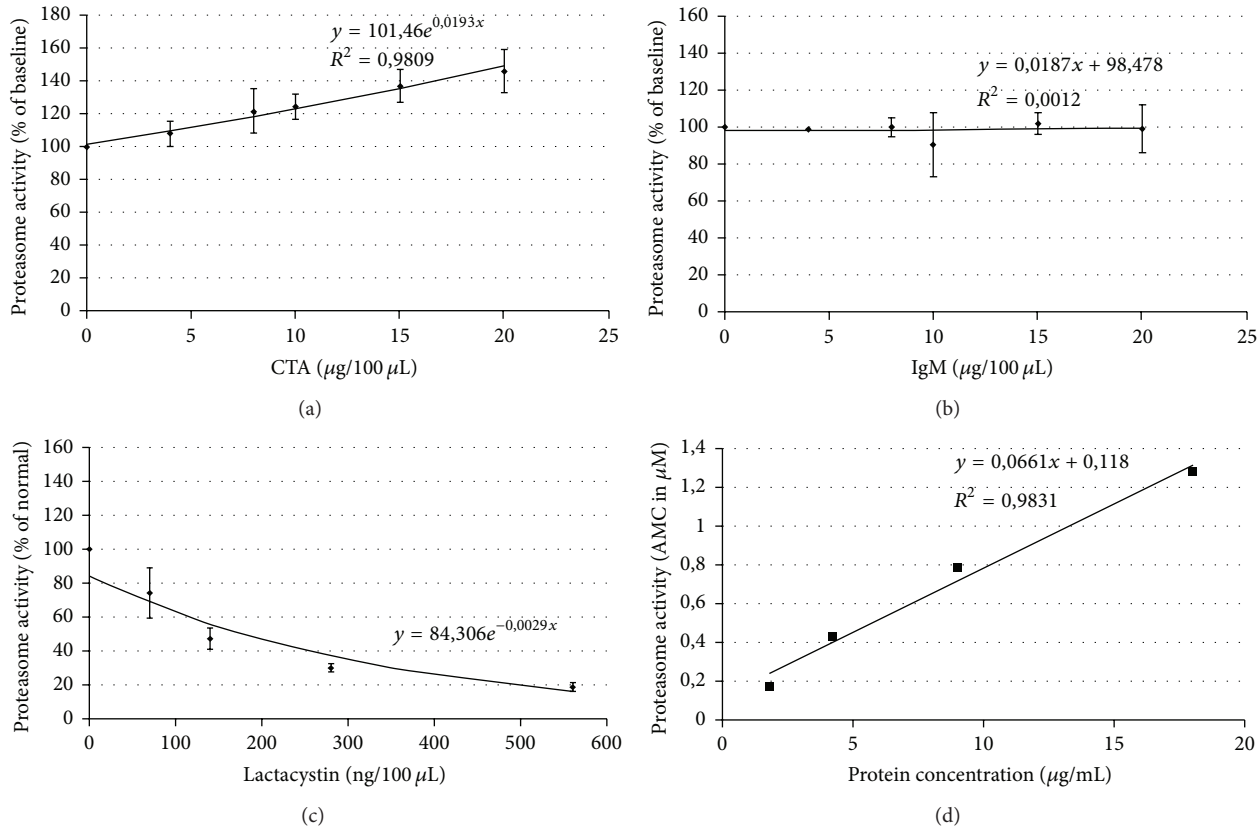

Figure 3: (a) CTA 157-2 specifically activates 20S proteasome and (b) control IgM antibody is without effect. (c) Proteasome inhibitor lactacystin reduces proteasome activity as expected. (d) Activation of the proteasome is purified membrane preparations with CTA 157-2 treatment.

detergents like CHAPS, Triton, or Tris, which leave tertiary structures of membrane proteins intact, allowed CTA 157-2 to detect the antigen indicating that the antigen-binding site represents a tertiary protein structure possibly composed of several protein subunits (Figure 2(c)). This also indicated a fairly strong attachment of the antigen detected by CTA 157-2 to the membrane fraction. The antigen was finally identified after chromatographic purification of membrane preparations of RHE A cells. Gel filtration of membrane fractions revealed that the antigen had a size around 700 kDa (Figure 2(d)). After further purification using ion exchange chromatography the antigen separated into several subunits on SDS page that were identified as 26 kDa α7 and 21 kDa β3 subunits of 20S proteasome using mass spectrometry (Figure 2(e)). These were the only rat proteins sequenced from the final CTA 157-2 positive fraction indicating that the purification strategy was successful.

3.4. Immunoprecipitates Generated with CTA 157-2 Are Identified as 20S Proteasome with a Polyclonal Rabbit Anti-Bovine 20S Proteasome Antibody on Western Blots. A second independent line of evidence is that CTA 157-2 bound 20S proteasome was generated after immunoprecipitation of cellular extracts with CTA 157-2 covalently linked to sepharase beads. Staining of immunoprecipitated extracts after gel electrophoreses and blotting with a second polyclonal rabbit anti-bovine 20S proteasome antibody revealed a band at 23 kDA corresponding to the 20S proteasome subunits reported to stain with this particular antibody (Figure 2(f)). This band was not detected in cellular extracts after immunoprecipitation with a control IgM and was only visible in immunoprecipitates of VR-EPC cellular extracts but not in cellular extracts from control cells that did not express the antigen in FACS analysis (Figure 2(f)).

3.5. CTA 157-2 Binds to Purified 20S Proteasome and Leads to Its Activation. We furthermore revealed a functional impact of CTA 157-2 on the proteasome when testing different concentrations of CTA on AMC cleavage from LLVY by 20S proteasome. CTA 157-2 specifically and concentration dependently activated reproducibly 20S proteasome (Figure 3(a)). We were able to exclude that this activation was due to unspecific effects of IgM (Figure 3(b)). Functionality of the assay was confirmed with the known proteasome inhibitor lactacystin (Figure 3(c)).

3.6. CTA 157-2 Elicits Proteasome Activity in Purified Membrane Fractions of VR-EPC. In order to confirm that proteasome activity is present in cell membranes we tested the effect

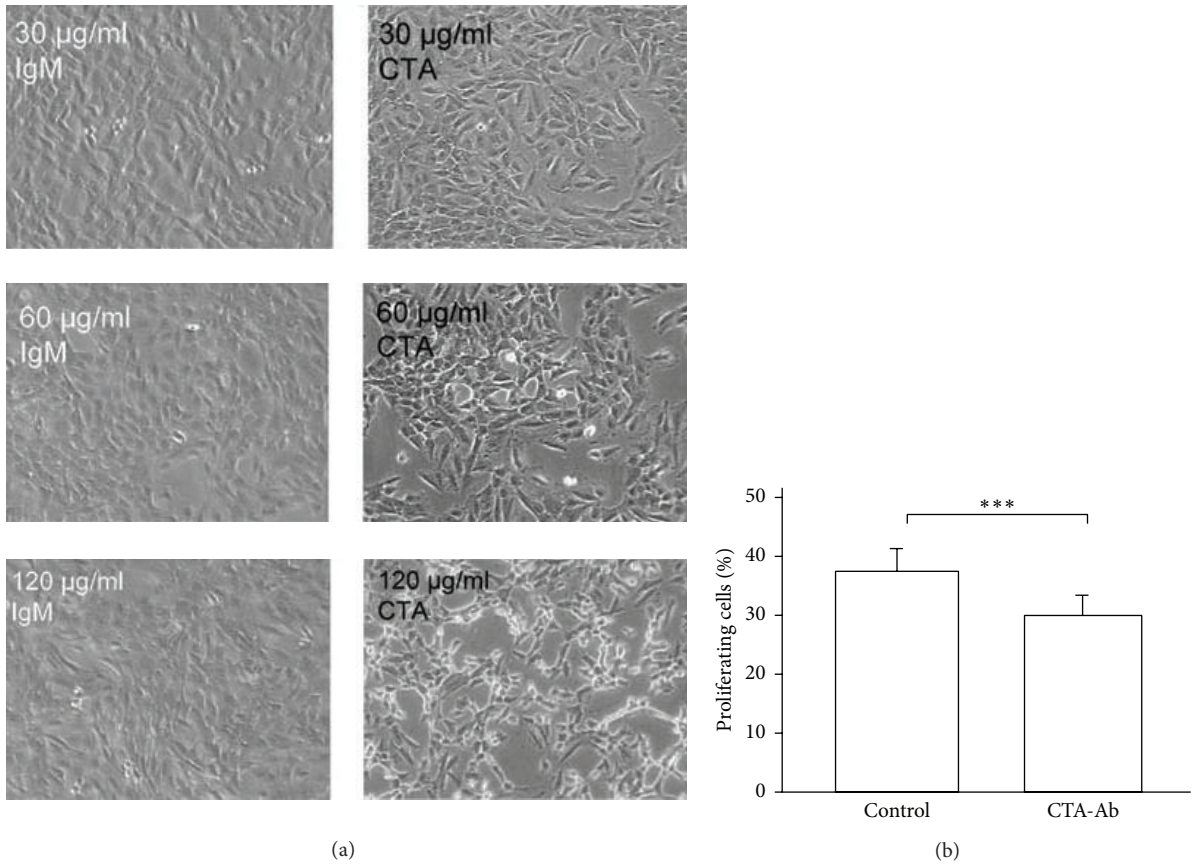

Figure 4: Concentration dependent decrease of VR-EPC proliferation by treatment with CTA157-2: (a) microscopic images after addition of control IgM and CTA 157-2 at different concentrations; (b) quantitative comparison of VR-EPC proliferation after addition of control IgM and CTA 157-2 as determined by BrdU incorporation; 5 experiments; $^{***}P < 0.001$.

of different membrane protein concentrations on AMC cleavage from LLVY with and without CTA 157-2 stimulation. In accordance with previous reports we were not able to detect any significant proteasome activity without stimulation. With CTA 157-2 stimulation, however, we were able to detect a concentration dependent proteasome activity of purified cell membranes (Figure 3(d)).

3.7. Proteasomal Activation via mAb CTA 157-2 Inhibits Concentration Dependently VR-EPC Proliferation In Vitro. In vitro CTA 157-2 reduced VR-EPCs proliferation concentration dependently (Figures 4(a) and 4(b): 37.2% ± 4.4% (IgM control) versus 29.7% ± 3.6% (CTA 157-2), $^{***}P < 0.001$ at 120 μg/mL).

3.8. Proteasomal Activation via mAb CTA 157-2 Inhibits Collateral Proliferation In Vivo. In order to investigate the impact of proteasomal activation on collateral growth we used the CTA 157-2 antibody in a collateral artery growth model previously described by our group [8, 17, 23]. In contrast to injection of an IgM control antibody local infusion of CTA 157-2 antibody reduced collateral proliferation and formation of collateral arteries in postmortem angiographies (Figures 5(a) and 5(d): proliferative index CTA 157-2 versus control IgM: 0.40 ± 0.14 versus 0.54 ± 0.17, $^{*}P < 0.05$; Figures 5(b), 5(c), and 5(e): number of visible collateral vessels CTA 157-2 versus control IgM 4.3±0.7 versus 5.3±0.4; $^{*}P < 0.05$). Furthermore we were able to demonstrate on a functional level infusion of CTA 157-2 reduced total collateral conductance after femoral artery occlusion as compared to control (Figure 5(f): box plot of total collateral conductance in mL/min/100 mmHg: CTA 157-2 versus control IgM: 0.93±0.02 mL/min/100 mmHg versus 1,61 ± 0.2 mL/min/100 mmHg, $^{*}P < 0.05$).

4. Discussion

In this study we demonstrate that transmembranous proteasomal activation controls vascular endothelial progenitor cell proliferation and collateral growth. The primary tool for our investigations was the monoclonal antibody CTA 157-2 that was generated against membrane preparations of growing collateral vessels in an attempt to identify novel membrane bound players in collateral growth. The collateral prone antibody CTA 157-2 was chosen because it predominantly stained the endothelial lining of proliferating collateral vessels, bound 100% of VR-EPCs in flow cytometric analysis, and was shown to significantly inhibit their proliferation concentration dependently *in vitro*. We furthermore were able to

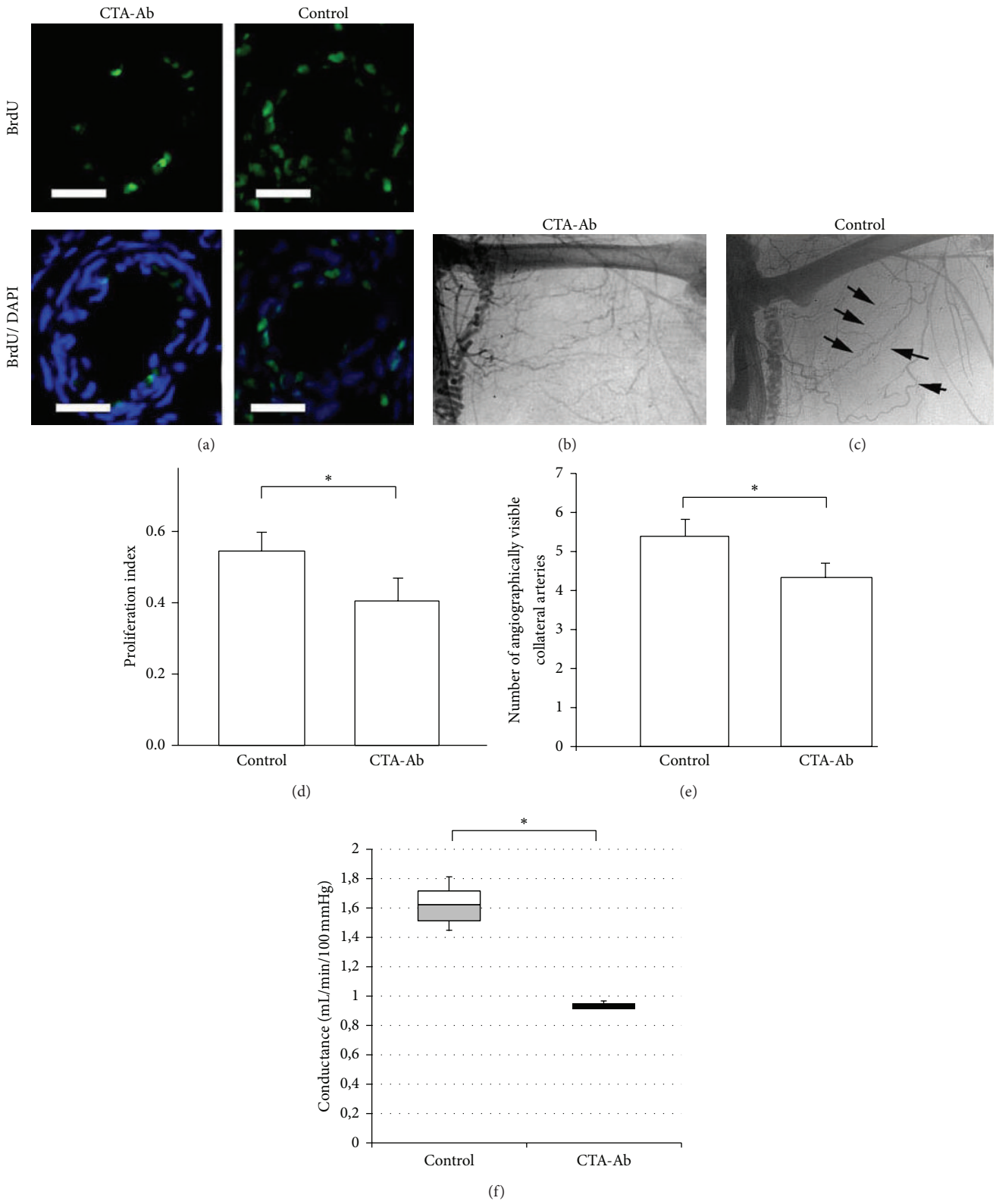

FIGURE 5: Decreased proliferation, number of collateral vessels, and total collateral conductance after *in vivo* injection of CTA 157-2 as compared to injection of control IgM: (a) BrdU incorporating nuclei (green/FITC) in relation to total nuclei (blue staining/DAPI) in collateral vessels of CTA 157-2 treated and control animals, (b) postmortem angiography of animal treated with CTA157-2, and (c) postmortem angiography of control animal (black arrows: collateral vessels). (d) Quantitative comparison of proliferation index (scale bar represents 100 μm; 6 animals per group, $^{*}P < 0.05$). (e) Quantification of visible collateral vessels using stereoscopic analysis (6 animals per group; $^{*}P < 0.05$). (f) Total collateral conductance in animals treated with CTA 157-2 as compared to control (3 animals per group; $^{*}P < 0.05$).

demonstrate that infusion of this antibody significantly inhibited collateral growth in contrast to infusion of an IgM control antibody.

Despite the challenging nature of the antibody and the antigen bound by this antibody we managed to obtain four lines of evidence that CTA 157-2 binds to cell membranes and activates the proteasome. A number of activators and inhibitors have been shown to regulate 20S proteasome *in vitro* [4]. Some activators like PA 28 bind to the end of the barrel shaped proteasome complex and stimulate peptidase activity. It appears possible that CTA 157-2 also binds to the ends of 20S proteasome and simulates activator functions [4].

More importantly we were able to demonstrate that the binding site of CTA 157-2 is exposed on the extracellular surface of vascular cell membranes via flow cytometric and immunohistochemical analysis of impermeabilized VR-EPCs. While the major part of the proteasome is located within the nuclear and cytoplasmic compartment it has long been recognized that the proteasome is also associated with cell membranes [24]. Lipopolysaccharide (LPS) components of Gram-negative bacteria have been shown to specifically bind to 20S proteasomes attached to the cell membrane of murine macrophages [25]. The presence of proteasomes at the surface of cell membranes was furthermore reported in human T and B lymphocytes [26]. Proteolytic active 20S proteasome was also detected in lung epithelial lining fluid of patients with acute respiratory distress syndrome [27]. Recently it was shown that functionally active 20S proteasome can be exported from activated immune cells by way of microparticles [28]. Although extracellular proteasome is known to be elevated in a number of inflammatory processes reports of its functional role during inflammation are scarce.

Inflammatory processes are strongly connected to arteriogenesis. In particular macrophage accumulation and activation have been shown to play a very important role in collateral growth [8–10, 17, 29]. A number of reports demonstrate that proteasomal activity is regulated by paracrine signals. It has, for example, been shown that cell attachment to extracellular matrices induces proteasomal degradation of the cyclin-dependent kinase 2 inhibitor p 21 [30]. To our knowledge, however, this is the first report demonstrating a functional role of extracellular 20S proteasome on progenitor cell function and vascular growth. Previous studies demonstrated that inhibition of the proteasome reduces angiogenesis and the growth of vascular cells, which at first sight appears to contradict our findings [31, 32]. However these studies investigated the effect of the proteasome on angiogenesis, the sprouting of capillaries, which considerably differs in its mechanisms from arteriogenesis, and the growth of collateral arteries from preexisting arteriolar anastomoses [10, 11]. Furthermore these studies primarily targeted the proteasome in nuclear and cytoplasmic compartments using different inhibitors and approaches whereas mAb CTA 157-2 only binds to the extracellular compartment *in vitro* and *in vivo*. For the same reason it appears counterintuitive to use proteasome inhibitors like lactacystin to test our hypothesis in cell culture or in *in vivo* experiments because it targets the proteasome in a different compartment and in different cells. To our knowledge there are no other agents that target specifically extracellular, respectively, transmembraneous proteasome apart from mAB CTA 157-2.

In this context it is interesting to note that the SOCS box protein 5 (asb5) that acts as a bridge between specific substrate-binding domains and E3 ubiquitin protein ligases has previously been shown to be upregulated in growing collateral vessels [33]. However a functional impact of this part of the ubiquitin-proteasome system on either vascular cell proliferation or collateral growth has not been demonstrated until now. Furthermore it was shown that adenoviral transfection of PR39, a protein that enhances hypoxia-inducible factor-1 alpha- (HIF-1 alpha-) dependent gene expression by selectively inhibiting proteasome degradation of this transcription factor, improves blood flow and myocardial function in a pig model of chronic myocardial ischemia by enhancing collateral formation [7].

5. Conclusion

Our study adds further evidence to the notion that the ubiquitin-proteasome system plays a decisive role in regulating collateral growth and demonstrates that extracellular 20S proteasome not only is released from cells but also plays a functional role in physiological processes.

Conflict of Interests

The authors declare that there is no conflict of interests regarding the publication of this paper.

Acknowledgments

The authors would like to thank Mrs. Juliane Bergmann for excellent technical assistance and helpful discussions. This work was supported by Grants from the German Research Foundation (DFG) IT-13/1, IT-13/2, and IT-13/3 (W.D. Ito) and Klinikum rechts der Isar, Technical University of Munich (H.-G. Machens). Dr. Ziyang Zhang is a recipient of the international scholarship from the China Scholarship Council.

References

[1] A. Helisch and W. Schaper, "Arteriogenesis: the development and growth of collateral arteries," *Microcirculation*, vol. 10, no. 1, pp. 83–97, 2003.

[2] P. Carmeliet, "Mechanisms of angiogenesis and arteriogenesis," *Nature Medicine*, vol. 6, no. 4, pp. 389–395, 2000.

[3] J.-S. Silvestre, D. M. Smadja, and B. I. Lévy, "Postischemic revascularization: from cellular and molecular mechanisms to clinical applications," *Physiological Reviews*, vol. 93, no. 4, pp. 1743–1802, 2013.

[4] M. Hochstrasser, "Ubiquitin-dependent protein degradation," *Annual Review of Genetics*, vol. 30, pp. 405–439, 1996.

[5] J. Li, M. Post, R. Volk et al., "PR39, a peptide regulator of angiogenesis," *Nature Medicine*, vol. 6, no. 1, pp. 49–55, 2000.

[6] T. Acker and K. H. Plate, "A role for hypoxia and hypoxia-inducible transcription factors in tumor physiology," *Journal of Molecular Medicine*, vol. 80, no. 9, pp. 562–575, 2002.

[7] M. J. Post, K. Sato, M. Murakami et al., "Adenoviral PR39 improves blood flow and myocardial function in a pig model of chronic myocardial ischemia by enhancing collateral formation," *American Journal of Physiology—Regulatory Integrative and Comparative Physiology*, vol. 290, no. 3, pp. R494–R500, 2006.

[8] S. Herzog, H. Sager, E. Khmelevski, A. Deylig, and W. D. Ito, "Collateral arteries grow from preexisting anastomoses in the rat hindlimb," *The American Journal of Physiology—Heart and Circulatory Physiology*, vol. 283, no. 5, pp. H2012–H2020, 2002.

[9] D. Scholz, W. Ito, I. Fleming et al., "Ultrastructure and molecular histology of rabbit hind-limb collateral artery growth (arteriogenesis)," *Virchows Archiv*, vol. 436, no. 3, pp. 257–270, 2000.

[10] W. Schaper and J. Schaper, *Arteriogenesis (Basic Science for the Cardiologist)*, vol. 1, Kluwer Academic Publishers, Boston, Mass, USA, 2004.

[11] W. D. Ito, M. Areas, D. Scholz, B. Winkler, P. Htun, and W. Schaper, "Angiogenesis but not collateral growth is associated with ischemia after femoral artery occlusion," *The American Journal of Physiology: Heart and Circulatory Physiology*, vol. 273, no. 3, pp. H1255–H1265, 1997.

[12] E. Zengin, F. Chalajour, U. M. Gehling et al., "Vascular wall resident progenitor cells: a source for postnatal vasculogenesis," *Development*, vol. 133, no. 8, pp. 1543–1551, 2006.

[13] K. Jujo, M. Ii, and D. W. Losordo, "Endothelial progenitor cells in neovascularization of infarcted myocardium," *Journal of Molecular and Cellular Cardiology*, vol. 45, no. 4, pp. 530–544, 2008.

[14] J. T. Egaña, S. Danner, M. Kremer et al., "The use of glandular-derived stem cells to improve vascularization in scaffold-mediated dermal regeneration," *Biomaterials*, vol. 30, no. 30, pp. 5918–5926, 2009.

[15] Y. Zhang, B.-S. Herbert, G. Rajashekhar et al., "Premature senescence of highly proliferative endothelial progenitor cells is induced by tumor necrosis factor-alpha via the p38 mitogen-activated protein kinase pathway," *The FASEB Journal*, vol. 23, no. 5, pp. 1358–1365, 2009.

[16] P. van Vliet, J. P. G. Sluijter, P. A. Doevendans, and M.-J. Goumans, "Isolation and expansion of resident cardiac progenitor cells," *Expert Review of Cardiovascular Therapy*, vol. 5, no. 1, pp. 33–43, 2007.

[17] E. Khmelewski, A. Becker, T. Meinertz, and W. D. Ito, "Tissue resident cells play a dominant role in arteriogenesis and concomitant macrophage accumulation," *Circulation Research*, vol. 95, no. 6, pp. E56–E64, 2004.

[18] Z. Zhang, W. D. Ito, U. Hopfner et al., "The role of single cell derived vascular resident endothelial progenitor cells in the enhancement of vascularization in scaffold-based skin regeneration," *Biomaterials*, vol. 32, no. 17, pp. 4109–4117, 2011.

[19] G. Kohler and C. Milstein, "Continuous cultures of fused cells secreting antibody of predefined specificity," *Nature*, vol. 256, no. 5517, pp. 495–497, 1975.

[20] C. J. Dean, "Preparation and testing of monoclonal antibodies to recombinant proteins," in *Immunochemical Protocols*, J. D. Pound, Ed., vol. 80 of *Methods in Molecular Biology*, pp. 23–37, Humana Press, Totowa, NJ, USA, 1998.

[21] N. Obermeyer, N. Janson, J. Bergmann, F. Buck, and W. D. Ito, "Proteome analysis of migrating versus nonmigrating rat heart endothelial cells reveals distinct expression patterns," *Endothelium*, vol. 10, no. 3, pp. 167–178, 2003.

[22] F. Pipp, M. Heil, K. Issbrücker et al., "VEGFR-1-selective VEGF homologue PlGF is arteriogenic—evidence for a monocyte-mediated mechanism," *Circulation Research*, vol. 92, no. 4, pp. 378–385, 2003.

[23] W. D. Ito, N. Lund, H. Sager, W. Becker, and U. Wenzel, "Differential impact of diabetes mellitus type II and arterial hypertension on collateral artery growth and concomitant macrophage accumulation," *Vasa*, vol. 44, no. 1, pp. 31–41, 2015.

[24] S. U. Sixt and B. Dahlmann, "Extracellular, circulating proteasomes and ubiquitin—incidence and relevance," *Biochimica et Biophysica Acta—Molecular Basis of Disease*, vol. 1782, no. 12, pp. 817–823, 2008.

[25] N. Qureshi, P.-Y. Perera, J. Shen et al., "The proteasome as a lipopolysaccharide-binding protein in macrophages: differential effects of proteasome inhibition on lipopolysaccharide-induced signaling events," *The Journal of Immunology*, vol. 171, no. 3, pp. 1515–1525, 2003.

[26] J. P. Bureau, M. Olink-Coux, N. Brouard et al., "Characterization of prosomes in human lymphocyte subpopulations and their presence as surface antigens," *Experimental Cell Research*, vol. 231, no. 1, pp. 50–60, 1997.

[27] S. U. Sixt, M. Beiderlinden, H. P. Jennissen, and J. Peters, "Extracellular proteasome in the human alveolar space: a new housekeeping enzyme?" *The American Journal of Physiology—Lung Cellular and Molecular Physiology*, vol. 292, no. 5, pp. L1280–L1288, 2007.

[28] I. Bochmann, F. Ebstein, A. Lehmann et al., "T lymphocytes export proteasomes by way of microparticles: a possible mechanism for generation of extracellular proteasomes," *Journal of Cellular and Molecular Medicine*, vol. 18, no. 1, pp. 59–68, 2014.

[29] M. Arras, W. D. Ito, D. Scholz, B. Winkler, J. Schaper, and W. Schaper, "Monocyte activation in angiogenesis and collateral growth in the rabbit hindlimb," *The Journal of Clinical Investigation*, vol. 101, no. 1, pp. 40–50, 1998.

[30] W. Bao, M. Thullberg, H. Zhang, A. Onischenko, and S. Strömblad, "Cell attachment to the extracellular matrix induces proteasomal degradation of p21CIP1 via Cdc42/Rac1 signaling," *Molecular and Cellular Biology*, vol. 22, no. 13, pp. 4587–4597, 2002.

[31] H. C. A. Drexler, W. Risau, and M. A. Konerding, "Inhibition of proteasome function induces programmed cell death in proliferating endothelial cells," *The FASEB Journal*, vol. 14, no. 1, pp. 65–77, 2000.

[32] T. Tamatani, N. Takamaru, K. Hara et al., "Bortezomib-enhanced radiosensitization through the suppression of radiation-induced nuclear factor-kappaB activity in human oral cancer cells," *International Journal of Oncology*, vol. 42, no. 3, pp. 935–944, 2013.

[33] K. Boengler, F. Pipp, B. Fernandez, A. Richter, W. Schaper, and E. Deindl, "The ankyrin repeat containing SOCS box protein 5: a novel protein associated with arteriogenesis," *Biochemical and Biophysical Research Communications*, vol. 302, no. 1, pp. 17–22, 2003.

Hindawi Publishing Corporation
BioMed Research International
Volume 2015, Article ID 142359, 13 pages
http://dx.doi.org/10.1155/2015/142359

Review Article

The Role of Mast Cell Specific Chymases and Tryptases in Tumor Angiogenesis

Devandir Antonio de Souza Junior, Ana Carolina Santana, Elaine Zayas Marcelino da Silva, Constance Oliver, and Maria Celia Jamur

Department of Cell and Molecular Biology and Pathogenic Bioagents, Ribeirão Preto Medical School, University of São Paulo, 14049-900 Ribeirão Preto, SP, Brazil

Correspondence should be addressed to Maria Celia Jamur; mjamur@fmrp.usp.br

Received 18 December 2014; Accepted 13 February 2015

Academic Editor: Francesco Moccia

An association between mast cells and tumor angiogenesis is known to exist, but the exact role that mast cells play in this process is still unclear. It is thought that the mediators released by mast cells are important in neovascularization. However, it is not known how individual mediators are involved in this process. The major constituents of mast cell secretory granules are the mast cell specific proteases chymase, tryptase, and carboxypeptidase A3. Several previous studies aimed to understand the way in which specific mast cell granule constituents act to induce tumor angiogenesis. A body of evidence indicates that mast cell proteases are the pivotal players in inducing tumor angiogenesis. In this review, the likely mechanisms by which tryptase and chymase can act directly or indirectly to induce tumor angiogenesis are discussed. Finally, information presented here in this review indicates that mast cell proteases significantly influence angiogenesis thus affecting tumor growth and progression. This also suggests that these proteases could serve as novel therapeutic targets for the treatment of various types of cancer.

1. Introduction

Angiogenesis is a dynamic process mediated by endothelial cells whereby new blood vessels are formed from existing ones [1, 2]. Angiogenesis is crucial during physiological processes such as embryonic development and corpus luteum formation, and it is also involved in the development of pathological conditions such as tumorigenesis and chronic inflammation [3, 4]. This process is highly regulated by the balance between proangiogenic and antiangiogenic factors within the vascular microenvironment and involves the participation of extracellular matrix (ECM) proteins, adhesion molecules, and proteolytic enzymes [5, 6]. The main proangiogenic factors include vascular endothelial growth factor (VEGF), fibroblast growth factor (FGF), transforming growth factor-beta (TGF-β) platelet-derived growth factor (PDGF), interleukin-8 (IL-8), and angiopoietin-1 [7, 8]. A change in the balance between proangiogenic and antiangiogenic factors towards the activation of usually quiescent endothelial cells initiates a series of sequential events that characterize the angiogenic process, that is, ECM degradation, migration and proliferation of endothelial cells, formation of tube-like structures on 2D matrices and sprouting in 3D matrices, spatial distribution of newly formed vessels, deposition of new ECM, and mobilization of pericytes for vessel stabilization, and finally a shift in the balance towards inhibition of angiogenesis returns the endothelial cells to their quiescent state [9–12].

The importance of angiogenesis for tumor development has long been investigated. In the beginning of the 20th century, Goldmann [13] had already envisioned the importance of the vascular system for tumor growth. However, it was not until 1971 that Folkman [14] showed that tumor growth was dependent on angiogenesis and proposed the use of antiangiogenic therapy against cancer. Today, tumor angiogenesis is considered crucial for cancer development through induction of tumor growth, invasion, and metastasis [15, 16]. Moreover, the use of antiangiogenic agents as adjuvants for cancer treatment has become a reality [17].

Tumor angiogenesis relies on the abnormal switch in the balance between positive and negative regulators, usually triggered by the release of angiostimulatory mediators from neoplastic and inflammatory cells. The binding of these mediators to their receptors on endothelial cells activates the angiogenesis cascade [18–20]. The pro- and antitumorigenic signals provided by tumor cells and resident and recruited immune cells are ultimately responsible for the outcome of tumor progression. These signals act in processes such as proliferation and survival of tumor cells, angiogenesis, immune system modulation, tissue remodeling, and metastasis [21]. Therefore, the interaction between tumor, stromal, and immune cells collaborates to establish a "proangiogenic/tumorigenic" microenvironment favoring the survival, development, and spreading of tumor cells [22].

The view that immune cells are critical in providing the angiogenic stimulus required for tumor growth and progression is supported by a number of studies assigning proangiogenic roles to various innate immune cell types, in particular macrophages and mast cells [23]. In this review article, the importance of mast cells in tumor angiogenesis with special reference on the role of mast cell proteases in this process will be discussed.

2. Mast Cell Biology

Mast cells are bone-marrow-derived multifunctional immune cells implicated in both physiological and pathological settings (reviewed in [24]). Mast cell progenitors leave the blood circulation to mature and reside in the connective tissue, at the interface between the host and the outside environment, predominantly in subepithelial regions and in the connective tissue surrounding blood vessels, nerves, lymphatic vessels, and mucus glands [25, 26]. Mast cell distribution relies on mechanisms of constitutive homing, enhanced recruitment, survival, and local maturation of mast cell progenitors. In physiological conditions, their numbers remain relatively constant; however, proliferation and the enhancement of the mechanisms described above lead to mast cell hyperplasia during hypersensitivity reactions and infections and in response to various disease processes [27–29].

Mast cells' functions are a direct consequence of the diversity of biologically active compounds that they are able to produce and secrete. Upon activation, mast cells can release a wide range of mediators belonging to three distinct classes: preformed mediators, which are stored in mast cell cytoplasmic granules; neoformed or lipid mediators, which are products of phospholipase A2 activation; and neosynthesized mediators, which are produced and released upon transcriptional activation [25].

Mast cells may be activated by distinct stimuli acting on the various surface receptors expressed by these cells. Moreover, the variety of mast cell responses to different stimuli, that is, the nature of the mediators released, is influenced by mast cell heterogeneity. This heterogeneity is ultimately dictated by the intrinsic and microenvironmental factors that these cells encounter in normal and pathological conditions [25, 30].

A distinct feature of mature mast cells is the high content of metachromatic, electron dense secretory granules present in their cytoplasm. These secretory granules store an extensive variety of preformed bioactive mediators, which are all stored in the active form and are promptly released by degranulation. Mast cell degranulation can be triggered by various mechanisms such as the crosslinking of FcεRI-bound IgE by specific antigens, crosslinking of FcγRIII by IgG immune complexes, complement receptor engagement by complement components such as C3a and C5a, c-kit receptor binding by stem cell factor (SCF), TLR2 (toll-like receptor 2) stimulation, or by binding of neuropeptides, and other peptides [31–37]. The preformed mediators include, but are not restricted to, biogenic amines, lysosomal enzymes, proteases, proteoglycans, cytokines, chemokines, growth factors, and peptides [31, 33, 36–38].

The major constituents of mast cell secretory granules are the mast cell specific proteases chymase, tryptase, and carboxypeptidase A3 (CPA3) (Table 1) [39]. These proteases are exclusively expressed by mast cells and they represent approximately 25% of the cell protein content. They are stored in their active form within the secretory granules [40–42]. The tryptases and chymases are serine proteases while CPA3 is a zinc-dependent metalloprotease [39, 43].

Like other positively charged preformed mediators, mast cell proteases are efficiently packed into mast cell secretory granules owing to their interaction with negatively charged serglycin proteoglycans [43, 44]. However, not all subtypes of mast cell proteases are dependent on serglycin for storage. A study using knockout mice for serglycin core protein showed that although the protease mRNA levels were similar between knockout and wild type mice the interaction of mast cell proteases with serglycin was necessary to regulate the storage of mouse mast cell protease- (mMCP-) 4, mMCP-5, mMCP-6, and CPA in the granules [45]. On the other hand, Braga et al. [46] showed that the storage of mMCP-7 and mMCP-1 was independent of serglycin. Moreover, Melo et al. [44] have recently shown that serglycin dependent storage of mast cell proteases is critical in the induction of apoptosis induced by permeabilization of the granule membrane.

The mast cell protease content varies according to the tissue distribution of mast cells as well as from species to species, and these differences are used to phenotypically classify mast cells (Table 1) [47]. Human mast cells are divided into MC_T that express tryptases α and β and MC_{TC} that express chymases, tryptases, and CPA3. A third phenotype expressing tryptases and CPA3 was recently described in airway epithelium and esophageal samples of patients with asthma and eosinophilic esophagitis [48, 49]. In rodents, mast cells are classified according to their distribution as connective tissue mast cells (CTMCs), which express chymases (α and β), tryptases, and CPA, and mucosal mast cells (MMCs), which express the β chymases, mMCP-1 and mMCP-2. It is noteworthy to mention that these mouse mast cell phenotypes can vary significantly according to mast cell location, animal strain, and whether or not the tissue is inflamed [50–53]. Mast cell proteases have been implicated

Table 1: Characteristics of major human and murine mast cell proteases.

Protein designation	Mast cell subtype	Chromosomal location	Gene name	Primary substrate specificity	Subunit structure
			Chymase		
			Human		
Chymase (CMA1)	MC_{TC}	14q11.2	*CMA1*	Chymotrypsin-like (aromatic amino acid)	Monomer
			Mouse		
mMCP-1	MMC	14C1/2	*Mcpt1*	Chymotrypsin-like (aromatic amino acid)	Monomer
mMCP-2	MMC	14C1/2	*Mcpt2*	Unknown (low enzymatic activity)	Monomer
mMCP-4	CTMC	14C1/2	*Mcpt4*	Chymotrypsin-like (aromatic amino acid)	Monomer
mMCP-5	CTMC	14C1/2	*Cma1/Mcpt5*	Elastase-like (Val/Ala/Ile)	Monomer
			Tryptase		
			Human		
Tryptase βII/βIII (human)	MC_{TC}/MC_{T}	16p13.3	*TPSB2*	Trypsin-like (Arg/Lys)	Tetramer
Tryptase αI/βI (human)	MC_{TC}/MC_{T}	16p13.3	*TPSAB1*	Trypsin-like (Arg/Lys)	Tetramer
			Mouse		
mMCP-6	CTMC	17A3.3	*Mcpt6*	Trypsin-like (Arg/Lys)	Tetramer
mMCP-7	CTMC	17A3.3	*Tpsab1*	Trypsin-like (Arg/Lys)	Tetramer
			Carboxypeptidase A3		
			Human		
MC-CPA	MC_{TC}	3q24	*CPA3*	CPA-like (C-terminal aromatic/aliphatic amino acids)	Monomer
			Mouse		
MC-CPA	CTMC	3A3	*Cpa3*	CPA-CPA-like (C-terminal aromatic/aliphatic amino acids)	Monomer

in a number of pathological states including arthritis, allergic airway inflammation, and tumor angiogenesis [54–59].

3. Mast Cells, Tumors, and Angiogenesis

The association between mast cells, inflammation, and cancer is conflicting and involves both promotion of and protection against tumor progression. The first association of mast cells with tumors dates back from the initial description of mast cells by Ehrlich in 1878, when he reported that mast cells were numerous in some tumors [60]. Since then, interest in the contribution of mast cells to tumor development has increased progressively. Mast cells have been shown to accumulate around several types of tumors and are generally the first inflammatory cells to infiltrate developing tumors such as malignant melanoma and breast and colorectal tumors [61–64]. This accumulation typically occurs around blood vessels within the tumor environment and correlates with both good and poor prognosis in different cancers demonstrating the paradoxical involvement of mast cells in tumor progression [65–67]. Mast cells are recruited by several tumor-derived factors including the angiogenic factors VEGF, PDGF, and FGF-2 [68]. Notably, Huang et al. [69], using an hepatocarcinoma model, showed that mast cells were unable to migrate in SCF-knockout tumors or in the presence of anti-c-kit antibodies, ultimately resulting in decreased tumor growth. In addition, SCF stimulation leads to the release of matrix metalloproteinase-9 (MMP-9), IL-6, TNF-α, VEGF, Cox2, i-NOS, and chemokine (C-C motif) ligand 2 (CCL2). These results suggest that mast cell recruitment and activation, with the consequent release of inflammatory mediators that participate in tissue remodeling and immune suppression, are mainly mediated by SCF and its receptor c-kit expressed on the mast cell surface. The contribution of mast cells to the promotion of cancer includes their action on immunosuppression, the release of proangiogenic and mitogenic factors, and degradation of the ECM [61].

Mast cells have been shown to be associated with angiogenesis and tumor progression in numerous types of cancer

[65, 70–80]. Stimulation of angiogenesis is undoubtedly the most significant role of mast cells in the promotion of tumor growth and development [81]. In fact, mast cell deficient mice showed a reduced angiogenesis and metastatic capacity during tumor induction [82]. The involvement of mast cells in these processes is most certainly related to the release of a plethora of potent proangiogenic mediators which include histamine, angiopoietin-1, VEGF, FGF-2, TGF-β, tumor necrosis factor-alpha (TNF-α), and IL-18 [81, 83, 84]. Furthermore, a role for mast cell specific proteases has gained increasing support [74, 85–89]. For instance, mast cell specific proteases are involved in the initial phases of tumor growth and also modulate vascular growth in the later stages of tumor progression [59]. Mast cell mediators can induce angiogenesis through their action at different stages of angiogenesis, that is, degradation of the ECM, migration and proliferation of endothelial cells, formation and distribution of new vessels, synthesis of ECM, and pericyte mobilization [10, 90].

Most angiogenic mediators released by mast cells are not exclusive to mast cells, so it is difficult to attribute their biological actions to mast cells alone. Therefore, the majority of recent investigations on the role of mast cells in tumor angiogenesis have focused on the ability of mast cells to synthesize, store, and release mast cell specific chymases and tryptases. The role of these proteases in tumor angiogenesis is the subject of this review.

4. Tryptases in Tumor Angiogenesis

Mast cell tryptase is a tetrameric neutral serine protease with a molecular weight of 134 kDa [54, 91]. Mast cells contain 10–35 pg tryptases per cell [92]. The enzyme consists of four noncovalently bound subunits. Each subunit has one active catalytic site and disruption of the tetramer into monomers causes inactivation of the tryptase [40, 93]. Tryptases were named because of their trypsin-like substrate specificity (Table 1). They cleave preferentially after Lys/Arg residues [39, 94]. Humans express two classes of tryptase (alpha and beta). Alpha-tryptase is the major circulating isoform and β-tryptase appears to be the major type stored in secretory granules [54, 94–96]. Three similar β-tryptases (βI–III) and one α-tryptase have been identified. The β-tryptases are 98-99% identical in amino acid sequence, while the α-tryptase is less closely related. The mast cell tryptases (MCP-6 and MCP-7) expressed in rodents most likely represent the counterparts to human α-tryptase and β-tryptases, respectively. Additionally, both subtypes are initially expressed as monomers in humans and rodents [95, 96] and then combine to form tetramers.

The first reports on the association between tryptase and tumor angiogenesis focused on the use of tryptase as a specific marker for mast cells. Kankkunen and colleagues [97] were among the first to study this relationship. They analyzed the number and distribution of tryptase- and chymase-positive mast cells in benign and malignant breast lesions [97]. Their results show that the number of tryptase-positive mast cells in malignant tumors was increased four times in relation to the benign lesions. Moreover, in malignant lesions, tryptase-positive mast cells were concentrated at the tumor edge within the "invasion zone." Since then several other studies have corroborated this correlation between tryptase and malignant tumors in various types of tumor, such as lung adenocarcinoma [98]; B-cell non-Hodgkin's lymphomas [80], brain [99] and cervical cancer [70], myelodysplastic syndrome [4], B-cell chronic lymphocytic leukemia [100], melanoma [101], hepatocellular carcinoma [102], gastrointestinal cancer [103], early breast cancer [104], and colorectal cancer [105]. During the last two decades, several studies, using tryptase as a mast cell marker, have shown that mast cells are strategically located in proximity to blood vessels where they have been associated with tumor angiogenesis. These studies on the correlation between tryptase-positive mast cells and angiogenesis also showed a positive association between tumor aggressiveness and poor prognosis [106–108].

Tryptases act on a variety of substrates [39, 96]. Processing of several of these substrates are known to be key factors in angiogenesis, such as degradation of extracellular matrix [109, 110], plasminogen activation [111], fibrinogen degradation [112, 113], activation of latent collagenase and matrix metalloproteinases [114, 115], and tryptase-induced endothelial barrier dysfunction [116, 117]. The correlation between the presence of tryptase-positive mast cells and angiogenesis as well as the action of tryptase on angiogenesis related substrates supports the hypothesis that the presence of tryptase is critical for the initiation of angiogenesis. In spite of the fact that these studies only showed the presence of mast cells at angiogenic sites, they provided a basis for further investigation on the direct relationship between tryptase and angiogenesis.

Blair et al. [118] were the first to investigate the potential of tryptase to induce *in vitro* angiogenesis using a tube formation angiogenesis assay. This assay involves plating endothelial cells on a gel matrix and assaying adhesion, migration, and formation of capillary or tube-like structures. These capillary-like structures consist of tubes and loops. Tubes are formed by endothelial cell sheets and go from one branch point to another branch point or to a loose end. Loops are the enclosed (or almost enclosed) spaces inside the tubes. In these experiments, they incubated human dermal microvascular endothelial cells (HDMECs), plated in matrigel-coated wells, in the presence of purified human lung tryptase for 16 hours. The tryptase induced an increase in capillary-like structures and proliferation of HDMECs. This effect was suppressed by the use of protease inhibitors. These results lead to the conclusion that tryptase interacts directly with endothelial cells via an unidentified mechanism to induce angiogenesis.

Compton et al. [119] also investigated the ability of tryptase to induce *in vitro* angiogenesis. However, in this study tryptase did not stimulate growth of human umbilical vein endothelial cells (HUVEC). They observed that tryptase induced the release of IL-8 in a dose-dependent manner. They also confirmed that this effect on HUVEC required enzymatically active tryptase. Release of IL-8 did not occur in the presence of heat inactivated enzyme or when the tryptase was preincubated with the protease inhibitors.

Using a mouse model of epithelial carcinogenesis, Coussens et al. [120] observed that, during the dysplasia stage,

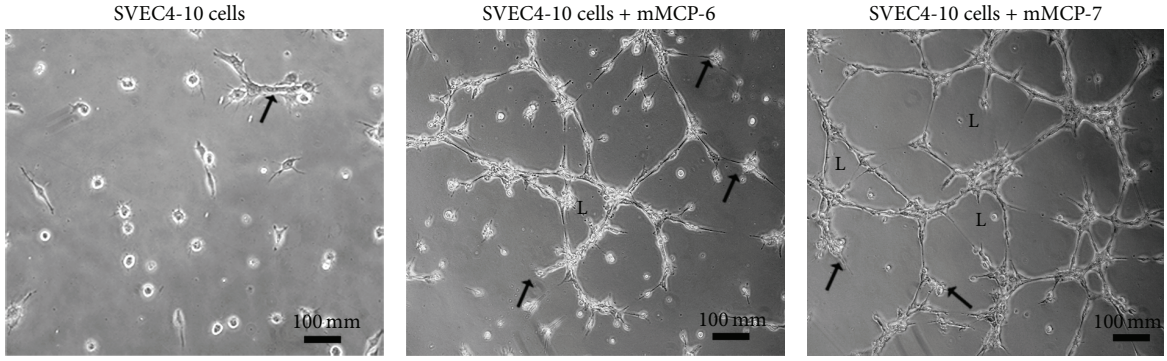

Figure 1: rmMCP-6 and rmMCP-7 induce tube formation by mouse endothelial cells.

vascular changes indicative of an angiogenic switch from vascular quiescence to modest neovascularization occurred in early modest to low-grade lesions [120]. At this stage, the researchers observed a significant increase in tryptase activity and mMCP-6 mRNA expression. In this same study, mMCP-6 did not directly affect the extracellular matrix, but mMCP-6 acted indirectly through the stimulation of procollagen synthesis by fibroblasts. The results of this elegant study indicate that tryptase can affect the extracellular matrix by stimulating the cellular components, thus altering its composition that then leads to neovascularization. Additionally, other studies have demonstrated the ability of tryptase to digest isolated extracellular matrix [109, 121, 122]. Further studies have shown that tryptase can also activate metalloproteinases thus inducing degradation of the extracellular matrix [114, 123]. Taken together, these results suggest that tryptase may have both a direct and indirect action in the remodeling and degradation of the extracellular matrix during angiogenesis. The role of tryptase in degradation/remodeling of the extracellular matrix may vary depending on the type of tumor and phase of tumor progression. This process of degradation/remodeling could increase the space available for neovascularization and contribute to the release of angiogenic factors present in the matrix such as VEGF and FGF-2 [113, 124].

Another direct effect of tryptase in various cell types, including endothelial cells, is stimulation of protease activated receptor-2 (PAR-2) [125, 126]. Yoshii and coworkers [74] studying the direct effects of tryptase on the proliferation and intracellular signaling in DLD-1 colorectal adenocarcinoma cells *in vitro* demonstrated that tryptase induces proliferation in DLD-1 cells through its proteolytic activity on PAR-2. The increase in proliferation was mediated in a cyclooxygenase- and MAP kinase-dependent manner. Recently, Zhi and colleagues [127] demonstrated *in vitro* that tryptase increased bEnd.3 mouse brain endothelial cell proliferation, migration, and tube formation, suggesting a role for tryptase in microvessel formation. They also observed that tryptase increased tissue plasminogen activator (tPA) and inhibited plasminogen activator inhibitor-1 (PAI-1) expression at both mRNA and protein levels in bEnd.3 cells.

Therefore, tryptase, through the activation of PAR-2, may have a role in modulating the balance between expression of urokinase plasminogen activator (uPA) and PAI-1. Expression of uPA and PAI-1 is PAR-dependent [128, 129]. Additionally, PAR-2 activation in vascular cells promotes angiogenesis during tissue repair as well as during neovascularization of the retina [130, 131]. PAR-2 also induces endothelial cell proliferation [132, 133] and cytokine expression in endothelial cells and other cell types [134–136]. Together these studies indicate that the activation of PAR-2 by tryptase is directly related to the role of mast cells in angiogenesis. The exact mechanism by which PAR-2 contributes to angiogenesis remains to be elucidated. Nevertheless, the involvement of tryptase in PAR-2 activation and angiogenesis is clear.

Tryptase (mMCP-6 and mMCP-7) expression and activity were increased during progression of skin tumors in mice [59]. Furthermore, the increase in tryptase activity was correlated with the tumor angiogenesis. mMCP-7 was not detectable in control animals but became measurable concomitantly with the initiation of angiogenesis during tumor progression. The ability of these two subtypes of tryptase to induce angiogenesis *in vitro* was compared. mMCP-6 and mMCP-7 were both able to induce tube formation in SVEC4-10 endothelial cells. However, mMCP-7 was more efficient in inducing cell spreading and tube formation than mMCP-6 (Figure 1). These data show that both subtypes of mast cell specific tryptases may interact with endothelial cells to promote neovascularization of tumors.

When endothelial cells were incubated in absence of tryptases a few SVEC4-10 cells are spread and an occasional tube is seen (arrow). When the SVEC4-10 cells were incubated with rmMCP-6, cells are spread, and tubes (arrows) and loops (L) are present. When the SVEC4-10 cells were incubated with rmMCP-7 tubes (arrows) and loops (L) are more prevalent. Endothelial cells (SVEC4-10) were cultivated in wells of μ-slides angiogenesis (ibidi GmbH, Martinsried, Germany) with Geltrex (Thermo Fisher Scientific Inc. Waltham, MA) for 5 hours at 37°C in the presence or absence of the subtypes of tryptase. Following incubation, the samples were fixed, viewed, and photographed using a Nikon Eclipse TE2000-U (Nikon Instruments Inc., Melville, NY) phase

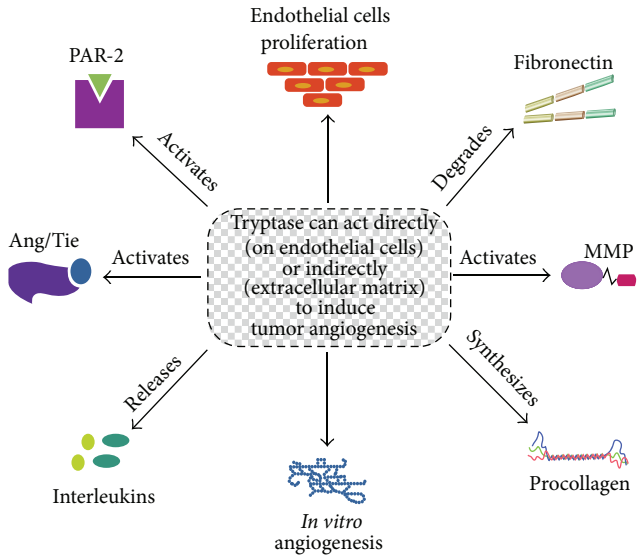

FIGURE 2: Tryptase can act directly or indirectly to induce tumor angiogenesis.

contrast inverted microscope equipped with a Nikon DXM-1200 digital camera.

Recently, Wang et al. [137] examined the involvement of mast cells in angiogenesis *in vitro* by coculturing myocardial microvascular endothelial cells (MMVEC) with rat peritoneal mast cells (activated or nonactivated) or with only the granules from rat peritoneal mast cells. Mast cells activated by 48/80 induced *in vitro* angiogenesis, but this was not detected with nonactivated mast cells. To confirm if the mast cell granules (MCG) alone can induce *in vitro* angiogenesis, MMVEC were cultivated with MCG. There was significantly higher migration, proliferation, and capillary tube-like formation in the presence of MCG than without MCG. In addition, in the presence of MCG a decrease in Angiopoietin-2 (Ang-2) protein expression and mRNA by endothelial cells was seen, indicating that the MCG had a suppressive effect on Ang-2 expression. In order to determine if tryptase or chymase was responsible for the induction of angiogenesis via Ang/Tie-2, myocardial microvascular endothelial cells were cultivated with MCG in the presence of tryptase or chymase inhibitors. The ability of MCG to induce angiogenesis could be reversed by either tryptase or chymase inhibitors, although the tryptase inhibitor was more effective. Therefore, tryptase may be more important than chymase in inducing angiogenesis. Also tryptase may be the major factor released by mast cells that promotes neovessel formation. Taken together the results indicate that tryptase affects angiogenesis in MMVEC via Ang/Tie-2.

Since tryptase is known to be involved in tumor angiogenesis (Figure 2), recently it has been suggested that tryptase may serve not only as a biomarker in different pathologies but also as a promising therapeutic target. Ammendola et al. [103] review the possible molecular mechanisms of three drugs targeting tryptase and discuss their possible role in cancer therapy. Furthermore, the authors suggest mast cell tryptase as potential antiangiogenic strategy.

5. Chymases and Tumor Angiogenesis

Chymases are mast cell specific proteases that belong to the family of serine proteases. Mast cell chymases are monomeric endopeptidases [138] that have chymotrypsin-like specificities (Table 1). They preferentially cleave proteins after aromatic amino acid residues, except rat and mouse chymase 5 (rMCP-5 and mMCP-5), which have elastase-like rather than chymotrypsin-like substrate specificity [139]. Different chymases have been identified in various species and have been divided into two groups (α- and β-chymases) according to their structure and substrate specificity [140, 141]. Both subgroups of chymases convert Angiotensin I to Angiotensin II, but only β-chymases degrade Angiotensin II. The α-chymases cleave the Phe^{8}-His^{9} bond of Angiotensin I [141] and are widely expressed in mammalian mast cells. The β-chymases can convert Angiotensin I to Angiotensin II but preferentially hydrolyze the Tyr^{4}-Ile^{5} bond of Ang I and Ang II, yielding inactive peptide fragments [142].

Many other chymase substrates have been reported such as procollagen [143], pro-matrix metalloproteinase-9 (pro-MMP-9) [144, 145], tissue inhibitor of metalloproteinase-1 (TIMP-1) [146], big-endothelin-1 and big-endothelin-2 [147, 148], TGF-β1 [149], and thrombin [150]. However, chymases are relatively promiscuous in terms of cleavage specificity, and they have the capacity to cleave a multitude of substrates and can even cleave the same substrate at multiple positions.

In mast cells, chymases are stored as active enzymes in a macromolecular complex together with heparin in secretory granules. Prior to secretion, mast cell chymases are activated by dipeptidyl peptidase I [151]. Once secreted into the extracellular fluid, chymases remain in a complex with heparin proteoglycan, which protects the chymases from inhibition by endogenous inhibitors of chymase present in the extracellular fluid [152].

In man chymases are found in mast cells around blood vessels, in the heart, and many other tissues [153], but not in plasma [138]. The fact that chymases are present in different tissues and that they cleave numerous substrates indicates that chymases can play many different roles in physiological and pathological conditions, including tumor angiogenesis, but these roles are not well characterized. Additionally, the distribution of mast cells and mast cell subtypes is variable depending on the type of tumor. In colorectal cancer, hepatocellular carcinoma, and intrahepatic cholangiocarcinoma, both MC_{TC} and MC_{T} proliferate or infiltrate in the tumor [154, 155]. In contrast, in some malignant tumors, a significant increase in mast cell number was found. This observation was due to an increase in MC_{T} at the invasion zone, whereas the number of MC_{TC} remained constant in this area [70, 156].

Muramatsu et al. [157], using a hamster sponge implant model of angiogenesis, suggested a possible involvement of chymase in angiogenesis. Both transfection of human prochymase cDNA and injections of purified chymase into implanted sponges demonstrated that chymase was a powerful angiogenic factor. The authors then went on to investigate chymase as an alternative Angiotensin II-generating enzyme in angiogenesis. Chymase inhibitors reduced mast cell mediated angiogenesis in hamster sponge implant model [86, 158].

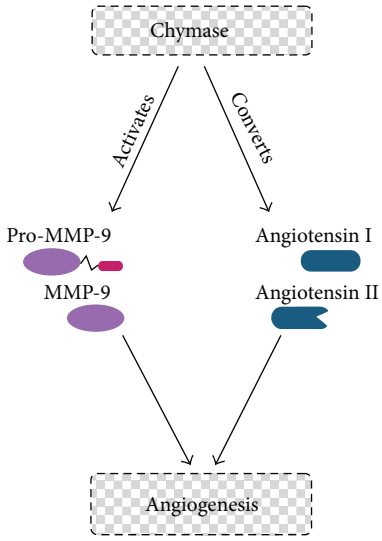

Figure 3: Chymase acts indirectly to induce angiogenesis. Chymase can activate MMP-9 or convert Angiotensin I to Angiotensin II.

Furthermore, chymostatin (a chymase inhibitor) and TCV-116 (an Angiotensin II (Ang II) type 1 receptor agonist) completely inhibited bFGF-induced angiogenesis [85]. These results suggest that hamster chymase generates Angiotensin II from Angiotensin I, triggering bFGF-induced angiogenesis (Figure 3). Additionally, chymase mRNA expression was detected in bFGF-induced angiogenesis, but not in the control hamsters treated with saline. The increased angiogenesis was accompanied by a considerable increase in chymase activity in the granuloma tissues [86].

Local injection of compound 48/80, a mast cell activator, also promoted angiogenesis in hamster sponge granulomas through a chymase-dependent mechanism [85] and enhanced VEGF mRNA expression [159]. Treatment with neutralizing antibody against VEGF or an antisense oligodeoxynucleotide against VEGF supressed Angiotensin II-induced angiogenesis, showing that VEGF is a downstream factor in Angiotensin II-induced angiogenesis [159]. Therefore, the chymase-Ang II-VEGF pathway in granulation tissue may be the primary functional mediator of angiogenesis.

Arbeit et al. [160] developed a mouse model of epithelial carcinogenesis, by targeting the early region of human papillomavirus type 16 (HPV16) to the basal cells of the squamous epithelium using a human keratin 14 (K14) enhancer/promoter. With time after birth, these mice develop epidermal hyperplasia, which advances to angiogenic dysplasias. After one year, these dysplasias can progress to invasive squamous cell carcinomas [120]. In this transgenic mouse model an increase in mast cell number was observed during progression of the disease, especially in dysplasia [120], which is characterized by increased angiogenesis. At the same time, there was a significant increase in chymase activity and mMCP-4 mRNA was detected in dysplastic skin. Finally, hyperplastic ear skin from the transgenic mice was incubated in medium containing mMCP-4 and subsequently embedded in a collagen gel containing randomly dispersed bovine capillary endothelial cells (BCEs). The BCEs showed a dramatic response to the presence of skin that had been preincubated with mMCP-4. The endothelial cells became radially aligned, had increased rates of proliferation and migration, and exhibited tube formation toward the dermal surface, but not the epidermal surface of the skin pieces. However, the addition of mMCP-4 directly to BCEs did not induce a response, indicating that the angiogenic activity came from sequestered factors in the skin pieces used in this assay. Furthermore, canine and human chymases can cleave pro-MMP-9 producing active MMP-9. This matrix metalloproteinase participates in extracellular matrix remodeling [161] and regulation of angiogenesis [162]. In order to verify that mMCP-4 contributes to angiogenesis by activating MMP-9, hyperplastic skin lysates (containing predominantly pro-MMP-9) were incubated with mMCP-4 and then subjected to gelatin-substrate zymography. A substantially increased amount of active MMP-9 was detected, confirming that mMCP-4 plays a role in angiogenesis by activating MMP-9 thus inducing extracellular matrix remodeling [120]. These results, taken together, suggest that mMCP-4 acts indirectly to induce angiogenesis by activating pro-MMP-9, thus releasing sequestered angiogenic factors (Figure 3).

MCP-5 is emerging as a key player in chymase induced angiogenesis. The level of rMCP-5 mRNA in the granulomatous tissue of λ-carrageenin-soaked sponge implants was significantly increased in comparison to control granulomas [163]. Furthermore, angiogenesis during granuloma formation could be blocked by chymostatin and by blocking rMCP-5 with a specific antisense oligonucleotide. Recently, de Souza Jr. et al. [59] reported increased mast cell and blood vessel numbers as well as blood vessel diameter during mouse skin tumor progression. mMCP-5 expression was not detected in the control animals but was present in all stages of tumor progression. Total chymase activity and mMCP-5 expression increased during tumor progression and were correlated with tumor angiogenesis. In contrast, although mMCP-4 expression could be detected in control animals and in all phases of tumor progression, there was no difference in expression at the various phases.

The majority of the studies attempting to define the role of specific mast cell proteases, such as chymase in tumor angiogenesis in humans, have been focused on a pathological examination of tumor biopsies. The stage of the tumor, mast cell numbers, and mast cell subtype, that is, MC_{TC} and MC_T, were all analyzed [78, 80, 156, 164–167]. These investigations have suggested a relation between chymase and angiogenesis in tumors. However, research into the chymase-containing mast cell subpopulations has been hampered by lack of suitable reagents.

In small sized adenocarcinomas of the lung, the mast cell number is increased in comparison with normal lung tissue and the ratio of MC_{TC} to total mast cells in the adenocarcinomas is significantly higher than that in normal lung. Furthermore, the accumulation of MC_{TC}, but not MC_T, correlates with a poor prognosis for patients with small sized lung adenocarcinoma. However, the numbers of both mast cell types correlated significantly with microvessel counts in small sized lung adenocarcinomas [168].

Mast cells are present in all three developmental phases of hemangiomas, which are benign, usually self-involuting tumors of the microvasculature [169]. In the initial proliferative phase, angiogenesis in hemangiomas is excessive but is followed by spontaneous regression, and the cellular parenchyma is gradually replaced with fibrofatty tissue. The mast cell number is the highest in the involuting phase, reduced in the involuted phase, and the least in the proliferative phase. However, the proportion of MC_{TC} decreases from the proliferative phase through the involuting phase to the involuted phase, indicating a proangiogenic role for chymase in this tumor. At the later stages, when the proportion of MC_T is increasing, these mast cells may be releasing tumor inhibitors.

In conclusion, the studies presented here support a relationship between mast cell chymases and tumor angiogenesis (Figure 3). However, additional studies are needed in order to elucidate the precise role of mast cell chymases in angiogenesis.

6. Conclusion

This review has presented evidence that tryptase and chymase act directly (on endothelial cells) or indirectly (on the extracellular matrix) to induce tumor angiogenesis. Most importantly, tryptase appears to play a more significant role in tumor progression than chymase. These findings support the use of mast cell proteases as novel tumor biomarkers as well as targets for antiangiogenic therapy. Furthermore, studies using chymase or tryptase knockout animals are necessary to demonstrate the functional impact of either chymase or tryptase on tumor angiogenesis.

Conflict of Interests

The authors declare that there is no conflict of interests regarding the publication of this paper.

References

[1] J. Folkman and Y. Shing, "Angiogenesis," *The Journal of Biological Chemistry*, vol. 267, no. 16, pp. 10931–10934, 1992.

[2] T. O. Daniel and D. Abrahamson, "Endothelial signal integration in vascular assembly," *Annual Review of Physiology*, vol. 62, pp. 649–671, 2000.

[3] D. Ribatti, "Genetic and epigenetic mechanisms in the early development of the vascular system," *Journal of Anatomy*, vol. 208, no. 2, pp. 139–152, 2006.

[4] D. Ribatti and E. Crivellato, "Mast cells, angiogenesis, and tumour growth," *Biochimica et Biophysica Acta—Molecular Basis of Disease*, vol. 1822, no. 1, pp. 2–8, 2012.

[5] D. Hanahan and J. Folkman, "Patterns and emerging mechanisms of the angiogenic switch during tumorigenesis," *Cell*, vol. 86, no. 3, pp. 353–364, 1996.

[6] M. L. Iruela-Arispe and H. F. Dvorak, "Angiogenesis: a dynamic balance of stimulators and inhibitors," *Thrombosis and Haemostasis*, vol. 78, no. 1, pp. 672–677, 1997.

[7] M. Sawatsubashi, T. Yamada, N. Fukushima, H. Mizokami, O. Tokunaga, and T. Shin, "Association of vascular endothelial growth factor and mast cells with angiogenesis in laryngeal squamous cell carcinoma," *Virchows Archiv*, vol. 436, no. 3, pp. 243–248, 2000.

[8] J. Talreja, M. H. Kabir, M. B. Filla, D. J. Stechschulte, and K. N. Dileepan, "Histamine induces Toll-like receptor 2 and 4 expression in endothelial cells and enhances sensitivity to Gram-positive and Gram-negative bacterial cell wall components," *Immunology*, vol. 113, no. 2, pp. 224–233, 2004.

[9] B. Hobson and J. Denekamp, "Endothelial proliferation in tumours and normal tissues: continuous labelling studies," *British Journal of Cancer*, vol. 49, no. 4, pp. 405–413, 1984.

[10] P. A. D'Amore and R. W. Thompson, "Mechanisms of angiogenesis," *Annual Review of Physiology*, vol. 49, pp. 453–464, 1987.

[11] A. Le Querrec, D. Duval, and G. Tobelem, "Tumour angiogenesis," *Bailliere's Clinical Haematology*, vol. 6, no. 3, pp. 711–730, 1993.

[12] M. Potente, H. Gerhardt, and P. Carmeliet, "Basic and therapeutic aspects of angiogenesis," *Cell*, vol. 146, no. 6, pp. 873–887, 2011.

[13] E. Goldmann, "The growth of malignant disease in man and the lower animals, with special reference to the vascular system," *Proceedings of the Royal Society of Medicine, Surgery Section*, vol. 1, pp. 1–13, 1908.

[14] J. Folkman, "Tumor angiogenesis: therapeutic implications," *The New England Journal of Medicine*, vol. 285, no. 21, pp. 1182–1186, 1971.

[15] G. Ranieri, C. D. Gadaleta, R. Patruno et al., "A model of study for human cancer: spontaneous occurring tumors in dogs. Biological features and translation for new anticancer therapies," *Critical Reviews in Oncology/Hematology*, vol. 88, no. 1, pp. 187–197, 2013.

[16] G. Ranieri, M. Pantaleo, M. Piccinno et al., "Tyrosine kinase inhibitors (TKIs) in human and pet tumours with special reference to breast cancer: a comparative review," *Critical Reviews in Oncology/Hematology*, vol. 88, no. 2, pp. 293–308, 2013.

[17] B. Al-Husein, M. Abdalla, M. Trepte, D. L. DeRemer, and P. R. Somanath, "Antiangiogenic therapy for cancer: an update," *Pharmacotherapy*, vol. 32, no. 12, pp. 1095–1111, 2012.

[18] A. W. Griffioen and G. Molema, "Angiogenesis: potentials for pharmacologic intervention in the treatment of cancer, cardiovascular diseases, and chronic inflammation," *Pharmacological Reviews*, vol. 52, no. 2, pp. 237–268, 2000.

[19] P. Carmeliet and R. K. Jain, "Molecular mechanisms and clinical applications of angiogenesis," *Nature*, vol. 473, no. 7347, pp. 298–307, 2011.

[20] F. Moccia, S. Dragoni, V. Poletto et al., "Orai1 and transient receptor potential channels as novel molecular targets to impair tumor neovascularization in renal cell carcinoma and other malignancies," *Anti-Cancer Agents in Medicinal Chemistry*, vol. 14, no. 2, pp. 296–312, 2014.

[21] T. Marichal, M. Tsai, and S. J. Galli, "Mast cells: potential positive and negative roles in tumor biology," *Cancer Immunology Research*, vol. 1, no. 5, pp. 269–279, 2013.

[22] D. Hanahan and R. A. Weinberg, "Hallmarks of cancer: the next generation," *Cell*, vol. 144, no. 5, pp. 646–674, 2011.

[23] D. Ribatti and E. Crivellato, "Immune cells and angiogenesis," *Journal of Cellular and Molecular Medicine*, vol. 13, no. 9, pp. 2822–2833, 2009.

[24] E. Z. M. da Silva, M. C. Jamur, and C. Oliver, "Mast cell function: a new vision of an old cell," *Journal of Histochemistry & Cytochemistry*, vol. 62, no. 10, pp. 698–738, 2014.

[25] S. J. Galli, J. Kalesnikoff, M. A. Grimbaldeston, A. M. Piliponsky, C. M. M. Williams, and M. Tsai, "Mast cells as 'tunable' effector and immunoregulatory cells: recent advances," *Annual Review of Immunology*, vol. 23, pp. 749–786, 2005.

[26] M. F. Gurish and K. F. Austen, "Developmental origin and functional specialization of mast cell subsets," *Immunity*, vol. 37, no. 1, pp. 25–33, 2012.

[27] M. F. Gurish and J. A. Boyce, "Mast cells: ontogeny, homing, and recruitment of a unique innate effector cell," *The Journal of Allergy and Clinical Immunology*, vol. 117, no. 6, pp. 1285–1291, 2006.

[28] K. D. Stone, C. Prussin, and D. D. Metcalfe, "IgE, mast cells, basophils, and eosinophils," *Journal of Allergy and Clinical Immunology*, vol. 125, no. 2, supplement 2, pp. S73–S80, 2010.

[29] M. C. Jamur and C. Oliver, "Origin, maturation and recruitment of mast cell precursors," *Frontiers in Bioscience*, vol. 3, no. 4, pp. 1390–1406, 2011.

[30] D. D. Metcalfe, R. D. Peavy, and A. M. Gilfillan, "Mechanisms of mast cell signaling in anaphylaxis," *Journal of Allergy and Clinical Immunology*, vol. 124, no. 4, pp. 639-646, 647–638, 2009.

[31] H. R. Katz, M. B. Raizman, C. S. Gartner, H. C. Scott, A. C. Benson, and K. F. Austen, "Secretory granule mediator release and generation of oxidative metabolites of arachidonic acid via Fc-IgG receptor bridging in mouse mast cells," *Journal of Immunology*, vol. 148, no. 3, pp. 868–871, 1992.

[32] J. W. Coleman, M. R. Holliday, I. Kimber, K. M. Zsebo, and S. J. Galli, "Regulation of mouse peritoneal mast cell secretory function by stem cell factor, IL-3 or IL-4," *The Journal of Immunology*, vol. 150, no. 2, pp. 556–562, 1993.

[33] S. J. Galli, A. Iemura, D. S. Garlick, C. Gamba-Vitalo, K. M. Zsebo, and R. G. Andrews, "Reversible expansion of primate mast cell populations in vivo by stem cell factor," *The Journal of Clinical Investigation*, vol. 91, no. 1, pp. 148–152, 1993.

[34] V. Supajatura, H. Ushio, A. Nakao et al., "Differential responses of mast cell Toll-like receptors 2 and 4 in allergy and innate immunity," *Journal of Clinical Investigation*, vol. 109, no. 10, pp. 1351–1359, 2002.

[35] S. J. Galli, S. Nakae, and M. Tsai, "Mast cells in the development of adaptive immune responses," *Nature Immunology*, vol. 6, no. 2, pp. 135–142, 2005.

[36] R. T. Venkatesha, E. B. Thangam, A. K. Zaidi, and H. Ali, "Distinct regulation of C3a-induced MCP-1/CCL2 and RANTES/CCL5 production in human mast cells by extracellular signal regulated kinase and PI3 kinase," *Molecular Immunology*, vol. 42, no. 5, pp. 581–587, 2005.

[37] S. J. Galli and M. Tsai, "Mast cells: versatile regulators of inflammation, tissue remodeling, host defense and homeostasis," *Journal of Dermatological Science*, vol. 49, no. 1, pp. 7–19, 2008.

[38] H. R. Katz, J. P. Arm, A. C. Benson, and K. F. Austen, "Maturation-related changes in the expression of FcγRII and FcγRIII on mouse mast cells derived in vitro and in vivo," *The Journal of Immunology*, vol. 145, no. 10, pp. 3412–3417, 1990.

[39] G. Pejler, M. Åbrink, M. Ringvall, and S. Wernersson, "Mast cell proteases," *Advances in Immunology*, vol. 95, pp. 167–255, 2007.

[40] L. B. Schwartz and T. R. Bradford, "Regulation of tryptase from human lung mast cells by heparin. Stabilization of the active tetramer," *Journal of Biological Chemistry*, vol. 261, no. 16, pp. 7372–7379, 1986.

[41] L. B. Schwartz, A. M. A. Irani, K. Roller, M. C. Castells, and N. M. Schechter, "Quantitation of histamine, tryptase, and chymase in dispersed human T and TC mast cells," *Journal of Immunology*, vol. 138, no. 8, pp. 2611–2615, 1987.

[42] C. Huang, G. Morales, A. Vagi et al., "Formation of enzymatically active, homotypic, and heterotypic tetramers of mouse mast cell tryptases. Dependence on a conserved Trp-rich domain on the surface," *Journal of Biological Chemistry*, vol. 275, no. 1, pp. 351–358, 2000.

[43] G. Pejler, S. D. Knight, F. Henningsson, and S. Wernersson, "Novel insights into the biological function of mast cell carboxypeptidase A," *Trends in Immunology*, vol. 30, no. 8, pp. 401–408, 2009.

[44] F. R. Melo, I. Waern, E. Rönnberg et al., "A role for serglycin proteoglycan in mast cell apoptosis induced by a secretory granule-mediated pathway," *The Journal of Biological Chemistry*, vol. 286, no. 7, pp. 5423–5433, 2011.

[45] M. Åbrink, M. Grujic, and G. Pejler, "Serglycin is essential for maturation of mast cell secretory granule," *The Journal of Biological Chemistry*, vol. 279, no. 39, pp. 40897–40905, 2004.

[46] T. Braga, M. Grujic, A. Lukinius, L. Hellman, M. Åbrink, and G. Pejler, "Serglycin proteoglycan is required for secretory granule integrity in mucosal mast cells," *Biochemical Journal*, vol. 403, no. 1, pp. 49–57, 2007.

[47] S. J. Galli, N. Borregaard, and T. A. Wynn, "Phenotypic and functional plasticity of cells of innate immunity: macrophages, mast cells and neutrophils," *Nature Immunology*, vol. 12, no. 11, pp. 1035–1044, 2011.

[48] J. P. Abonia, C. Blanchard, B. B. Butz et al., "Involvement of mast cells in eosinophilic esophagitis," *Journal of Allergy and Clinical Immunology*, vol. 126, no. 1, pp. 140–149, 2010.

[49] R. H. Dougherty, S. S. Sidhu, K. Raman et al., "Accumulation of intraepithelial mast cells with a unique protease phenotype in T_H2-high asthma," *The Journal of Allergy and Clinical Immunology*, vol. 125, no. 5, pp. 1046.e8–1053.e8, 2010.

[50] R. L. Stevens, D. S. Friend, H. P. Mcneil, V. Schiller, N. Ghildyal, and K. F. Austen, "Strain-specific and tissue-specific expression of mouse mast cell secretory granule proteases," *Proceedings of the National Academy of Sciences of the United States of America*, vol. 91, no. 1, pp. 128–132, 1994.

[51] M. F. Gurish, W. S. Pear, R. L. Stevens et al., "Tissue-regulated differentiation and maturation of a v-abl-immortalized mast cell-committed progenitor," *Immunity*, vol. 3, no. 2, pp. 175–186, 1995.

[52] D. S. Friend, N. Ghildyal, K. F. Austen, M. F. Gurish, R. Matsumoto, and R. L. Stevens, "Mast cells that reside at different locations in the jejunum of mice infected with *Trichinella spiralis* exhibit sequential changes in their granule ultrastructure and chymase phenotype," *Journal of Cell Biology*, vol. 135, no. 1, pp. 279–290, 1996.

[53] W. Xing, K. F. Austen, M. F. Gurish, and T. G. Jones, "Protease phenotype of constitutive connective tissue and of induced mucosal mast cells in mice is regulated by the tissue," *Proceedings of the National Academy of Sciences of the United States of America*, vol. 108, no. 34, pp. 14210–14215, 2011.

[54] H. P. McNeil, K. Shin, I. K. Campbell et al., "The mouse mast cell-restricted tetramer-forming tryptases mouse mast cell protease 6 and mouse mast cell protease 7 are critical mediators in inflammatory arthritis," *Arthritis and Rheumatism*, vol. 58, no. 8, pp. 2338–2346, 2008.

[55] K. Shin, G. F. M. Watts, H. C. Oettgen et al., "Mouse mast cell tryptase mMCP-6 Is a critical link between adaptive and innate immunity in the chronic phase of *Trichinella spiralis* infection," *Journal of Immunology*, vol. 180, no. 7, pp. 4885–4891, 2008.

[56] Q. Sun, W. Li, R. She et al., "Evidence for a role of mast cells in the mucosal injury induced by Newcastle disease virus," *Poultry Science*, vol. 88, no. 3, pp. 554–561, 2009.

[57] L. Scandiuzzi, W. Beghdadi, E. Daugas et al., "Mouse mast cell protease-4 deteriorates renal function by contributing to inflammation and fibrosis in immune complex-mediated glomerulonephritis," *Journal of Immunology*, vol. 185, no. 1, pp. 624–633, 2010.

[58] A. Lambiase, A. Micera, and S. Bonini, "Multiple action agents and the eye: do they really stabilize mast cells?" *Current Opinion in Allergy and Clinical Immunology*, vol. 9, no. 5, pp. 454–465, 2009.

[59] D. A. de Souza Jr., V. D. Toso, M. R. D. C. Campos, V. S. Lara, C. Oliver, and M. C. Jamur, "Expression of mast cell proteases correlates with mast cell maturation and angiogenesis during tumor progression," *PLoS ONE*, vol. 7, no. 7, Article ID e40790, 2012.

[60] P. Ehrlich, *Beiträge zur Theorie und Praxis der Histologischen Färbung*, 1878.

[61] S. Ch'ng, R. A. Wallis, L. Yuan, P. F. Davis, and S. T. Tan, "Mast cells and cutaneous malignancies," *Modern Pathology*, vol. 19, no. 1, pp. 149–159, 2006.

[62] M. Gulubova and T. Vlaykova, "Prognostic significance of mast cell number and microvascular density for the survival of patients with primary colorectal cancer," *Journal of Gastroenterology and Hepatology*, vol. 24, no. 7, pp. 1265–1275, 2009.

[63] G. Ranieri, M. Ammendola, R. Patruno et al., "Tryptase-positive mast cells correlate with angiogenesis in early breast cancer patients," *International Journal of Oncology*, vol. 35, no. 1, pp. 115–120, 2009.

[64] A. Mangia, A. Malfettone, R. Rossi et al., "Tissue remodelling in breast cancer: human mast cell tryptase as an initiator of myofibroblast differentiation," *Histopathology*, vol. 58, no. 7, pp. 1096–1106, 2011.

[65] I. Takanami, K. Takeuchi, and M. Naruke, "Mast cell density is associated with angiogenesis and poor prognosis in pulmonary adenocarcinoma," *Cancer*, vol. 88, no. 12, pp. 2686–2692, 2000.

[66] S. Dabiri, D. Huntsman, N. Makretsov et al., "The presence of stromal mast cells identifies a subset of invasive breast cancers with a favorable prognosis," *Modern Pathology*, vol. 17, no. 6, pp. 690–695, 2004.

[67] P. Conti, M. L. Castellani, D. Kempuraj et al., "Role of mast cells in tumor growth," *Annals of Clinical and Laboratory Science*, vol. 37, no. 4, pp. 315–322, 2007.

[68] B. L. Gruber, M. J. Marchese, and R. Kew, "Angiogenic factors stimulate mast-cell migration," *Blood*, vol. 86, no. 7, pp. 2488–2493, 1995.

[69] B. Huang, Z. Lei, G.-M. Zhang et al., "SCF-mediated mast cell infiltration and activation exacerbate the inflammation and immunosuppression in tumor microenvironment," *Blood*, vol. 112, no. 4, pp. 1269–1279, 2008.

[70] L. Benítez-Bribiesca, A. Wong, D. Utrera, and E. Castellanos, "The role of mast cell tryptase in neoangiogenesis of premalignant and malignant lesions of the uterine cervix," *Journal of Histochemistry and Cytochemistry*, vol. 49, no. 8, pp. 1061–1062, 2001.

[71] M. P. Wymann, K. Björklöf, R. Calvez et al., "Phosphoinositide 3-kinase γ: a key modulator in inflammation and allergy," *Biochemical Society Transactions*, vol. 31, part 1, pp. 275–280, 2003.

[72] M. A. Grimbaldeston, A. L. Pearce, B. O. Robertson et al., "Association between melanoma and dermal mast cell prevalence in sun-unexposed skin," *British Journal of Dermatology*, vol. 150, no. 5, pp. 895–903, 2004.

[73] D. Ribatti, N. Finato, E. Crivellato et al., "Neovascularization and mast cells with tryptase activity increase simultaneously with pathologic progression in human endometrial cancer," *The American Journal of Obstetrics and Gynecology*, vol. 193, no. 6, pp. 1961–1965, 2005.

[74] M. Yoshii, A. Jikuhara, S. Mori et al., "Mast cell tryptase stimulates DLD-1 carcinoma through prostaglandin- and MAP kinase-dependent manners," *Journal of Pharmacological Sciences*, vol. 98, no. 4, pp. 450–458, 2005.

[75] N. C. Diaconu, R. Kaminska, A. Naukkarinen, R. J. Harvima, and I. T. Harvima, "The increase in tryptase- and chymase-positive mast cells is associated with partial inactivation of chymase and increase in protease inhibitors in basal cell carcinoma," *Journal of the European Academy of Dermatology and Venereology*, vol. 21, no. 7, pp. 908–915, 2007.

[76] N. Nonomura, H. Takayama, K. Nishimura et al., "Decreased number of mast cells infiltrating into needle biopsy specimens leads to a better prognosis of prostate cancer," *British Journal of Cancer*, vol. 97, no. 7, pp. 952–956, 2007.

[77] A. Fleischmann, T. Schlomm, J. Köllermann et al., "Immunological microenvironment in prostate cancer: high mast cell densities are associated with favorable tumor characteristics and good prognosis," *Prostate*, vol. 69, no. 9, pp. 976–981, 2009.

[78] M. J. Carlini, M. C. L. Dalurzo, J. M. Lastiri et al., "Mast cell phenotypes and microvessels in non-small cell lung cancer and its prognostic significance," *Human Pathology*, vol. 41, no. 5, pp. 697–705, 2010.

[79] A. Johansson, S. Rudolfsson, P. Hammarsten et al., "Mast cells are novel independent prognostic markers in prostate cancer and represent a target for therapy," *The American Journal of Pathology*, vol. 177, no. 2, pp. 1031–1041, 2010.

[80] D. Ribatti, D. Guidolin, A. Marzullo et al., "Mast cells and angiogenesis in gastric carcinoma," *International Journal of Experimental Pathology*, vol. 91, no. 4, pp. 350–356, 2010.

[81] G. Dyduch, K. Kaczmarczyk, and K. Okoń, "Mast cells and cancer: enemies or allies?" *Polish Journal of Pathology*, vol. 63, no. 1, pp. 1–7, 2012.

[82] D. Ribatti, A. Vacca, B. Nico, E. Crivellato, L. Roncali, and F. Dammacco, "The role of mast cells in tumour angiogenesis," *British Journal of Haematology*, vol. 115, no. 3, pp. 514–521, 2001.

[83] E. Crivellato, C. A. Beltrami, F. Mallardi, and D. Ribatti, "The mast cell: an active participant or an innocent bystander?" *Histology and Histopathology*, vol. 19, no. 1, pp. 259–270, 2004.

[84] X. Tan, S. Essengue, J. Talreja, J. Reese, D. J. Stechschulte, and K. N. Dileepan, "Histamine directly and synergistically with lipopolysaccharide stimulates cyclooxygenase-2 expression and prostaglandin I_2 and E_2 production in human coronary artery endothelial cells," *Journal of Immunology*, vol. 179, no. 11, pp. 7899–7906, 2007.

[85] M. Muramatsu, J. Katada, M. Hattori, I. Hayashi, and M. Majima, "Chymase mediates mast cell-induced angiogenesis in hamster sponge granulomas," *European Journal of Pharmacology*, vol. 402, no. 1-2, pp. 181–191, 2000.

[86] M. Muramatsu, J. Katada, I. Hayashi, and M. Majima, "Chymase as a proangiogenic factor. A possible involvement of chymase-angiotensin-dependent pathway in the hamster sponge angiogenesis model," *The Journal of Biological Chemistry*, vol. 275, no. 8, pp. 5545–5552, 2000.

[87] T. Tth, R. Tth-Jakatics, S. Jimi, S. Takebayashi, and N. Kawamoto, "Cutaneous malignant melanoma: correlation between neovascularization and peritumor accumulation of mast cells overexpressing vascular endothelial growth factor," *Human Pathology*, vol. 31, no. 8, pp. 955–960, 2000.

[88] K. Norrby, "Mast cells and angiogenesis," *Acta Pathologica, Microbiologica et Immunologica Scandinavica*, vol. 110, no. 5, pp. 355–371, 2002.

[89] I. Feoktistov, S. Ryzhov, A. E. Goldstein, and I. Biaggioni, "Mast cell-mediated stimulation of angiogenesis: cooperative interaction between A2B and A3 adenosine receptors," *Circulation Research*, vol. 92, no. 5, pp. 485–492, 2003.

[90] M. Juczewska and L. Chyczewski, "Angiogenesis in cancer," *Roczniki Akademii Medycznej w Białymstoku*, vol. 42, supplement 1, pp. 86–100, 1997.

[91] L. B. Schwartz, R. A. Lewis, and K. F. Austen, "Tryptase from human pulmonary mast cells. Purification and characterization.," *The Journal of Biological Chemistry*, vol. 256, no. 22, pp. 11939–11943, 1981.

[92] L. B. Schwartz, "Tryptase, a mediator of human mast cells," *Journal of Allergy and Clinical Immunology*, vol. 86, no. 4, pp. 594–598, 1990.

[93] V. Payne and P. C. A. Kam, "Mast cell tryptase: a review of its physiology and clinical significance," *Anaesthesia*, vol. 59, no. 7, pp. 695–703, 2004.

[94] G. Pejler, E. Rönnberg, I. Waern, and S. Wernersson, "Mast cell proteases: multifaceted regulators of inflammatory disease," *Blood*, vol. 115, no. 24, pp. 4981–4990, 2010.

[95] H.-Z. Xia, C. L. Kepley, K. Sakai, J. Chelliah, A.-M. A. Irani, and L. B. Schwartz, "Quantitation of tryptase, chymase, FcεRlα, and FcεRlγ mRNAs in human mast cells and basophils by competitive reverse transcription-polymerase chain reaction," *Journal of Immunology*, vol. 154, no. 10, pp. 5472–5480, 1995.

[96] S. Wernersson and G. Pejler, "Mast cell secretory granules: armed for battle," *Nature Reviews Immunology*, vol. 14, no. 7, pp. 478–494, 2014.

[97] J. P. Kankkunen, I. T. Harvima, and A. Naukkarinen, "Quantitative analysis of tryptase and chymase containing mast cells in benign and malignant breast lesions," *International Journal of Cancer*, vol. 72, no. 3, pp. 385–388, 1997.

[98] A. Imada, N. Shijubo, H. Kojima, and S. Abe, "Mast cells correlate with angiogenesis and poor outcome in stage I lung adenocarcinoma," *European Respiratory Journal*, vol. 15, no. 6, pp. 1087–1093, 2000.

[99] B. Nico, A. Marzullo, P. Corsi, A. Vacca, L. Roncali, and D. Ribatti, "A possible role of tryptase in angiogenesis in the brain of mdx mouse, a model of Duchenne muscular dystrophy," *Neuroscience*, vol. 123, no. 3, pp. 585–588, 2004.

[100] D. Ribatti, S. Molica, A. Vacca et al., "Tryptase-positive mast cells correlate positively with bone marrow angiogenesis in B-cell chronic lymphocytic leukemia," *Leukemia*, vol. 17, no. 7, pp. 1428–1430, 2003.

[101] D. Ribatti, M. G. Ennas, A. Vacca et al., "Tumor vascularity and tryptase-positive mast cells correlate with a poor prognosis in melanoma," *European Journal of Clinical Investigation*, vol. 33, no. 5, pp. 420–425, 2003.

[102] V. Goffredo, C. D. Gadaleta, A. Laterza, A. Vacca, and G. Ranieri, "Tryptase serum levels in patients suffering from hepatocellular carcinoma undergoing intra-arterial chemoembolization: possible predictive role of response to treatment," *Molecular and Clinical Oncology*, vol. 1, no. 2, pp. 385–389, 2013.

[103] M. Ammendola, R. Sacco, G. Donato et al., "Mast cell positivity to tryptase correlates with metastatic lymph nodes in gastrointestinal cancer patients treated surgically," *Oncology*, vol. 85, no. 2, pp. 111–116, 2013.

[104] I. Marech, M. Ammendola, R. Sacco et al., "Serum tryptase, mast cells positive to tryptase and microvascular density evaluation in early breast cancer patients: possible translational significance," *BMC Cancer*, vol. 14, article 534, 2014.

[105] I. Marech, M. Ammendola, C. Gadaleta et al., "Possible biological and translational significance of mast cells density in colorectal cancer," *The World Journal of Gastroenterology*, vol. 20, no. 27, pp. 8910–8920, 2014.

[106] T. C. Theoharides, K.-D. Alysandratos, A. Angelidou et al., "Mast cells and inflammation," *Biochimica et Biophysica Acta*, vol. 1822, no. 1, pp. 21–33, 2012.

[107] A. Malfettone, N. Silvestris, C. Saponaro et al., "High density of tryptase-positive mast cells in human colorectal cancer: a poor prognostic factor related to protease-activated receptor 2 expression," *Journal of Cellular and Molecular Medicine*, vol. 17, no. 8, pp. 1025–1037, 2013.

[108] M. Ammendola, Ch. Leporini, I. Marech et al., "Targeting mast cells tryptase in tumor microenvironment: a potential antiangiogenetic strategy," *BioMed Research International*, vol. 2014, Article ID 154702, 16 pages, 2014.

[109] C. M. Kielty, M. Lees, C. A. Shuttleworth, and D. Woolley, "Catabolism of intact type VI collagen microfibrils: susceptibility to degradation by serine proteinases," *Biochemical and Biophysical Research Communications*, vol. 191, no. 3, pp. 1230–1236, 1993.

[110] D. Ribatti and G. Ranieri, "Tryptase, a novel angiogenic factor stored in mast cell granules," *Experimental Cell Research*, 2014.

[111] M. S. Stack and D. A. Johnson, "Human mast cell tryptase activates single-chain urinary-type plasminogen activator (prourokinase)," *The Journal of Biological Chemistry*, vol. 269, no. 13, pp. 9416–9419, 1994.

[112] L. B. Schwartz, T. R. Bradford, B. H. Littman, and B. U. Wintroub, "The fibrinogenolytic activity of purified tryptase from human lung mast cells," *Journal of Immunology*, vol. 135, no. 4, pp. 2762–2767, 1985.

[113] C. Huang, G. W. Wong, N. Ghildyal et al., "The tryptase, mouse mast cell protease 7, exhibits anticoagulant activity in vivo and in vitro due to its ability to degrade fibrinogen in the presence of the diverse array of protease inhibitors in plasma," *The Journal of Biological Chemistry*, vol. 272, no. 50, pp. 31885–31893, 1997.

[114] B. L. Gruber, M. J. Marchese, K. Suzuki et al., "Synovial procollagenase activation by human mast cell tryptase dependence upon matrix metalloproteinase 3 activation," *The Journal of Clinical Investigation*, vol. 84, no. 5, pp. 1657–1662, 1989.

[115] K. C. Fang, P. J. Wolters, M. Steinhoff, A. Bidgol, J. L. Blount, and G. H. Caughey, "Mast cell expression of gelatinases A and B is regulated by kit ligand and TGF-beta," *Journal of Immunology*, vol. 162, no. 9, pp. 5528–5535, 1999.

[116] T. Sendo, T. Sumimura, Y. Itoh et al., "Involvement of proteinase-activated receptor-2 in mast cell tryptase-induced barrier dysfunction in bovine aortic endothelial cells," *Cellular Signalling*, vol. 15, no. 8, pp. 773–781, 2003.

[117] Y. Itoh, T. Sendo, T. Hirakawa et al., "Role of sensory nerve peptides rather than mast cell histamine in paclitaxel hypersensitivity," *The American Journal of Respiratory and Critical Care Medicine*, vol. 169, no. 1, pp. 113–119, 2004.

[118] R. J. Blair, H. Meng, M. J. Marchese et al., "Human mast cells stimulate vascular tube formation. Tryptase is a novel, potent

angiogenic factor," *The Journal of Clinical Investigation*, vol. 99, no. 11, pp. 2691–2700, 1997.

[119] S. J. Compton, J. A. Cairns, S. T. Holgate, and A. F. Walls, "The role of mast cell tryptase in regulating endothelial cell proliferation, cytokine release, and adhesion molecule expression: tryptase induces expression of mRNA for IL-1β and IL-8 and stimulates the selective release of IL-8 from human umbilical vein endothelial cells," *The Journal of Immunology*, vol. 161, no. 4, pp. 1939–1946, 1998.

[120] L. M. Coussens, W. W. Raymond, G. Bergers et al., "Inflammatory mast cells up-regulate angiogenesis during squamous epithelial carcinogenesis," *Genes and Development*, vol. 13, no. 11, pp. 1382–1397, 1999.

[121] J. Lohi, I. Harvima, and J. Keski-Oja, "Pericellular substrates of human mast cell tryptase: 72,000 dalton gelatinase and fibronectin," *Journal of Cellular Biochemistry*, vol. 50, no. 4, pp. 337–349, 1992.

[122] R. Kaminska, P. Helisalmi, R. J. Harvima, A. Naukkarinen, M. Horsmanheimo, and I. T. Harvima, "Focal dermal-epidermal separation and fibronectin cleavage in basement membrane by human mast cell tryptase," *Journal of Investigative Dermatology*, vol. 113, no. 4, pp. 567–573, 1999.

[123] M. Lees, D. J. Taylor, and D. E. Woolley, "Mast cell proteinases activate precursor forms of collagenase and stromelysin, but not of gelatinases A and B," *European Journal of Biochemistry*, vol. 223, no. 1, pp. 171–177, 1994.

[124] W. Zhang, G. Stoica, S. I. Tasca, K. A. Kelly, and C. J. Meininger, "Modulation of tumor angiogenesis by stem cell factor," *Cancer Research*, vol. 60, no. 23, pp. 6757–6762, 2000.

[125] I. A. Akers, M. Parsons, M. R. Hill et al., "Mast cell tryptase stimulates human lung fibroblast proliferation via protease-activated receptor-2," *The American Journal of Physiology—Lung Cellular and Molecular Physiology*, vol. 278, no. 1, pp. L193–L201, 2000.

[126] C. Lu, F. D. Zhao, X. B. Li, and L. H. Yin, "Up-regulation of interleukin-8 expressions induced by mast cell tryptase via protease activated receptor-2 in endothelial cell line," *Chinese Medical Journal (English Edition)*, vol. 118, no. 22, pp. 1900–1906, 2005.

[127] X. Zhi, C. Xu, H. Zhang et al., "Tryptase promotes atherosclerotic plaque haemorrhage in ApoE-/- mice," *PLoS ONE*, vol. 8, no. 4, Article ID e60960, 2013.

[128] T. A. McEachron, F. C. Church, and N. MacKman, "Regulation of thrombin-induced plasminogen activator inhibitor-1 in 4T1 murine breast cancer cells," *Blood Coagulation and Fibrinolysis*, vol. 22, no. 7, pp. 576–582, 2011.

[129] T. A. McEachron, R. Pawlinski, K. L. Richards, F. C. Church, and N. Mackman, "Protease-activated receptors mediate crosstalk between coagulation and fibrinolysis," *Blood*, vol. 116, no. 23, pp. 5037–5044, 2010.

[130] A. F. Milia, M. B. Salis, T. Stacca et al., "Protease-activated receptor-2 stimulates angiogenesis and accelerates hemodynamic recovery in a mouse model of hindlimb ischemia," *Circulation Research*, vol. 91, no. 4, pp. 346–352, 2002.

[131] M. Belting, M. I. Dorrell, S. Sandgren et al., "Regulation of angiogenesis by tissue factor cytoplasmic domain signaling," *Nature Medicine*, vol. 10, no. 5, pp. 502–509, 2004.

[132] H. Mirza, V. Yatsula, and W. F. Bahou, "The proteinase activated receptor-2 (PAR-2) mediates mitogenic responses in human vascular endothelial cells: molecular characterization and evidence for functional coupling to the thrombin receptor," *Journal of Clinical Investigation*, vol. 97, no. 7, pp. 1705–1714, 1996.

[133] C. Cicala, "Protease activated receptor 2 and the cardiovascular system," *British Journal of Pharmacology*, vol. 135, no. 1, pp. 14–20, 2002.

[134] G. M. Hjortoe, L. C. Petersen, T. Albrektsen et al., "Tissue factor-factor VIIa-specific up-regulation of IL-8 expression in MDA-MB-231 cells is mediated by PAR-2 and results in increased cell migration," *Blood*, vol. 103, no. 8, pp. 3029–3037, 2004.

[135] V. M. Shpacovitch, T. Brzoska, J. Buddenkotte et al., "Agonists of proteinase-activated receptor 2 induce cytokine release and activation of nuclear transcription factor kappaB in human dermal microvascular endothelial cells," *Journal of Investigative Dermatology*, vol. 118, no. 2, pp. 380–385, 2002.

[136] N. Asokananthan, P. T. Graham, J. Fink et al., "Activation of protease-activated receptor (PAR)-1, PAR-2, and PAR-4 stimulates IL-6, IL-8, and prostaglandin E_2 release from human respiratory epithelial cells," *The Journal of Immunology*, vol. 168, no. 7, pp. 3577–3585, 2002.

[137] Z. H. Wang, W. Zhu, J. P. Tao, Q. Y. Zhang, and M. Wei, "Stimulated mast cells promote maturation of myocardial microvascular endothelial cell neovessels by modulating the angiopoietin-Tie-2 signaling pathway," *Brazilian Journal of Medical and Biological Research*, vol. 46, no. 11, pp. 920–928, 2013.

[138] H. Urata, A. Kinoshita, K. S. Misono, F. M. Bumpus, and A. Husain, "Identification of a highly specific chymase as the major angiotensin II-forming enzyme in the human heart," *The Journal of Biological Chemistry*, vol. 265, no. 36, pp. 22348–22357, 1990.

[139] Y. Kunori, M. Koizumi, T. Masegi et al., "Rodent α-chymases are elastase-like proteases," *European Journal of Biochemistry*, vol. 269, no. 23, pp. 5921–5930, 2002.

[140] U. M. Chandrasekharan, S. Sanker, M. J. Glynias, S. S. Karnik, and A. Husain, "Angiotensin II-forming activity in a reconstructed ancestral chymase," *Science*, vol. 271, no. 5248, pp. 502–505, 1996.

[141] G. H. Caughey, W. W. Raymond, and P. J. Wolters, "Angiotensin II generation by mast cell α- and β-chymases," *Biochimica et Biophysica Acta*, vol. 1480, no. 1-2, pp. 245–257, 2000.

[142] S. Sanker, U. M. Chandrasekharan, D. Wilk, M. J. Glynias, S. S. Karnik, and A. Husain, "Distinct multisite synergistic interactions determine substrate specificities of human chymase and rat chymase-1 for angiotensin II formation and degradation," *The Journal of Biological Chemistry*, vol. 272, no. 5, pp. 2963–2968, 1997.

[143] M. W. Kofford, L. B. Schwartz, N. M. Schechter, D. R. Yager, R. F. Diegelmann, and M. F. Graham, "Cleavage of type I procollagen by human mast cell chymase initiates collagen fibril formation and generates a unique carboxyl-terminal propeptide," *The Journal of Biological Chemistry*, vol. 272, no. 11, pp. 7127–7131, 1997.

[144] K. C. Fang, W. W. Raymond, S. C. Lazarus, and G. H. Caughey, "Dog mastocytoma cells secrete a 92-kD gelatinase activated extracellularly by mast cell chymase," *The Journal of Clinical Investigation*, vol. 97, no. 7, pp. 1589–1596, 1996.

[145] E. Tchougounova, A. Lundequist, I. Fajardo, J.-O. Winberg, M. Åbrink, and G. Pejler, "A key role for mast cell chymase in the activation of pro-matrix metalloprotease-9 and pro-matrix metalloprotease-2," *The Journal of Biological Chemistry*, vol. 280, no. 10, pp. 9291–9296, 2005.

[146] B. T. Frank, J. C. Rossall, G. H. Caughey, and K. C. Fang, "Mast cell tissue inhibitor of metalloproteinase-1 is cleaved and inactivated extracellularly by alpha-chymase," *Journal of Immunology*, vol. 166, no. 4, pp. 2783–2792, 2001.

[147] A. Nakano, F. Kishi, K. Minami, H. Wakabayashi, Y. Nakaya, and H. Kido, "Selective conversion of big endothelins to tracheal smooth muscle-constricting 31-amino acid-length endothelins by chymase from human mast cells," *Journal of Immunology*, vol. 159, no. 4, pp. 1987–1992, 1997.

[148] S. Takai, N. Shiota, D. Jin, and M. Miyazaki, "Chymase processes big-endothelin-2 to endothelin-2-(1–31) that induces contractile responses in the isolated monkey trachea," *European Journal of Pharmacology*, vol. 358, no. 3, pp. 229–233, 1998.

[149] J. Taipale, J. Lohi, J. Saarinen, P. T. Kovanen, and J. Keski-Oja, "Human mast cell chymase and leukocyte elastase release latent transforming growth factor-beta 1 from the extracellular matrix of cultured human epithelial and endothelial cells," *The Journal of Biological Chemistry*, vol. 270, no. 9, pp. 4689–4696, 1995.

[150] G. Pejler and A. Karlstrom, "Thrombin is inactivated by mast cell secretory granule chymase," *The Journal of Biological Chemistry*, vol. 268, no. 16, pp. 11817–11822, 1993.

[151] G. H. Caughey, "New developments in the genetics and activation of mast cell proteases," *Molecular Immunology*, vol. 38, no. 16–18, pp. 1353–1357, 2002.

[152] L. Lindstedt, M. Lee, and P. T. Kovanen, "Chymase bound to heparin is resistant to its natural inhibitors and capable of proteolyzing high density lipoproteins in aortic intimal fluid," *Atherosclerosis*, vol. 155, no. 1, pp. 87–97, 2001.

[153] H. Urata, S. Hoffmann, and D. Ganten, "Tissue angiotensin II system in the human heart," *European Heart Journal*, vol. 15, pp. 68–78, 1994.

[154] T. Terada and Y. Matsunaga, "Increased mast cells in hepatocellular carcinoma and intrahepatic cholangiocarcinoma," *Journal of Hepatology*, vol. 33, no. 6, pp. 961–966, 2000.

[155] S.-Y. Tan, Y. Fan, H.-S. Luo, Z.-X. Shen, Y. Guo, and L.-J. Zhao, "Prognostic significance of cell infiltrations of immunosurveillance in colorectal cancer," *World Journal of Gastroenterology*, vol. 11, no. 8, pp. 1210–1214, 2005.

[156] A. Cabanillas-Saez, J. A. Schalper, S. M. Nicovani, and M. I. Rudolph, "Characterization of mast cells according to their content of tryptase and chymase in normal and neoplastic human uterine cervix," *International Journal of Gynecological Cancer*, vol. 12, no. 1, pp. 92–98, 2002.

[157] M. Muramatsu, J. Katada, I. Hayashi, and M. Majima, "Involvement of chymase in angiogenesis in hamster sponge granulomas," *Nihon Yakurigaku Zasshi*, vol. 114, supplement 1, pp. 48P–54P, 1999.

[158] M. Muramatsu, M. Yamada, S. Takai, and M. Miyazaki, "Suppression of basic fibroblast growth factor-induced angiogenesis by a specific chymase inhibitor, BCEAB, through the chymase-angiotensin-dependent pathway in hamster sponge granulomas," *British Journal of Pharmacology*, vol. 137, no. 4, pp. 554–560, 2002.

[159] J. Katada, M. Muramatsu, I. Hayashi, M. Tsutsumi, Y. Konishi, and M. Majima, "Significance of vascular endothelial cell growth factor up-regulation mediated via a chymase-angiotensin-dependent pathway during angiogenesis in hamster sponge granulomas," *The Journal of Pharmacology and Experimental Therapeutics*, vol. 302, no. 3, pp. 949–956, 2002.

[160] J. M. Arbeit, K. Münger, P. M. Howley, and D. Hanahan, "Progressive squamous epithelial neoplasia in K14-human papillomavirus type 16 transgenic mice," *Journal of Virology*, vol. 68, no. 7, pp. 4358–4368, 1994.

[161] L. M. Coussens and Z. Werb, "Matrix metalloproteinases and the development of cancer," *Chemistry and Biology*, vol. 3, no. 11, pp. 895–904, 1996.

[162] E. I. Deryugina and J. P. Quigley, "Pleiotropic roles of matrix metalloproteinases in tumor angiogenesis: contrasting, overlapping and compensatory functions," *Biochimica et Biophysica Acta*, vol. 1803, no. 1, pp. 103–120, 2010.

[163] A. Russo, G. Russo, M. Peticca, C. Pietropaolo, M. Di Rosa, and T. Iuvone, "Inhibition of granuloma-associated angiogenesis by controlling mast cell mediator release: role of mast cell protease-5," *British Journal of Pharmacology*, vol. 145, no. 1, pp. 24–33, 2005.

[164] I. G. Rojas, M. L. Spencer, A. Martínez, M. A. Maurelia, and M. I. Rudolph, "Characterization of mast cell subpopulations in lip cancer," *Journal of Oral Pathology and Medicine*, vol. 34, no. 5, pp. 268–273, 2005.

[165] M. Białas, G. Dyduch, J. Szpor, S. Demczuk, and K. Okoń, "Microvascular density and mast cells in benign and malignant pheochromocytomas," *Polish Journal of Pathology*, vol. 63, no. 4, pp. 235–242, 2012.

[166] T. Globa, L. Şaptefrţi, R. A. Ceauşu, P. Gaje, A. M. Cimpean, and M. Raica, "Mast cell phenotype in benign and malignant tumors of the prostate," *Polish Journal of Pathology*, vol. 2, pp. 147–153, 2014.

[167] M. Wilk, Ł. Liszka, P. Paleń, A. Gabriel, and P. Laudański, "Intensity of angiogenesis and mast cell infiltration in cervical intraepithelial and invasive lesions—are they correlated?" *Pathology Research and Practice*, vol. 206, no. 4, pp. 217–222, 2010.

[168] M. Nagata, N. Shijubo, A. F. Walls, S. Ichimiya, S. Abe, and N. Sato, "Chymase-positive mast cells in small sized adenocarcinoma of the lung," *Virchows Archiv*, vol. 443, no. 4, pp. 565–573, 2003.

[169] S. T. Tan, R. A. Wallis, Y. He, and P. F. Davis, "Mast cells and hemangioma," *Plastic and Reconstructive Surgery*, vol. 113, no. 3, pp. 999–1011, 2004.

Hindawi Publishing Corporation
BioMed Research International
Volume 2015, Article ID 652474, 8 pages
http://dx.doi.org/10.1155/2015/652474

Research Article

Production of Human Endothelial Cells Free from Soluble Xenogeneic Antigens for Bioartificial Small Diameter Vascular Graft Endothelization

Juliana Lott de Carvalho, Alessandra Zonari, Ana Cláudia Chagas de Paula, Thaís Maria da Mata Martins, Dawidson Assis Gomes, and Alfredo Miranda Goes

Laboratory of Cellular and Molecular Immunology, Department of Biochemistry and Immunology, Institute of Biological Sciences, Universidade Federal de Minas Gerais, 31270-901 Belo Horizonte, MG, Brazil

Correspondence should be addressed to Juliana Lott de Carvalho; julianalott@gmail.com

Received 19 November 2014; Accepted 29 January 2015

Academic Editor: Francesco Moccia

Arterial bypass graft implantation remains the primary therapy for patients with advanced cardiovascular disease, but most lack adequate saphenous vein or other conduits for bypass procedures and would benefit from a bioartificial conduit. This study aimed to produce human endothelial cells (hECs) in large scale, free from xenogeneic antigens, to develop a small diameter, compatible vessel for potential use as a vascular graft. Human adipose-derived stromal cells (hASCs) were isolated, cultured, and differentiated in the presence of human serum and used for the reendothelization of a decellularized rat aorta. hASC derived ECs (hASC-ECs) expressed VEGFR2, vWf and CD31 endothelial cell markers, the latter in higher levels than hASCs and HUVECs, and were shown to be functional. Decellularization protocol yielded aortas devoid of cell nuclei, with preserved structure, including a preserved basement membrane. When seeded with hASC-ECs, the decellularized aorta was completely reendothelized, and the hASC-ECs maintained their phenotype in this new condition. hASCs can be differentiated into functional hECs without the use of animal supplements and are capable of reendothelizing a decellularized rat aorta while maintaining their phenotype. The preservation of the basement membrane following decellularization supported the complete reendothelization of the scaffold with no cell migration towards other layers. This approach is potentially useful for rapid obtention of compatible, xenogeneic-free conduit.

1. Introduction

Approximately one-third of the 500.000 coronary bypass patients operated on in the USA every year [1] lack sufficient or healthy autologous tissue for vascular grafting [2]. Such patients then rely on synthetic grafts, which are a useful alternative to fill such gap, since they present favorable patency properties [2]. Currently, though, these grafts suffer from high thrombogenicity rates for small diameter vessels (<6 mm) [3], leaving a great unmet need for small diameter vascular grafting.

One of the strategies adopted so far to prevent graft failure is to cover graft interface with primary human endothelial cells (hECs), even though this procedure is hindered by low cell yield, limited cell plasticity, and loss of differentiation capacity of hECs following prolonged expansion *in vitro* [4]. In such scenario, the search for alternative sources of hECs is of interest. Human adipose-derived stromal cells (hASCs) have been shown to be easily isolated, expanded, and differentiated into hECs *in vitro*, constituting an excellent option for large-scale production of compatible and functional hECs. However, current cell culture supplements contain xenogeneic proteins, which may be source of infections [5, 6] and generate specific immune responses [7].

Recently, our group has shown that human allogeneic serum (aHS) is a suitable cell culture supplement for hASCs [8]. In addition to successfully maintaining hASCs *in vitro*, it maintains hASCs multipotency and induces higher proliferation rates without promoting cell senescence or loss of differentiation capacity [8–10]. Therefore, the use of aHS may be beneficial for tissue engineering approaches.

In the present study, we aimed to produce functional hECs and use them to promote the reendothelization of rat decellularized aortas. We propose that the association of hECs originated from human adipose-derived stromal cells (hASC-ECs) and a xenogeneic extracellular matrix (ECM) is feasible and may potentially constitute a fast and efficient strategy to develop a compatible vessel free from xenogeneic soluble antigens for potential use as a small-diameter vascular graft.

2. Material and Methods

2.1. aHS Obtention. The aHS was obtained from the whole blood of healthy donors from all blood group types, as previously described by our group [8]. Briefly, whole blood was collected and allowed to clot spontaneously. Serum was then separated by centrifugation and pooled to produce the aHS. The aHS was inactivated at 56°C for 30 min and aliquoted in sterile tubes, which were kept frozen until use. This procedure was approved by the Ethics Committee in Research from the Federal University of Minas Gerais (number ETIC 21176413.9.0000.5149).

2.2. Basal Medium. Basal Medium (BM) consisted of Dulbecco's modified Eagle medium-high glucose (DMEM) (Sigma-Aldrich) supplemented with 5 mM sodium bicarbonate (Cinética Química Ltda), penicillin (100 U/mL), streptomycin (0.1 mg/mL), amphotericin B (0.25 mg/mL; Sigma-Aldrich), gentamicin (60 mg/L; Schering-Plough), and 10% aHS.

2.3. Endothelial Medium. Endothelial medium (EM) was composed of DMEM supplemented with 5 mM sodium bicarbonate (Cinética Química Ltda), penicillin (100 U/mL), streptomycin (0.1 mg/mL), amphotericin B (0.25 mg/mL), (Sigma-Aldrich), gentamicin (60 mg/L; Schering-Plough), 1% aHS, 1 mg/mL VEGF (Invitrogen), and 0.1 mg/mL bFGF (Invitrogen).

2.4. hASCs Isolation and Culture. Human adipose tissue was harvested from healthy patients, which had abdominal reduction surgery for aesthetic reasons. This study was approved by the Ethics Committee of the Federal University of Minas Gerais (number ETIC 21176413.9.0000.5149). The isolation and culture of hASCs were performed as described, with minor modifications [8, 11]. Briefly, the excess of blood in the raw lipoaspirates was removed with phosphate-buffered saline (PBS) washes and enzymatic digestion of adipose tissue was performed with the incubation of the tissue in a solution of 0.075% type I collagenase I (Life Technologies) in PBS at 37°C for 1 h. Then, the stromal vascular fraction was isolated by centrifugation at 252 g for 10 min, and the pellet was suspended in BM and plated into cell culture flasks (Sarstedt). The flasks were incubated at 37°C in 5% CO_2 and a humidified atmosphere. After 12–28 h of incubation, plastic adherent cells were isolated with media change and those were termed hASCs. BM was changed every 2-3 days. Subculture was performed every time cell population achieved 80–90% confluency, with incubation of the cells in 0.05% Trypsin-EDTA (Invitrogen) solution for 3–5 min, when cells began to detach from tissue culture flasks. Trypsin solution was then inactivated by adding the same volume of BM supplemented with human serum to flasks, and the resulting cell suspension was replated in new cell culture flasks. The cells were expanded this way until passage 4, when they were used in the assays.

2.5. Flow Cytometry. Phenotypic characterization of isolated hASCs was performed as recommended by the Mesenchymal and Tissue Stem Cell Committee of the International Society for Cellular Therapy [12] and performed as already described elsewhere [8]. Briefly, fourth passage undifferentiated hASCs were detached from cell culture surface and counted. About one million cells were then washed with PBS and incubated with the following primary unconjugated mouse monoclonal antibodies: CD29 (Santa Cruz Cat. number sc-9970), CD44 (Santa Cruz Cat. number sc-7297), CD34 (Abcam Cat. number ab8147-500), and CD45 (from BD Biosciences, Cat. number 616256) and with the following conjugated antibodies: HLA-ABC-fluorescein isothiocyanate (FITC) (Abcam, Cat. number ab20313-100) and HLA-DR-FITC (Abcam, Cat. number ab36775-500). Secondary antibodies used were Alexa Fluor 488 goat anti-mouse IgG (Invitrogen, Cat. number A11001). Flow cytometry was performed using a Guava easyCyte 6-2L Flow Cytometer (Millipore). Five thousand events were acquired using the software Incyte (Millipore), analyzed using FlowJo 7.5.6 and compared to isotype controls.

2.6. Endothelial Differentiation. Endothelial differentiation was performed with the culture of 7.5×10^4 cells in endothelial medium. Briefly, hASCs were detached from tissue culture flasks, counted, and seeded in BM at a density of 10^3 cells/cm^2 in T75 cell culture flasks (Sarstedt). Twenty-four hours later, the BM was removed and EM was used thereafter up to 21 days. EM was changed every 2-3 days.

2.7. RT-PCR. The differentiation of hASCs towards endothelial cell fate was assessed according to gene expression of the endothelial markers VEGF receptor type 2 (VEGFR2) and Von Willebrand Factor (vWF). In order to do that, at the end of the induction period, total RNA was extracted using TRIzol and reverse transcripted into cDNA using RevertAidTM H Minus M-MuLV RT. PCR was performed for VEGFR2 (forward primer (FP): 5′ GGAATACCCCTTGAGTCC3′, reverse primer (RP): 5′ CCTCCAACTGCCAATACC3′), vWF (FP: 5′ CGCTCCAGGATGGCTGTG3′, RP: 5′ GTACATGGCTTTGCTGGC3′), GAPDH (FP: 5′ GGTATCGTGGAAGGACTCATGAC3′, and RP: 5′ ATGCCAGTGAGCTTCCCGTTCAGC3′). mRNA was also isolated from human umbilical vein endothelial cells (HUVECs) as positive control. PCR cycles were as follows: 94°C for 2 min, 94°C for 30 s, 56°C (for vWF and VEGFR2) and 60°C (for GAPDH) for 45 s and 72°C for 45 s (30 cycles), and 72°C for 10 min. The RT-PCR products were analyzed through 1% agarose gel electrophoresis and visualized with ethidium bromide.

2.8. Immunofluorescence. At the end of the differentiation period, cells were stained for endothelial markers. Immunofluorescence was performed following cell fixation with 4% paraformaldehyde. Afterwards, cells were washed, permeabilized, and incubated with primary antibodies overnight at 4°C. Cells were then washed and incubated with secondary antibodies for 1 h at room temperature. Finally, cell nuclei were stained with DAPI and slides were mounted using Hydromount. Primary antibodies used were mouse anti-vWF (Abcam, Cat. number ab129948) and rabbit anti-VEGFR (Abcam, Cat. number 2349-500). Secondary antibodies used were Alexa Fluor goat anti-mouse 488 (Molecular Probes, Cat. number A21428), and Alexa Fluor goat anti-rabbit 555 (Molecular Probes, Cat. number A11001). HUVECs were stained and considered positive control.

The same antibodies were also used for tissue immunostaining of the recellularized aortas. Tissue sections were washed in water and protocol was similar to described for cells.

2.9. Tube Formation Assay. The capacity of hASC-ECs to form tubes in matrigel was assessed as previously described as an *in vitro* assay to assess endothelial cell function [13]. For this assay, 4×10^4 cells were seeded on each well of a 24-well plate coated with 225 μL of previously solidified Matrigel (BD Biosciences) and incubated overnight at 37°C in 5% CO_2 incubator. Cells were then incubated in 3 μg/mL Calcein-AM (Invitrogen) diluted in PBS for 30 min at 37°C in 5% CO_2 incubator, protected from light. Finally, tube formation was observed, quantified and tube area was measured both under light microscopy and under fluorescence microscope, using the ImageJ 1.47 software.

2.10. Aorta Decellularization and Animal Information. Lewis LEW-Tg (EGFP) F455.5/Rrrc rats 6–8 weeks old, which express enhanced fluorescence green fluorescent protein (EGFP), were obtained from the Rat Resource and Research Center, Missouri, USA. The animals were housed in a climate-controlled environment under a 12 h light/dark cycle with free access to rat chow and water. All experimental protocols were performed in accordance with the guidelines for the humane use of laboratory animals established at our Institution. This study was approved by the Committee of Ethics in Research at the Federal University of Minas Gerais (Protocol number 140/2011).

Aorta decellularization was performed according to the protocol published by [14], with minor modifications, as described by [15]. Briefly, the isolated aorta was perfused with 1% SDS and 1% Triton X-100 solutions and sterilized by perfusion of PBS supplemented with 100 U/mL penicillin-G, 100 U/mL streptomycin, and amphotericin B. After, Aorta was isolated from the heart and cannulated in its other end to mount a closed perfusion system. Following decellularization, approximately 50 mg of tissue was processed using DNAzol reagent (Life Technologies) for genomic DNA isolation, following manufacturer's instructions. Isolated DNA was quantified using Nanodrop ND-1000 spectrophotometer (Life Technologies, USA).

2.11. Aorta Reendothelization. hASC-EC were evaluated according to their potential of reendothelizing a decellularized aorta in the presence of EM with human serum. In order to do so, endothelial cells were harvested and counted. 2.5×10^6 cells were then perfused into the decellularized matrix with an initial static period overnight, followed by 7 days of continuous perfusion with EM.

2.12. Decellularized Aorta Processing for Histology and Immunofluorescence. Following fixation in 4% paraformaldehyde, aortas were embedded in paraffin or OCT (Optimal Cutting Temperature). 5 μm tissue slices were cut for histology and immunostaining. Hematoxylin and Eosin staining was performed. ECM proteins laminin and collagen I were stained following tissue slice production, following the same steps of immunofluorescence cell staining. Primary antibodies used were mouse anti-rat collagen I and rabbit anti-rat laminin (both from Abcam, UK). Secondary antibodies were the same used for cell staining.

3. Results

3.1. hASCs Characterization. Isolated hASCs cultured in BM were positive for CD29 (98.3%) and CD44 (99.6%) and lacked the expression of hematopoietic stem cell-associated markers CD34 (0.38%) and CD45 (0.72%). In addition, hASCs expressed HLA-ABC (99.8%) and lacked HLA-DR (0.15%) (Figure 1(a)).

Functionally, isolated hASCs proved their multilineage differentiation potential and were capable of generating osteoblasts, chondrocytes, and adipocytes following differentiation (data not shown). Those were capable of mineralizing the ECM, depositing proteoglycan in ECM, and storing lipid droplets in their cytoplasm, respectively. Therefore, isolated hASCs attended to the criteria of mesenchymal stromal cell (MSC) characterization both phenotypically and functionally.

3.2. hASCs Endothelial Differentiation in Induction Medium Containing Human Serum. Endothelial differentiation of hASCs in the presence of aHS was confirmed by gene and protein expression of endothelial markers; therefore, they were regarded as hASC-ECs. First, expressions of VEGFR2 and vWF were assessed by PCR. As expected, hASC-ECs were capable of expressing both markers related to the endothelial lineage. Undifferentiated hASCs also expressed such genes in discrete smaller levels, similar to HUVECs, which were used as positive control (Figure 1(b)). In a quantitative approach, the expression of CD31 was also assessed (Figure S.1 in Supplementary Material available online at http://dx.doi.org/10.1155/2015/652474) and indicated that hASC-ECs had approximately 11 times higher CD31 expression compared to both hASCs and HUVECs, which had statistically similar expression of this marker, even though the latter had a slightly higher CD31 expression level then hASCs.

The expression of both VEGFR and vWF was assessed at protein level by immunofluorescence. Our results show

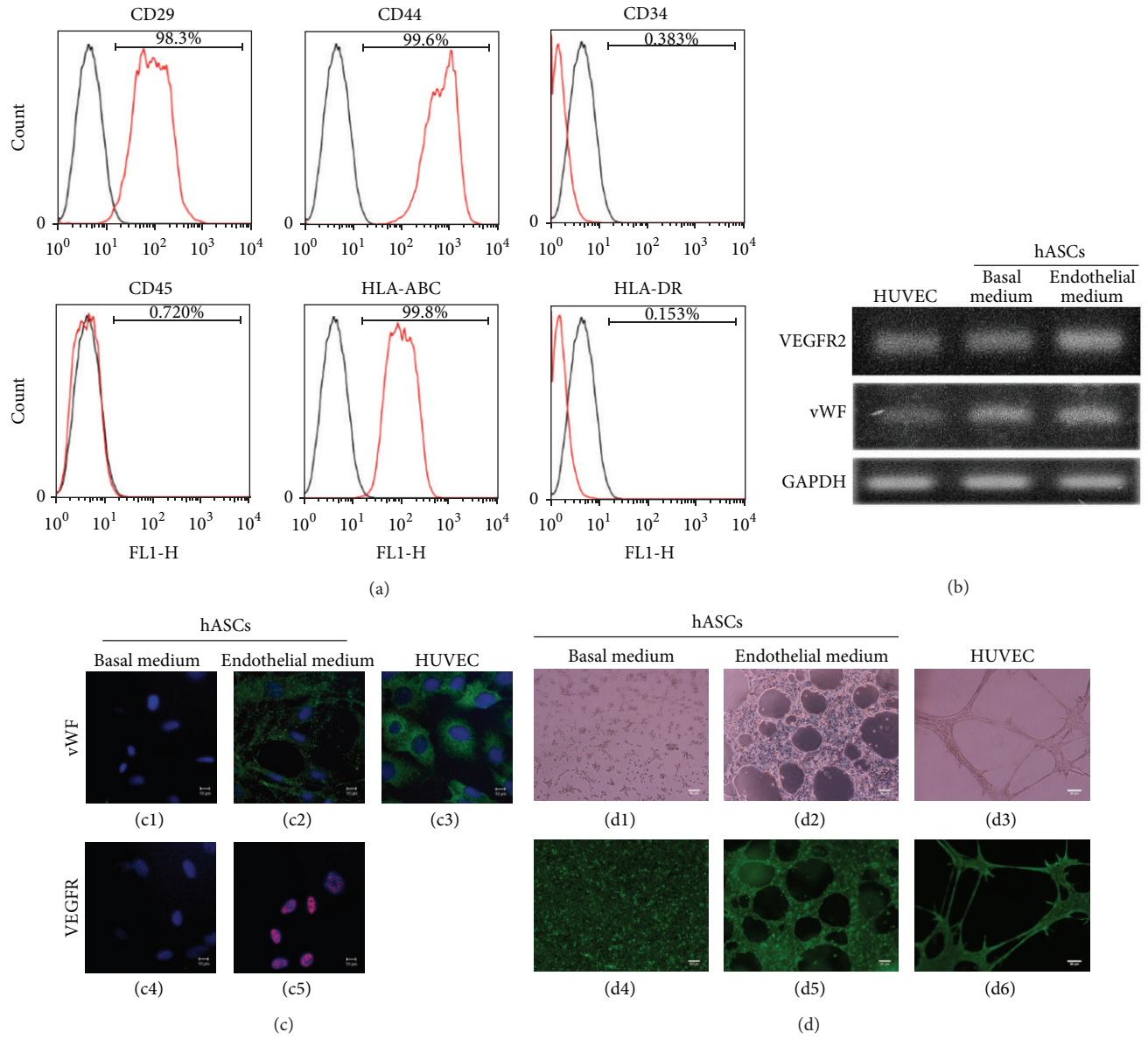

Figure 1: hASCs characterization and endothelial differentiation. (a) Flow cytometry analysis of hASCs expression of mesenchymal stem cell markers. Black line indicates isotype-matched monoclonal antibody controls and red line indicates positive stained cells. (b) RT-PCR analysis of VEGFR2 and vWF mRNA expression during endothelial differentiation of hASCs. The expression of those markers was also assessed at protein level by immunohistochemistry (c). Green fluorescence corresponds to vWF protein presence (c1, c2, and c3), red corresponds to VEGFR protein expression (c4 and c5), and blue corresponds to cell nuclei (c1–c5). (d) Functional analysis of endothelial cell differentiation, as assessed by tube formation assay. In (d1) to (d3), inverted microscopy was used to document tube formation. In (d4) to (d6), cells were stained with calcein-AM and observed under fluorescence microscope, in order to show cell viability in addition to tube formation. $n = 3$ for each experiment.

once again the consistent differentiation of hASC-ECs into the endothelial phenotype, as both hASC-ECs and HUVECs exhibited VEGFR and vWF proteins. hASCs presented no expression of those proteins, evidentiating the difference between undifferentiated hASCs and their hASC-ECs derivatives (Figure 1(c)).

3.3. Tube Formation Assay. One of the functional assays to assess endothelial differentiation consists on investigating the capacity of hECs of forming tubes when cultured in Matrigel in the presence of stimulus. Since the undifferentiated hASCs express VEGFR and vWF in discrete levels, this assay is necessary to differentiate hASCs from functional hECs. To do so, first, we cultured HUVECs in such condition and showed their capacity to form tubes. Following, hASCs and hASC-ECs were also used in the experiment and only differentiated hASCs (hASC-ECs) and HUVECs were capable of forming tubes once stimulated in Matrigel (Figure 1(d)). Even though hASCs express some hECs markers, those are not present at the protein level and hASCs are not able to form tubes when

seeded on Matrigel. Cell viability was assessed with Calcein-AM. The qualitative observation was confirmed by quantitative analysis of the relative numbers of tube formation and the median size of those tubes. Once again, HUVECs showed high capacity of forming tubes, presenting an average of 8 per field, with average size of 22431 μm^2. HUVECs were closely followed by hASC-ECs, which were also able to generate tubes under the tested conditions, with 14 tubes per field (average size: 8599 μm^2). Tube formation by hASCs was not observed and considered virtually absent.

3.4. Aorta Reendothelization. Finally, the reendothelization of a decellularized aorta was performed in order to assess the applicability of using hASC-ECs to promote construct viability *in vivo*. First, aorta decellularization was verified by histology and DNA isolation. As expected, decellularized aorta was shown to be deployed of cell nuclei and DNA. Additionally, decellularized aortas presented laminin preserved along their layers, including the basement membrane (Figures 2(a) and 2(b)).

After a period of static seeding, hASC-ECs were reperfused and cultured for 7 days in the closed system in order to attach and proliferate in the matrix. Following such period, cells formed continuous sheets of viable cells, as shown by histology and immunofluorescence (Figures 2(c) and 2(d)). Even after 7 days of culture in a perfusion biorreactor, hASC-ECs still expressed VEGFR and vWF and strongly adhered to the basement membrane of the decellularized aorta (Figure 2(d)), evidentiating the stability of the construct in a perfusion system for 7 days.

4. Discussion

The search for vascular substitutes has proven to be difficult, specially when considering small diameter grafts. Major problems concerning vascular engineering comprise thrombogenesis, calcification, and patency maintenance. An effective strategy to prevent such events to occur is to protect materials from circulation by covering them with hECs. Therefore, disregarding the vascularization strategy used to substitute occluded or diseased vessels, hECs are always a key component. A continuous endothelium on the flow surface maintains graft patency and prevents platelet deposition, thrombosis, and neointimal hyperplasia [16]. Also, it excludes the need of fixation steps and prevents the presence of cell debris and the attraction of calcium by glutaraldehyde, both related to the process of calcification [17]. Beyond that, hECs are in direct contact to several lymphoid cell types and may initiate rejection in an allograft context, functioning as antigen presenting cells and directly activating lymphocytes [18]. Therefore, they must not be different from host nor present xenogeneic antigens.

Endothelization of vascular grafts is observed *in vivo* within weeks to months postgrafing. Monoclonal antibodies, recombinant proteins, and aptamers have been used to accelerate graft endothelization [19]. We propose that endothelization *in vitro* is faster and more efficient, since it has been shown that despite being reendothelized *in vivo* vascular grafts lacking a continuous endothelium still show thrombosis and calcification. In this scenario, obtaining high numbers of autologous hECs is imperative. hECs can be easily isolated from patients as circulating progenitors [20, 21] or from vessel wall biopsies [22, 23]. However, those approaches are hindered by low cell yield, limited plasticity, and differentiation capacity following prolongated expansion *in vitro* [24]. Here, we show that adipose tissue constitutes a promising cell source for hECs generation, as it does not suffer from the aforementioned limitations. In addition, adipose tissue may prove to be a more reliable source of autologous stem cells than blood or bone marrow, where the presence of diabetes and other comorbidities may significantly decrease the availability of stem cells for clinical use.

hASCs are easily isolated from adipose tissue and have a clear potential for clinical applications. Indeed, several clinical trials using these cells have been performed aiming for the treatment of various injuries and diseases (clinicaltrials.gov). hASCs may be obtained from the patient in times of health, in order to be used when needed, or from healthy donors. Therefore, the isolation of hASCs and further differentiation towards endothelial lineage constitute faster and more reliable approach for tissue engineered vascular graft (TEVG).

hASCs endothelial differentiation *in vitro* is consistent and reproducible [25–27]. Most differentiation protocols are based on induction with VEGF and bFGF [25, 27]. Even though the mechanism for hECs induction is not clear, it is known that VEGF induces hECs differentiation in a Rho-GTPase-dependent manner. Physical stimuli (shear stress) also promote hASCs endothelial differentiation [26, 28]. In the present work, we associate both stimuli for hASCs differentiation. Our results indicate that generation of hASC-ECs in the presence of aHS was succesful. hASC-ECs presented CD31, VEGFR2 (also known as KDR), and vWF. Among those markers, CD31 is the most specific, since KDR may be expressed in progenitors and pluripotent stem cells [29, 30], and vWF may be released by platelets [31]. Therefore, CD31 expression was assessed quantitatively, by qPCR (Figure S.1), and revealed that hASC-ECs had the higher expression of this surface marker among samples tested, which also included hASC and HUVECs. This data can indicate that the HUVEC cell line maintained in our lab may have lost the expression of such marker or that maybe our culture conditions did not promote the maintenance of CD31 expression. Nevertheless, other markers were assessed and shown to be present at HUVECs, in addition to hASCs and hASC-ECs, both at the mRNA and protein levels. Those markers were VEGFR2 and vWF. Even though those markers can be related to other events, it is known that the former plays a major role in the *in vivo* angiogenesis and contributes with matrix-metalloproteinase to the formation of capillary-like structures seen *in vitro* [29]. The latter mediates the adhesion of blood platelets at sites of vascular injury, stabilizes clotting factor VIII, and contributes to hECs anchoring to ECM [30]. Even though they are also expressed in discrete amounts at mRNA level in hASCs, those markers are not present at the protein level. Cell populations under investigation in the present work were also assessed in terms of

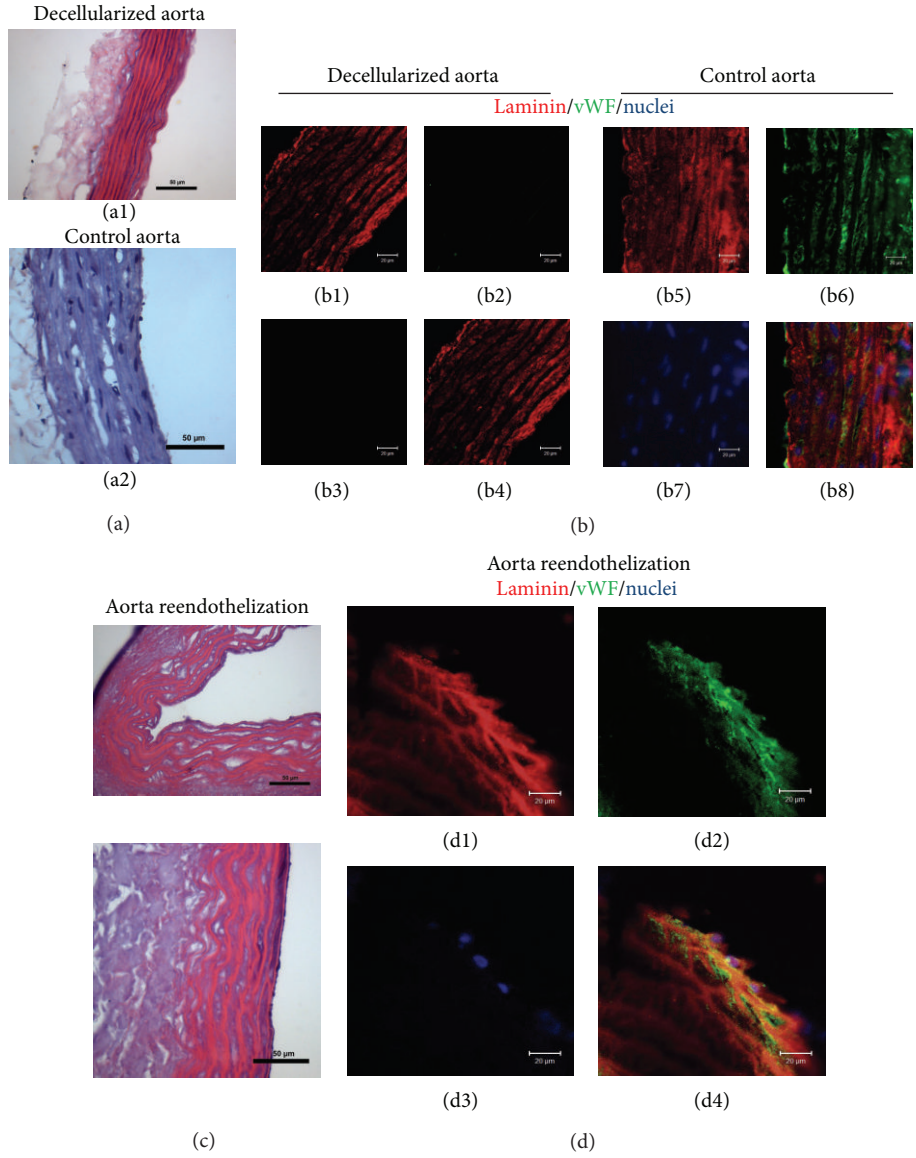

Figure 2: Decellularization of rat aortas and recellularization with hASC-ECs. (a) Perfusion-decellularized rat aortas (a1) presented intact ultrastructure but were devoid of cell nuclei, in contrast to nondecellularized control rat aortas (a2). (b) Decellularization process (b1 to b4) did not compromise laminin content, as compared to nondecellularized control aorta (b5 to b8). (b1) and (b5) correspond to laminin staining (red), (b2) and (b6) correspond to vWF staining (green), (b3) and (b7) show cell nuclei content (blue), and (b4) and (b8) are image overlays. (c) Recellularized rat aortas present continuous endothelium in their inner surface (c2), absent in decellularized controls (c1). Recellularization with hASC-ECs rebuilt the endothelium of decellularized aorta, which maintained laminin content (red, d1) and regained vWF (green, d2) and nuclei (d3) in their endothelium. Image overlay (d4). $n = 3$ for each experiment.

functionality, in order to further strengthen our claim of having generated hASC-ECs in nonxenogeneic conditions. As expected, hASCs are not functional hECs and were unable to generate tubes when seeded on Matrigel. In contrast, hASC-ECs were able to generate tubes under the tested conditions, confirming their endothelial phenotype, as well as HUVECs. Even though hASC-ECs formed tubes in higher amounts and smaller diameters compared to HUVECs, those differences emphasize the higher proliferative potential of hASC-ECs [31], which is a positive feature, considering the proposed objectives of the present work. This assay also confirmed that the HUVEC cell line maintained in our lab may have lost CD31 expression but is still functional and is representative of the endothelial phenotype.

The seeding of hASC-ECs in biomaterials and decellularized matrices has been performed with exciting results [19, 31]. It has been described that hEC coated TEVG is feasible and safe, but the developed strategy used autologous primary cultures of hECs and took several weeks to achieve complete graft endothelization [32]. With our approach, this time can be shortened, due to high proliferation rates of hASCs cultured with aHS.

The production of the aforementioned TEVG requires the investigation of ways to exclude soluble animal antigens from cell culture, before performing hASCs differentiation. Use of animal origin reagents is controversial due to the possibility of zoonosis disease transmission. The risk of prion infection can be avoided, but the use of an average of 20% FBS in cell culture, regardless of the type, results in MSC carrying between 7 and 30 mg of bovine serum proteins, resulting in specific immune reaction in humans [33].

Animal-free alternatives have emerged for immortalized cell cultures, but few products exist for primary adult human cells, and they typically provide suboptimal results. Previously, our group has described that allogeneic human serum is a suitable supplement for proliferation and differentiation of hASCs [8]. In this work, the results indicate that hASCs not only maintained their classic phenotype in such condition (e.g., cell markers and multipotent differentiation capacity), but also were able to differentiate into functional hECs, as shown by the tube formation assay. Finally, functional hECs were able to generate a continuous cell sheet in the preserved basement membrane of a rat aorta, in the presence of shear stress. Here, we generated functional hECs free from animal soluble antigens and showed that they are functional and able to be used for TEVG approaches, in a potentially faster and safer manner.

Conflict of Interests

The authors declare that there is no conflict of interests regarding the publication of this paper.

Authors' Contribution

Juliana Lott de Carvalho performed experiment design, cell culture and differentiation, aorta decellularization and seeding, immunostainings, data analysis, and paper writing. Alessandra Zonari contributed to experiment design, data analysis, and paper revision. Ana Cláudia Chagas de Paula contributed to experiment design, allogeneic serum obtention, cell isolation, and culture and differentiation, in addition to paper revision. Thaís Maria de Mata Martins contributed to experiment design, data analysis, figure preparation, and paper revision. Dawidson Assis Gomes and Alfredo Miranda Goes performed study conception and design, data analysis and interpretation, provision of study materials, and paper writing.

Acknowledgments

Confocal laser-scanning microscopy was performed at Centro de Aquisição e Processamento de Imagens (CAPI). This work was supported by CNPq, CAPES, and FAPEMIG agencies.

References

[1] L. J. Kozak, M. J. Hall, and M. F. Owings, "National Hospital discharge survey: 2000 annual summary with detailed diagnosis and procedure data," *Vital and Health Statistics Series*, vol. 13, no. 153, pp. 1–194, 2000.

[2] M. Avci-Adali, N. Perle, G. Ziemer, and H. P. Wendel, "Current concepts and new developments for autologous in vivo endothelialisation of biomaterials for intravascular applications," *European Cells and Materials*, vol. 21, pp. 157–176, 2011.

[3] M. Peck, D. Gebhart, N. Dusserre, T. N. McAllister, and N. L'Heureux, "The evolution of vascular tissue engineering and current state of the art," *Cells Tissues Organs*, vol. 195, no. 1-2, pp. 144–158, 2011.

[4] L. Gui, A. Muto, S. A. Chan, C. K. Breuer, and L. E. Niklason, "Development of decellularized human umbilical arteries as small-diameter vascular grafts," *Tissue eEngineering. Part A*, vol. 15, no. 9, pp. 2665–2676, 2009.

[5] R. Knight, "The risk of transmitting prion disease by blood or plasma products," *Transfusion and Apheresis Science*, vol. 43, no. 3, pp. 387–391, 2010.

[6] G. A. Erickson, S. R. Bolin, and J. G. Landgraf, "Viral contamination of fetal bovine serum used for tissue culture: risks and concerns.," *Developments in Biological Standardization*, vol. 75, pp. 173–175, 1991.

[7] T. A. Selvaggi, R. E. Walker, and T. A. Fleisher, "Development of antibodies to fetal calf serum with arthus-like reactions in human immunodeficiency virus-infected patients given syngeneic lymphocyte infusions," *Blood*, vol. 89, no. 3, pp. 776–779, 1997.

[8] A. C. C. de Paula, A. A. C. Zonari, T. M. da Mata Martins et al., "Human serum is a suitable supplement for the osteogenic differentiation of human adipose-derived stem cells seeded on poly-3-hydroxibutyrate-co-3-hydroxyvalerate scaffolds," *Tissue Engineering Part A*, vol. 19, no. 1-2, pp. 277–289, 2012.

[9] C. Escobedo-Lucea, C. Bellver, C. Gandia et al., "A xenogeneic-free protocol for isolation and expansion of human adipose stem cells for clinical uses," *PLoS ONE*, vol. 8, no. 7, Article ID e67870, 2013.

[10] A. Kocaoemer, S. Kern, H. Klüter, and K. Bieback, "Human AB serum and thrombin-activated platelet-rich plasma are suitable alternatives to fetal calf serum for the expansion of mesenchymal stem cells from adipose tissue," *Stem Cells*, vol. 25, no. 5, pp. 1270–1278, 2007.

[11] P. A. Zuk, M. Zhu, H. Mizuno et al., "Multilineage cells from human adipose tissue: implications for cell-based therapies," *Tissue Engineering*, vol. 7, no. 2, pp. 211–228, 2001.

[12] M. Dominici, K. Le Blanc, I. Mueller et al., "Minimal criteria for defining multipotent mesenchymal stromal cells. The International Society for Cellular Therapy position statement," *Cytotherapy*, vol. 8, no. 4, pp. 315–317, 2006.

[13] S. M. Mihaila, A. M. Frias, R. P. Pirraco et al., "Human adipose tissue-derived SSEA-4 subpopulation multi-differentiation potential towards the endothelial and osteogenic lineages," *Tissue Engineering—Part A*, vol. 19, no. 1-2, pp. 235–246, 2013.

[14] H. C. Ott, T. S. Matthiesen, S.-K. Goh et al., "Perfusion-decellularized matrix: using nature's platform to engineer a bioartificial heart," *Nature Medicine*, vol. 14, no. 2, pp. 213–221, 2008.

[15] J. L. Carvalho, P. H. de Carvalho, D. A. Gomes, and A. M. Goes, "Characterization of decellularized heart matrices as biomaterials for regular and whole organ tissue engineering and initial in-vitro recellularization with ips cells," *Journal of Tissue Science & Engineering*, vol. 3, p. S11, 2012.

[16] T. Nishibe, Y. Kondo, A. Muto, and A. Dardik, "Optimal prosthetic graft design for small diameter vascular grafts," *Vascular*, vol. 15, no. 6, pp. 356–360, 2007.

[17] F. J. Schoen, R. J. Levy, and H. R. Piehler, "Pathological considerations in replacement cardiac valves," *Cardiovascular Pathology*, vol. 1, no. 1, pp. 29–52, 1992.

[18] R. S. Al-Lamki, J. R. Bradley, and J. S. Pober, "Endothelial cells in allograft rejection," *Transplantation*, vol. 86, no. 10, pp. 1340–1348, 2008.

[19] C. Quint, Y. Kondo, R. J. Manson, J. H. Lawson, A. Dardik, and L. E. Niklason, "Decellularized tissue-engineered blood vessel as an arterial conduit," *Proceedings of the National Academy of Sciences of the United States of America*, vol. 108, no. 22, pp. 9214–9219, 2011.

[20] Q. Shi, S. Rafii, M. H. Wu et al., "Evidence for circulating bone marrow-derived endothelial cells," *Blood*, vol. 92, no. 2, pp. 362–367, 1998.

[21] M. Yamada, H. Kubo, K. Ishizawa, S. Kobayashi, M. Shinkawa, and H. Sasaki, "Increased circulating endothelial progenitor cells in patients with bacterial pneumonia: evidence that bone marrow derived cells contribute to lung repair," *Thorax*, vol. 60, no. 5, pp. 410–413, 2005.

[22] M. Massa, V. Rosti, M. Ferrario et al., "Increased circulating hematopoietic and endothelial progenitor cells in the early phase of acute myocardial infarction," *Blood*, vol. 105, no. 1, pp. 199–206, 2005.

[23] G. C. Schatteman, M. Dunnwald, and C. Jiao, "Biology of bone marrow-derived endothelial cell precursors," *The American Journal of Physiology—Heart and Circulatory Physiology*, vol. 292, no. 1, pp. H1–H18, 2007.

[24] G. C. Schatteman and O. Awad, "In vivo and in vitro properties of $CD34^+$ and $CD14^+$ endothelial cell precursors," *Advances in Experimental Medicine and Biology*, vol. 522, pp. 9–16, 2003.

[25] A. Zonari, S. Novikoff, N. R. P. Electo et al., "Endothelial differentiation of human stem cells seeded onto electrospun polyhydroxybutyrate/polyhydroxybutyrate-co-hydroxyvalerate fiber mesh," *PLoS ONE*, vol. 7, no. 4, Article ID e35422, 2012.

[26] K. J. Portalska, A. Leferink, N. Groen et al., "Endothelial differentiation of mesenchymal stromal cells," *PLoS ONE*, vol. 7, no. 10, Article ID e46842, 2012.

[27] N. Wang, R. Zhang, S.-J. Wang et al., "Vascular endothelial growth factor stimulates endothelial differentiation from mesenchymal stem cells via Rho/myocardin-related transcription factor-A signaling pathway," *International Journal of Biochemistry and Cell Biology*, vol. 45, no. 7, pp. 1447–1456, 2013.

[28] U. Liny, A. Nas, O. Gus, and A. Mas, "High-level shear stress stimulates endothelial differentiation and VEGF secretion by human mesenchymal stem cells," *Cellular and Molecular Bioengineering*, vol. 6, no. 2, pp. 220–229, 2013.

[29] S. J. Kattman, A. D. Witty, M. Gagliardi et al., "Stage-specific optimization of activin/nodal and BMP signaling promotes cardiac differentiation of mouse and human pluripotent stem cell lines," *Cell Stem Cell*, vol. 8, no. 2, pp. 228–240, 2011.

[30] H. Kataoka, N. Takakura, S. Nishikawa et al., "Expressions of PDGF receptor alpha, c-Kit and Flk1 genes clustering in mouse chromosome 5 define distinct subsets of nascent mesodermal cells," *Development Growth and Differentiation*, vol. 39, no. 6, pp. 729–740, 1997.

[31] S. Kanaji, S. A. Fahs, Q. Shi, S. L. Haberichter, and R. R. Montgomery, "Contribution of platelet vs. endothelial VWF to platelet adhesion and hemostasis," *Journal of Thrombosis and Haemostasis*, vol. 10, no. 8, pp. 1646–1652, 2012.

[32] J. Oswald, S. Boxberger, B. Jørgensen et al., "Mesenchymal stem cells can be differentiated into endothelial cells in vitro," *Stem Cells*, vol. 22, no. 3, pp. 377–384, 2004.

[33] J. E. Sadler, "von Willebrand factor assembly and secretion," *Journal of Thrombosis and Haemostasis*, vol. 7, supplement S1, no. 1, pp. 24–27, 2009.

Hindawi Publishing Corporation
BioMed Research International
Volume 2015, Article ID 742646, 11 pages
http://dx.doi.org/10.1155/2015/742646

Research Article

Expression of Adiponectin Receptors on Peripheral Blood Leukocytes of Hypertensive Children Is Associated with the Severity of Hypertension

Lidia Gackowska,[1] Mieczyslaw Litwin,[2] Joanna Trojanek,[3] Andrzej Eljaszewicz,[1] Izabela Kubiszewska,[1] Anna Niemirska,[2] Aldona Wierzbicka,[4] and Jacek Michalkiewicz[1,3]

[1]*Chair of Immunology, Collegium Medicum in Bydgoszcz, Nicolaus Copernicus University of Torun, 85-094 Bydgoszcz, Poland*
[2]*Department of Nephrology and Arterial Hypertension, The Children's Memorial Health Institute, 07-730 Warsaw, Poland*
[3]*Department of Microbiology and Immunology, The Children's Memorial Health Institute, 07-730 Warsaw, Poland*
[4]*Department of Biochemistry and Experimental Medicine, The Children's Memorial Health Institute, 07-730 Warsaw, Poland*

Correspondence should be addressed to Lidia Gackowska; lidiagackowska@gmail.com

Received 27 November 2014; Revised 30 January 2015; Accepted 25 February 2015

Academic Editor: Alessandra Micera

The aim of the study was to find out whether peripheral blood leukocyte adiponectin receptors 1 and 2 (AdipoR1, AdipoR2) protein expression patterns (flow cytometry) differ between the primary hypertension children ($n = 57$) and healthy controls ($n = 19$) and if their expression levels are related to selected clinical parameters. The group of 26 patients [AdipoR(−)] showed lower and the group of 31 patients [AdipoR(+)] showed higher AdipoRs protein expression than the control and each other ($P < 0.01$ for neutrophils, $P < 0.05$ for monocytes). The AdipoR(+) leukocytes expressed higher AdipoR1 mRNA levels (RT-PCR) than AdipoR(−) ones and controls ($P = 0.022$ and $P = 0.007$, resp.). Despite greater BMI, the AdipoR(−) patients had unchanged serum adiponectin levels. In contrast, AdipoR(+) patients had lower serum adiponectin concentrations than the AdipoR(−) ones and controls ($P < 0.001$). The AdipoR(+) patients had higher blood pressure ($P = 0.042$) and greater carotid intima-media thickness ($P = 0.017$) than the AdipoR(−) ones. The stage of hypertension was associated with increased neutrophil but not monocyte AdipoR1 density (AdipoR1 MFI) ($P < 0.05$). Severe ambulatory hypertension was presented more often in AdipoR(+) patients than in AdipoR(−) ones (51.6% versus 26.9%, resp.; $P < 0.01$). In conclusion, neutrophil AdipoRs upregulation was associated with early stages of vascular injury, hypertension severity, and low serum levels of adiponectin.

1. Introduction

Primary hypertension (PH) is a complex disease consisting of hemodynamic, metabolic, and immune abnormalities. The primary reason for these defects is still unknown, but immune abnormalities are now considered to be the leading factors in the PH pathogenesis [1]. Low-grade systemic inflammation, including innate and adaptive immune response components, seems to play a role in the pathogenesis of PH [2]. It was found that the serum systemic inflammatory markers, including C-reactive protein, cytokines, and chemokines, are related mainly to metabolic abnormalities and oxidative stress components or even to target organ damage (TOD) but are rather weakly associated with blood pressure elevation per se [3]. Recently we found that peripheral blood leukocytes (PBLs) of PH children showed an upregulation of renin-angiotensin system (RAS) genes [4]. These observations, as well as other results, may indicate that leukocyte activation profiles are much more related to blood pressure elevation than the serum acute phase response components. The reason of this phenomenon is currently unclear, but its presence may suggest that human PH is related to some alterations in leukocyte functions, as it has previously been suggested in animal models [5]. We previously reported that the PH children serum adiponectin levels correlated negatively with increased carotid intima-media thickness [6, 7]. Here we hypothesized that the PH

children PBLs adiponectin receptors (AdipoRs) expression profile might be related to a stage of arterial hypertension and TOD. We found here that upregulation of AdipoRs expression in the PH children leukocytes (neutrophils) was associated with both blood pressure elevation and TOD increase. This is a novel finding suggesting an engagement of the innate immune system in the development and maintenance of PH in children.

2. Patients and Methods

The study has been conducted according to the Declaration of Helsinki and with the approval of the Ethics Committee. All patients and parents gave consent to participate in the study. Out of 122 consecutively referred pediatric patients with newly diagnosed primary hypertension (PH), 57 children (43 boys), in mean age 15.0 ± 2.6 years, who underwent all laboratory procedures, were included in the study. The exclusion criteria were the presence of any significant chronic disease (except for PH), including diabetes and chronic kidney disease, any acute illness, including infections in the 6 weeks preceding enrollment, and incomplete data. Arterial hypertension was diagnosed according to the 4th Task Force Report and confirmed by 24-hour ambulatory blood pressure monitoring (ABPM) [8]. PH was diagnosed after exclusion of secondary hypertension according to guidelines. Blood pressure status was defined according to ABPM classification [9]. All hypertensive children underwent full protocol of assessment of TOD and biochemical investigations. The control group consisted of 19 (10 boys) healthy children, mean age 13.9 ± 3.5 years.

2.1. Anthropometric Measurements. Body mass index (BMI) and waist circumference (WC) were expressed as absolute values and as standard deviation scores (SDS), from the median of the norm. Current reference normative values of anthropometrical parameters for Polish population have been used to calculate SDS values [10].

2.2. Assessment of Target Organ Damage (TOD). TOD was assessed using left ventricular mass index (LVMi), common carotid artery intima-media thickness (cIMT), and carotid wall cross-sectional area (WCSA).

2.3. Echocardiography. All echocardiographic (ECHO) examinations were performed by one examiner, who knew the clinical diagnosis but was unaware of the severity of hypertension and the effectiveness of treatment. ECHO measurements were performed according to the American Society of Echocardiography guidelines. To standardize the left ventricular mass to height, LVMi was calculated according to the de Simone formula [11]. Left ventricular hypertrophy (LVH) was defined as an LVMi value above the 95th percentile for age and gender, based on the reference data, and severe LVH as LVMi equal to or greater than 51 g/m$^{2.7}$ [12].

2.4. IMT Measurements. cIMT was evaluated by ultrasound technique, according to the previously described methodology [13, 14]. Mean wall cross-sectional area of the carotid artery (WCSA) was calculated from the equation WCSA = π(dD/2 + IMT)2 − π(dD/2)2, where dD is the mean diastolic diameter and sD is the mean systolic diameter. Mean and standard deviation (SD) of normal values for cIMT and WCSA were taken from recently published normative data of cIMT for age- and sex-matched healthy children [13].

2.5. Laboratory Investigations. Blood samples were taken after 12 h of fasting. Lipid profile, serum uric acid (UA), and high sensitive C-reactive protein (hsCRP) were assessed in all patients. The hsCRP concentration was determined using highly sensitive immunoturbidimetry (Orion Diagnostica).

2.6. Immunoassays. Circulating levels of serum mediators were measured by means of commercially available ELISA kits: DuoSet, R&D Systems (MMP-9, TIMP-1, sCD14), DRG International Inc. (adiponectin, leptin), and BD Bioscience (IL-12p70, IL-1beta, and TNF-alpha), according to the manufacturer's instructions. Before performing the tests, the serum samples were diluted according to each kit's protocol and the final results were obtained by appropriate multiplication. The protein level in the diluted sample was calculated from a reference curve generated for a given assay by using reference standards containing known concentrations of appropriate protein. Results were expressed as nanograms or picograms per mL. Values below detection limit were considered as 0 [15, 16].

2.7. Assessment of Leukocyte Adiponectin Receptor Expression by Flow Cytometry. The leukocyte adiponectin receptor expressions (AdipoR1 and AdipoR2) were determined in heparin-collected whole blood samples with the use of direct and indirect three-color flow cytometry. First, the blood samples were washed with PBS, and 100 μL of blood was incubated with primary, unstained antibodies: goat anti-human AdipoR1 and goat anti-human AdipoR2 (Santa Cruz Biotechnology Inc.) in two independent tubes. The blood samples were then washed with washing buffer, preincubated with donkey serum to avoid nonspecific binding, and stained with donkey anti-goat FITC-conjugated secondary antibodies (Santa Cruz Biotechnology Inc.). The erythrocytes were removed with the use of BD Bioscience FACS lysing solution. The stained leukocytes were suspended in cold PBS and analyzed immediately with flow cytometry (BD FACSCan). The cells stained solely with secondary antibody were used as negative control (isotype control) [17, 18]. For the leukocyte phenotype analysis, a gate was set on the neutrophil and monocyte by means of both the morphological features (a forward scatter FS versus 90° light scatter-side scatter SS) and the fluorescence characteristics of the cells labeled with phycoerythrin- (PE-) coupled anti-CD16 (neutrophils) and Peridinin Chlorophyll Protein Complex- (PerCP-) coupled anti-CD14 (monocytes) (BD Biosciences) as gating parameters. A histogram of log green fluorescence of each adiponectin receptor was used for the determination

of the percentage of positive cells (%) and the mean fluorescence intensity (MFI) of each sample. The background fluorescence level for each specimen was established using the isotype control. The cells with AdipoRs fluorescence expression levels higher than those of the isotype controls were counted as positive: here as AdipoR(+). Accordingly, the cells with AdipoRs fluorescence expression levels lower than those of isotype controls were described here as AdipoRs(−). Autocomp using Calibrite beads (BD Biosciences) was used to standardize instrument electronics. Data acquisition was performed using the BD CellQuest Pro software (BD Biosciences) and the analysis with FlowJo 7.5.5 (Tree Star Inc.).

2.8. RNA Isolation and Real Time PCR Technique. PBLs were isolated from venous blood by means of Histopaque (Sigma-Aldrich 1119) gradient centrifugation. Total RNA was isolated with Chomczyński method using Trizol Reagent (Invitrogen), as described previously [4, 19]. RNA sample concentration was determined spectrophotometrically at 260 nm, and the purity was confirmed by 260/280 ratio. One microgram of total RNA for each sample was converted into cDNA in the Reverse Transcription Polymerase Chain Reaction (RT-PCR) by using Taq Man Reverse Transcription Reagents. Quantitative RT-PCR (real time PCR) for *ADIPOR1* target gene and endogenous control (reference gene) glyceraldehydes-3-phosphate dehydrogenase (G3PDH) were performed on Viia 7 Real Time System, according to the manufacturer's recommendation. For one reaction, 50 ng of cDNA with SYBR Green PCR Master Mix and 10 nmol/L of each of the forward and reverse primers [*ADIPOR1* F: ACA AGG TCT GGG AGG GAC GT; *ADIPOR1* R: CAT GGG AGG TCT ATG ACC ATG; *G3PDH* F: GCG GGG CTC TCC AGA ACA TCA T; *G3PDH* R: CCA GCC CCA GCG TCA AAG GTG] were applied, and analysis of each sample was performed at least in duplicate. The specificity of the amplification reaction was verified by analyzing the melting curve. The gene expression level was expressed as fold change of target gene expression according to basic level (=1) of the same gene expression in the control group's leukocytes, after normalization by expression of the reference gene G3PDH, by using Pfaffl's mathematical model, as previously described [4, 20]. All reagents, equipment, and other supplies for Q-PCR technique were provided by Applied Biosystems (now Life Technologies).

2.9. Statistical Analysis. Statistical analysis was performed using Statistica (StatSoft, Inc., 2011, STATISTICA, version 10.0, http://www.statsoft.com/). Normal distribution of the analyzed variables was tested with Kolmogorov-Smirnov test with Lilliefors correction. The t-test for independent measures and chi-square test were used for intergroup comparisons of continuous and categorical variables, respectively. Comparisons between groups presenting with different clinical stages were performed by using a generalized regression model (GRM), while linear regression analysis (Pearson's or Spearman's, depending on variable distribution) was performed to assess the relationship between continuous variables. In all analyses, $P < 0.05$ was considered as statistically significant. A probability value ranging between 0.05 and 0.1 was regarded as a statistical tendency. The results are depicted in the graphs in the form of mean values and their standard deviations.

3. Results

3.1. Assessment of Adiponectin Receptor Expression on Peripheral Blood Leukocytes. The group of 26 patients (45%) showed very low neutrophil and monocyte surface AdipoR1 and AdipoR2 expression levels (AdipoR(−)), both in terms of the percentage of positive cells and receptor density (MFI).

In contrast, the other 31 patients (55%) showed a significantly greater proportion of AdipoR positive leukocytes (AdipoR(+)) than the AdipoR(−) ones and the controls ($P < 0.01$ for neutrophils, $P < 0.05$ for monocytes) (Figures 1(a)–1(d)). This distribution profile was dependent on neutrophils but not monocytes. As much as 29% and 48% of hypertensive children versus 16% and 21% of control had elevated proportion of AdipoR1 and AdipoR2 bearing neutrophils, respectively. In contrast, the percentage of patients having AdipoR1^{high} and AipoR2^{high} monocytes (25% and 30%, resp.) did not differ from that of control (26% and 21%, resp.).

The percentage of AdipoRs on neutrophils correlated with the proportion of AdipoR positive monocytes ($r = 0.6211$, $P < 0.0001$ for AdipoR1 and $r = 0.6041$, $P < 0.0001$ for AdipoR2). Both AdipoRs were correlated with each other ($r = 0.8603$, $P < 0.001$ for AdipoR1 versus AdipoR2 in neutrophils, and $r = 0.909$, $P < 0.001$ for AdipoR1 versus AdipoR2 in monocytes) (Figures 1(e)–1(h)).

Patients from AdipoR(−) and AdipoR(+) groups did not differ in terms of BMI and WC (Table 1). There were no statistical differences in the AdipoR1 and AdipoR2 leukocyte expression profiles between female and male patients ($P > 0.05$).

The leukocytes from AdipoR(+) patients showed significantly higher total leukocyte AdipoR1 mRNA levels than those from AdipoR(−) patients or from the controls ($P = 0.022$ and $P = 0.007$, resp.) (Figure 2(a)). AdipoR1 mRNA expression correlated positively solely with the percentage of AdipoR1-bearing neutrophils, but not monocytes ($r = 0.373$, $P = 0.005$) (Figure 2(c)).

3.2. Serum Parameters Distribution in the AdipoR(−) and AdipoR(+) Patients. AdipoR(+) patients had significantly lower adiponectin concentrations (6.0 ± 1.9 μg/mL), as compared to AdipoR(−) patients (9.2 ± 3.8 μg/mL) and controls (10.3 ± 2.9 μg/mL) ($P = 0.0029$ and $P < 0.001$, resp.) (Figure 2(b)). Serum adiponectin levels correlated inversely with AdipoR-bearing neutrophil, but not monocyte or leukocyte AdipoR1 mRNA expression ($r = -0.406$, $P = 0.006$) (Figure 2(d)).

AdipoR(+) patients had slightly, albeit significantly, lower sCD14 concentration (779.4 ± 174.1 ng/mL) than the AdipoR(−) ones (885.4 ± 304.2 ng/mL) and controls (998.5 ± 152.3 ng/mL) ($P < 0.01$, Table 1). sCD14 levels were inversely related to neutrophil and monocyte AdipoR protein expressions (Table 2) and tended to correlate positively with adiponectin levels ($r = 0.318$, $P = 0.08$).

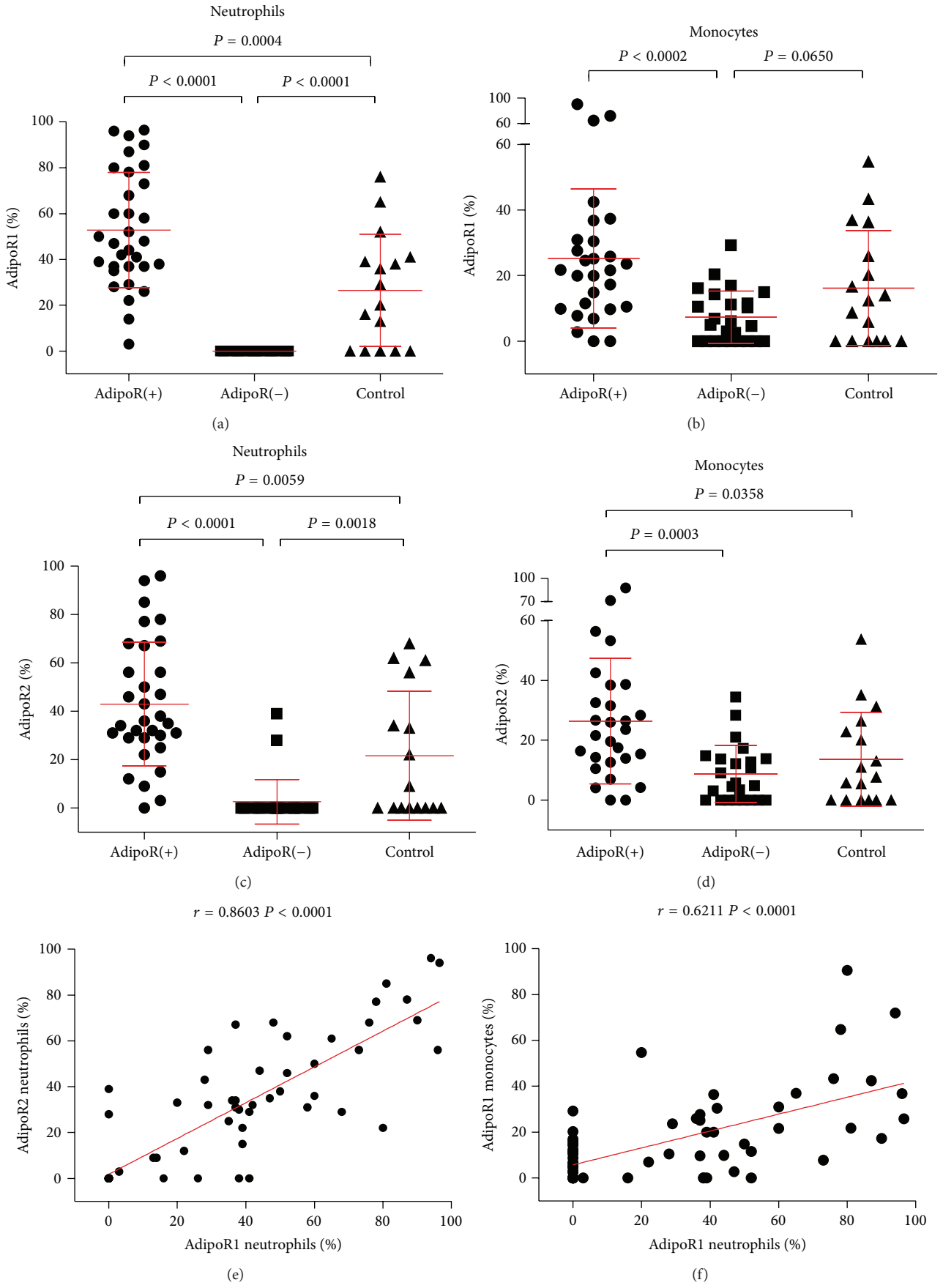

Figure 1: Continued.

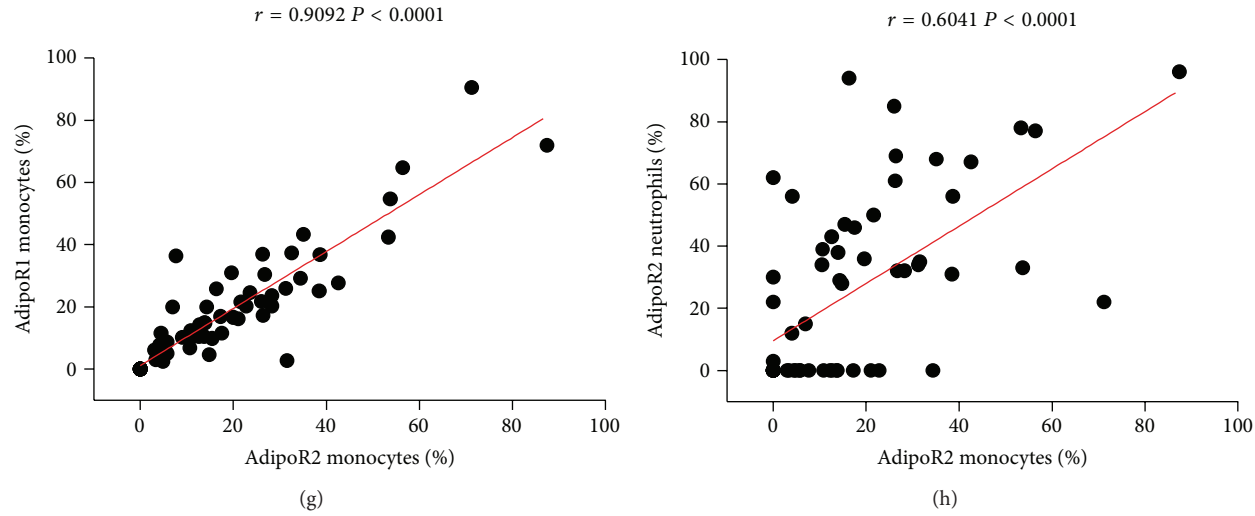

Figure 1: Expression and correlations of AdipoR on neutrophils and monocytes in PH children and normotensive control. The summary of analyses of AdipoR1 and AdipoR2 expression in neutrophils and monocytes in PH children (AdipoR(+) and AdipoR(−)) and normotensive control. (a) Percentage of neutrophils showing AdipoR1 receptor expression (AdipoR1%). (b) Mean levels of AdipoR1 receptor expression (AdipoR1%) in monocytes. (c) Percentage of neutrophils showing AdipoR2 receptor expression (AdipoR2%). (d) Mean levels of AdipoR2 receptor expression (AdipoR2%) in monocytes. All results (a–d) presented as means ± SD. AdipoR(+), $n = 31$, AdipoR(−), $n = 26$, controls, $n = 19$. (e) Correlations between AdipoR1 and AdipoR2 surface expression levels in neutrophils. (f) Correlations between the percentage of AdipoR1-positive neutrophils and AdipoR1-positive monocytes. (g) Correlations between the percentage of monocytes showing expression of AdipoR1 and AdipoR2. (h) Correlations between the percentage of AdipoR2-positive neutrophils and AdipoR2-positive monocytes.

The serum concentrations of leptin, sCRP, MMP-9, TIMP1, IL-12p70, and IL-1 beta did not correlate with leukocyte AdipoR expression profile, on either protein or mRNA levels (data not shown).

3.3. Relation of Clinical Variables and Target Organ Damage Markers to Leukocyte AdipoR Expression Profiles. The AdipoR(+) patients had significantly higher mean 24-hour systolic blood pressure and higher cIMT values than the AdipoR(−) patients (Table 1). Furthermore, neutrophil AdipoR1 mean fluorescence intensity (MFI) values positively correlated with the 24-hour SBP values ($r = 0.26$, $P = 0.045$), and the proportions of AdipoR2 bearing neutrophils were related to 24-hour DBP ($r = 0.28$, $P = 0.043$). Disease severity, as assessed by the stage of hypertension, was related to neutrophil but not monocyte AdipoR upregulation. The stage of hypertension (according to ABPM blood pressure classification) was associated with increased neutrophil AdipoR1 fluorescence intensity (AdipoR1 MFI) ($P < 0.05$) (Figure 3(c)).

Severe ambulatory hypertension also presented more often in patients with high AdipoR expression, as compared to the AdipoR(−) ones (51.6% versus 26.9%, resp.; $P < 0.01$). The neutrophil AdipoR1 and AdipoR2 protein expression profiles were not associated with anthropometric data, such as the age, body height, body weight, or BMI. In striking contrast, the monocyte AdipoR protein expression (MFI), as well as total leukocyte AdipoR1 mRNA, was both inversely related to the anthropometric parameters (Table 2), as well as to adiponectin levels ($r = -0.297$, $r = -0.484$, $r = -0.445$, and $r = -0.335$, resp., $P < 0.05$). Furthermore, LVMI did not differ between the patient groups (Table 1) but also correlated negatively with the monocyte but not neutrophil, AdipoR MFI (Table 2).

4. Discussion

The analysis of PBL gene expression pattern proved to be useful to describe intermediate phenotype of the hypertensive disorder. There is a high gene expression concordance rate (over 80%) between PBLs and other tissues, both in humans and other species [21]. Leukocytes continuously interact with virtually every tissue and organ in the body and thus their gene and surface receptor expression profiles may serve as early markers of many abnormalities [22]. Moreover, leukocytes are important mediators of TOD in animals with experimentally induced hypertension [1, 23, 24].

The AdipoR1 and AdipoR2 protein expression levels were the highest in monocytes and neutrophils, but they were relatively low in lymphocytes (not shown). These data are consistent with the results published by Pang and Narendran [18] and Rossi and Lord [25]. We found that neutrophil and monocyte AdipoRs protein expression levels were closely related to each other and to total leukocyte AdipoR1 mRNA. However, the PBLs of PH children showed either high (AdipoRs(+) patients) or low AdipoR expression (AdipoR(−) patients) profiles, which were strictly related to different disease severity and TOD. Only AdipoR(+) patients presented with increased cIMT and had severe ambulatory hypertension, alongside low serum adiponectin concentrations. Strikingly, neutrophil (but not monocyte) AdipoR protein expression levels (MFI) were negatively related to serum

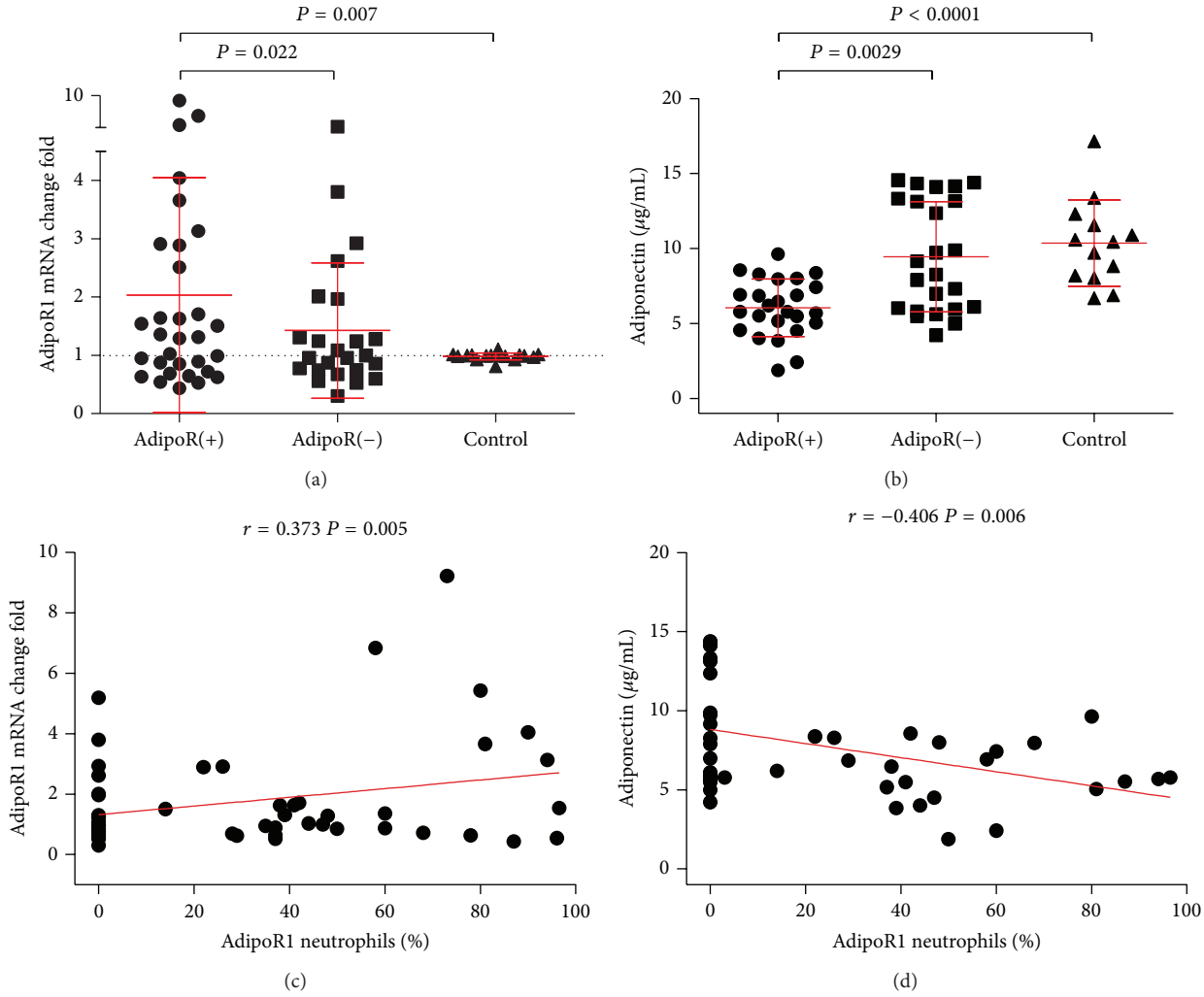

FIGURE 2: AdipoR1 mRNA expression in leukocytes and the serum adiponectin concentration in PH children and normotensive controls. (a) AdipoR1 gene expression levels (AdipoR1 mRNA). Results presented as means ± SD; AdipoR(+), $n = 31$, AdipoR(−), $n = 16$, controls, $n = 24$. (b) Serum adiponectin levels. Results presented as means ± SD; AdipoR(+), $n = 25$, AdipoR(−), $n = 25$, control, $n = 13$. (c) Correlations between the percentage of neutrophils showing expression of AdipoR1 and AdipoR1 mRNA leukocyte expression. (d) Correlations between the percentage of AdipoR1-positive neutrophils and serum adiponectin concentrations.

adiponectin concentrations but positively related to the severity of hypertension. These changes occurred independently of other studied systemic factors, including biochemical, anthropometric, and immune parameters.

In contrast to neutrophil, monocyte AdipoR expression levels (expressed as MFI), as well as total AdipoR1 mRNA, turned out to be independent of serum adiponectin concentrations but showed negative correlations with some serum immune mediators (sCD14, TNF-alpha), anthropometric parameters (body mass, BMI, WC), and LMVI (Table 2).

Altogether, these data suggest that neutrophil AdipoR upregulation in conditions of low adiponectin levels is related to vascular changes (described hereby as increased cIMT) and disease severity. The involvement of neutrophils in the pathogenesis of PH and vascular changes has long been postulated. Hypertensive adult patients exhibit several alterations in neutrophil characteristics, including an increased neutrophil count [26] and activated neutrophil functions, such as upregulation of CD11b and rapid release of neutrophil primary granules (CD69 expression) on short incubation with PBS or TPA [27]. Similarly, PBLs from PH children have been revealed to show an altered expression of inflammatory molecules and elements of renin-angiotensin system. This altered pattern of gene expression changed during nonpharmacological treatment [4].

Our study showed that different neutrophil AdipoR expression profiles were associated with hypertension severity and subclinical arterial injury. Neutrophils normally show AdipoR expression levels that are equal to those of monocytes, as found also in our present study, and both of them react with adiponectin [25]. Adiponectin has been shown to modulate both neutrophil phenotype and functions, but its significance in the PH development remains unknown. Adiponectin exerts a variety of effects related to neutrophil

Table 1: Comparison of demographic, anthropometric, and laboratory data in control group and AdipoR(+) and AdipoR(−) group of hypertensive children.

Variables	Control ($n = 19$)	Group of hypertensive children		
		AdipoR(+) ($n = 31$)	AdipoR(−) ($n = 26$)	P Value AdipoR(+) *versus* AdipoR(−)
Age (years)	13.9 ± 3.5	15.0 ± 2.6	15.0 ± 2.6	0.964
Growth, cm	157.8 ± 22.9	170.7 ± 14.8†	167 ± 13.8	0.383
Weight, kg	55.1 ± 21.8	75.5 ± 17.9†	72.5 ± 20.5‡	0.570
BMI	21.0 ± 4.3	25.6 ± 4.3†	25.5 ± 4.6‡	0.896
BMI-SDS	0.5 ± 1.0	1.3 ± 0.8†	1.3 ± 0.9‡	0.942
Waist circumference, cm	68.8 ± 8.5	82.7 ± 8.3†	83.6 ± 12.9‡	0.782
Waist circumference SDS	0.7 ± 0.6	1.4 ± 0.7	1.3 ± 1.1	0.690
24 h SBP, mm Hg	110.3 ± 14.4	130.5 ± 8.7†	125 ± 9.4‡	0.042*
24 h DBP, mm Hg	62.7 ± 5.5	73.0 ± 5.7†	71.1 ± 6.1‡	0.225
24 h MAP, mm Hg	88.6 ± 9.8	92.3 ± 5.9	89.4 ± 5.9	0.073
24 h heart rate, beats/min	75.1 ± 13.8	78.0 ± 14.1	79.1 ± 13.4	0.740
Left ventricular mass index, g/m$^{2.7}$	28.2 ± 5.8	32.7 ± 6.5	34.5 ± 8.9	0.383
Carotid intima-media thickness, m	0.42 ± 0.03	0.45 ± 0.04	0.42 ± 0.04	0.017*
Carotid intima-media thickness Z-score	0.7 ± 0.7	1.57 ± 1.2	1.04 ± 1.0	0.073
Carotid wall cross-sectional area, mm^2	6.8 ± 0.9	8.0 ± 1.5†	7.5 ± 1.4	0.092
Total cholesterol, mg/DL	178.6 ± 28.3	171.8 ± 35.1	174.5 ± 30.3	0.760
HDL cholesterol, mg/dL	53.4 ± 19.8	50.9 ± 13.9	51.4 ± 13.8	0.890
LDL cholesterol, mg/dL	109.0 ± 24.7	96.7 ± 29.4	101.9 ± 25.0	0.471
Triglycerides, mg/dL	85.9 ± 42.0	127.2 ± 79.3	111.7 ± 50.5	0.389
Uric acid mg/dL	5.1 ± 0.9	6.0 ± 1.4	5.8 ± 1.2	0.457
hsCRP, mg/L	0.2 ± 0.08	0.32 ± 0.2	0.28 ± 0.1	0.488
sCD14 ng/mL	998.5 ± 152.3	779.4 ± 174.1†	885.4 ± 304.1	0.008*

Results presented as mean ± SD. BMI indicates body mass index; DBP, diastolic blood pressure; HDL, high-density lipoprotein, hsCRP, high sensitivity C-reactive protein; LDL, low-density lipoprotein; MAP, mean arterial pressure; SBP, systolic blood pressure. Statistically significant differences are given as follows: *AdipoR(+) *versus* AdipoR(−), †AdipoR(+) *versus* control, ‡AdipoR(−) *versus* control, $P < 0.05$ is considered significant.

Table 2: Correlation of adiponectin receptors and AdipoR1 mRNA with selected cytokines and anthropometric parameters and LVMI.

	Neutrophils				Monocytes				
	AdipoR1		AdipoR2		AdipoR1		AdipoR2		AdipoR1 mRNA
	r [%]	r [MFI]	r [%]	r [MFI]	r [%]	r [MFI]	r [%]	r [MFI]	
sCD14	−0.257*	−0.307*	−0.339*	−0.384*	−0.289*	−0.342*	−0.291*	−0.429*	−0.050
Body mass	0.012	0.032	0.069	0.023	−0.043	−0.300*	−0.044	−0.333*	−0.298*
BMI	0.019	0.020	0.009	−0.030	0.075	−0.349*	0.017	−0.371*	−0.079
WC	−0.095	−0.063	−0.099	−0.106	−0.017	−0.336*	−0.092	−0.365*	−0.370*
LVMI	−0.023	−0.039	−0.116	−0.065	−0.197	−0.314*	−0.189	−0.331*	−0.067

AdipoR indicates adiponectin receptor, BMI, body mass index; WC, waist circumference, and LVMI, left ventricular hypertrophy. $^{*}P < 0.05$ is considered significant.

biology, including (a) inhibition of *E. coli* phagocytosis by suppression of PKB and ERK1/2 MAPK signaling pathways, and Mac-1 activation [25], (b) suppression of reactive oxygen species formation by inhibition of NADPH oxidase activation [28], (c) increase in neutrophil survival rate by inhibition of their apoptosis via activation of AMPK, PI3K/PKB, and ERK pathways, stabilization of antiapoptotic Mcl-1 molecule, and reduction of cell membrane ceramide accumulation [29], (d) downregulation of granulopoiesis by suppression of GM colony formation [30], and (e) acting as growth factor for hematopoietic stem cells [31].

In the steady state, serum adiponectin levels are rather low, but its receptor expression levels are higher in PBLs of obese people than in the control subjects, possibly due to alterations in insulin levels and insulin sensitivity [32]. Adiponectin increases insulin sensitivity, but insulin down-regulates both AdipoR expression (especially AdipoR1) and insulin sensitivity [33]. In conditions of insulin deficiency

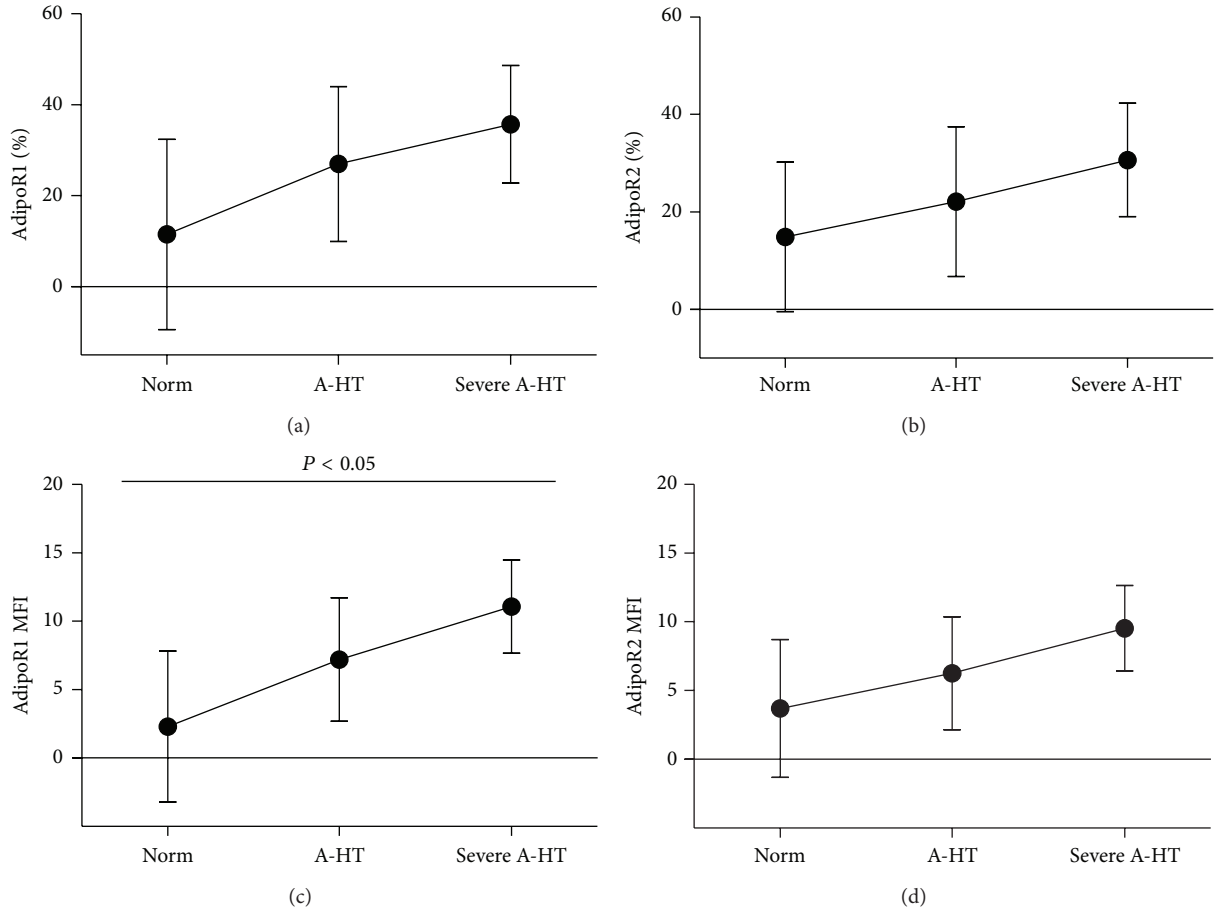

Figure 3: Expression of adiponectin receptors in neutrophils and stage of hypertension. Results presented as means ± SD. A-HT, ambulatory hypertension; (a) AdipoR1% and (b) AdipoR2%, percentage of neutrophils showing expression of adiponectin receptors; (c) AdipoR1 MFI and (d) AdipoR2 MFI, mean density of adiponectin receptors on the surface of neutrophils expressed as mean fluorescence intensity of positive cells.

(like in type 1 diabetes) AdipoR expression is high, but serum adiponectin levels are also elevated [34]. Furthermore, increased serum adiponectin level has been associated with higher all-cause mortality in type 1 diabetes patients [35]. On the other hand, reduced or low serum adiponectin levels have long been linked to metabolic syndrome components, such as visceral obesity and insulin resistance [36], and PH children with low serum adiponectin concentrations had increased cIMT [6, 7]. Our study showed that greater expression of AdipoRs on PBLs was associated with low serum adiponectin levels, blood pressure elevation, and increased cIMT. However, it is difficult to distinguish if increased cIMT results from lower adiponectin concentrations or higher blood pressure. Our findings are consistent with the previous reports indicating that hypoadiponectinemia is a strong predictor of future hypertension, even after adjusting for the confounding systemic factors, such as mean blood pressure, C-reactive protein, BMI, and WC [37]. In fact, these factors were not associated with neutrophil AdipoR upregulations in our patients. This suggests that other, probably genetic, factors control both neutrophil AdipoR expression profile and adiponectin levels.

In contrast to neutrophils, AdipoR expression on monocytes did not correlate with hypertension severity, expressed here as cIMT values and blood pressure elevation. Furthermore, we found inverse correlation between monocyte AdipoR expression level and LVMI. This finding corresponds with the recent report on the role of neutrophils, but not monocytes, in the left ventricular hypertrophy caused by angiotensin II infusion in mice [23].

Monocyte AdipoR expression profiles have been shown to be related to coronary artery disease (CAD) progression in adult patients, in whom AdipoR mRNA and protein upregulation correlated with arterial stiffness and cIMT. However, contrary to our results, AdipoR upregulation was positively related to systemic low-grade inflammation markers (increase in serum MMP-9 and CRP levels) and elevation of serum adiponectin concentration [22, 38, 39]. Furthermore, serum adiponectin levels, monocyte AdipoR expression, and adiponectin-induced synthesis of IL-10 by monocytes were downregulated in the overweight CAD patients, as compared to overweight patients without CAD [39]. Altogether, these data point to a protective role of AdipoR monocyte expression in CAD patients.

In contrast to the abovementioned adults with clinically evident cardiovascular disease, the PH children present the earliest stage of the pathological process. Thus, increased neutrophil, but not monocyte, AdipoR expression that was related to low serum adiponectin, may reflect the first phase of arterial disease (increased cIMT and blood pressure) that occurs without other systemic inflammatory effects. Moreover, PH is not the same as atherosclerosis and CAD which are distinct clinical entities although they may share common risk factors with PH. Some discrepancies may also be explained in terms of the technical differences. We tested AdipoR expression in whole blood leukocytes with flow cytometry (in the cells gated as monocytes and neutrophils) and with RT-PCR (total leukocyte AdipoR1 mRNA). In contrast, the authors mentioned above used PBMC (flow cytometry) and monocyte AdipoR1/2 mRNA. The isolation procedure may change both distribution of leukocyte subpopulations and their activation state, thus altering the profile of AdipoR expression.

We found a slight, albeit significant, increase in serum sCD14 levels (in the AdipoR(−) patients) that were inversely related to neutrophil and monocyte AdipoR expression and tended to correlate positively with serum adiponectin concentrations. These findings may suggest that lipopolysaccharides (LPS) (often present in obese individuals) of the AdipoR(−) patients can be bound by sCD14, transferred to HDL serum fraction and subsequently inactivated. Thus, CD14- and toll-like receptor-dependent inflammatory reactions are limited [40–42]. This effect may eventually be facilitated by adiponectin [43] and sCD14 can also limit the amount of LPS bound by monocytes, by increasing LPS efflux from these cells [44]. On the other hand, sCD14 elevation was reported to be associated with an increase in arterial stiffness in adult hypertensive patients [45]. Considering pro- or anti-inflammatory actions of sCD14 proteins, their significance in AdipoR- and adiponectin-controlled immune responses [41, 46] warrants further investigations.

5. Conclusion

To the best of our knowledge, there are no other data concerning the leukocyte AdipoR expression profiles in the onset of PH in children. We found that upregulation of neutrophil AdipoR expression was associated with early stages of vascular injury, hypertension severity, and low serum levels of adiponectin. These phenomena were not associated with involvement of systemic activities concerning immune, metabolic, and anthropometric parameters. Inverse associations between AdipoR expression profiles on neutrophils and monocytes and serum adiponectin concentrations are worth emphasizing. Our findings point to different roles of neutrophils and monocytes in the pathogenesis of PH and arterial injury; earlier activation of neutrophils may result in early vascular inflammation and subsequent monocyte involvement that is related to more systemic responses.

The main limitation of the study is its cross-sectional design. It does not allow assessing changes in AdipoR expression related to treatment. Similarly, it does not allow evaluating if treatment efficacy is associated with AdipoR expression. The other limitation is associated with measuring total adiponectin concentrations, rather than its different molecular forms. The strength of the study is recruitment of homogenous population of yet untreated hypertensive children without other cardiovascular risk factors, such as diabetes, smoking, and widespread atherosclerosis. Moreover, all children underwent full diagnostic approach with the assessment of hypertensive TOD. It allows the analysis of immune phenomena on the earliest phase of cardiovascular disease.

The results of our study give perspectives for further analysis of leukocyte-mediated, AdipoR-dependent immune reactions, and their role in the development of PH and hypertensive TOD. The relationship between insulin resistance and leukocyte AdipoR expression profiles still remains unclear. Also the effects of both nonpharmacological and pharmacological treatment on leukocyte AdipoR expression pattern were not studied. One may assume that different antihypertensive drugs may exert different effects on AdipoR expression profiles. Furthermore, the patients who differ in terms of AdipoR expression profiles may also differ in their responsiveness to pharmacological or nonpharmacological treatment. The other challenge is the analysis of different roles of neutrophils and monocytes in the pathogenesis of hypertensive TOD, especially in relation to absence or presence of AdipoRs in connection to other leukocyte phenotype characteristics, such as expression of ROS and apoptosis markers. The other issue is description of AdipoR patterns in relation to sex and ethnicity of PH children.

Abbreviations

TOD: Target organ damage
PBLs: Peripheral blood leukocytes.

Conflict of Interests

The authors declare that they have no conflict of interests.

Acknowledgments

The study was partly supported by a grant from the National Science Centre Poland 2011/01/B/NZ6/02661 and 2013/11/B/NZ4/03832.

References

[1] D. G. Harrison, T. J. Guzik, H. E. Lob et al., "Inflammation, immunity, and hypertension," *Hypertension*, vol. 57, no. 2, pp. 132–140, 2011.

[2] J. Zubcevic, H. Waki, M. K. Raizada, and J. F. R. Paton, "Autonomic-immune-vascular interaction: an emerging concept for neurogenic hypertension," *Hypertension*, vol. 57, no. 6, pp. 1026–1033, 2011.

[3] M. Litwin, J. Michałkiewicz, and L. Gackowska, "Primary hypertension in children and adolescents is an immunometabolic disease with hemodynamic consequences," *Current Hypertension Reports*, vol. 15, no. 4, pp. 331–339, 2013.

[4] M. Litwin, J. Michałkiewicz, J. Trojanek, A. Niemirska, A. Wierzbicka, and M. Szalecki, "Altered genes profile of renin-angiotensin system, immune system, and adipokines receptors in leukocytes of children with primary hypertension," *Hypertension*, vol. 61, no. 2, pp. 431–436, 2013.

[5] D. G. Harrison, P. J. Marvar, and J. M. Titze, "Vascular inflammatory cells in hypertension," *Frontiers in Physiology*, vol. 3, article 128, 2012.

[6] M. Litwin, J. Śladowska, J. Antoniewicz et al., "Metabolic abnormalities, insulin resistance, and metabolic syndrome in children with primary hypertension," *The American Journal of Hypertension*, vol. 20, no. 8, pp. 875–882, 2007.

[7] M. Litwin, J. Michałkiewicz, A. Niemirska et al., "Inflammatory activation in children with primary hypertension," *Pediatric Nephrology*, vol. 25, no. 9, pp. 1711–1718, 2010.

[8] National High Blood Pressure Education Program Working Group on High Blood Pressure in Children and Adolescents, "The fourth report on the diagnosis, evaluation, and treatment of high blood pressure in children and adolescents," *Pediatrics*, vol. 114, pp. 555–576, 2004.

[9] J. T. Flynn, S. R. Daniels, L. L. Hayman et al., "Update: ambulatory blood pressure monitoring in children and adolescents: a scientific statement from the American heart association," *Hypertension*, vol. 63, pp. 116–135, 2014.

[10] Z. Kulaga, M. Litwin, A. Grajda et al., "Normy rozwojowe wysokosci i masy ciała, wskaznika masy ciała, obwodu talii i cisnienia tetniczego dzieci i młodziezy w wieku 3–18 lat," *Standardy Medyczne*, vol. 10, pp. 3–12, 2013.

[11] G. de Simone, R. B. Devereux, S. R. Daniels, M. J. Koren, R. A. Meyer, and J. H. Laragh, "Effect of growth on variability of left ventricular mass: assessment of allometric signals in adults and children and their capacity to predict cardiovascular risk," *Journal of the American College of Cardiology*, vol. 25, no. 5, pp. 1056–1062, 1995.

[12] P. R. Khoury, M. Mitsnefes, S. R. Daniels, and T. R. Kimball, "Age-specific reference intervals for indexed left ventricular mass in children," *The Journal of the American Society of Echocardiography*, vol. 22, no. 6, pp. 709–714, 2009.

[13] A. Doyon, D. Kracht, A. K. Bayazit et al., "Carotid artery intima-media thickness and distensibility in children and adolescents: reference values and role of body dimensions," *Hypertension*, vol. 62, no. 3, pp. 550–556, 2013.

[14] C. Jourdan, E. Wühl, M. Litwin et al., "Normative values for intima-media thickness and distensibility of large arteries in healthy adolescents," *Journal of Hypertension*, vol. 23, no. 9, pp. 1707–1715, 2005.

[15] T. Morioka, M. Emoto, Y. Yamazaki et al., "Leptin is associated with vascular endothelial function in overweight patients with type 2 diabetes," *Cardiovascular Diabetology*, vol. 13, no. 1, article 10, 2014.

[16] V. A. Belo, D. C. Souza-Costa, M. R. Luizon et al., "Matrix metalloproteinase-9 genetic variations affect MMP-9 levels in obese children," *International Journal of Obesity*, vol. 36, no. 1, pp. 69–75, 2012.

[17] P. Restituto, I. Colina, J. J. Varo, and N. Varo, "Adiponectin diminishes platelet aggregation and sCD40L release. Potential role in the metabolic syndrome," *American Journal of Physiology—Endocrinology and Metabolism*, vol. 298, no. 5, pp. E1072–E1077, 2010.

[18] T. T. L. Pang and P. Narendran, "The distribution of adiponectin receptors on human peripheral blood mononuclear cells," *Annals of the New York Academy of Sciences*, vol. 1150, pp. 143–145, 2008.

[19] P. Chomczynski and N. Sacchi, "Single-step method of RNA isolation by acid guanidinium thiocyanate-phenol-chloroform extraction," *Analytical Biochemistry*, vol. 162, no. 1, pp. 156–159, 1987.

[20] M. W. Pfaffl, "A new mathematical model for relative quantification in real-time RT-PCR," *Nucleic Acids Research*, vol. 29, no. 9, article e45, 2001.

[21] C.-C. Liew, J. Ma, H.-C. Tang, R. Zheng, and A. A. Dempsey, "The peripheral blood transcriptome dynamically reflects system wide biology: a potential diagnostic tool," *Journal of Laboratory and Clinical Medicine*, vol. 147, no. 3, pp. 126–132, 2006.

[22] I. Halvatsiotis, P. C. Tsiotra, I. Ikonomidis et al., "Genetic variation in the adiponectin receptor 2 (*ADIPOR2*) gene is associated with coronary artery disease and increased ADIPOR2 expression in peripheral monocytes," *Cardiovascular Diabetology*, vol. 9, article 10, 2010.

[23] Y. Wu, Y. Li, C. Zhang et al., "S100a8/a9 released by $CD11b^{+}Gr1^{+}$ neutrophils activates cardiac fibroblasts to initiate angiotensin II-induced cardiac inflammation and injury," *Hypertension*, vol. 63, no. 6, pp. 1241–1250, 2014.

[24] P. J. Marvar, S. R. Thabet, T. J. Guzik et al., "Central and peripheral mechanisms of T-lymphocyte activation and vascular inflammation produced by angiotensin II-induced hypertension," *Circulation Research*, vol. 107, no. 2, pp. 263–270, 2010.

[25] A. Rossi and J. Lord, "Adiponectin inhibits neutrophil phagocytosis of *Escherichia coli* by inhibition of PKB and ERK 1/2 MAPK signalling and Mac-1 activation," *PLoS ONE*, vol. 8, no. 7, Article ID e69108, 2013.

[26] M. Madjid, I. Awan, J. T. Willerson, and S. W. Casscells, "Leukocyte count and coronary heart disease: implications for risk assessment," *Journal of the American College of Cardiology*, vol. 44, no. 10, pp. 1945–1956, 2004.

[27] N. J. M. Fardon, R. Wilkinson, and T. H. Thomas, "Rapid fusion of granules with neutrophil cell membranes in hypertensive patients may increase vascular damage," *The American Journal of Hypertension*, vol. 14, no. 9, pp. 927–933, 2001.

[28] P. Chedid, M. Hurtado-Nedelec, B. Marion-Gaber et al., "Adiponectin and its globular fragment differentially modulate the oxidative burst of primary human phagocytes," *American Journal of Pathology*, vol. 180, no. 2, pp. 682–692, 2012.

[29] A. Rossi and J. M. Lord, "Adiponectin inhibits neutrophil apoptosis via activation of AMP kinase, PKB and ERK 1/2 MAP kinase," *Apoptosis*, vol. 18, no. 12, pp. 1469–1480, 2013.

[30] L. J. A. Crawford, R. Peake, S. Price, T. C. M. Morris, and A. E. Irvine, "Adiponectin is produced by lymphocytes and is a negative regulator of granulopoiesis," *Journal of Leukocyte Biology*, vol. 88, no. 4, pp. 807–811, 2010.

[31] L. DiMascio, C. Voermans, M. Uqoezwa et al., "Identification of adiponectin as a novel hemopoietic stem cell growth factor," *Journal of Immunology*, vol. 178, no. 6, pp. 3511–3520, 2007.

[32] B. E. Wolfe, D. C. Jimerson, C. Orlova, and C. S. Mantzoros, "Effect of dieting on plasma leptin, soluble leptin receptor, adiponectin and resistin levels in healthy volunteers," *Clinical Endocrinology*, vol. 61, no. 3, pp. 332–338, 2004.

[33] A. Tsuchida, T. Yamauchi, Y. Ito et al., "Insulin/Foxo1 pathway regulates expression levels of adiponectin receptors and adiponectin sensitivity," *The Journal of Biological Chemistry*, vol. 279, no. 29, pp. 30817–30822, 2004.

[34] H. Leth, K. K. Andersen, J. Frystyk et al., "Elevated levels of high-molecular-weight adiponectin in type 1 diabetes," *Journal of Clinical Endocrinology and Metabolism*, vol. 93, no. 8, pp. 3186–3191, 2008.

[35] A. Jorsal, L. Tarnow, J. Frystyk et al., "Serum adiponectin predicts all-cause mortality and end stage renal disease in patients with type I diabetes and diabetic nephropathy," *Kidney International*, vol. 74, no. 5, pp. 649–654, 2008.

[36] M. Chandran, S. A. Phillips, T. Ciaraldi, and R. R. Henry, "Adiponectin: more than just another fat cell hormone?" *Diabetes Care*, vol. 26, no. 8, pp. 2442–2450, 2003.

[37] K. Ohashi, N. Ouchi, and Y. Matsuzawa, "Adiponectin and hypertension," *The American Journal of Hypertension*, vol. 24, no. 3, pp. 263–269, 2011.

[38] I. Ikonomidis, N. Kadoglou, P. C. Tsiotra et al., "Arterial stiffness is associated with increased monocyte expression of adiponectin receptor mRNA and protein in patients with coronary artery disease," *American Journal of Hypertension*, vol. 25, no. 7, pp. 746–755, 2012.

[39] A. Kollias, P. C. Tsiotra, I. Ikonomidis et al., "Adiponectin levels and expression of adiponectin receptors in isolated monocytes from overweight patients with coronary artery disease," *Cardiovascular Diabetology*, vol. 10, article 14, 2011.

[40] C. J. Vesy, R. L. Kitchens, G. Wolfbauer, J. J. Albers, and R. S. Munford, "Lipopolysaccharide-binding protein and phospholipid transfer protein release lipopolysaccharides from gram-negative bacterial membranes," *Infection and Immunity*, vol. 68, no. 5, pp. 2410–2417, 2000.

[41] J. M. Fernández-Real, S. P. del Pulgar, E. Luche et al., "CD14 modulates inflammation-driven insulin resistance," *Diabetes*, vol. 60, no. 8, pp. 2179–2186, 2011.

[42] V. K. Topkara, S. Evans, W. Zhang et al., "Therapeutic targeting of innate immunity in the failing heart," *Journal of Molecular and Cellular Cardiology*, vol. 51, no. 4, pp. 594–599, 2011.

[43] N. Yamaguchi, J. G. M. Argueta, Y. Masuhiro et al., "Adiponectin inhibits Toll-like receptor family-induced signaling," *FEBS Letters*, vol. 579, no. 30, pp. 6821–6826, 2005.

[44] R. L. Kitchens, P. A. Thompson, S. Viriyakosol, G. E. O'Keefe, and R. S. Munford, "Plasma CD14 decreases monocyte responses to LPS by transferring cell-bound LPS to plasma lipoproteins," *The Journal of Clinical Investigation*, vol. 108, no. 3, pp. 485–493, 2001.

[45] J. Amara, J. B. Ruidavets, B. D. Sollier et al., "Soluble CD14 and aortic stiffness in a population-based study," *Journal of Hypertension*, vol. 21, no. 10, pp. 1869–1877, 2003.

[46] D. L. Mann, "The emerging role of innate immunity in the heart and vascular system: for whom the cell tolls," *Circulation Research*, vol. 108, no. 9, pp. 1133–1145, 2011.

Hindawi Publishing Corporation
BioMed Research International
Volume 2015, Article ID 965271, 14 pages
http://dx.doi.org/10.1155/2015/965271

Research Article

Regulation of Angiogenic Functions by Angiopoietins through Calcium-Dependent Signaling Pathways

Irene Pafumi,[1] Annarita Favia,[1] Guido Gambara,[1,2] Francesca Papacci,[1] Elio Ziparo,[1] Fioretta Palombi,[1] and Antonio Filippini[1]

[1]*Department of Anatomy, Histology, Forensic Medicine and Orthopaedics, Unit of Histology and Medical Embryology, Sapienza University of Rome, 00161 Rome, Italy*
[2]*Institute of Vegetative Anatomy, Charité Universitätsmedizin, Neuromuscular Group, 10115 Berlin, Germany*

Correspondence should be addressed to Antonio Filippini; antonio.filippini@uniroma1.it

Received 19 December 2014; Revised 12 February 2015; Accepted 15 February 2015

Academic Editor: Jie-Hui Li

Angiopoietins are vascular factors essential for blood vessel assembly and correct organization and maturation. This study describes a novel calcium-dependent machinery activated through Angiopoietin-1/2-Tie receptor system in HUVECs monolayer. Both cytokines were found to elicit intracellular calcium mobilization. Targeting intracellular Ca^{2+} signaling, antagonizing IP_3 with 2-APB or cADPR with 8Br-cADPR, was found to modulate *in vitro* angiogenic responses to Angiopoietins in a specific way. 2-APB and 8Br-cADPR impaired the phosphorylation of AKT and FAK induced by Ang-1 and Ang-2. On the other hand, phosphorylation of ERK1/2 and p38, as well as cell proliferation, was not affected by either inhibitor. The ability of ECs to migrate following Angs stimulation, evaluated by "scratch assay," was reduced by either 2-APB or 8Br-cADPR following Ang-2 stimulation and only slightly affected by 2-APB in cells stimulated with Ang-1. These results identify a novel calcium-dependent machinery involved in the complex interplay regulating angiogenic processes showing that IP_3- and cADPR-induced Ca^{2+} release specifically regulates distinct Angs-mediated angiogenic steps.

1. Introduction

Angiogenesis is a complex remodeling process characterized by the sprouting of new blood vessels from preexisting ones, occurring mainly during embryonic development and in pathological processes such as cancer. During the early stages of this process, endothelial cells (ECs) are stimulated to form new capillaries by growth factors such as vascular endothelial growth factor (VEGF) and fibroblast growth factor (FGF). Angiopoietins (Angs) play a fundamental role in the subsequent maturation step, in which microvessels acquire a layer of mural cells, pericytes, and smooth muscle cells, which are critical for the development and maintenance of functional vasculature [1, 2]. Experimental evidence identifies the Angs and their Tie receptors as important regulators of tumor-induced angiogenesis and metastasis [3, 4]. So far, a major effort in the field of angiogenesis control has centered on the VEGF-VEGF receptor system [5, 6]. However, despite partial success, resistance to anti-VEGF therapy, resulting from a variety of mechanisms, remains a major obstacle [7–9]. The search for novel key downstream effectors as a possible common "signaling hub" between Angs and other known growth factors is therefore of potential significance in the perspective of angiogenesis control in cancer.

The Tie receptors and their Angiopoietin (Ang) ligands have been identified as the second vascular tissue-specific tyrosine kinase receptor system. Angs-Tie system is essential during embryonic vessel assembly and for the correct organization and maturation of newly formed vessels and functions as a key regulator of adult vascular homeostasis in the later stages of the angiogenic cascade. Thus, whereas VEGF signals promote initiating events in angiogenesis, such as ECs sprouting and proliferation, Ang-Tie signals appear to promote ECs survival and vascular assembly, stability, and maturation [10]. The best-characterized Angs are Angiopoietin-1 (Ang-1) and Angiopoietin-2 (Ang-2),

which are secreted glycoproteins with a dimeric structure and molecular weight of approximately 75 kDa [11] showing about 60% amino acid sequence homology. Ang-1 is expressed by smooth muscle cells and other perivascular cells and acts in a paracrine manner as agonist of the endothelial Tie-2 receptor, whereas Ang-2 is considered as its antagonist although also reported to context-dependently act as a Tie-2 agonist inducing receptor phosphorylation [12–14]. The molecular basis for agonistic versus antagonistic functions of Ang-2 has not been unraveled. Cell type specific effects, the degree of endothelial confluence, the duration of Ang-2 stimulation, concentration dependent effects, and the presence of the coreceptors such as Tie-1 have all been implicated in controlling agonistic versus antagonistic function of Ang-2 [15–18]. Ang-1 induces tyrosine phosphorylation of Tie-2 in ECs and activates downstream signaling pathways such as mitogen-activated protein kinase (MAPK) pathways. In adult tissues, Ang-1 does not induce endothelial chemotaxis or proliferation but exerts a dual role: it stimulates angiogenesis at sites of vascular remodeling contributing to the formation of capillary sprouts, while it stimulates prosurvival pathways and promotes vascular quiescence in mature vessels, preventing apoptosis and inflammation through the activation of PI3K-AKT and MAPK/ERK signaling pathways [19–21]. Ang-2 is almost exclusively expressed by ECs where it is stored in Weibel-Palade bodies (WPB) [22, 23]. Following cytokine activation of the endothelium, Ang-2 is rapidly released and acts in an autocrine manner on Tie-2 receptor binding as homodimers or multimers. Under physiological conditions, in the adult tissues Ang-2 is expressed in regions of vascular remodelling, during vascularization of the retina or during vessel formation/regression of ovarian corpus luteum. Ang-2 expression is also upregulated under pathological conditions, for example, in the endothelium of tumors [24–26]. Interestingly, experimental evidence indicates that signaling downstream of Tie-2 activation is influenced by the subcellular localization of the receptor, which is different in confluent versus sparse ECs [1, 27]. In these studies, Ang-1 produced stronger AKT signaling in confluent cells, in which Tie-2 was localized at cell/cell junctions, and stronger ERK activation when cells were sparse and Tie-2 was localized at cell/matrix junction, indicating that the effect of Ang-1 on Tie-2 activation may depend on the nature of cell/cell or cell/matrix contacts. Less well known is the role of calcium (Ca^{2+}) in the regulation of angiogenic processes. Ca^{2+} is a crucial point of intersection for many distinct molecular signaling pathways that promote and modulate angiogenesis. Specific Ca^{2+} signatures rely upon spatiotemporal variations in $[Ca^{2+}]_i$ [28] and are mainly based on three second messengers, namely, inositol trisphosphate (IP_3) and cyclic adenosine diphosphoribose (cADPR), which mobilize Ca^{2+} from endoplasmic reticulum (ER) stores, and nicotinic acid adenine-dinucleotide phosphate (NAADP), which triggers Ca^{2+} release from acidic organelles [29, 30]. We have previously demonstrated that histamine H1 receptors mediate NAADP-dependent Ca^{2+} signaling in ECs [31] and have recently identified that in HUVECs (human umbilical vein endothelial cells) VEGF increases $[Ca^{2+}]_i$ by mobilizing Ca^{2+} from internal stores. The latter study demonstrated the direct role of NAADP in VEGF-induced Ca^{2+} mobilization from acidic organelles and its important involvement in the control of angiogenic processes [32]. To our knowledge, the role of Ca^{2+} signaling in the regulation of Ang-1/Ang-2-induced angiogenesis has not been investigated yet. In the present work, we identify a novel pathway for Angs-Tie signaling whereby receptor activation leads to IP_3- and cADPR-dependent Ca^{2+} release and show that each of these Ca^{2+} mobilizing second messengers specifically controls distinct Angs-mediated angiogenic steps.

2. Materials and Methods

2.1. Cell Culture. Human umbilical vein endothelial cells (HUVECs) were obtained from Lonza Sales Ltd., cultured in EGM-2 Endothelial Cell Growth Medium-2 (Endothelial Basal Medium EBM-2 + EGM-2 Bullet Kit, Lonza), + 100 mM penicillin/streptomycin (Sigma). Cells were maintained at 37°C in a humified 5% (vol/vol) incubator and grown to reach the confluence. Monolayers were used at passages 1 to 6.

2.2. Calcium Imaging. Cells were incubated in EGM-2 containing 3.5 μM Fura-2-AM (Invitrogen) for 1 h at 37°C and then rinsed with Hanks' Balanced Salt Solution (HBSS Sigma) or Krebs-Henseleit-HEPES (KHH) buffer (140 mM Na^+, 5.3 mM K^+, 132.4 mM Cl^-, 0.98 mM PO_4^{2-}, 1.25 mM Ca^{2+}, 0.81 mM Mg^{2+}, 5.5 mM glucose, and 20 mM HEPES). Plates were placed into a culture chamber kept at 37°C controlled temperature on the stage of an inverted microfluorimeter (Nikon TE2000E) connected to a cooled CCD camera (512B Cascade, Princeton Instruments). Samples were illuminated alternately at 340 and 380 nm using a random access monochromator (Photon Technology International) and emission was detected using a 510 nm emission filter. Images were acquired (1 image/sec ratio) using MetaFluor software (Universal Imaging Corporation). Calibration of the signal was obtained at the end of each experiment by maximally increasing intracellular Ca^{2+}-dependent Fura-2-AM fluorescence with 5 μM ionomycin (ionomycin calcium salt from *Streptomyces conglobatus*, Sigma) followed by recording minimal fluorescence in Ca^{2+}-free medium. $[Ca^{2+}]_i$ was calculated according to previously described formulas [33].

2.3. Western Blot. Cells were first starved in EBM-2 for 4 h and then incubated with BAPTA-AM (Sigma, 20 μM), 2-APB (Sigma 75 μM), or 8Br-cADPR (Sigma 30 μM) for 30 min before stimulation for 20 min with 100 ng/mL Angiopoietin-1 or 200 ng/mL Angiopoietin-2 (PeproTech). Cells were washed with cold PBS before adding lysis buffer 10X (Cell Signaling), PI, and PMSF (Sigma 1 mM). After determining protein concentration by a BCA kit (Thermo Scientific), 25 μg–35 μg protein of each sample was loaded on 8%–10% SDS-PAGE. The proteins were subsequently blotted onto a nitrocellulose membrane and the membrane treated with a blocking solution TTBS + 5% milk (ECL prime blocking agent, GE Healthcare). The following primary antibodies were used: Phospho-p42/44 MAPK (T202/Y204: E10, Cell

Signaling, 1 : 1,000), Phospho-AKT (Ser-473, Cell Signaling, 1 : 1,000), Phospho-FAK (Tyr925, Cell Signaling, 1 : 1,000), Phospho-p38 MAP Kinase (Thr180/Tyr182, Cell Signaling, 1 : 1,000), AKT (Cell Signaling, 1 : 1,000), ERK 2 (Santa Cruz, 1 : 1,000), p38 (Santa Cruz, 1 : 1,000), and FAK (Cell Signaling, 1 : 1,000). All the antibodies were diluted in TTBS 5% BSA. After three washes in TTBS, the membrane was incubated with a secondary HRP-conjugated stabilized goat anti-mouse (Pierce, 1 : 10,000) and stabilized peroxidase-conjugated polyclonal goat anti-rabbit (Bio-Rad, 1 : 10,000) 1 h at RT. To ensure equal loading membranes were reprobed with monoclonal HRP-conjugated anti-β-actin (Sigma). The intensity of Western blot bands was quantified by Image J software from at least three independent experiments, normalized to both total amount of the protein indicated and β-actin content, and compared with control (vehicle) set as 1.

2.4. Scratch Assay. Confluent ECs monolayers plated in 35 mm dishes were scraped along a straight line with a p10 pipette tip to create a narrow gap (scratch). The scratch created was of similar size in the different experimental conditions to minimize any possible variation caused by differences in the width. Debris were removed by a wash with PBS prior to incubation in fresh medium containing Angs in the presence or absence of inhibitors. To record cell migration, images of the wound were acquired at time zero and again 24 h later in an inverted microscope (Nikon Eclipse TS100) equipped with a digital camera (Nikon Ds Fi2, Nis elements F 4.00.00 software). Five random microscopic fields along each wound were photographed.

2.5. In Vitro Matrigel Assay. Capillary-like endothelial tube formation was evaluated by an angiogenesis *in vitro* angiogenesis assay. 130 μL Matrigel basement membrane matrix growth factor reduced (BD Biosciences) was added to each well of precooled 24-well tissue culture plates. Pipette tips and Matrigel solution were kept cold during the procedure to avoid solidification. The plates were incubated for 1 h at 37°C to allow matrix solution to solidify. 4×10^4 cells in a final volume of 500 μL EBM-2 were seeded onto the surface of each well containing the polymerized matrix. Cells were pretreated with the pharmacological inhibitors indicated or with vehicle alone and stimulated with the specific agonists 100 ng/mL Ang-1 or 200 ng/mL Ang-2 for 4-5 hours at 37°C. Tube formation was inspected under an inverted microscope (Nikon Eclipse TS100) at 20x magnification and images were acquired by a digital camera (Nikon Ds Fi2, Nis elements F 4.00.00 software). The closed polygons formed in five random microscopic fields per well were counted and values averaged.

2.6. Statistical Analysis. Data are presented as the mean ± s.e.m. resulting from at least three independent experiments. Student's t-test was used for statistical comparison between means where applicable. Consider $^{*}P < 0.05$, $^{**}P < 0.01$, and $^{***}P < 0.001$. Statistical analysis of the data in Figures 1(a) and 1(b) was performed using the one-way ANOVA test. Consider $^{****}P$ value < 0.0001, $^{*}P$ value < 0.05. Bands on Western blots were quantified by densitometric scanning of films from three or more independent experiments.

3. Results and Discussion

3.1. Ang-1 and Ang-2 Mobilize Calcium from Intracellular Calcium Stores. In the present study, the involvement of Ca^{2+} in the signaling of Angs was tested and analysed to investigate in ECs if Ca^{2+} is involved in responses to Angs. We performed Ca^{2+} imaging experiments in HUVECs monolayer using microfluorimetric analysis. First, we performed dose response experiments stimulating Fura-2-AM-loaded HUVECs with Angs at different concentrations (5 ng/mL–400 ng/mL) using HBSS buffer that allows Ca^{2+} entry from the extracellular environment. The maximum increase in intracellular Ca^{2+} concentration was found to take place at the concentration of 100 ng/mL for Ang-1 and 200 ng/mL for Ang-2 (Figures 1(a) and 1(b)). These two concentrations were therefore used in all the subsequent experiments. In order to investigate the involvement of extracellular Ca^{2+} influx, we performed Ca^{2+} imaging experiments in Ang-1/Ang-2-stimulated cells using Krebs-Henseleit-HEPES buffer (KHH) and a Ca^{2+}-free buffer containing the extracellular Ca^{2+} chelator EGTA (Figures 1(c1) and 1(d1)). Representative $[Ca^{2+}]_i$ profiles are shown in Figures 1(c2) and 1(d2). The response to Angs was found to be buffer-independent, indicating the involvement of intracellular stores. Taken together, these data show for the first time that Angs stimulation triggers intracellular Ca^{2+} signaling. The substantially equal values observed in presence or absence of extracellular Ca^{2+} prompted us to evaluate the involvement of different intracellular compartments in Angs-induced intracellular Ca^{2+} mobilization. We adopted a pharmacological approach using bafilomycin A1, which inhibits pH-dependent Ca^{2+} uptake into acidic stores by inhibition of the vacuolar-type H^+-ATPase pump, and thapsigargin, which inhibits ER SERCA pumps [29]. Angs-induced Ca^{2+} release was significantly impaired by thapsigargin (Figures 2(a) and 2(c)) but not by bafilomycin A1 (Figures 2(b) and 2(d)), demonstrating that Ca^{2+} stores different from acidic compartments are involved in this process.

3.2. Both cADPR and IP_3 Are Involved in $[Ca^{2+}]_i$ Increase Induced by Ang-1 and Ang-2. Many cell stimuli act on receptors that are coupled to phospholipase C (PLC) that hydrolyses phosphatidylinositol 4,5-bisphosphate (PIP_2) producing IP_3, in turn recognised by receptors located on the ER resulting in the release of Ca^{2+}. The spatially and temporally organized pattern of Ca^{2+} release is a remarkably versatile signaling system controlling a multitude of processes in many different cell types [34]. Another Ca^{2+} mobilizing messenger, unrelated to IP_3, has been identified as cyclic ADP-ribose (cADPR) which activates the ryanodine receptors (RyRs) in the sarco/ER [28]. To explore the involvement of these two different second messengers responsible for Ang-1- and Ang-2-dependent intracellular Ca^{2+} mobilization from ER stores, a pharmacological approach was adopted using inhibitors specifically targeting either of them at different levels. The involvement of IP_3 was studied through Ca^{2+} imaging experiments in cells pretreated for 20 min with 2 μM

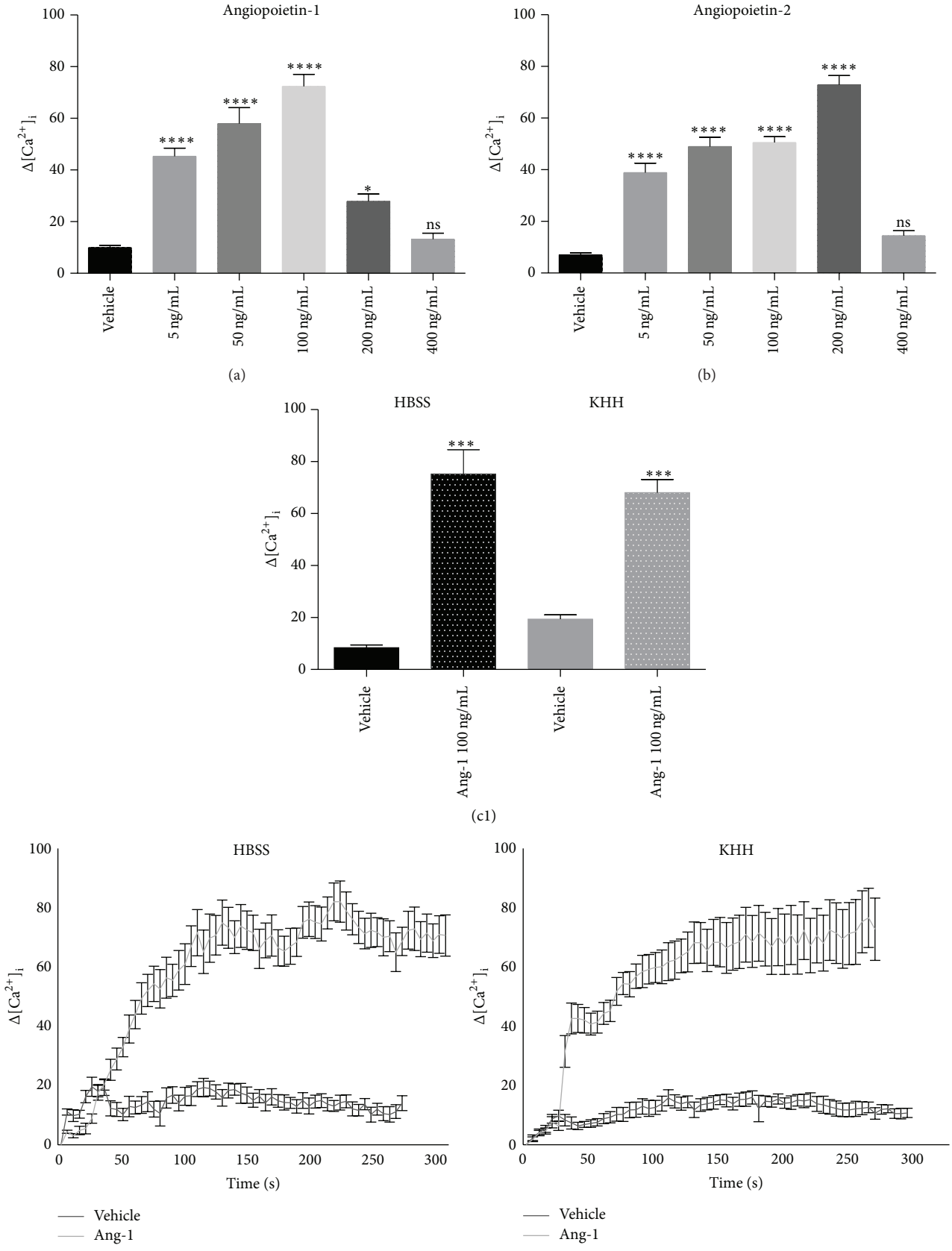

Figure 1: Continued.

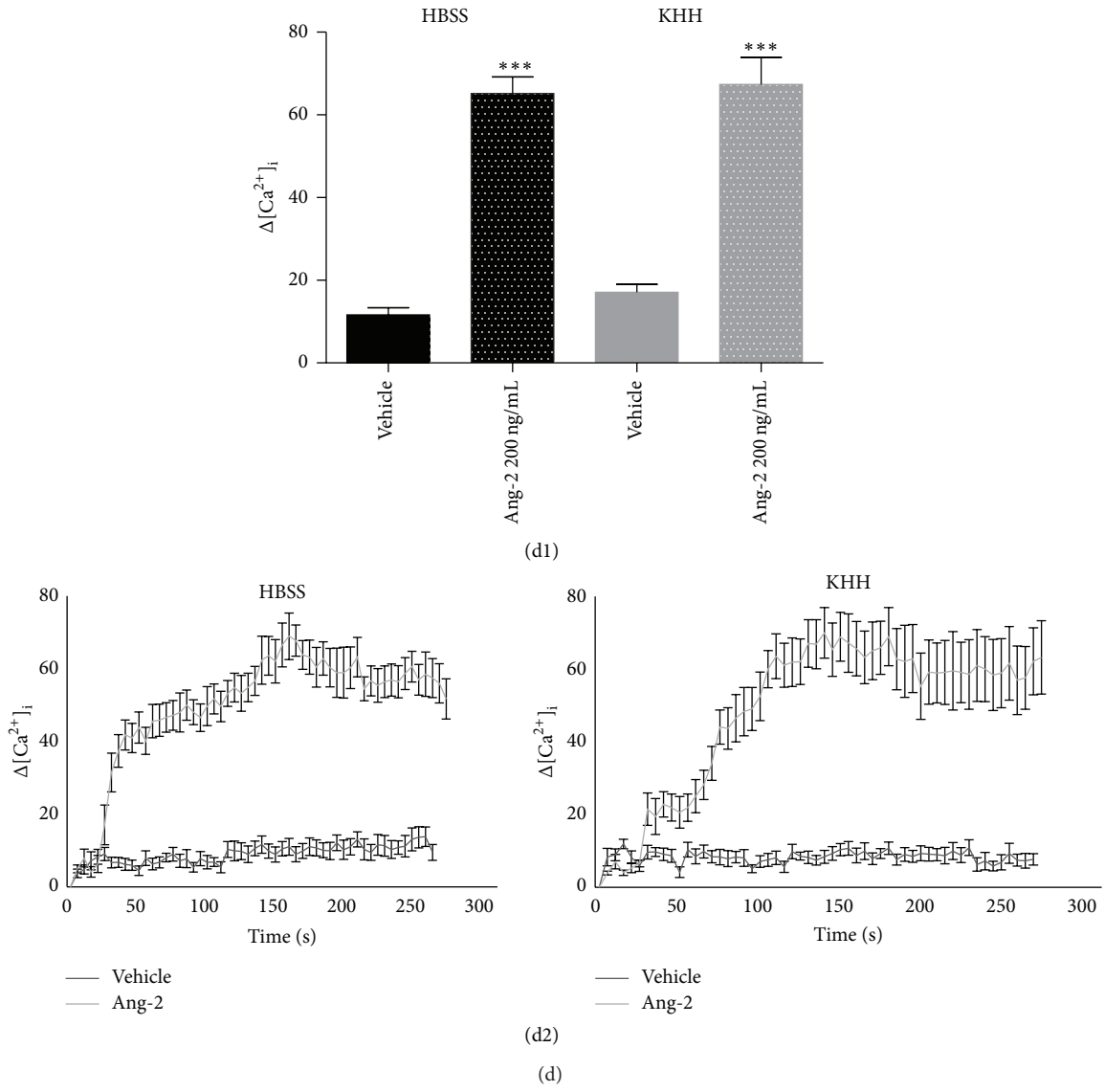

Figure 1: $[Ca^{2+}]_i$ is increased by Ang-1 and Ang-2 stimulation. Live imaging in Fura-2-AM-loaded single cells. $[Ca^{2+}]_i$ increases (nM) following stimulation with either Ang-1 or Ang-2 at different concentrations (5 to 400 ng/mL) in Ca^{2+} containing HBSS buffer. Identification of 100 ng/mL Ang-1 and 200 ng/mL Ang-2 as agonist concentrations is most effective in increasing $[Ca^{2+}]_i$ levels (a, b). Data in bar charts represent mean ± s.e.m. from three independent experiments. Statistical analysis of the data was performed using one-way ANOVA test. $^{****}P$ value < 0.0001, $^{*}P$ value < 0.05. Lack of contribution from Ca^{2+} influx, tested in absence or presence of extracellular calcium (resp., in KHH or HBSS buffer) (c, d). Changes in $[Ca^{2+}]_i$ levels (nM) are shown as maximum concentration in bar charts (c1, d1) and as representative traces (c2, d2) in cells stimulated with Ang-1 or Ang-2, at the respective maximal concentrations, or with vehicle alone. Agonist-stimulated $[Ca^{2+}]_i$ increases are substantially the same in the presence or absence of extracellular Ca^{2+}. Data in bar charts represent mean ± s.e.m. from three independent experiments. Cell number = 78–155. $^{***}P < 0.001$ versus vehicle by Student's t-test. $[Ca^{2+}]_i$ values in representative traces are expressed as increase with respect to basal Ca^{2+} concentrations (Δ).

U73122, the antagonist of PLC, or U73343, its nonfunctional analogue, and in cells pretreated for 30 min with 75 μM 2-APB, the selective antagonist of IP_3 receptor, and stimulated with 10 μM ATP as positive control or Ang-1 or Ang-2. Pretreatment with either inhibitor significantly impaired Ang-1- and Ang-2-induced Ca^{2+} release (Figures 3(a3), 3(a5), 3(b3), and 3(b5)) and, as expected, blocked ATP-evoked Ca^{2+} mobilization, known to be dependent by IP_3 (Figures 3(a1) and 3(b1)). Representative $[Ca^{2+}]_i$ traces are shown in Figures 3(a2), 3(a4), 3(a6), 3(b2), 3(b4), and 3(b6).

To identify the possible involvement of cADPR, Ca^{2+} imaging experiments were performed on cells pretreated for 30 min with 30 μM 8Br-cADPR, the cell permeant antagonist of cADPR, that binds ER RyRs and then stimulated with Ang-1 or Ang-2. As shown in Figure 4, intracellular Ca^{2+} release after stimulation with either Ang was significantly

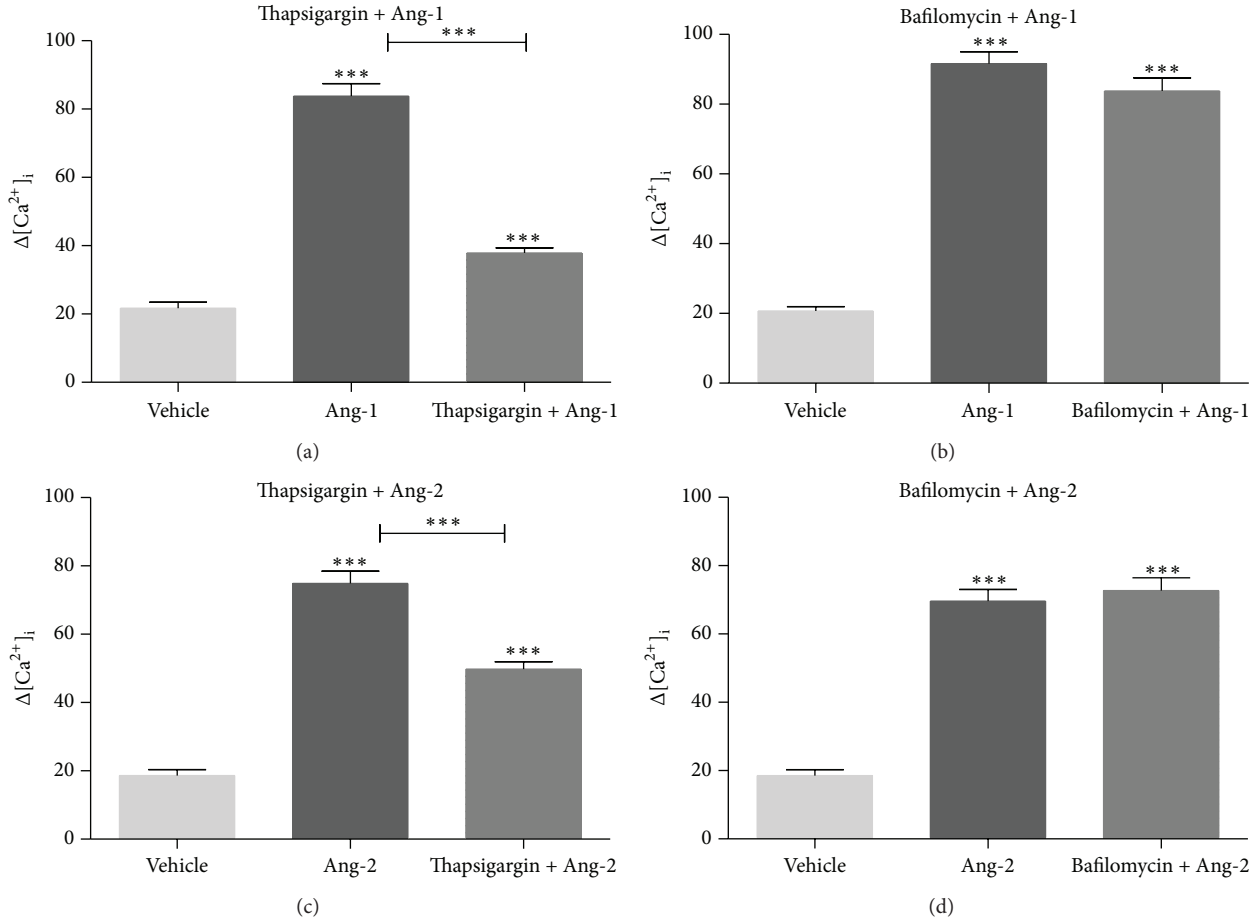

FIGURE 2: Ang-1 and Ang-2 mobilize $[Ca^{2+}]_i$ from ER but not from acidic stores. Live imaging in Fura-2-AM-loaded single cells. Identification of Ang-1- and Ang-2-activated $[Ca^{2+}]_i$ stores. Histograms represent Ca^{2+} release in cells stimulated with 100 ng/mL Ang-1 or 200 ng/mL Ang-2 after pretreatment with vehicle alone, or with 1 μM thapsigargin for 15 min (a, c), or with 500 nM bafilomycin A1 for 1 h in Ca^{2+}-free medium KHH (b, d). Δ on the y-axes = nM. Data in bar charts represent mean ± s.e.m. from three independent experiments. Cell number = 68–187. $^{***}P < 0.001$ by Student's t-test.

reduced in cells pretreated with this inhibitor (Figures 4(a1) and 4(a3)). Representative $[Ca^{2+}]_i$ traces are shown in Figures 4(a2) and 4(a4). These observations demonstrate that Angs mobilize Ca^{2+} from ER stores through IP_3 and cADPR signaling and that the involvement of either pathway is Ang-1/2 isoform specific. In particular, the unexpected partial insensitivity to thapsigargin, U73122, 2-APB, and 8Br-cADPR, observed with Ang-2 stimulation, suggests that this agonist might possibly rely upon additional Ca^{2+} storing compartments/subcompartments [35].

3.3. Ang-1- and Ang-2-Dependent MAPK Pathways Are Differently Regulated by IP_3 and cADPR. Ang-1/Ang-2 signaling via Tie-2 receptor is known to control specific essential steps during angiogenesis, a process involving a complex network of intracellular transduction pathways. The interaction of Ang-1 with Tie-2 in the adult vascular system is essential for ECs survival, migration, and vascular repair. It is known that in ECs Ang-1 induces phosphorylation of AKT [36], ERK1/2 [27], and p38 mitogen-activated protein kinase (MAPKs) [37]. Alitalo's group [38] demonstrated that Ang-1 and Tie-2 form distinct signaling complexes depending on the presence or absence of inter-ECs adhesion linked to the predominant phosphorylation of AKT and weaker activation of ERK in HUVECs monolayer. The intracellular phosphatidylinositol 3-kinase (PI3K)/AKT pathway is a key regulator of several cellular processes and promotes cell survival in response to various stresses such as nutrient deprivation. Among the many signaling pathways that respond to stress, the members of MAPK family are also essential for maintaining cell viability. Several studies demonstrated that Ang-1 promotes cell survival activating the MAPK and PI3K/AKT pathways [16, 19]. During the early stages of angiogenesis, neovascular sprouts are composed primarily by ECs. As they mature, microvessels acquire a coating of mural cells, which are critical for the development and maintenance of functional vasculature. In a rat aorta model [39] p38 MAPK has been shown to transduce signals critical for vascular remodeling and maturation. With the aim of identifying the involvement of Ca^{2+} in Angs-dependent signaling events, we evaluated the

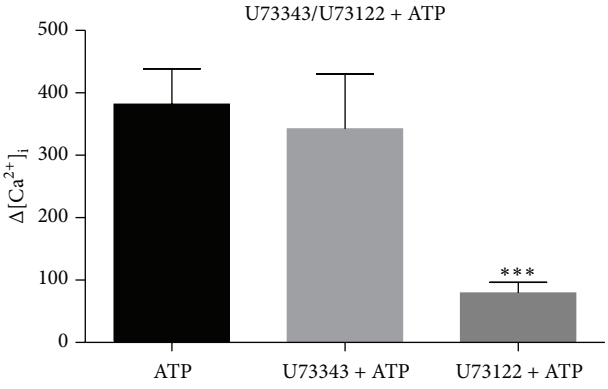

(a1)

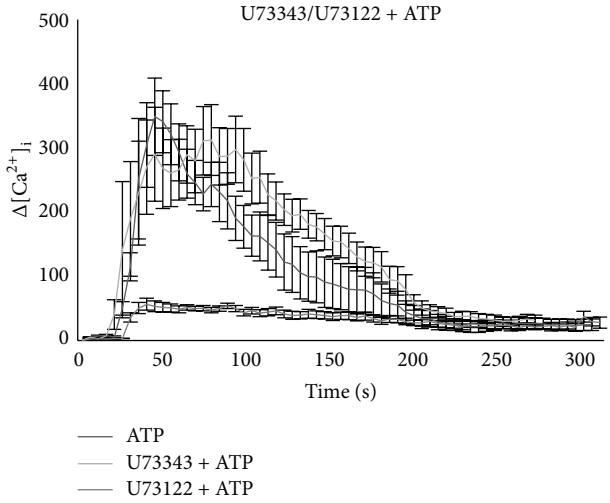

(a2)

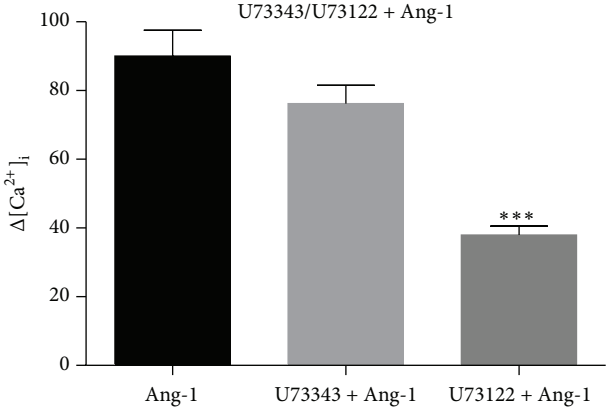

(a3)

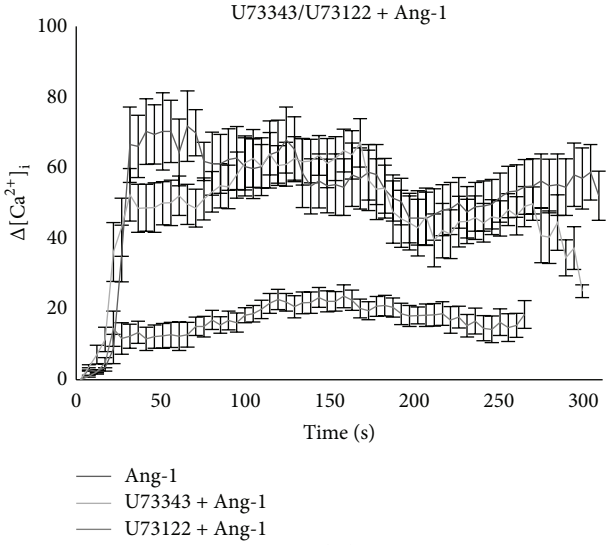

(a4)

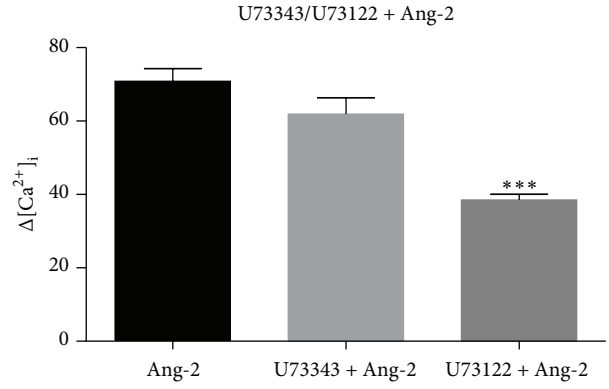

(a5)

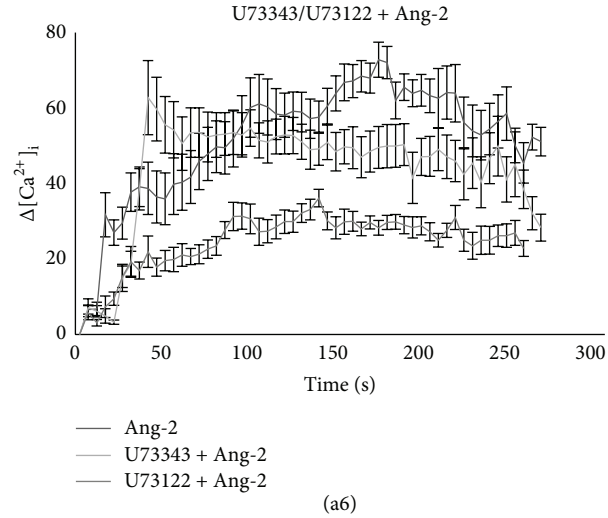

(a6)

(a)

Figure 3: Continued.

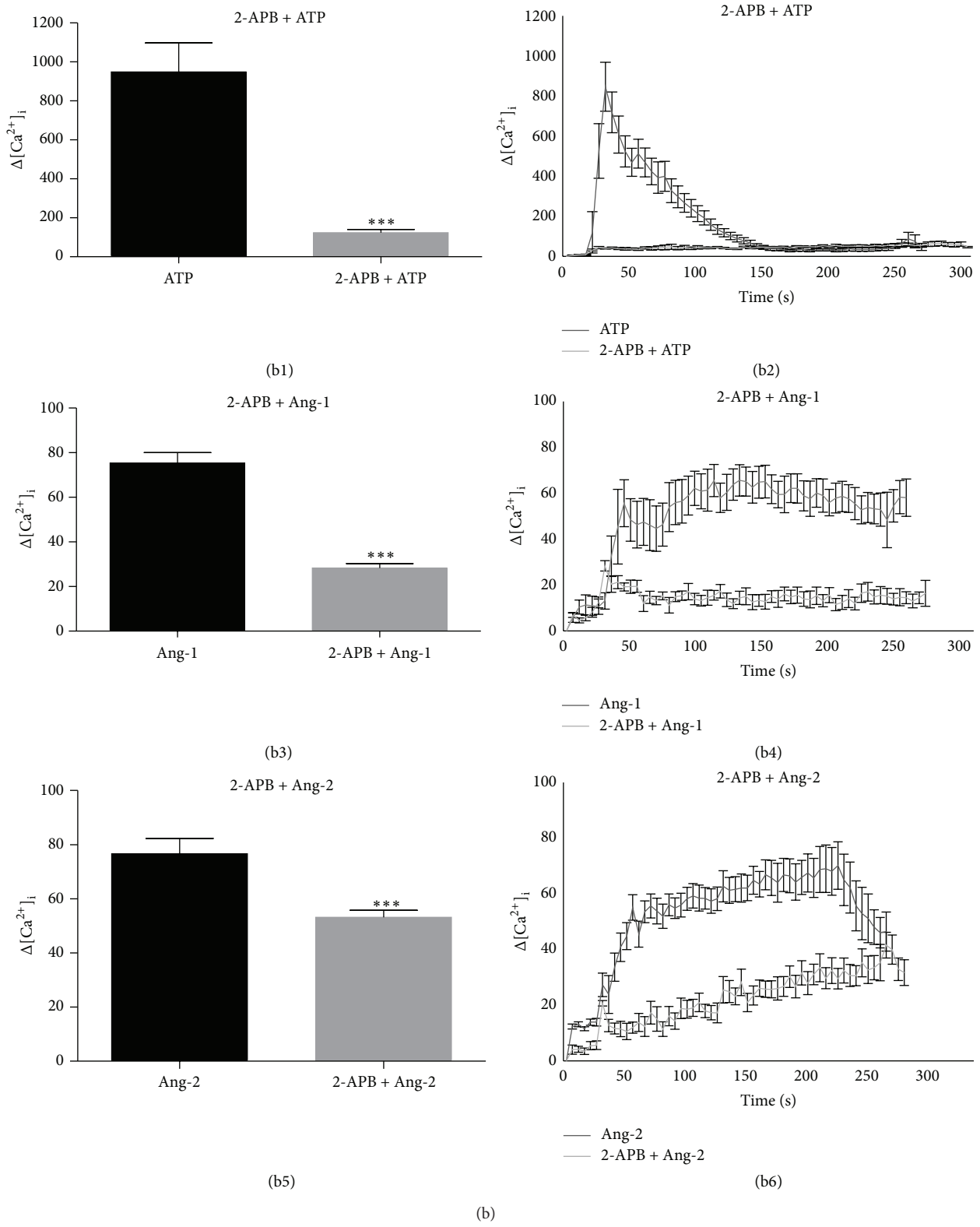

FIGURE 3: Ang-1- and Ang-2-dependent $[Ca^{2+}]_i$ mobilization is inhibited by antagonists of PLC and of IP_3R. Cells pretreated for 20 min with 2 μM U73122 (antagonist of PLC) or U73343 (its nonfunctional analogue) and cells pretreated for 30 min with 75 μM 2-APB (selective antagonist of IP_3 receptor) were stimulated with 10 μM ATP (positive control) or Angs in Ca^{2+}-free medium KHH. Statistical evaluation of $\Delta[Ca^{2+}]_i$ in response to each agonist in the presence or absence of the indicated inhibitors (a1, a3, a5, b1, b3, and b5). Changes in $[Ca^{2+}]_i$ levels are shown as representative traces indicating the effect of U73122/U73343 or 2-APB on cells stimulated with ATP or Ang-1 or Ang-2 in Ca^{2+}-free medium (a2, a4, a6, b2, b4, and b6). Δ on the y-axes = nM. Data in bar charts represent mean ± s.e.m. from three independent experiments. Cell number = 88–140. $^{***}P < 0.001$ versus agonists by Student's t-test. $[Ca^{2+}]_i$ values in representative traces are expressed as increase with respect to basal Ca^{2+} concentrations (Δ).

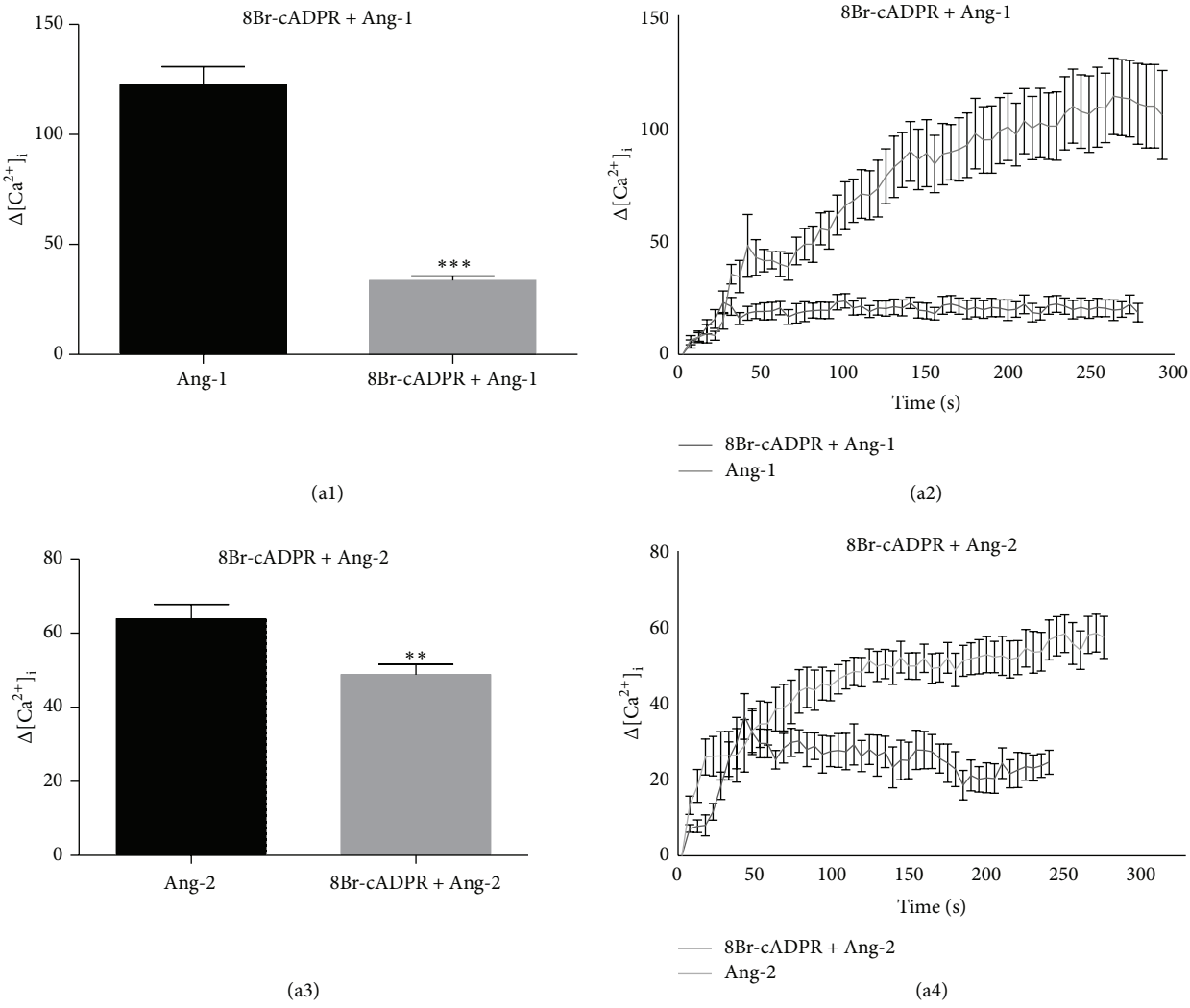

FIGURE 4: RyR inhibition abates both Ang-1- and Ang-2-mediated intracellular calcium mobilization. Cells were pretreated for 30 min with 30 μM 8Br-cADPR (inactive analogue of cADPR) and then stimulated with Ang-1 or Ang-2 in Ca^{2+}-free medium KHH. Histograms show changes in $[Ca^{2+}]_i$ levels in response to each agonist in the presence or absence of the indicated inhibitor (a1, a3). Representative traces showing the effect of 8Br-cADPR on Ang-1-stimulated (a2) and Ang-2-stimulated (a4) cells. Δ on the y-axes = nM. Data in bar charts represent mean ± s.e.m. of three independent experiments. Cell number = 96–132. $^{**}P < 0.01$, $^{***}P < 0.001$ versus agonist by Student's t-test. $[Ca^{2+}]_i$ values in representative traces are expressed as increase with respect to basal Ca^{2+} concentrations (Δ).

activation of their known protein targets ERK1/2, AKT, and p38. HUVECs were pretreated or not with the Ca^{2+} chelator BAPTA-AM at the concentration of 20 μM. As shown in Figure 5(a) and Figures S1 A–F (in Supplementary Material available online at http://dx.doi.org/10.1155/2015/965271), both Angs activate the phosphorylation of AKT, ERK1/2, and p38 and the combined treatment with BAPTA-AM was found to inhibit both Ang-1- and Ang-2-dependent AKT phosphorylation, while the phosphorylation of ERK1/2 was not affected. The lack of intracellular calcium had an opposite effect on p38 phosphorylation. To further evaluate the specific contribution of the different Ca^{2+} mobilizing second messengers in AKT phosphorylation, we performed Western blot analysis of cells with two specific inhibitors, either 2-APB (for IP_3/IP_3R) or 8Br-cADPR (for cADPR/RyR) prior to Angs stimulation. As shown in Figures 5(b) and 5(c) and Figures S1 G–L, the phosphorylation of AKT is differentially regulated by the two Angs. Pretreatment with 2-APB specifically reduced the extent of AKT phosphorylation resulting from stimulation with Ang-1 suggesting the requirement of IP_3-dependent Ca^{2+} release (Figures 5(b1) and 5(c1)), while cADPR/RyR signaling is significantly not involved in this response to either Ang-1 or Ang-2 (Figures 5(b2) and 5(c2)).

3.4. Different Ca^{2+} Signatures Regulate the Cell Migratory Response to Ang-1 and Ang-2. During neovascularization and angiogenesis ECs degrade the basement membrane and migrate into the perivascular stroma in response to a gradient of angiogenic factors. Cell migration and invasion of extracellular matrix beneath the basement membrane are essential steps involving reorganization of the actin cytoskeleton. The

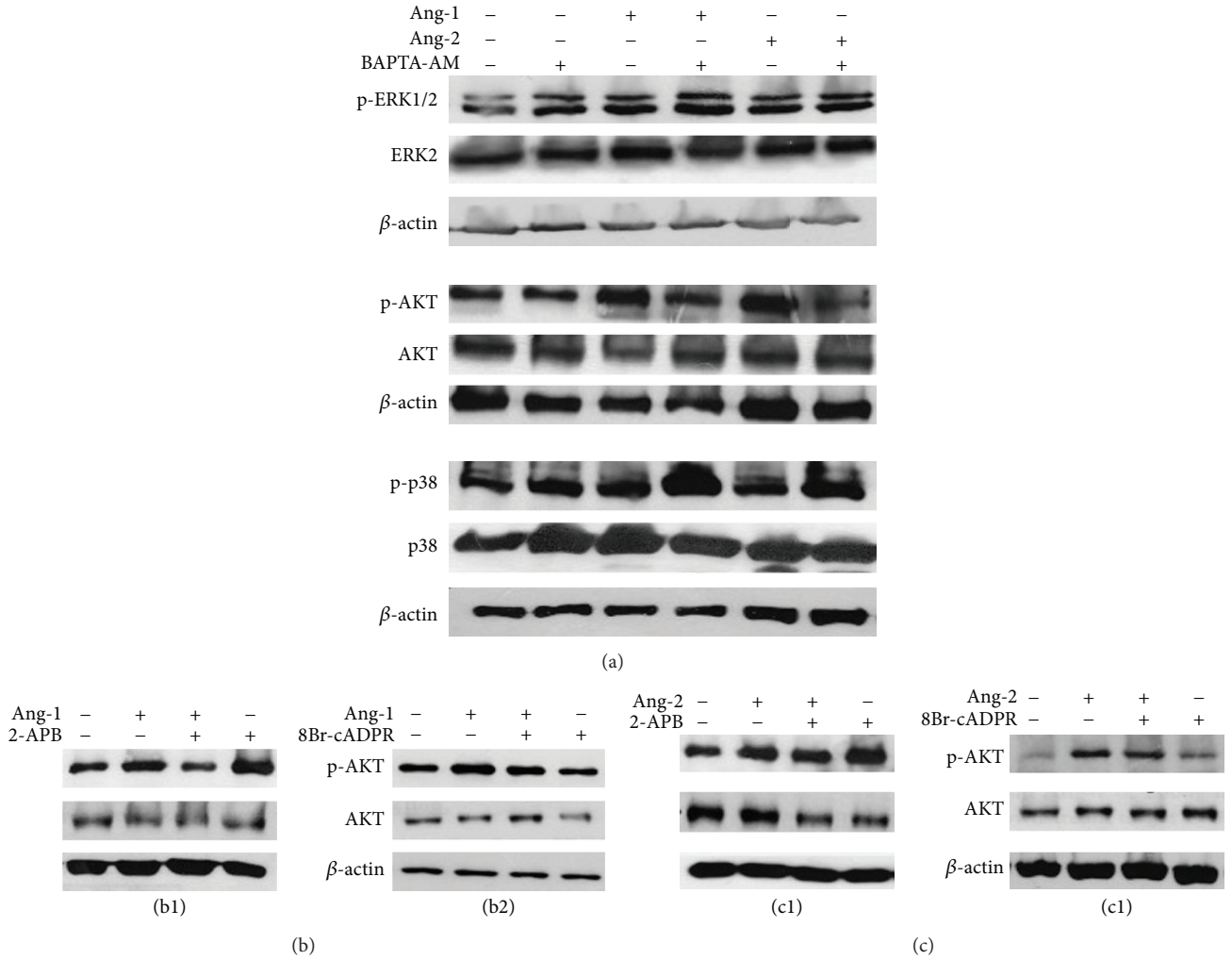

Figure 5: Calcium-dependent AKT and MAPK activation upon Ang-1/Ang-2 stimulation. Ang-1 and Ang-2 induce Ca^{2+}-dependent AKT, ERK1/2, and p38 phosphorylation. Confluent HUVECs were pretreated or not with 20 μM BAPTA-AM for 1 h and stimulated with 100 ng/mL Ang-1 or 200 ng/mL Ang-2 for 30 min. Blots of total cell lysate were probed for the phosphorylation of downstream targets AKT, ERK1/2, and p38. To ensure equal loading membranes were reprobed for the total amount of the indicated proteins and for β-actin. Representative blots are shown from three to five independent experiments (a). Cells pretreated or not with 75 μM 2-APB or 30 μM 8Br-cADPR and stimulated with either Ang-1 or Ang-2. Blots of total cell lysate were probed for the phosphorylation of downstream target AKT. To ensure equal loading membranes were reprobed for the total amount of the indicated protein and for β-actin. Representative blots are shown from three independent experiments (b1, b2, c1, and c2).

focal adhesion kinase FAK, a member of nonreceptor tyrosine kinases, plays a key role in regulating the dynamic changes in actin cytoskeleton reorganization involved in migration and adhesion. Ang-1 induces capillary sprouting activity through nondirectional and directional migration mediated by Tie-2 but not Tie-1 receptor and induces tyrosine phosphorylation of FAK which is dependent on PI3K activity [40–43]. To identify the possible involvement of $[Ca^{2+}]_i$ rise in Angs-dependent activation of p-FAK, we performed Western blot analysis in cells treated or not with the Ca^{2+} chelator BAPTA-AM at the concentration of 20 μM prior to stimulation with either Ang-1 or Ang-2. We observed that both Angs activate p-FAK through a Ca^{2+}-dependent mechanism (Figure 6(a), Figures S2 A-B). To evaluate the contribution of the different second messengers involved, cells were pretreated with two specific inhibitors, 2-APB and 8Br-cADPR. FAK phosphorylation induced by Angs was found to depend on IP_3 signal in cells stimulated with Ang-1 (Figures 6(b1) and 6(b2)) and strongly by both second messengers in those stimulated with Ang-2 (Figures 6(c1) and 6(c2), Figures S2 C–F). To further test the specific involvement of IP_3 and cADPR in Ang-1- and Ang-2-induced cell motility, we performed a "scratch assay" in which confluent ECs monolayer is manually wounded along a narrow line and subsequent cell migration to reform the monolayer can be studied. The advantage of this method is that cell migration can be monitored over time, thus allowing us to estimate the rate of migratory response. Quantification is arbitrary, depending on size of wound and

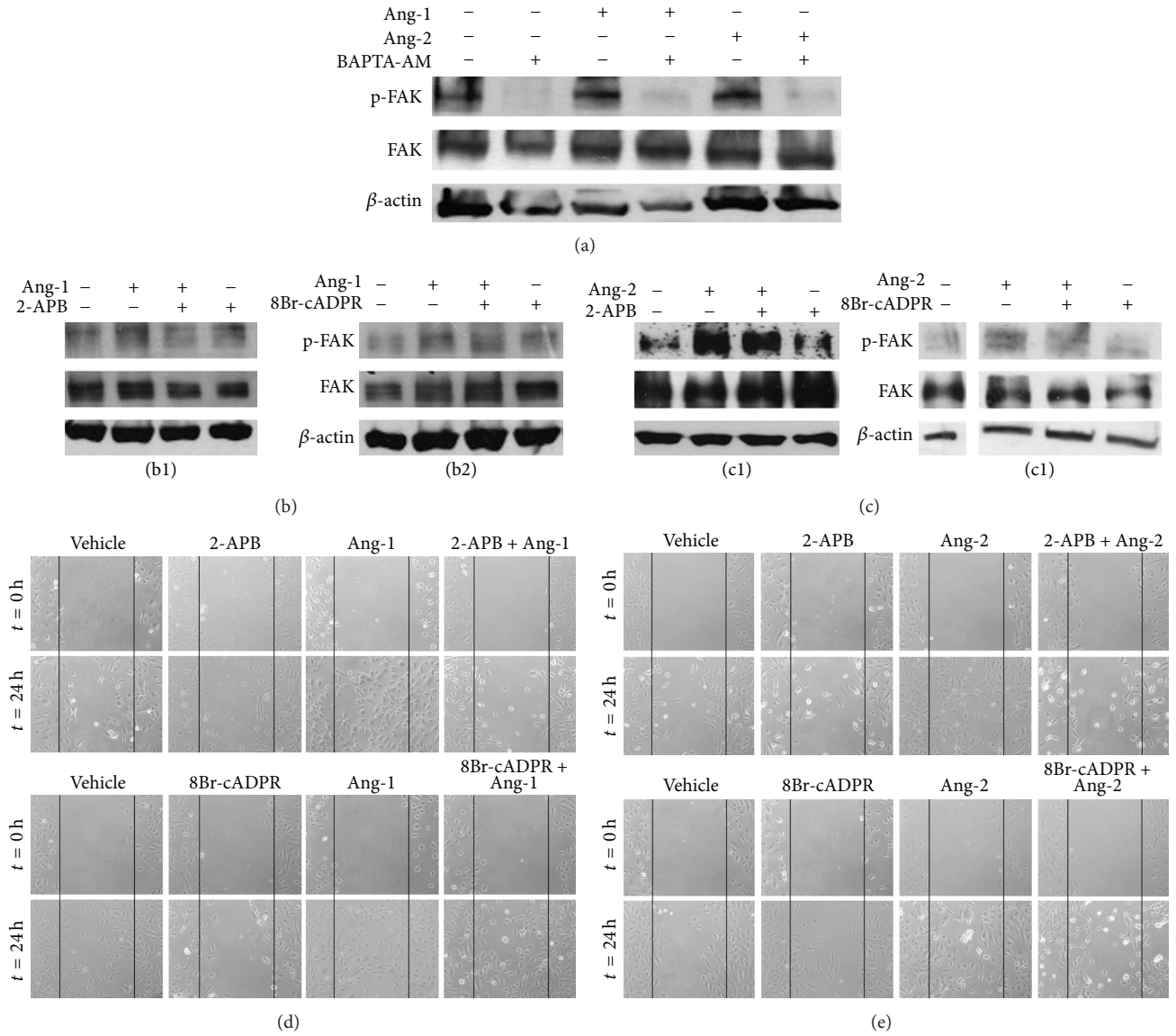

Figure 6: 2-APB and 8Br-cADPR impair Angs-dependent cell migration on HUVECs. Ang-1 and Ang-2 induce Ca^{2+}-dependent FAK phosphorylation. Confluent HUVECs were pretreated or not with 20 μM BAPTA-AM for 1 h and stimulated with 100 ng/mL Ang-1 or 200 ng/mL Ang-2 for 30 min. Blots of total cell lysate were probed for the phosphorylation of downstream target FAK. To ensure equal loading membranes were reprobed for the total amount of the indicated protein and for β-actin (a). Cells pretreated or not with 75 μM 2-APB or 30 μM 8Br-cADPR and stimulated with either Ang-1 or Ang-2 (b1, b2, c1, and c2). Representative blots are shown from three to five independent experiments. Ang-1-induced EC migration is affected by treatment with the second messengers inhibitor 2-APB while Ang-2-induced cell migration appears to be both IP_3- and cADPR-dependent. Scratch assay to evaluate the cell migration capability in the indicated experimental conditions. Wounded monolayers at the time of manual damage (t = 0 h upper panel) and after 24 h treatment (lower panel) with Ang-1 (d), Ang-2 (e), and inhibitors as indicated. Pictures are representative of three independent experiments.

cell growth. In order to discriminate between migration and proliferation, flow cytometric assessment of cell proliferation with propidium iodide (PI) was performed (Figure S3). This assay showed that, in the culture conditions of the wound healing assay, ECs do not proliferate under Angs stimulation. From a qualitative point of view, the wound healing assay clearly demonstrated that the capability of ECs to move in 24 h under Ang-1 stimulation is modified by the treatment with 2-APB, while under Ang-2 stimulation cell migration is reduced by the treatment with either 8Br-cADPR or 2-APB (Figures 6(d) and 6(e)).

3.5. Capillary-Like Network Formation Controlled by Ang-1 Is IP_3-Dependent. The formation of capillary-like structures *in vivo* is considered as representative of later, differentiative stages of angiogenesis and is commonly assayed to test the efficiency of compounds with pro- or antiangiogenic functions. The Angs-Tie axis is essential for vasculogenesis,

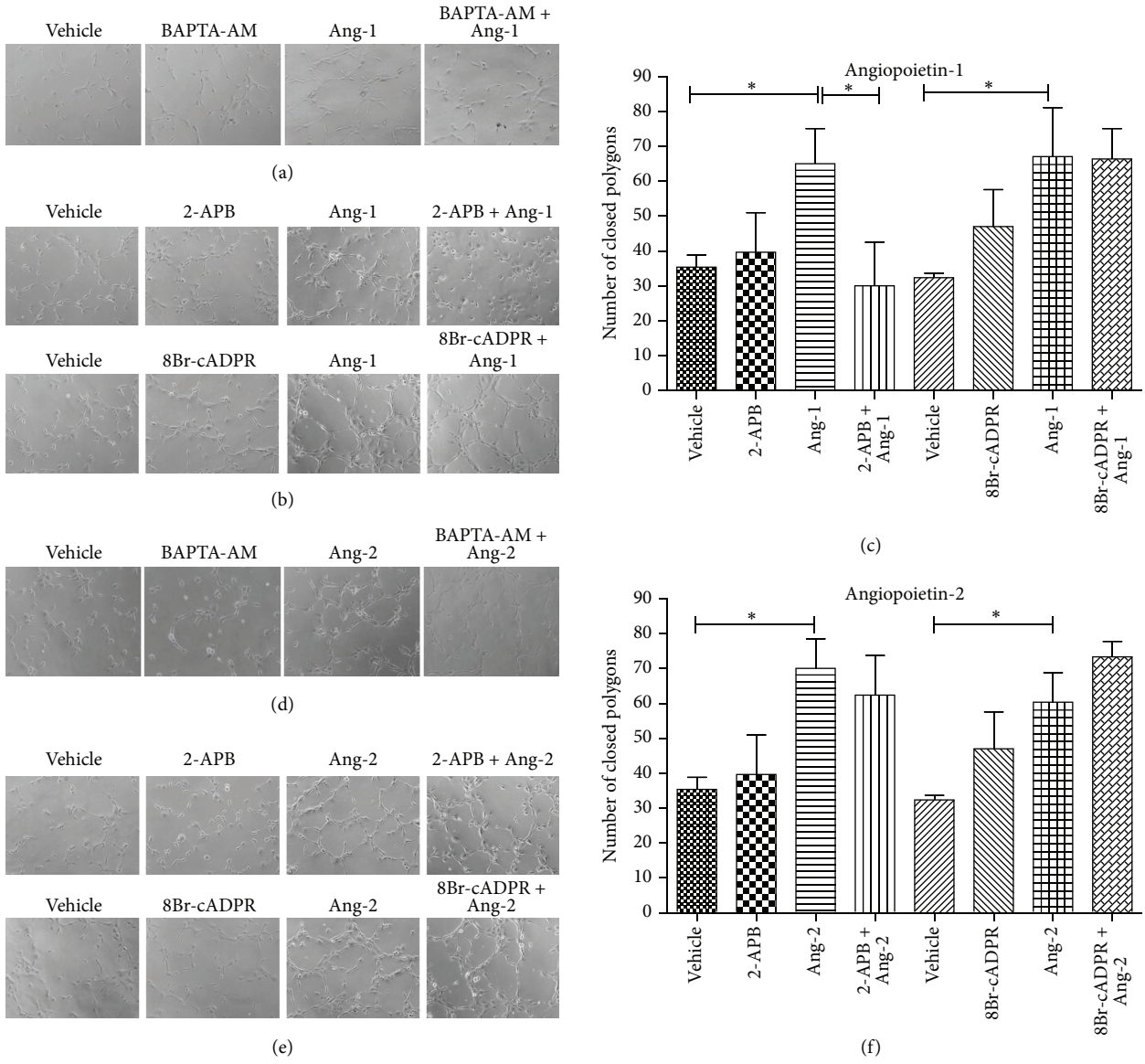

FIGURE 7: IP_3 pathway inhibition impairs Ang-1-induced capillary-like formation *in vitro*. Cells were plated in Matrigel-coated dishes and incubated in EBM-2 + 2% FBS for 5 h in the presence or absence of Angs or/and inhibitors as indicated. Each condition was tested in triplicate. Representative images of one of three independent experiments (Ang-1: a, b; Ang-2: d, e). Quantitative evaluation of tube formation as the number of closed polygons formed in seven fields for each experimental condition (c, f). Data in bar charts represent mean ± s.e.m. of three independent experiments. $^*P < 0.05$ by Student's t-test.

normal vascular development, and angiogenesis. When ECs are plated onto a layer of gel matrix, they are stimulated to migrate and differentiate into tubular-like structures simulating the *in vivo* process [44]. Matrigel, a complex compound that mimics the extracellular matrix, containing extracellular and basement membrane proteins, is known to be the most potent matrix for tubule formation. This is usually assayed in the presence of potential modulators of angiogenesis and tubule development is observed over a 4 to 24 h period. Cord-like capillary structures are visualized as close polygons and the degree of complexity of the structure can be quantitatively evaluated counting the number of close polygons or associating a score depending on the number of ECs composing each of them. As shown in Figures 7(a) and 7(d), when plated on Matrigel matrices at high densities, HUVECs form cord-like capillary structures within a few hours, and this process is enhanced by Ang-1 and Ang-2. To evaluate the possible involvement of calcium signals in the regulation of this angiogenic process, cells were pretreated with the Ca^{2+} chelator BAPTA-AM at the concentration of 20 μM. The formation of Angs-induced capillary-like structures was impaired by this inhibitor in Ang-1 stimulated samples but unaffected in cells stimulated with Ang-2, indicating that this response to Ang-2 is $[Ca^{2+}]_i$-independent. To further assess whether Ca^{2+} signal is dispensable for Ang-2 to induce capillary-like formation, we performed the Matrigel assay in

the presence of second messengers inhibitors as shown in Figures 7(e) and 7(f) and found no evident inhibition of tube formation. Moreover, to identify by which second messenger Ang-1 controls the formation of capillary-like structures, cells were pretreated with the same second messenger inhibitors. Representative images show that this response to Ang-1 was inhibited by 2-APB pretreatment (Figure 7(b)). An approximate estimate of the efficiency of this process can be inferred by the extent of cellular network formation, whereby cells first align to form linear segments and subsequently interconnect to form closed polygonal structures. As shown in Figure 7(c), the number of closed polygons formed in cells stimulated with Ang-1 in the presence of 2-APB is significantly reduced compared with samples stimulated with Ang-1 alone, indicating the involvement of IP_3-mediated Ca^{2+} signaling in capillary-like formation *in vitro*.

4. Conclusions

During the complex process of angiogenesis, a variety of growth factors and cytokines are upregulated and exert their functions through autocrine/paracrine signaling. Among these, Ang-1 and Ang-2 play important roles. Ang-1 does not stimulate ECs growth but rather promotes stabilization of vascular network and branching morphogenesis in *in vitro* and *in vivo* angiogenesis; conversely, Ang-2, a somehow context-dependent antagonist of Ang-1, promotes vessels destabilization favouring pericytes detachment [45]. In the present study, we identified a novel Ca^{2+}-dependent machinery activated by Angs which controls angiogenic processes, including migration and the ability to induce capillary-like structures *in vitro*. Our data suggest that Ca^{2+} signaling might be envisaged as a possible "signaling hub" for Angs and other angiogenic factors. Given the therapeutic potential of angiogenesis-blocking therapies based on the inhibition of specific signaling pathways, this concept could open the way to novel experimental approaches in this field.

Conflict of Interests

The authors declare no conflict of interests.

Authors' Contribution

Irene Pafumi and Antonio Filippini designed research; Irene Pafumi and Annarita Favia performed research; Irene Pafumi, Annarita Favia, Guido Gambara, Francesca Papacci, Elio Ziparo, and Antonio Filippini analyzed data; Irene Pafumi, Annarita Favia, Fioretta Palombi, and Antonio Filippini wrote the paper.

Acknowledgments

This work was supported by grants from Ministero dell'Istruzione, dell'Università e della Ricerca (MIUR) and Agenzia Spaziale Italiana (to Antonio Filippini) and from Fondazione Roma (to Elio Ziparo).

References

[1] S. Fukuhara, K. Sako, K. Noda, K. Nagao, K. Miura, and N. Mochizuki, "Tie2 is tied at the cell-cell contacts and to extracellular matrix by Angiopoietin-1," *Experimental & Molecular Medicine*, vol. 41, no. 3, pp. 133–139, 2009.

[2] S. Davis, T. H. Aldrich, P. F. Jones et al., "Isolation of angiopoietin-1, a ligand for the TIE2 receptor, by secretion-trap expression cloning," *Cell*, vol. 87, no. 7, pp. 1161–1169, 1996.

[3] H. Huang, A. Bhat, G. Woodnutt, and R. Lappe, "Targeting the ANGPT-TIE2 pathway in malignancy," *Nature Reviews Cancer*, vol. 10, no. 8, pp. 575–585, 2010.

[4] L. Eklund and P. Saharinen, "Angiopoietin signaling in the vasculature," *Experimental Cell Research*, vol. 319, no. 9, pp. 1271–1280, 2013.

[5] K. J. Kim, B. Li, J. Winer et al., "Inhibition of vascular endothelial growth factor-induced angiogenesis suppresses tumour growth *in vivo*," *Nature*, vol. 362, no. 6423, pp. 841–844, 1993.

[6] H. Hurwitz, L. Fehrenbacher, W. Novotny et al., "Bevacizumab plus irinotecan, fluorouracil, and leucovorin for metastatic colorectal cancer," *The New England Journal of Medicine*, vol. 350, no. 23, pp. 2335–2342, 2004.

[7] N. M. Biel and D. W. Siemann, "Targeting the Angiopoietin-2/Tie-2 axis in conjunction with VEGF signal interference," *Cancer Letters*, 2014.

[8] P. Carmeliet and R. K. Jain, "Principles and mechanisms of vessel normalization for cancer and other angiogenic diseases," *Nature Reviews Drug Discovery*, vol. 10, no. 6, pp. 417–427, 2011.

[9] G. Bergers and D. Hanahan, "Modes of resistance to anti-angiogenic therapy," *Nature Reviews Cancer*, vol. 8, no. 8, pp. 592–603, 2008.

[10] H. G. Augustin, G. Y. Koh, G. Thurston, and K. Alitalo, "Control of vascular morphogenesis and homeostasis through the angiopoietin—Tie system," *Nature Reviews Molecular Cell Biology*, vol. 10, no. 3, pp. 165–177, 2009.

[11] M. Thomas and H. G. Augustin, "The role of the angiopoietins in vascular morphogenesis," *Angiogenesis*, vol. 12, no. 2, pp. 125–137, 2009.

[12] P. C. Maisonpierre, C. Suri, P. F. Jones et al., "Angiopoietin-2, a natural antagonist for Tie2 that disrupts in vivo angiogenesis," *Science*, vol. 277, no. 5322, pp. 55–60, 1997.

[13] N. W. Gale, G. Thurston, S. F. Hackett et al., "Angiopoietin-2 is required for postnatal angiogenesis and lymphatic patterning, and only the latter role is rescued by angiopoietin-1," *Developmental Cell*, vol. 3, no. 3, pp. 411–423, 2002.

[14] T. C. M. Seegar, B. Eller, D. Tzvetkova-Robev et al., "Tie1-Tie2 interactions mediate functional differences between angiopoietin ligands," *Molecular Cell*, vol. 37, no. 5, pp. 643–655, 2010.

[15] G. Thurston and C. Daly, "The complex role of angiopoietin-2 in the angiopoietin-Tie signaling pathway," *Cold Spring Harbor Perspectives in Medicine*, 2012.

[16] I. Kim, J.-H. Kim, S.-O. Moon, H. J. Kwak, N.-G. Kim, and G. Y. Koh, "Angiopoietin-2 at high concentration can enhance endothelial cell survival through the phosphatidylinositol 3′-kinase/Akt signal transduction pathway," *Oncogene*, vol. 19, no. 39, pp. 4549–4552, 2000.

[17] K. Teichert-Kuliszewska, P. C. Maisonpierre, N. Jones et al., "Biological action of angiopoietin-2 in a fibrin matrix model of angiogenesis is associated with activation of Tie2," *Cardiovascular Research*, vol. 49, no. 3, pp. 659–670, 2001.

[18] C. Daly, E. Pasnikowski, E. Burova et al., "Angiopoietin-2 functions as an autocrine protective factor in stressed endothelial cells," *Proceedings of the National Academy of Sciences of the United States of America*, vol. 103, no. 42, pp. 15491–15496, 2006.

[19] K. Fujikawa, I. de Aos Scherpenseel, S. K. Jain, E. Presman, R. A. Christensen, and L. Varticovski, "Role of PI 3-kinase in angiopoietin-1-mediated migration and attachment-dependent survival of endothelial cells," *Experimental Cell Research*, vol. 253, no. 2, pp. 663–672, 1999.

[20] I. Kim, H. G. Kim, J.-N. So, J. H. Kim, H. J. Kwak, and G. Y. Koh, "Angiopoietin-1 regulates endothelial cell survival through the phosphatidylinositol 3′-kinase/Akt signal transduction pathway," *Circulation Research*, vol. 86, no. 1, pp. 24–29, 2000.

[21] D. P. Hughes, M. B. Marron, and N. P. J. Brindle, "The antiinflammatory endothelial tyrosine kinase Tie2 interacts with a novel nuclear factor-κB inhibitor ABIN-2," *Circulation Research*, vol. 92, no. 6, pp. 630–636, 2003.

[22] U. Fiedler, M. Scharpfenecker, S. Koidl et al., "The Tie-2 ligand Angiopoietin-2 is stored in and rapidly released upon stimulation from endothelial cell Weibel-Palade bodies," *Blood*, vol. 103, no. 11, pp. 4150–4156, 2004.

[23] Y.-Q. Huang, J.-J. Li, L. Hu, M. Lee, and S. Karpatkin, "Thrombin induces increased expression and secretion of angiopoietin-2 from human umbilical vein endothelial cells," *Blood*, vol. 99, no. 5, pp. 1646–1650, 2002.

[24] I. Helfrich, L. Edler, A. Sucker et al., "Angiopoietin-2 levels are associated with disease progression in metastatic malignant melanoma," *Clinical Cancer Research*, vol. 15, no. 4, pp. 1384–1392, 2009.

[25] K. M. Detjen, S. Rieke, A. Deters et al., "Angiopoietin-2 promotes disease progression of neuroendocrine tumors," *Clinical Cancer Research*, vol. 16, no. 2, pp. 420–429, 2010.

[26] V. Goede, O. Coutelle, J. Neuneier et al., "Identification of serum angiopoietin-2 as a biomarker for clinical outcome of colorectal cancer patients treated with bevacizumab-containing therapy," *British Journal of Cancer*, vol. 103, no. 9, pp. 1407–1414, 2010.

[27] S. Fukuhara, K. Sako, T. Minami et al., "Differential function of Tie2 at cell-cell contacts and cell-substratum contacts regulated by angiopoietin-1," *Nature Cell Biology*, vol. 10, no. 5, pp. 513–526, 2008.

[28] M. J. Berridge, M. D. Bootman, and H. L. Roderick, "Calcium signalling: dynamics, homeostasis and remodelling," *Nature Reviews Molecular Cell Biology*, vol. 4, no. 7, pp. 517–529, 2003.

[29] A. Galione and G. C. Churchill, "Interactions between calcium release pathways: multiple messengers and multiple stores," *Cell Calcium*, vol. 32, no. 5-6, pp. 343–354, 2002.

[30] A. J. Morgan, F. M. Platt, E. Lloyd-Evans, and A. Galione, "Molecular mechanisms of endolysosomal Ca^{2+} signalling in health and disease," *Biochemical Journal*, vol. 439, no. 3, pp. 349–374, 2011.

[31] B. Esposito, G. Gambara, A. M. Lewis et al., "NAADP links histamine H1 receptors to secretion of von Willebrand factor in human endothelial cells," *Blood*, vol. 117, no. 18, pp. 4968–4977, 2011.

[32] A. Favia, M. Desideri, G. Gambara et al., "VEGF-induced neoangiogenesis is mediated by NAADP and two-pore channel-2-dependent Ca^{2+} signaling," *Proceedings of the National Academy of Sciences of the United States of America*, vol. 111, no. 44, pp. E4706–E4715, 2014.

[33] G. Grynkiewicz, M. Poenie, and R. Y. Tsien, "A new generation of Ca^{2+} indicators with greatly improved fluorescence properties," *The Journal of Biological Chemistry*, vol. 260, no. 6, pp. 3440–3450, 1985.

[34] M. J. Berridge, "Inositol trisphosphate and calcium signalling mechanisms," *Biochimica et Biophysica Acta—Molecular Cell Research*, vol. 1793, no. 6, pp. 933–940, 2009.

[35] M. Brini and E. Carafoli, "Calcium pumps in health and disease," *Physiological Reviews*, vol. 89, no. 4, pp. 1341–1378, 2009.

[36] A. Papapetropoulos, D. Fulton, K. Mahboubi et al., "Angiopoietin-1 inhibits endothelial cell apoptosis via the Akt/survivin pathway," *The Journal of Biological Chemistry*, vol. 275, no. 13, pp. 9102–9105, 2000.

[37] W.-H. Zhu, J. Han, and R. F. Nicosia, "Requisite role of p38 MAPK in mural cell recruitment during angiogenesis in the rat aorta model," *Journal of Vascular Research*, vol. 40, no. 2, pp. 140–148, 2003.

[38] P. Saharinen, L. Eklund, J. Miettinen et al., "Angiopoietins assemble distinct Tie2 signalling complexes in endothelial cell-cell and cell-matrix contacts," *Nature Cell Biology*, vol. 10, no. 5, pp. 527–537, 2008.

[39] W. H. Zhu, A. MacIntyre, and R. F. Nicosia, "Regulation of angiogenesis by vascular endothelial growth factor and angiopoietin-1 in the rat aorta model: distinct temporal patterns of intracellular signaling correlate with induction of angiogenic sprouting," *The American Journal of Pathology*, vol. 161, no. 3, pp. 823–830, 2002.

[40] I. Kim, H. G. Kim, S. O. Moon et al., "Angiopoietin-1 induces endothelial cell sprouting through the activation of focal adhesion kinase and plasmin secretion," *Circulation Research*, vol. 86, no. 9, pp. 952–959, 2000.

[41] M. Felcht, R. Luck, A. Schering et al., "Angiopoietin-2 differentially regulates angiogenesis through TIE2 and integrin signaling," *The Journal of Clinical Investigation*, vol. 122, no. 6, pp. 1991–2005, 2012.

[42] I. Cascone, E. Audero, E. Giraudo et al., "Tie-2-dependent activation of RhoA and Rac1 participates in endothelial cell motility triggered by angiopoietin-1," *Blood*, vol. 102, no. 7, pp. 2482–2490, 2003.

[43] B. Witzenbichler, P. C. Maisonpierre, P. Jones, G. D. Yancopoulos, and J. M. Isner, "Chemotactic properties of angiopoietin-1 and -2, ligands for the endothelial-specific receptor tyrosine kinase Tie2," *The Journal of Biological Chemistry*, vol. 273, no. 29, pp. 18514–18521, 1998.

[44] C. A. Staton, M. W. R. Reed, and N. J. Brown, "A critical analysis of current *in vitro* and *in vivo* angiogenesis assays," *International Journal of Experimental Pathology*, vol. 90, no. 3, pp. 195–221, 2009.

[45] E. Fagiani and G. Christofori, "Angiopoietins in angiogenesis," *Cancer Letters*, vol. 328, no. 1, pp. 18–26, 2013.